

Universidade do Minho

Escola de Engenharia

Alexandre António Antunes Barros

**Biodegradable urological stent
systems based on natural origin
polymers**

Tese de Doutoramento

Programa Doutoral em Engenharia de Tecidos
Medicina Regenerativa e Células Estaminais

Supervisores

Doutora Ana Rita Cruz Duarte

**Professor Doutor Estevão Augusto Rodrigues
Lima**

março de 2017

STATEMENT OF INTEGRITY

I hereby declare having conducted my thesis with integrity. I confirm that I have not used plagiarism or any form of falsification of results in the process of the thesis elaboration.

I further declare that I have fully acknowledged the Code of Ethical Conduct of the University of Minho.

University of Minho, 8th March 2017

Full name: Alexandre António Antunes Barros

Signature: _____

"A smooth sea never made a skilled sailor"

English Proverb

To my Mom

ACKNOWLEDGMENTS

While it is my name that comes on the front cover of this thesis, the work here described would have never been possible if it wasn't for the support and understanding of my supervisors, my friends and my family. To all the people that somehow were involved in the construction of this thesis, I am deeply thankful. Although many names will be left unsaid, I need to emphasize some of the people that directly contributed to my happiness during this period of my life.

I would like to start by acknowledge my supervisors Dra. Ana Rita Duarte and Professor Estevão Lima who taught me so much along all these years. It is time to sincerely thank you for the patience, assistance, availability and encouragement. Thank you for giving me the freedom to pursue my ideas, helping me on becoming a more independent researcher. Most importantly, thank you for the friendship.

To Professor Rui L. Reis, the director of 3B's Research group, I express a special recognition for believing in me and for the possibility of developing my PhD thesis at the European Institute of Excellence for Tissue Engineering and Regenerative Medicine. Thank you for the opportunity to work with you along all these years and broaden my horizons, preparing me for the competitive scientific world.

I would also express my thankfulness to Professor Kevin Healy for accepting to receive me at his laboratory at University of Berkeley, California, during my international collaboration. I am thankful for an unforgettable experience to work in one of the most prestigious universities in the world and also to integrate his group.

I would also like to acknowledge the foundation for Science and Technology (FCT) for my personal doctoral grant (SFRH/BD/97203/2013).

Doctor Carlos Oliveira, who has not only been a co-author of the works described in the thesis, but also my friend, also deserves a special acknowledgment. The work, special *In vivo*, on this thesis would have never been possible if it wasn't for his disponibility and sacrifices. Thank you.

I also deeply acknowledge all the 3B's technicians and management team. Your work made mine easier and, most importantly, possible. To my other colleagues at 3B's, thank you for all the support and help.

Special thanks to Ivo, João, Dianinha, Clara, Lucília, Joaninha, Diana Pereira, Pedro Babo, Ana Gonçalves, Mariana and Cristiana thank you for the friendship during the past years and for all the good moments.

Finally, I would like to thank my dear friends Tiago, André and César, beloved Lau, my little Camila and my family. Lau, thank you for all your patience, for celebrating my achievements and for giving me strength in the hardest moments. I am profoundly grateful to my mother, Ana and Leandro. This thesis is dedicated to them. Thank you for your unconditional support and love. There are no words to describe the luck I have for having a family like you.



ABSTRACT

Ureteral stents are one of the most commonly used devices in urological practices. Ureteral stents are used for temporary or permanent relief of ureteral obstruction to maintain the flow of urine through the ureter after urological surgical procedures or in case of intrinsic or extrinsic obstruction. Nonetheless, they are related with common problems including encrustation, infection, pain and discomfort. As these problems restrict optimal stent function, including maintenance of suitable urine drainage and decrease of hydronephrosis, new ureteral stent biomaterials and designs are required. In last years, progress has been made in the development of biodegradable ureteral stents (BUS) and drug-eluting ureteral stents. These new technologies may provide ureteral stents with increased biocompatibility, decreased vulnerability to encrustation and improved drug-elution features. In the present thesis, it is proposed a BUS based on natural origin polymers (i.e., gelatin, alginate and gellan gum) produced after a combination of template gelation and critical point drying. The proposed biodegradable ureteral stent underwent an improvement in mechanical properties and indwelling time throughout the thesis, by testing different formulations and optimizing process parameters. The BUS developed was first successfully validated *in vitro* showing a degradation profile which occurs by surface erosion, without any fragmentation, in artificial urine solution. The performance of the BUS developed was also tested *in vivo*, in a porcine model, supporting the biocompatibility and the homogenous degradation observed *in vitro*. *In vivo* testing of the BUS compared with a commercial non-degradable ureteral stent has shown less hydronephrosis and capacity to provide a temporary urine drainage as good as the non-degradable commercial stents. In this thesis, the drug-eluting capacity of the developed BUS was also investigated. BUS was impregnated with anti-inflammatory (ketoprofen) and anti-cancer (paclitaxel, doxorubicin, epirubicin and gemcitabine) compounds by supercritical carbon dioxide impregnation. The ketoprofen-eluting biodegradable ureteral stents developed showed a very promising locally delivery of the active compounds within the 72h, which is the timeframe for the description of anti-inflammatory agents after the surgical procedure. In the case of drug-eluting BUS impregnated with anti-cancer drugs, cancer cells, when in contact with this stents, after 72h reduced their viability by 75%. Results further demonstrate minimal cytotoxic effect of the stents on non-cancer cells used as control. These novel biodegradable ureteral stents might overcome some of the common problems associated with ureteral stenting and avoid the second surgical procedure for stent removal.

RESUMO

Os cateteres ureterais são dos dispositivos mais comumente utilizados em Urologia. Estes dispositivos são utilizados para o alívio temporário ou permanente da obstrução ureteral no sentido de manter o fluxo de urina através do ureter dos rins para a bexiga, após procedimentos cirúrgicos urológicos ou em caso de obstrução intrínseca ou extrínseca. No entanto, estão relacionados com problemas comuns como incrustação, infecção, dor e desconforto. Estes limitam a função do cateter, nomeadamente a manutenção da drenagem urinária e a atenuação da hidronefrose, daí a necessidade de desenvolvimento de novos biomateriais e modelos de cateteres ureterais. Nos últimos anos, observaram-se progressos no âmbito do desenvolvimento de cateteres ureterais biodegradáveis (BUS) e de cateteres ureterais com libertação de fármacos. Estas novas tecnologias levam à produção de cateteres ureterais com uma melhor biocompatibilidade, menor vulnerabilidade à incrustação e possibilidade de libertação localizada de fármacos. Na presente tese, propõe-se um BUS baseado em polímeros de origem natural (i.e., gelatina, alginato e goma de gelano) produzidos por uma combinação de vários passos de processamento e secagem supercrítica. O cateter ureteral biodegradável proposto foi sendo melhorado no que diz respeito as propriedades mecânicas e ao tempo de permanência, testando-se diferentes formulações e otimizando-se diferentes parâmetros do processo. O BUS desenvolvido foi inicialmente validado com sucesso *In vitro*, mostrando numa solução artificial de urina um perfil de degradação que ocorre por erosão superficial, sem qualquer fragmentação. Posteriormente, o BUS foi testado *in vivo*, num modelo suíno, mantendo a biocompatibilidade e degradação homogénea observada *in vitro*. Na comparação *in vivo* do BUS desenvolvido com um cateter ureteral comercial não degradável, o primeiro mostrou menor hidronefrose e semelhante capacidade de drenagem urinária temporária. Neste trabalho foi também investigada a capacidade de libertação de fármacos. Os BUS foram impregnados com compostos anti-inflamatórios (cetoprofeno) e anticancerígenos (paclitaxel, doxorubicina, epirubicina e gencitabina) por impregnação com dióxido de carbono supercrítico. Os BUS com cetoprofeno revelaram uma libertação local muito promissora dos compostos ativos dentro das 72h, período de tempo para a prescrição de agentes anti-inflamatórios após cirurgia. No caso dos BUS impregnados com fármacos anticancerígenos, foi verificado que as células cancerígenas, quando em contacto com estes cateteres, reduziram a sua viabilidade em 75% após 72h. Os resultados demonstraram para além disso um efeito citotóxico mínimo dos cateteres impregnados sobre células não cancerígenas utilizadas como

controle. Os resultados obtidos no âmbito desta tese demonstram a possibilidade destes novos cateteres ureterais biodegradáveis desenvolvidos poderem superar muitos dos problemas comuns associados aos cateteres comerciais, evitando assim um segundo procedimento cirúrgico para remoção dos mesmos. para além disso foi ainda demonstrada a capacidade destes cateteres poderem vir a ser utilizados como agentes de libertação controlada.

TABLE OF CONTENTS

ACKNOWLEDGMENTS	IX
ABSTRACT	XI
RESUMO	XIII
TABLE OF CONTENTS	XV
LIST OF ABBREVIATIONS.....	XXIII
LIST OF EQUATIONS	XXXI
LIST OF FIGURES	XXXIII
LIST OF TABLES.....	XLI
SHORT CURRICULUM VITAE	XLIII
LIST OF PUBLICATIONS	XLV
INTRODUCTION TO THE THESIS FORMAT.....	XLIX
CHAPTER I	1
URETERAL STENTS TECHNOLOGY: BIODEGRADABLE AND DRUG-ELUTING PERSPECTIVE	1
ABSTRACT	3
<i>I-1. Introduction</i>	5
I-1.1. Medical Motivation for development of biodegradable ureteral stents	7
<i>I-2. Biomaterials in Ureteral stents</i>	8
I-2.1. Polymeric ureteral stents.....	8
I-2.2. Metal Ureteral Stents.....	9
<i>I-3. Ureteral Stents coatings</i>	10
I-3.1. Hydrophilic Coating.....	11
I-3.2. Glycosaminoglycan coatings	12
I-3.3. Biostable coatings	12
I-3.4. Biomimetic coatings.....	13
<i>I-4. biodegradable ureteral stents material</i>	15
I-4.1. Synthetic polymers	16
I-4.2. Natural origin polymers	18
I-4.3. Magnesium-based metal	19
<i>I-5. Drug-eluting ureteral stents</i>	21
I-5.1. Anti-bacterial eluting	21

I-5.2.	Anti-inflammatory eluting.....	22
I-5.3.	Biodegradable designs	23
I-6.	<i>Tissue-engineered stents</i>	27
I-7.	<i>Conclusions and future perspectives</i>	28
REFERENCES	28
CHAPTER II	35
MATERIALS AND METHODS	35
OVERVIEW	37
II-1.	<i>Materials</i>	39
II-1.1.	Biodegradable ureteral stents core material	39
II-1.1.1.	Gelatin	39
II-1.1.1.1	Genipin crosslinking gelatin	41
II-1.1.2.	Alginate	41
II-1.1.3.	Gellan Gum.....	43
II-1.1.4.	Bismuth (III) carbonate basic.....	44
II-1.2.	Biodegradable ureteral stents coating material	44
II-2.	<i>Production of Biodegradable ureteral stents</i>	45
II-2.1.1.	Supercritical carbon dioxide drying.....	47
II-2.1.2.	Supercritical fluid impregnation process.....	48
II-3.	<i>Methods</i>	50
II-3.1.	Physicochemical characterization of BUS developed	50
II-3.1.1.	Scanning Electron Microscopy	50
II-3.1.2.	Artificial Urine Uptake and swelling studies.....	51
II-3.2.	Study the biodegradation of the BUS developed in Artificial Urine Solution	51
II-3.2.1.	<i>In vitro</i> and <i>In vivo</i> degradation studies	51
II-3.2.2.	Tensile mechanical tests	52
II-3.2.3.	Gel permeation chromatography.....	53
II-3.2.4.	Ion coupled plasma	54
II-3.3.	Bacterial Adhesion Studies.....	54
II-3.4.	Drug-eluting BUS impregnation study	55
II-3.4.1.	Impregnation Yield	55
II-3.4.2.	<i>In vitro</i> release kinetics in AUS	55
II-3.4.3.	Scanning calorimetry analysis	56
II-3.4.4.	Fourier Transformed InfraRed spectroscopy	56
II-3.4.5.	Permeability studies.....	57
II-3.5.	<i>In vitro</i> biological evaluation of the developed BUS	59
II-3.5.1.	Cells Sources.....	59
II-3.5.1.1	Cell lines	59
II-3.5.1.2	Primary Cells	59

II-3.5.2.	Cytotoxicity assay	60
II-3.5.3.	Half maximal inhibitory concentration (IC ₅₀) determination.....	61
II-3.5.4.	<i>In vitro</i> anti-cancer effect of anti-cancer drug-eluting BUS.....	62
II-3.6.	<i>In vivo</i> studies of BUS development.....	63
II-3.6.1.	Surgical procedure validation.....	63
II-3.6.2.	Hydronephrosis level.....	64
II-3.6.3.	Histological procedures and stainings.....	64
II-3.6.3.1	Hematoxylin & eosin	65
II-3.6.3.2	Masson's trichrome	65
II-4.	<i>Statistical analysis</i>	65
REFERENCES	66
CHAPTER III	71
BIODEGRADABLE URETERAL STENTS FROM NATURAL ORIGIN POLYMERS	71
ABSTRACT	73
III-1.	<i>Introduction</i>	75
III-2.	<i>Materials and Methods</i>	77
III-2.1.	Materials	77
III-2.2.	Preparation of polymer solutions	77
III-2.3.	Sample drying	77
III-2.4.	Characterization.....	78
III-2.4.1.	Scanning electron microscopy (SEM)	78
III-2.4.2.	Artificial urine uptake.....	78
III-2.4.3.	Swelling	79
III-2.4.4.	Indwelling time.....	79
III-2.5.	Tensile mechanical analysis	79
III-2.6.	Encrustation development.....	80
III-2.7.	Bacterial adhesion studies	80
III-2.8.	Cytotoxicity and cell adhesion studies	81
III-2.8.1.	Cell culture	81
III-2.8.2.	Indirect cytotoxicity studies	81
III-2.8.3.	Direct contact studies	81
III-3.	<i>Statistical Analysis</i>	82
III-4.	<i>Results</i>	82
III-4.1.	Stents from natural origin polymers	82
III-4.1.1.	Scanning electron microscopy.....	83
III-4.2.	Characterization.....	83
III-4.2.1.	Artificial urine uptake and indwelling time	83
III-4.2.2.	Mechanical tests	85
III-4.2.3.	Encrustation development.....	85

III-4.2.4. Bacterial adhesion studies	86
III-4.2.5. Cytotoxicity and cell adhesion studies	87
III-5. Discussion.....	88
III-6. Conclusion	93
ACKNOWLEDGEMENTS.....	93
REFERENCES	94
CHAPTER IV	97
KETOPROFEN-ELUTING BIODEGRADABLE URETERAL STENTS BY CO₂ IMPREGNATION: <i>IN</i>	
VITRO STUDY.....	97
ABSTRACT	99
IV-1. Introduction	101
IV-2. Material and Methods	103
IV-2.1. Materials	103
IV-2.2. Preparation of biodegradable ureteral stents	103
IV-2.3. Supercritical CO ₂ impregnation of ketoprofen.....	104
IV-2.4. Characterization	104
IV-2.4.1. Surface Morphology.....	104
IV-2.4.2. Fourier transform infrared spectroscopy.....	104
IV-2.4.3. Scanning calorimetry analysis (DSC)	105
IV-2.4.4. In vitro release Kinetics in Artificial Urine Solution (AUS).....	105
IV-2.4.5. Diffusion coefficient calculation procedure	106
IV-2.4.6. The impregnation yield of ketoprofen-eluting biodegradable ureteral stents	106
IV-2.4.7. Indirect cytotoxicity studies	106
IV-3. Results and discussion.....	107
IV-3.1. Morphological analysis	107
IV-3.2. <i>In vitro</i> release kinetics in Artificial Urine Solution (AUS)	111
IV-3.3. Cytotoxicity studies.....	115
IV-4. Conclusion	116
ACKNOWLEDGEMENTS.....	117
REFERENCES	117
CHAPTER V	123
GELATIN-BASED BIODEGRADABLE URETERAL STENTS WITH ENHANCED MECHANICAL	
PROPERTIES	123
ABSTRACT	125
V-1. Introduction	127
V-2. Materials and Experimental.....	128

V-2.1.	Materials	128
V-2.2.	Preparation of second generation of biodegradable ureteral stents	129
V-2.3.	Scanning electron microscopy	130
V-2.4.	Postoperative X-ray.....	130
V-2.5.	Degradation Study	130
V-2.5.1.	Gel permeation chromatography (GPC)	131
V-2.5.2.	Inductive coupled plasma (ICP).....	132
V-2.5.3.	Cytotoxicity evaluation of the leachables	132
V-2.6.	Tensile mechanical analysis	132
V-2.7.	Surgical procedure and <i>In vivo</i> placement validation	133
V-2.8.	Statistical analysis	133
V-3.	<i>Results and discussion</i>	134
V-3.1.	Morphology	135
V-3.2.	X-Ray validation	135
V-3.3.	<i>In vitro</i> degradation study.....	136
V-3.4.	Gel permeation chromatography (GPC)	137
V-3.5.	Inductive Couple Plasma (ICP)	138
V-3.6.	Leachables cytotoxicity	139
V-3.7.	Tensile mechanical tests	140
V-3.8.	<i>In vivo</i> placement technique validation	143
V-4.	<i>Conclusions</i>	146
	ACKNOWLEDGEMENTS.....	146
	REFERENCES	147
	CHAPTER VI.....	151
	DRUG-ELUTING BIODEGRADABLE URETERAL STENT: NEW APPROACH FOR UROTHELIAL	
	TUMORS OF UPPER URINARY TRACT	151
	ABSTRACT	153
VI-1.	<i>Introduction</i>	155
VI-2.	<i>Material and Methods</i>	157
VI-2.1.	Materials	157
VI-2.2.	Preparation of biodegradable ureteral stents	157
VI-2.3.	Supercritical CO ₂ impregnation of anti-cancer drugs.....	157
VI-2.4.	Characterization.....	159
VI-2.4.1.	Impregnation yield.....	159
VI-2.4.2.	Determination of anti-cancer drugs release from biodegradable ureteral stents.....	159
VI-2.4.3.	Cell culture	159
VI-2.4.4.	In vitro efficacy of anti-cancer drugs against T24 cells and HUVECs - IC ₅₀ determination	

VI-2.4.5. In vitro anti-cancer effect of anti-cancer drug-eluting biodegradable ureteral stents by indirect and direct contact with T24 cells and HUVECs	161
VI-2.4.6. Light microscopy	161
VI-2.4.7. Statistical analysis	162
VI-3. Results and Discussion	162
VI-3.1. Preparation of biodegradable ureteral stents impregnated with anticancer drugs	162
VI-3.2. <i>In vitro</i> release kinetics in Artificial Urine Solution	164
VI-3.3. Determination of IC ₅₀ of anti-cancer drugs against T24 and HUVEC	165
VI-3.4. In vitro study of anti-tumoral effect of anti-cancer biodegradable ureteral stents.....	169
VI-4. Conclusion	173
ACKNOWLEDGEMENTS.....	173
REFERENCES	174
CHAPTER VII.....	177
IN VITRO AND EX-VIVO PERMEABILITY STUDIES OF PACLITAXEL AND DOXORUBICIN FROM DRUG-ELUTING BIODEGRADABLE URETERAL STENTS.....	177
ABSTRACT	179
<i>VII-1. Introduction</i>	<i>181</i>
<i>VII-2. Material and Methods</i>	<i>182</i>
VII-2.1. Materials	182
VII-2.2. Preparation of biodegradable ureteral stents	183
VII-2.3. Supercritical CO ₂ impregnation of Paclitaxel and Doxorubicin	183
VII-2.4. Franz-cell diffusion test.....	184
VII-2.4.1. Experimental permeability setups.	184
VII-2.4.2. Histology and morphology of the ureter tissue layer	185
VII-2.5. Transwell® diffusion test.....	186
VII-2.5.1. Cell culture	186
VII-2.5.2. Experimental setups	186
VII-2.5.3. Calculations and mathematical model.....	188
VII-2.5.4. Statistical analysis	189
<i>VII-3. Results and Discussion</i>	<i>189</i>
VII-3.1. Permeability study of paclitaxel and doxorubicin.....	190
VII-3.2. Permeability study of drugs delivery from biodegradable ureteral stent.....	192
<i>VII-4. Conclusion</i>	<i>196</i>
ACKNOWLEDGEMENTS.....	197
REFERENCES	198
CHAPTER VIII.....	201

NATURAL ORIGIN POLYMER-BASED BIODEGRADABLE URETERAL STENT: <i>IN VIVO</i>	
EVALUATION IN A PORCINE MODEL	201
ABSTRACT	203
<i>VIII-1. Introduction</i>	<i>205</i>
<i>VIII-2. Materials and Methods.....</i>	<i>206</i>
VIII-2.1. Materials	206
VIII-2.2. Preparation of biodegradable ureteral stents (BUS)	207
VIII-2.2.1. <i>In vitro</i> cytotoxicity	207
VIII-2.3. <i>In vivo</i> evaluation in a porcine model.....	208
VIII-2.3.1. Stent insertion technique	208
VIII-2.3.2. Excretory Urogram	208
VIII-2.3.3. <i>In vitro</i> and <i>In vivo</i> degradation study	209
VIII-2.3.4. Tensile mechanical analysis	209
VIII-2.3.5. Euthanasia and Necropsy.....	210
VIII-2.4. Statistical analysis.....	210
<i>VIII-3. Results and discussion.....</i>	<i>211</i>
VIII-3.1. <i>In vivo</i> evaluation in a porcine model	212
VIII-3.2. <i>In vitro</i> and <i>In vivo</i> stent degradation	214
VIII-3.3. Tensile mechanical tests	216
VIII-3.4. Hydronephrosis	217
VIII-3.5. Histopathological analysis	219
<i>VIII-4. Conclusions</i>	<i>224</i>
ACKNOWLEDGEMENTS.....	224
REFERENCES	225
CHAPTER IX.....	227
BUSINESS PLAN	227
<i>IX-1. Executive Summary.....</i>	<i>229</i>
IX-1.1. Elevator Pitch:	229
IX-1.2. Market Validation:	229
IX-1.3. Problem:.....	229
IX-1.4. Solution:.....	230
IX-1.5. Technology:.....	230
IX-1.6. Market Opportunity:.....	230
IX-1.7. Why Invest:	230
<i>IX-2. Business opportunity.....</i>	<i>231</i>
<i>IX-3. Background</i>	<i>236</i>
<i>IX-4. . Go to Market Strategy</i>	<i>240</i>
IX-4.1. Value Proposition.....	240

IX-4.2.	Industry Analysis/Competitive Environment	241
IX-4.3.	Pricing and Costing.....	245
<i>IX-5.</i>	<i>Milestones and Action Plan.....</i>	<i>246</i>
<i>IX-6.</i>	<i>Investment and key financial indicators.....</i>	<i>249</i>
<i>IX-7.</i>	<i>Major risks and mitigations strategies.....</i>	<i>251</i>
IX-7.1.	Mitigation strategy.....	252
CHAPTER X.....		253
GENERAL CONCLUSIONS, FINAL REMARKS AND FUTURE PERSPECTIVES		253
<i>X-1.</i>	<i>General conclusions and final remarks</i>	<i>255</i>
<i>X-2.</i>	<i>Future research directions.....</i>	<i>257</i>

LIST OF ABBREVIATIONS

A

Å	angstrom
<i>A</i>	Effective area
AA	Acetic acid
AC	Alternating current
AFM	Atomic force microscopy
ALB	Albumin
ALG	Alginate
ALP	Alkaline phosphatase
ANOVA	Analysis of variance
API	Active pharmaceutical compound
ARH	Adult rat hepatocytes
ASTM	American society for testing materials
ATDC 5	Murine chondrocyte cell line
ATR	Attenuated total reflection
Au	Gold
AUS	Artificial urine solution
ca.	Approximately
α	alpha

B

BMAP28	Cathelicidin
BALB/C3T3	Mouse embryo fibroblast
BMS	Bare metal stent

BPH	Benign prostatic hyperplasia
BMP	Bone morphogenetic protein
BMSCs	Bone marrow derived mesenchymal stromal cells
BSA	Bovine serum albumin
β	beta
β-TCP/HAP	β-Tricalciumphosphate hydroxyapatite

C

Ca ²⁺	Calcium ions
CaCl ₂	Calcium chloride
CaCO ₃	Calcium carbonate
CHX	Chlorhexidine
CARs	Carrageenans
CEL	Cellulose
<i>C_f</i>	Final concentration
CIP	Ciprofloxacin
CHI	Chitosan
<i>C₀</i> or <i>C_i</i>	Initial concentration
CIS	Carcinoma in situ
CLSM	Confocal laser scanning microscopy
cm	centimeter
CMC	Carboxymethyl cellulose

CMP	Carboxymethyl pullulan	DOPA	3,4-Dihydroxy-L-phenylalanine
CO ₂	carbon dioxide	DOX	Doxorubicin
COL	Collagen	DSC	Differential scanning calorimetry
C _p	heat capacity	dsDNA	Double-stranded DNA
CPD	Critical point dryer	°C	degree Celsius
CS	Chondroitin sulphate	S-S	Disulfide bonds
C _t	Receptor compartment concentration	δ	delta
χ ²	chi-square	ΔD	Variation of dissipation
D		E	
D	Diffusion coefficient	ε	epsilon
D ₂ O	Deuterated water	E	Young modulus
Da	Dalton	e.g.	'for example', form latin <i>exempli gratia</i>
DAPI	4',6-diamidino-2-phenylindole	E'	Elastic modulus
DCI	Deuterated hydrochloric acid	E''	Loss modulus
DCM	Dichloromethane	E _a	Apparent modulus
DD	Deacetylation degree	ECC	European collection of cell cultures
DES	Drug-eluting stent	ECGS	Endothelial cell growth supplement
DMA	Dynamic mechanical analysis	ECM	Extracellular matrix
DMEM	Dulbecco's modified Eagle's medium	ECs	Endothelial cells
DMF	Dimethylformamide	EDC	1-ethyl-3-(3-dimethylaminopropyl)
DMSO	Dimethylsulfoxide	EDS	Energy dispersive spectroscopy
DN	Dopamine analogue	EDTA	Ethylenediaminetetraacetic acid
DNA	Deoxyribonucleic acid	ELas	Elastins
DNS	Dinitrosalicylic acid		
DLC	Diamond-like coating		

ELRs	Elastin-like recombinamers	G	
ϵ_{\max}	Maximum extension	GAGs	Glycosaminoglycan's
EP	Epirubicin	GAL	Galactomannans
ePTFE	Expanded Polytetrafluorethylene	GEL	Gelatin
ESCs	Embryonic stem cells	GF(s)	Growth factor(s)
<i>et al.</i>	And others	GLU	Glucan
etc.	'and others', from the latin <i>et cetera</i>	GLYs	Glycan sulphate
η	eta	GRAS	Generally recognized as safe
F		GSH	Glutathione
F	Resonant frequencies	γ	gamma
FA	Folic acid	H	
FBS	Fetal bovine serum	$^1\text{H-NMR}$	Hydrogen-1 nuclear magnetic resonance
FCT	Foundation of Science and Technology	h	hours
FDA	Food and Drug Administration	<i>h</i>	Thickness
FGF	Fibroblast growth factor	H&E	Haematoxylin & eosin
FIBR	Fibrinogen	HA	Hyaluronic acid
FITC	Fluorescein isothiocyanate	HA-s	Sulphated hyaluronic acid
FLSPCs	Fetal Liver stem progenitor cells	hASCs	Human adipose stem cells
FN	Fibronectin	HA-SH	Hyaluronic acid modified with thiol groups
FTIR	Fourier transform infrared spectroscopy	H_{av}	Height average value
FUC	Fuicoidan	HBMSCs	Human bone marrow derived mesenchymal stromal cells
FURC	Furcelan	HCS-2/8	Human chondrosarcoma cells derived from a chondrocyte cell line
ΔF	Variation of frequency	HEP	Heparin

HepG2	Human hepatocellular carcinoma
HFCC	Human foreskin fibroblasts
HFHb	Human fetal hepatoblasts
hPDLCs	Human periodontal ligament
HpoB	Human primary osteoblasts
HSC	Hepatic stellate cell
HT-29	Human colon cancer cells
hTGSCs	Human tooth germ stem cells
HUVECs	Human umbilical vein endothelial cells
Hz	hertz

I

ι	iota
i.e.	'that is', from the latin <i>id est</i>
IL-6	Interleukin-6
IPM	Intercellular matrix
IPN	Interpenetrating polymer network
IgG	Immunoglobulin G

K

κ	kappa
KBr	Potassium bromide
K _d	Partition coefficient
kDa	kilodalton
Ke	Keratin

keV	kiloelectronvolt
Kg	kilogram
kHz	kilohertz
kN	kilonewton
kV	kilovolt

L

L	liter (unit)
L	Span
L929	Murine fibroblast cell line
LA	Laminin
LB	Langmuir-Blodgett
LbL	Layer-by-layer
Lec	Lectin
LEC	Lens epithelial cell line
LEV	Levan
L _{MW}	Low molecular weight
LPS	Lipopolysaccharide
LUM	Lumican
λ	lambda

M

μ	mu
μL	microliter
μm	micrometer
μmol	micromole
m	meter
M	molar
MAPs	Mussel adhesive proteins
mbar	millibar
MC3T3	Mouse pre-osteoblast cells
mg	milligram
MHz	megahertz

min	minute	NH ₃	Ammonia
mPEG-DOPA ₃	Methoxy polyethylene glycol-dihydroxyphenylalanine	NHDF	Normal human dermal fibroblasts
mL	milliliter	NIH/3T3	Mouse embryonic fibroblasts
mM	milimolar	NIR	Near-infrared
mm	millimeter	NiTi	Nitinol
M _{MW}	Medium molecular weight	nm	nanometer
MNPs	Magnetic nanoparticles	NMR	Nuclear magnetic resonance
mol	mole	NO	Nitric oxide
MPa	megapascal	Non X-linked	Non-cross-linked
MSCs	Mesenchymal derived stromal cells	NPs	Nanoparticles
MSNs	Silica nanoparticles	NSAID	Nonsteroidal anti-inflammatory drug
MTS	3-(4,5-dimethylthiazol-2-yl)-2,5-diphenyltetrazolium bromide	NSPCs	Neuronal stem progenitor cells
MUC	Mucin	s-NHS	N-hydroxysulfosuccinimide
MUO	Malignant ureteral obstruction	v	nu
mV	millivolt	O	
M _w	Molecular weight	ω	omega
Δm	Variation of adsorbed film mass	P	
N		% (v/v)	Percentage of volume/volume
N	newton	% (w/v)	Percentage of mass/volume
NAC	N-acetylcysteine	%	Percentage
NaCl	Sodium chloride	P	Permeability
NADH	Nicotinamide adenine	P	Statistical level of significance
NaOH	Sodium hydroxide		
NCL	Non-cross-linked		

Pa	Pascal	pK _a	Acidic constant
PAA	Poly (acrylic acid)	PL	Platelet lysate
PAH	Poly (allylamine)	PLGA	Poly (lactide-co-glycolide)
PAM	Polyacrylamide	PLL	Poly (L-lysine)
Parg	Poly-L-arginine	PLLA	Poly (L-lactic acid)
Pasp	Poly (aspartic acid)	PMA-MS	Poly (maleic acid-co- α -methylstyrene)
PBAE(s)	Poly β -amino ester(s)	PP	Polypropylene
PBS	Phosphate-buffered saline	PRP	Platelet-rich-plasma
PC	Phosphorylcholine	PRT	Plasma recalcification time
PCL/ β -TCP	Poly ϵ -caprolactone / β tricalcium phosphate	PSS	Poly (styrene sulfonate)
PDDA	Poly (diallyldimethylammonium chloride)	PU	Polyurethane
PDL	Poly (D-lysine)	PUL	Pullulan
PDMS	Poly (dimethylsiloxane)	PVA	Poly (vinyl alcohol)
PD-MSCs	Placenta derived mesenchymal stromal cells	PVC	Poly (vinyl chloride)
PEC	Pectin	PVS	Poly (vinyl sulphate)
PEG	Poly (ethylene glycol)	Q	
PEI	Polyethylenimine	QCM-D	Quartz crystal microbalance with dissipation monitoring
PEM(s)	Polyelectrolyte multilayer(s)	R	
PES	Polyethersulfone	RBMSCs	Rat bone marrow derived mesenchymal stromal cells
PET	Polyethyleneterephthalate	Rch	Rabbit chondrocytes
PGA	Poly (L-glutamic acid)	Ref.	Reference
Pgal	Poly galacturonic acid	RIP	RNAIII-inhibiting peptide
PGGA	Poly (γ -glutamic acid)	RGD	Arginine-glycine-aspartic acid (Arg-Gly-Asp)
PGs	Proteoglycans	RHC	Rat hepatic cells
pH	Potential hydrogenionic	Rhd	Rhodamine
PI	Propidium iodide		

RMS	Root-mean-square	T24	Human Urothelial cancer cells
rpm	Rotations per minute	TGF- β	Transform growth factor-beta
R_{RMS}	Root mean squared roughness	THP-1	Cell line human leukemic monocyte
RT	Room temperature	Th_w	Wet thickness
R_t	Thickness recovery ratio	Ti	Titanium
ρ	rho	TNF- α	Tumor necrosis factor alpha
S			
CEL-s	Sulphated cellulose	TOB	Tobramycin
s	seconds	TR	Texas red
SAMs	Self-assembled monolayers	Tris	2-Amino-2-hydroxymethyl-propane-1,3-diol
SaOs-2	Human primary osteosarcomas	T_t	Transition temperature
scCO ₂	Supercritical fluid carbon dioxide	TZP	Piperacillin-tazobactam
SD	Standard deviation	U	
SEM	Scanning electronic microscopy	UV	Ultraviolet
SMCs	Smooth muscle cells	σ_{max}	Ultimate strength
SMGS	Smooth muscle growth supplement	V	
SNase	Staphylococcal nuclease	V	Volume
T			
2D	Two-dimensional	Vb	Vinyl benzene
3D	Three-dimensional	VEGF	Vascular endothelial growth factor
t	Time	VERO-1	Monkey kidney cells
tan δ	Loss factor	VN	Vitronectin
TCPS	Tissue culture polystyrene	W	
TE	Tissue engineering	w/v	Weight/volume
		WCA	Water contact angle
		W_d	Dry weight

	WEHI 265.1	Skin fibroblast cell line (from mouse)	Z	
	W_w	Swollen weight	Z	Vertical direction
X			ζ	Zeta potential
	X-linked	Cross-linked	ZES	Zotarolimus-eluting stent

LIST OF EQUATIONS

Equation II-1 Determination of Artificial Urine Uptake	51
Equation II-2 Determination of wight loss.	52
Equation II-3 Determination of impregnation Yield.	55
Equation II-4 Determination of permeability.....	58
Equation II-5 Determination of the diffusion coefficient	59
Equation II-6 Determination of partition coefficient	59

LIST OF FIGURES

- Figure I-1 Mechanism of bacterial adhesion, after ureteral stent insertion, 1) urine components deposits on stent surface 2) allowing create an ions and minerals spots on surface 3) building of the urinary conditioning film 4) bacterial adhesion and consequently infection. 5) In addition the interaction of ions and minerals with biofilm components and bacterial induced crystallization and the encrustation occurs in the stent surface.6
- Figure I-2 Strategies to avoid the ureteral stent-associated problems, a) Hydrophilic coatings have a significant water content decrease the bacterial fixation b) Ureteral stents surface coated with antimicrobial peptides, not allowing the bacterial reach the stent surface and break up the bacterial membrane c) Drug-eluting technology, stent release specific drugs (antibiotics) in the ureter, allowing it to interact with the bacteria d) biodegradable ureteral stents, with dynamic surface due the constant degradation would provide non stable surface for bacteria to attach.....11
- Figure I-3 Biodegradable ureteral stents a) degradable braided thin-walled ureteral stent composed of multifilaments of PGA and PLGA (4) b) Uriprene™ (Poly-Med Inc, Greenville, SC) composed of L-lactide, glycolide, and copolyester components (5) c) Natural polymer based ureteral stents composed by fully hydrogel of gelatin and alginate (15).....16
- Figure II-1. Schematic overview of the materials studied, processing and characterization techniques. Essentially, five materials were used throughout the thesis for the formulation of the biodegradable ureteral stent (BUS): gelatin; alginate; gellan gum; bismuth and polycaprolactone (PCL). Two crosslinking agents were used: calcium chloride (CaCl₂) and genipin. Five active pharmaceuticals ingredients (APIs) were tested in the development of drug-eluting BUS: ketoprofen (Chapter IV), paclitaxel, doxorubicin, epirubicin and gemcitabine (chapter VI and VII). The techniques used to characterize the materials/ structures are here summarized. (SEM - Scanning electron microscopy; FTIR- Fourier transform infrared spectroscopy; DSC - Differential scanning calorimetry; GPC - Gel Permeation Chromatography; ICP – Ion coupled plasma; IC50 - half maximal inhibitory concentration; IVP – Intravenous pyelogram).....38

Figure II-2 Crosslinking reaction of gelatin by genipin with: a) first reaction through Michael addition to form stable intermediate; and b) second reaction with nucleophilic substitution of free lysine amine molecules into genipin activated ester. Adpated from Rose <i>et al.</i> (13)	41
Figure II-3 Chemical structure of Alginate (M: manuronic repeating unit; G: glucuronic repeating unit).	42
Figure II-4 Repeating units of chemical structure of a) native and b) deacetylated gellan gum.....	44
Figure II-5 Schematic representation of methodologies adopted to fabricate the biodegradable ureteral stents and their evolution.	45
Figure II-6 The Phase Diagram of Carbon Dioxide. Adapted from Silberberg et al(56)	48
Figure II-7 Schematic representation of the three phases of the impregnation process.	49
Figure II-8 A) Tensile test on BUS using a tensile universal machine and B) Typical stress-strain curve with the different regions depicted on the graph.	53
Figure II-9 Schematic representation of the a) Franz-cells and b) Transwell® diffusion test used in the permeability studies with drug-eluting BUS.	57
Figure II-10 Conventional method of determining IC50 using the dose-response curve.	62
Figure II-11 Schematic representation of the BUS placement at ICVS, University of Minho, Braga, Portugal and the materials used.	64
Figure III-1 Methodology used to generate the different stents.	83
Figure III-2 SEM micrographs of the gellan gum : gelatin stent (60:40% wt/wt)	83
Figure III-3 AUS uptake by the developed stents (A—alginate; AG—alginate:gelatine, GG—gellan gum; GGG—gellan gum:gelatine) during a timeframe of 60 days, and swelling images using a magnifying lens (2×), showing a change in the internal diameter from 1.0 mm to 1.8 mm. Biosoft® duo, Porges Stent was used as a control.....	84
Figure III-4 Weight loss of the developed stents (A—alginate; AG—alginate:gelatine, GG—gellan gum; GGG—gellan gum:gelatine) during a time frame of 60 days (indwelling time). Biosoft® duo, Porges Stent was used as a control.	85
Figure III-5 SEM micrographs and EDS spectra of the surface of the stents prepared with the different polymers before and after immersion in AUS—last time point corresponds to 14 days	

for alginate-based stents and 60 days for gellan gum-based ones. Biosoft® duo, Porges Stent was used as a control.	86
Figure III-6 Bacterial adhesion on the stents incubated with approximately 1×10^8 (a) <i>S. aureus</i> bacterias (Gram+), (b) <i>E. coli</i> DH5 alpha (Gram–), and (c) <i>K. oxytoca</i> (Gram–) for 4 h. Values indicate mean \pm standard deviation from a single experiment performed in triplicate, which was representative of three independent experiments. Fold adhesion reduction between each tested stents and the commercial stent is indicated on top of each bar. Significance of the values between each tested stents and the commercial stent was determined by the t-student test (** $p < 0.001$). A–alginate; AG–alginate:gelatine, GG–gellan gum; GGG–gellan gum:gelatine.....	87
Figure III-7 Cytotoxicity and cell adhesion studies: (a) cell viability measured after 72 h and (b) cell adhesion on the surface of the different stents. Biosoft® duo, Porges Stent was used as a control. Statistical significant differences were considered as *** $p < 0.001$; ** $p < 0.01$; * $p < 0.05$	88
Figure IV-1 Supercritical fluid process impregnation and apparatus. TIC–temperature controller, P–pressure transducer, FM–flow meter.....	104
Figure IV-2 Biodegradable ureteral stent with the formulation AG (diameter 6 Fr).	108
Figure IV-3 Scanning electron microscopy image of the biodegradable stents before (AG–alginate-based; GG–gellan gum-based) and after ketoprofen CO ₂ impregnation (AG50, GG50–50 °C at 100 bar).	109
Figure IV-4 Fourier Transform Infrared Spectroscopy spectra of raw material alginate (AG), gellan gum (GG), gelatin (GLT), ketoprofen (KET) and after the ketoprofen impregnation by CO ₂ (AG35, GG35–35 °C at 100 bar).	110
Figure IV-5 Differential scanning calorimetry spectra of ketoprofen (a) and biodegradable stents before and after the ketoprofen impregnation (b).	111
Figure IV-6 Accumulative mass of ketoprofen released of (a) alginate-based stent (b) gellan gum-based stent, impregnated at 35 °C, 40 °C, 50 °C and 100 bar during 2 h for the release period of 72 h.....	112

Figure IV-7 Percentage of ketoprofen released from alginate and gellan gum-based impregnated at 40 °C and 100 bar during 2 h for the release period of 72 h.....	112
Figure IV-8 Cell viability measured after 72 h of ketoprofen-eluting biodegradable stents.	116
Figure V-1 SEM micrographs of the biodegradable ureteral stent (6 Fr, formulation 2, 0.48M) a) before coating, b) after coating, c) higher magnificence of one-layer hydrogel d) higher magnificence of two layers coating and hydrogel.....	135
Figure V-2 Radiograph in abdomen mode of a) commercial ureteral stent (Biosoft® duo, Porges, Coloplast) and b) biodegradable ureteral stent developed (formulation 2, 0.48M).....	136
Figure V-3 Weight loss of developed biodegradable ureteral stents a) Different formulations tests and b) Formulation 2 with different crosslinking concentration.	137
Figure V-4 GPC chromatograms of stent raw materials (alginate and gelatin) and the leachables at 1, 3, 6 and 9 days' time points.	138
Figure V-5 Cytotoxicity study by cell viability measured after 72 h.	140
Figure V-6 Mechanical properties of the biodegradable stents (0.48M crosslinking concentration) before and after PCL coating in terms of a) maximum load (N) b) maximum tensile strain (%) and c) young modulus (MPa). d) Images of biodegradable stents before and after coating in dry state and in wet state immersion in AUS (scale bar 2mm). Ctr - (Biosoft® duo, Porges, Coloplast). Values are represented as average ± SD, n = 3. Statistical differences (*p < 0.05, **p < 0.01) using one way-ANOVA followed by a Tukey post-test.	142
Figure V-7 Mechanical properties of the biodegradable stents prepared with the formulation 2 with different concentrations of crosslinking agent before and after PCL coating in terms of a) maximum load (N), b) maximum tensile strain (%), c) young modulus (MPa) and d) maximum tensile strain (%) of ureteral stent formulation 2 during the degradation time. Values are represented as average ± SD, n = 3. Statistical differences (*p < 0.05, **p < 0.01) using one way-ANOVA followed by a Tukey post-test.	143
Figure V-8 Conventional ureteroscopy of the stented ureter <i>In vivo</i> in a pig model: a) biodegradable ureteral stent placement b) biodegradable ureteral stent inside the right ostium pig ureter at placement time c) biodegradable ureteral stent after 3 days at the entrance of the right ostium pig ureter d) after 3 days with the biodegradable ureteral stent (image taken in the	

middle of the stent) e) after 10 days of the biodegradable ureteral stent f) right ostium pig ureter after the degradation at day 10.	145
Figure VI-1 Illustration of the concept of anti-cancer drug eluting biodegradable ureteral stent as a potential drug delivery system for UTUC therapy.....	156
Figure VI-2 Supercritical fluid process impregnation and apparatus of the anticancer drugs used in biodegradable ureteral stent.....	158
Figure VI-3 Section of commercial non-degradable ureteral stent (Biosoft® duo, Porges, Coloplast) BUS coated with PCL resin and BUS stents prepared after impregnation.....	163
Figure VI-4 Cumulative anti-cancer drugs release from biodegradable and non-biodegradable ureteral stents in Artificial Urine Solution AUS (pH 5.5) at 37°C, for different conditions tested. The stent degraded after 9 days.....	165
Figure VI-5 In vitro viability of T24 cells and HUVEC cells after exposure to the anti-cancer drugs at different concentrations for 4 h or 72 h. Cell viability is expressed as % of control. Vertical line represents the amount of drug impregnated by scCO ₂ in BUS. Data shown is the average of at least 3 independent experiments.	167
Figure VI-6 Cell viability of T24 cancer cell line after 72 h exposure by indirect contact. Statistical significant differences were considered as *p < 0.05, **p < 0.01 and ***p < 0.001.	169
Figure VI-7 Cell viability of T24 cancer cell line and HUVEC cells after 72 h exposure by direct contact. BUScoat is the BUS with the PCL coating without anti-cancer drugs impregnated. Statistical significant differences were considered as *p < 0.05, **p < 0.01 and ***p < 0.001.....	171
Figure VI-8 Light microscopy images (10x) of T24 cells morphology after 4 h and 72 h of exposure by direct contact to biodegradable ureteral stents impregnated with the anti-cancer drugs. Control experiments were carried out in T24 cells and drug-free stents for 72 h.	172
Figure VII-1 Paclitaxel and doxorubicin impregnation apparatus by supercritical fluid process in biodegradable ureteral stent, 100 bar, 90 min at 40°C.	183
Figure VII-2 Representative Representative photomicrographs show ureter sections from single <i>ex vivo</i> porcine urinary tract obtained by stereo microscope (A and B). Masson trichrome	

staining (C) of ureter section with measures and Hematoxylin and Eosin (H&E) staining (D)of ureter section. Scale bar indicates 200 μm (A, C and D) and 100 μm (B).	185
Figure VII-3 Schematic of A) Franz-type diffusion cell load with PES, B) Transwell® diffusion test with a HUVEC cells monolayer C) Franz-type diffusion cell load with porcine ureter tissue.	187
Figure VII-4 Inverted microscope images of confluent monolayer HUVEC cells on Transwell® before (A, B) and after diffusion test with paclitaxel (C) and doxorubicin (D). E) donor compartment of Franz-cell setup with the delivery of paclitaxel from BUS and permeation through the ureter tissue after 5 min, 30 min and 60 min.	187
Figure VII-5 Permeation of paclitaxel and doxorubicin through PES and ex vivo porcine ureter using a Franz-cell setup and through a confluent monolayer HUVEC cells on Transwell®.	191
Figure VII-6 Permeability profile of Paclitaxel (PA) and Doxorubicin (DOX), and Stent impregnated with paclitaxel (PAStent) and doxorubicin (DOXStent) through PES, HUVEC cell layer and porcine ureter (<i>ex-vivo</i>).	193
Figure VII-7 Release profile in the donor compartment and permeability profile obtained with the A) paclitaxel and B) doxorubicin delivered from BUS.	194
Figure VII-8 Percentage of Paclitaxel (PA) and Doxorubicin (DOX), and Stent impregnated with paclitaxel (PAStent) and doxorubicin (DOXStent) recovered after 8 h of permeability test in donor and receptor compartment, in BUS and in <i>ex vivo</i> porcine ureter.....	196
Figure VIII-1 a) Schematic illustration of the BUS cross-linking. b) 6-Fr Biodegradable ureteral stent – BUS (left) and 6-Fr Biosoft® duo, Porges, Coloplast - commercial (right). c) Cytotoxicity study by cell viability measured after 72h.	212
Figure VIII-2 X-ray image of biodegradable ureteral stent at a) day 0 and b) day 1. c) Commercial ureteral stent at day 1.....	213
Figure VIII-3 a) In vitro BUS degradation in AUS and b) <i>in vivo</i> degradation in a porcine model. BUS intact recovered after d) 5 days and e) 7 days in a porcine model.	215
Figure VIII-4 In vitro and <i>in vivo</i> values of maximum tensile strain (%), young modulus (MPa) and Mass loss (%) of BUS and commercial ureteral stents. Aterisks mark – data from in vitro results.	217

Figure VIII-5 a) A 10-min pyelogram at day 10 after BUS degradation. b) Hydronephrosis score measured by mean of IVP of all animals at day 0,1, 5 and 10 days of BUS and commercial ureteral stent, based on time until contrast (Omnipaque™ 1200mg/Kg) was seen in kidneys and ureters. 0.0, less than 3 minutes. 1.0, 3 to 10 minutes. 2.0, 10 to 20 minutes. 3.0, greater than 20 minutes. Values are represented as average. Statistical differences (*p≤0.05, **p≤0.01, ***p≤0.001)..... 218

Figure VIII-6 Macroscopic images representative of urinary tract after a) 5 days, b) 7 days and c) 10 days with BUS. d) Representative image of urinary tract after stented with commercial stent. e) Hydronephrosis case verified after stented with commercial stent. Asterisks mark the ureters that were stented. Arrow points the BUS stent after 7 days indweeling..... 219

Figure VIII-7 Width of BUS and commercial stented kidneys and ureters vs respective non-stented controls, including upper, mid and distal ureter. Values are represented as average. Statistical differences (*p≤0.05, **p≤0.01, ***p≤0.001). 221

Figure VIII-8 Representative Hematoxylin and Eosin (H.E) and Masson’s Trichrome (M.T.) images of ureters stented with biodegradable ureteral stent (BUS), Commercial stent (commercial) and non-stented ureters (control), on day 10. Examples of: mcv - mucinous cytoplasmic vacuolation, i – infiltrated, m – muscle, ep- epithelium, l- lumen ureter, e – edema, a – adipose tissue, arrow - epithelium destruction; arrow dashed- blood vessels, and arrow head – erythrocytes; All images were taken with a 4x, 10x and 40x magnification microscope objectives. 223

Figure IX-1 Incidence of ureteral stents in urological disorders..... 231

Figure IX-2 Uniqueness of HydrUStent in comparison with commercially available stents 234

Figure IX-3 HydrUStent stage of development and next steps. 238

Figure IX-4 Desired features of ureteral stents as referred in the survey 239

Figure IX-5 HydrUStent Porter ´ s five force analysis 242

Figure IX-6 HydrUStent business model canvas..... 243

Figure IX-7 Eight years’ financial projections for HydrUStent..... 250

LIST OF TABLES

Table I-1 Ureteral stents coatings.....	14
Table I-2 Biodegradable Ureteral Stents	20
Table I-3 Drug-eluting Technologies	24
Table II-1 Polymer, cross-linking agent concentrations and active pharmaceutical compounds (APIs) used along the thesis.	47
Table III-1 Polymer and cross-linking agent concentrations used to prepare the stents	77
Table III-2 Composition of the artificial urine solution (AUS).....	78
Table III-3 Mechanical properties of the stents prepared.....	85
Table IV-1 Polymer and cross-linking agent concentrations used to prepare the biodegradable stents	103
Table IV-2 Composition of the artificial urine solution (AUS).....	105
Table IV-3 Correlated parameters of the ketoprofen released kinetics.....	113
Table IV-4 Impregnation yield of the experiments carried out during 2 h at 100 bar.	114
Table V-1 Summary of the formulations tested to prepare the different biodegradable ureteral stents.	129
Table V-2 Crosslinking agent concentrations used to prepare the different biodegradable ureteral stents.	130
Table V-3 Composition of the artificial urine solution (AUS).....	131
Table V-4 Concentration of bismuth obtained by ICP, in immersion solution (AUS) during the degradation.	139
Table VI-1 Nomenclature of each condition study of anti-cancer drugs impregnated by supercritical fluid process.....	158
Table VI-2 Quantity of drug impregnated by scCO ₂ (operating conditions 90 min, 100 bar and 40 °C) (µg drug /mg polymer).....	164

Table VI-3 IC50 of the anti-cancer drugs at 4 h and 74 h for the T24 and HUVEC cells (\pm STD).	168
Table VII-1 Tissue layer measurements of ex vivo porcine ureter.....	186
Table VII-2 Characteristics of experimental setups used in the present study to assess the permeability of paclitaxel through the PES, HUVEC cell layer and porcine ureter (ex-vivo)..	189
Table VII-3 Permeability (P), Diffusion (D) and Partition (Kd) coefficients of paclitaxel and doxorubicin on PES, HUVEC cell layer and porcine ureter (ex vivo).	192
Table VII-4 Drug permeated and Cumulative paclitaxel and doxorubicin mass after 8h permeation test in the receptor compartment through different membranes studied for drug alone (PA and DOX) and paclitaxel or doxorubicin release from the BUS (PAStent and DOXStent).....	194
Table VIII-1 Preoperative (day 0) and postoperatively (day 10) follow-up serum and urine parameters of commercial and BUS ureteral stent.....	213
Table VIII-2 Biocompatibility parameters of BUS and commercial stents group in the kidney and the ureters.....	220
Table IX-1 Feature-Advantage-Benefit (FAB) model of HydrUStent	235
Table IX-2 Results obtained from the doctors survey about the problems associated with the current solutions for ureteral stents.	238
Table IX-3 HydrUStent project roadmap (Months after Investment)	239
Table IX-4 Competitive landscape of urological device market.....	241
Table IX-5 Unit Cost breakdown for HydrUStent production	245
Table IX-6 Milestone Actions and deadline set for HydrUStent development.	248
Table IX-7 Forecasted P&L statement (all figures in '000 EUR)	249
Table IX-8 Forecasted Cash Flow statement (all figures in '000 EUR).....	250
Table IX-9 Risk assessment of HydrUStent.....	251

SHORT CURRICULUM VITAE

Alexandre António Antunes Barros was born on the 27th of October 1988, in Braga, Portugal. He is currently a PhD student at 3B's Research Group (Biomaterials, Biodegradables and Biomimetics), at University of Minho, Headquarters of the European Institute of Excellence on Tissue Engineering and Regenerative Medicine at Avepark, Caldas das Taipas, Guimarães, Portugal. This is a research unit that has been classified by the Foundation of Science and Technology (FCT) as excellent and is part of the Portuguese Associate Laboratory ICVs/3B's. He received his BSc degree in 2010 in Biotechnology, at Polytechnic institute of Viana do Castelo, Portugal with a final grade of 15 (0-20). In his thesis, he spends a year at CeNTI- Centre of Nanotechnology and Smart Materials, Vila Nova de Famalicão, working under the supervision of Doctor Carla Joana Silva, where developed an alternative environmentally friendly process for colouring natural and synthetic fibres for his BSc thesis obtaining a score in thesis of 20/20 and an international patent that has been explored in the industry. MSc degree in 2012 in Properties and technology of polymers, at University of Minho, Braga, Portugal with a final grade of 17 (0-20). In his master thesis at the 3B's Research Group working under the supervision of Professor Rui L. Reis and Dr Ricardo Pires. The work was performed in his master thesis entitled "Aluminium-free and polysaccharide-based glass ionomer bone cements", obtaining a final classification of 16/20 (0-20 scale). In May 2014, he started pursuing his PhD at 3B's Research Group, at University of Minho, Portugal, under the supervision of Dra Ana Rita C. Duarte and Professor Estevão Lima. During four months, he was a visiting student at Healy Laboratory, at University of Berkeley, California, USA, supported by Luso-American Foundation, studying and developing anti-cancer drug-eluting biodegradable ureteral stent. Scientifically, Alexandre has contributed to the field of biomaterials so far with 12 peer-reviewed papers in international journals, 22 oral communications, 16 poster communications 7 patents and 1 book chapter. In 2014 he was a finalist of Building Global Innovators-MIT initiative with his PhD work, and he has participated in 2015 on the Boston Global Immersion program promoted by Building Global Innovators, IUL MIT-Portugal Accelerator and which was held in Boston, USA. In 2015, Alexandre has been awarded several prizes, the grand prize of Novo Banco Innovation Award, APU- Jaba Recordati Award granted by National Urology association.

LIST OF PUBLICATIONS

The work performed under the scope of this PhD thesis resulted in the publications listed below.

Papers in international scientific journals with referees

1. **Barros AA**, Oliveira C, Reis RL, Lima E, Duarte ARC, “Natural origin polymers-based biodegradable ureteral stent: In vivo evaluation in a porcine model”, Submitted, 2017.
2. **Barros AA**, Silva J, Craveiro R, Paiva A, Reis RL, Duarte ARC, “Green solvents for enhanced impregnation processes in biomedicine”, Accepted in Current opinion in green and sustainable chemistry, 2017.
3. **Barros AA**, Oliveira C, Reis RL, Lima E, Duarte ARC, “*In vitro* and *ex-vivo* permeability studies of paclitaxel and doxorubicin drug-eluting biodegradable ureteral stents”, Accepted in Journal of Pharmaceutical Sciences, 2017.
4. **Barros AA**, Browne S, Oliveira C, Lima E, Duarte ARC, Healy KE, Reis RL” Drug-eluting biodegradable ureteral stent: New approach for urothelial tumors of upper urinary tract cancer”, International Journal of Pharmaceutics, 2016, 513(1-2):227-237.
5. **Barros AA**, Oliveira C, Lima E, Duarte ARC, Reis RL, “Gelatin-based biodegradable ureteral stents with enhanced mechanical properties”, Applied Materials Today, 2016, (5):9-18.
6. **Barros AA**, Oliveira C, Reis RL, Lima E, Duarte ARC, “Ketoprofen-eluting biodegradable ureteral stents by CO₂ impregnation: *In vitro* study”, International Journal of Pharmaceutics, 2015, 495(2):651–659.
7. **Barros AA**, Duarte ARC, Pires RA, Marques B, Ludovico P, Lima E, Mano JF, Reis RL, “Bioresorbable ureteral stents from natural origin polysaccharides”, Journal of Biomedical Materials Research: Part B - Applied Biomaterials, 2015, 103(3):608-17.

Conference abstracts published in international scientific journals

1. **Barros AA**, Duarte ARC, Pires RA, Mano JF, Lima E, Reis RL, “Tailor made degradable ureteral stents from natural origin polysaccharides”, Proc. of the 10th Conference on Supercritical Fluids and their Applications, Italy, 2013

Book Chapter

1. **Barros AA**, Oliveira C, Lima E, Duarte ARC, Healy K, Reis RL. Ureteral stents technology: biodegradable and drug-eluting perspective, Reference Module in Materials Science and Materials Engineering, DOI: 10.1016/B978-0-12-803581-8.10189-4, 12 January 2017 (Online).

Conference oral presentations

1. **Barros AA**, Browne S, Oliveira C, Lima E, Duarte ARC, Healy KE, Reis RL, "Anti-cancer drug-eluting biodegradable stent - Aerogel approach toward the preparation of new therapies for urothelial cancer", 3rd International Seminar on Aerogels, Sophia Antipolis, France, 2016.
2. **Barros AA**, Browne S, Oliveira C, Lima E, Duarte ARC, Healy KE, Reis RL " Upper urinary tract urothelial tumors targeted with biodegradable drug-eluting stents", ESUT16 - Athens, Greece, 2016.
3. **Barros AA**, "HydrUStent – Biodegradable ureteral stent", TERMIS-EU, Business Plan competition, Uppsala, Sweden, 2016.
4. **Barros AA**, Browne S, Oliveira C, Lima E, Duarte ARC, Healy KE, Reis RL "Targeting urothelial tumors of upper urinary tract with drug-eluting stents impregnated by supercritical fluids", WBC2016 - World Biomaterials Congress, Montreal, Canada, 2016.
5. **Barros AA**, Browne S, Oliveira C, Lima E, Duarte ARC, Healy KE, Reis RL, "Anti-cancer Drugs Impregnated by CO₂ Supercritical Fluid Technology in Biodegradable Ureteral Stents", EMSF 2016 – 15th European Meeting on Supercritical Fluids, May 8-11, Essen, Germany, 2016.
6. **Barros AA**, Browne S, Oliveira C, Lima E, Duarte ARC, Healy KE, Reis RL "Biodegradable drug-eluting stents: targeting urothelial tumors of upper urinary tract", American Urology Association Meeting 2016 (AUA), May 6-10, San Diego, USA, 2016.
7. **Barros AA**, Browne S, Oliveira C, Lima E, Duarte ARC, Healy KE, Reis RL, "Masterclass in Minimally invasive surgeries", ICVS, 15 April 2016, Braga, Portugal, 2016.
8. **Barros AA**, Browne S, Oliveira C, Lima E, Duarte ARC, Healy KE, Reis RL, "Biodegradable drug-eluting stents: Targeting urothelial tumors of upper urinary tract", 31th Annual Congress of the European Association of Urology - EAU16, Munich, 2016.

9. **Barros AA**, Oliveira C, Reis RL, Lima E, Duarte ARC, "Ketoprofen-eluting biodegradable ureteral stent by carbon dioxide impregnation," ISSF15- 11th International Symposium on Supercritical Fluids – World Congress, Seoul, South Korea, 2015.
10. **Barros AA**, Oliveira C, Reis RL, Lima E, Duarte ARC, "Biodegradable ureteral stents: influence of critical point carbon dioxide drying for success in surgical procedure" ISSF15- 11th International Symposium on Supercritical Fluids – World Congress, Seoul, South Korea, 2015.
11. **Barros AA**, "Biomaterials in Urology", APU15 – National Congresso f Urology, Braga, 2015.
12. **Barros AA**, Oliveira C, Reis RL, Lima E, Duarte ARC, "Bioresorbable urological stent systems based on natural polymers: update", 5th Meeting ICVS/3B's, Braga, Portugal, 2015.
13. **Barros AA**, Mano JF, Reis RL, Lima E, Duarte ARC, "Bioresorbable urological stent systems based on natural polymers", 4th Meeting ICVS/3B's, Braga, Portugal, 2014.
14. **Barros AA**, Duarte ARC, Pires RA, Mano JF, Reis RL, Lima E, "Tailor made degradable ureteral stents from natural origin polymers", 3rd Meeting ICVS/3B's, Braga, Portugal, 2013.
15. **Barros AA**, Duarte ARC, Pires RA, Mano JF, Lima E, Reis RL, "Patient Compliant Biodegradable Urinary Stents", Termis-EU Meeting Istanbul, Turkey 2013.
16. **Barros AA**, Duarte ARC, Pires RA, Mano JF, Lima E, Reis RL, "Aerogel hollow tubes from natural-origin polysaccharides as tailor-made urinary stents", Seminar on Aerogels properties, manufacture and applications, Nancy, France 2012.
17. **Barros AA**, Duarte ARC, Pires RA, Mano JF, Lima E, Reis RL, "Tailor-made biodegradable urological stents", IMED conference, Lisboa, Portugal 2012.

Conference posters

1. **Barros AA**, Browne S, Oliveira C, Lima E, Duarte ARC, Healy KE, Reis RL, "Gelatin-based Biodegradable Ureteral Stents for the treatment of Urothelial Tumors of the Upper Urinary Tract Cancer", TERMIS-AM, San Diego, USA, 2016.
2. **Barros AA**, Oliveira C, Reis RL, Lima E, Duarte ARC, "Drug-eluting biodegradable ureteral stents: as a new approach for urothelial tumors of upper urinary tract cancer", TERMStem, Guimarães, Portugal, 2016.

3. **Barros AA**, Browne S, Oliveira C, Lima E, Duarte ARC, Healy KE, Reis RL, Biodegradable ureteral stents for the treatment of urothelial tumors of the upper urinary tract cancer, TERMIS-EU, Uppsala, Sweden, 2016.
4. **Barros AA**, Browne S, Oliveira C, Lima E, Duarte ARC, Healy KE, Reis RL, "Anti-cancer drug eluting stents prepared by supercritical fluid technology targeting urothelial tumors of upper urinary tract.", Prosciba2016 – IV Iberoamerican conference on supercritical fluids, Vinã del Mar, Chile, 2016.
5. **Barros AA**, Oliveira C, Reis RL, Lima E, Duarte ARC, Biodegradable Ureteral Stent, Business Plan Competition, TERMIS-WC, BOSTON, MA, USA, 08-11 September 2015.
6. **Barros AA**, Oliveira C, Reis RL, Lima E, Duarte ARC, Drug-eluting Bioresorbable Ureteral Stent by CO₂ Impregnation, TERMIS-WC, BOSTON, MA, USA, 08-11 September 2015.
7. **Barros AA**, Oliveira C, Reis RL, Lima E, Duarte ARC, "Drug-eluting degradable ureteral stents by supercritical fluid impregnation", TermStem, Guimarães, Portugal, 2015.
8. **Barros AA**, Oliveira C, Reis RL, Lima E, Duarte ARC, "Bioresorbable ureteral stent translation for *in vivo* model", Society for Biomaterials – Annual Meeting & Exposition, Charlotte, NC, USA, April 15-18, 2015.
9. **Barros AA**, Oliveira C, Reis RL, Lima E, Duarte ARC, "Tailor made degradable ureteral stents from natural origin polysaccharides", Proc. of the 10th Conference on Supercritical Fluids and their Applications, Italy, 2013.

Patents

1. PT Patent application, **Barros AA**, Oliveira C, Reis RL, Lima E, Duarte ARC "Biodegradable ureteral stents: new approach for urothelial tumors of upper urinary tract cancer", application 109229, registered on 11/03/2016.
2. PCT Patent application, **Barros AA**, Oliveira C, Correia-Pinto J, Reis RL, Lima E, Duarte ARC, "An ureteral stent, method and uses thereof", application WO2016181371A1, Priority date 2015-05-14, Filing date 2016-05-17
3. PT Patent PI106593, "Cateteres à base de polímeros de origem natural produzidos utilizando tecnologias limpas", **Barros AA**, Duarte ARC, Pires RA, Mano JF, Lima E, Reis RL, application 20121000079210 registered on 19/10/2013, publication at Revista de Propriedade Industrial, 77/2014, on March 21, 2014

INTRODUCTION TO THE THESIS FORMAT

The present thesis is divided into five main sections containing ten chapters. This structure was adopted to allow a proper organization of the data presented in the various chapters, preceded by a general introduction (first section), as well as an overall materials and methods section (second section). The third section shows the experimental results obtained in the context of this thesis and their discussion, focusing on biodegradable and drug-eluting ureteral stent based on natural origin polymer-based. The fourth section shows a business plan approached to translate into the urologic market the patented biodegradable ureteral stent. And the fifth section finalizes this thesis with concluding remarks.

The main body of the thesis is based on a series of publications published in international journals or submitted for publication. Each chapter is presented in a manuscript form, i.e., abstract, introduction, experimental section, results and discussion (or in two separate sections, i.e., results plus discussion), conclusion, and acknowledgements. A list of relevant references is also provided as a subsection within each chapter. The contents of each part and chapter are described below in more detail.

Section I – General introduction - Background

Chapter I – Ureteral Stents Technology: Biodegradable and Drug-eluting Perspective: This chapter provides a general introduction to the ureteral stent technologies focus on last advances regarding biodegradable ureteral stents as drug-eluting ureteral stents.

Section II – Detailed description of experimental materials and methodologies

Chapter II – Materials and Methods: A list of the materials used and methods applied to obtain the results described further on is provided, being the basis to the whole work described in this thesis.

Section III – Development of biodegradable ureteral stents

Chapter III – Biodegradable ureteral stents from natural origin polymers: This chapter describes the production of biodegradable ureteral stent from natural origin polysaccharides, following a combination of templated gelation and critical point carbon dioxide drying.

Chapter IV – Ketoprofen-eluting biodegradable ureteral stents by CO₂ impregnation: *In vitro* study: This chapter describes the production of biodegradable ureteral stents impregnated with ketoprofen by CO₂ impregnation. The ketoprofen release was evaluated in artificial urine solution while stent degraded.

Chapter V – Gelatin-based biodegradable ureteral stents with enhanced mechanical properties: Similarly, to chapter I, biodegradable ureteral stents were developed using the process previous optimized and different stent formulation was studied. In this case, besides the mechanical properties, the degradation study and cytotoxicity of the leachables were also evaluated. Conventional surgical procedure in *In vivo* model was performed.

Chapter VI – Drug-eluting biodegradable ureteral stent: New approach for urothelial tumors of upper urinary tract cancer: In this chapter, the impregnation of anticancer drugs by CO₂ impregnation process in biodegradable ureteral stent was studied. Non-degradable conventional ureteral stent was also impregnated using the same process and compared with biodegradable stent. The killing effect was evaluated using a urothelial cancer cell line.

Chapter VII – *In vitro* and *ex-vivo* permeability studies of paclitaxel and doxorubicin drug-eluting biodegradable ureteral stents: This chapter aims to understand the permeability profile of the anti-cancer drugs released from the anti-cancer biodegradable ureteral stents developed in the chapter VI. Transurothelial permeability was evaluated using an ex vivo porcine approach.

Chapter VIII – Natural origin polymers-based biodegradable ureteral stent: *In vivo* evaluation in a porcine model: In this chapter the biodegradable ureteral stents developed in Chapter V, with an enhance in crosslinking were used in *In vivo* porcine model study. The objective was to confirmed the *in vitro* results and to provide a better understanding of its complexity.

Section IV – Business Plan

Chapter IX – Business Plan - HydrUStent: This section of the thesis presents an overview of the ureteral stent market and the explore the steps to place the biodegradable ureteral stent developed into the market.

Section V – Concluding remarks

Chapter X – General Conclusions, Final Remarks and Future Perspectives: The final section of the thesis presents the general conclusions and implications, current limitations and potential of the work described for biodegradable ureteral stents.

Chapter I

Ureteral Stents Technology: Biodegradable and Drug- eluting perspective

Chapter I

Ureteral Stents Technology: Biodegradable and Drug-eluting perspective *

ABSTRACT

An ureteral stent is a versatile and indispensable common medical device in the management of several urological diseases. Nonetheless, the actual stent technology is far from the ideal. The ureteral stents available in the market are associated with clinical complications including bacterial adhesion, infection, encrustation development, pain and discomfort for the patients. Innovative stent materials and more research of new ureteral stent designs are necessary in order to avoid these complications and pursue the ideal stent, i.e., a stent that can maintain the adequate urine flow from the kidney to the bladder and mitigation of hydronephrosis. In past years different approaches have been explored, including novel stent coatings, drug-eluting stent and biodegradable ureteral stents. The common goal of these new technologies is to increase the biocompatibility of the biomaterials and avoid the stent-related symptoms. New developments in ureteral stent field, namely drug-eluting biodegradable ureteral stents, are also envisaged to address new urological clinical scenarios. In summary, there is no perfect ureteral stent that avoids all ureteral stent associated complications but there have been significant advances in last years in stent technology and particularly technologies such biodegradable drug-eluting stents are seen as very promising.

* This chapter is based on the following publication:

Barros AA, Oliveira C, Lima E, Duarte ARC, Healy K, Reis RL. Ureteral stents technology: biodegradable and drug-eluting perspective, Reference Module in Materials Science and Materials Engineering, DOI: 10.1016/B978-0-12-803581-8.10189-4, 12 January 2017 (Online).

I-1. INTRODUCTION

Every day thousands of ureteral stents are placed worldwide in urological practice, as a routine medical device. In 1978, Finney *et al.* (1) presented to the urology community the double-J and single-pigtail stent, and since then this medical device has become one of the most standard procedures and crucial device in urology. Ureteral stent design and materials have been improved in the last decades improving the efficacy of this medical device. The clinical scenarios that normally required the use of ureteral stents are the treatment of urolithiasis, to avoid obstruction of the ureter particularly in stone-forming patients, to stimulate ureteral restorative or to help urinary function. It can also be placed preoperatively to signalize the ureter during the operation (2). However, after all these years of use and intense research the ureteral stents available in the market may produce significantly stent symptoms, like infection, encrustation, patient discomfort and all required a second procedure to take out the stent by cystoscopic removal. **Figure I-1** shows the steps following stent insertion that lead to bacterial adhesion, infection and encrustation. The problems start when, after placement of stent in the ureter, upon the passage of urine, the deposition of ion and minerals occurs, and the urine components begin to deposit around the surface of the stent, creating anchor points where bacteria may adhere and start to grow. This situation facilitates the creation of a “conditioning film” and therefore the development the encrustation on the surface of the device (3-5). The ideal ureteral stent biomaterial would be able to prevent all of these problems it does not allow any deposition of material on the surface (6, 7). Research in this field has been focused on improving the safety and the comfort of stents. The design of stents is changing to make stents with anti-bacterial surfaces, e.g. like hydrogel-coated stents (8) , surfaces that allow the delivery of drugs (9, 10) avoiding encrustation and designs that make stents more flexible, allowing the device to adjust to the morphology of the ureter as the patients moves (11). The urologist prescribes oral agents as a management strategy to overcome pain and discomfort, however this procedure is associated with minimal efficacy and side effects (12, 13). Drug-eluting ureteral stents is one of the approaches explored based on the delivery of drugs incorporated on the ureteral stents, either by drug-coated or by drug-eluting technologies, with the objective to deliver the drug locally and accelerate the cure or preventing any side effects (14). From an other perspective, biodegradable ureteral stents have been appointed as the next generation of ureteral stents and may be the solution for the ureteral stent associated

complications. Biodegradable ureteral stents would avoid the second procedure for stent removal and theoretically be more comfortable for the patients as they are made from softer materials. Regarding the bacterial adhesion and encrustation problems these ureteral stents have a dynamic surface due the constantly degradation not promoting the appearance of the anchor points which lead to “conditioning film” development (11, 15, 16). The combination of the eluting-technology with ureteral stents made of biodegradable materials starts to get some attention in urology (17, 18) but have already been extensively used in some cardiovascular applications.

This review provides an overview of the last developments in ureteral stents focused on biodegradable ureteral stents technologies. It provides a description of the different approaches reported in literature with a comprehensive understanding of the problems reported with previous biodegradable ureteral stents and prospectively the drug-eluting biodegradable ureteral stents.

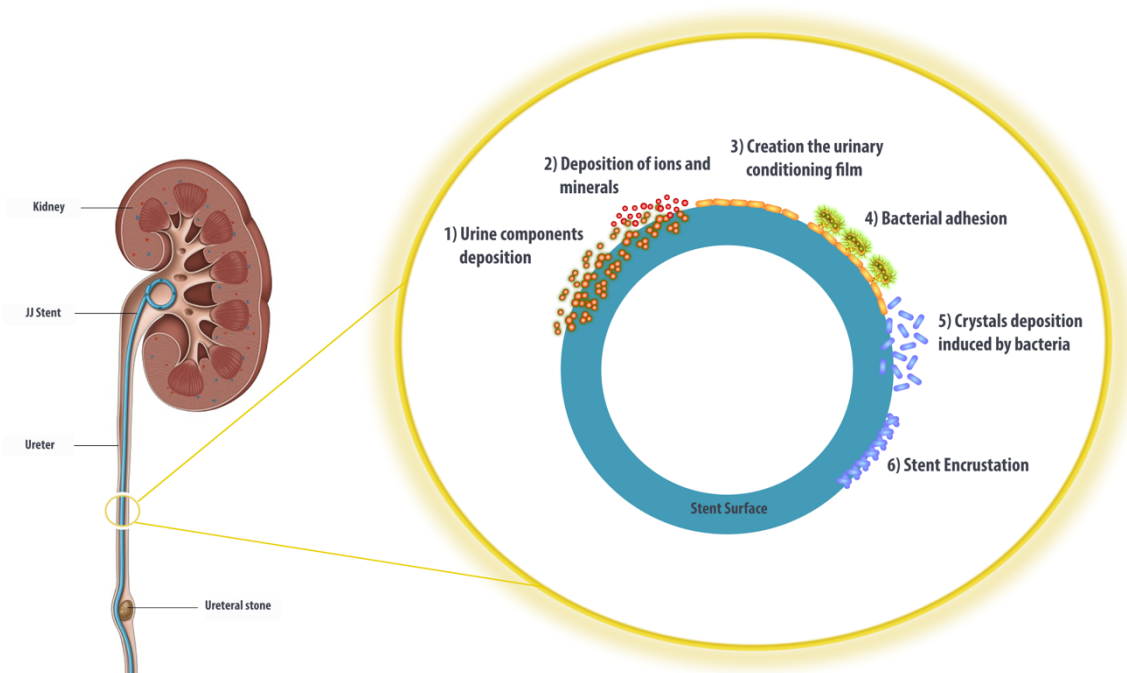


Figure I-1 Mechanism of bacterial adhesion, after ureteral stent insertion, 1) urine components deposits on stent surface 2) allowing create an ions and minerals spots on surface 3) building of the urinary conditioning film 4) bacterial adhesion and consequently infection. 5) In addition the interaction of ions and minerals with biofilm components and bacterial induced crystallization and the encrustation occurs in the stent surface.

I-1.1. Medical Motivation for development of biodegradable ureteral stents

Since their introduction in 1967 by Zimskind *et al.*(19), ureteral stents have become an invaluable tool in the urologist's armamentarium. They are widely used in routine urological clinical practice to establish or improve drainage in cases of extrinsic or intrinsic obstruction of urinary passage. They are also used after iatrogenic injuries to the ureter and prophylactically in complex urinary tract reconstructive surgeries. As it is a foreign body inside the genitourinary system, it has the potential to cause complications. It was reported that more than half of the patients with a stent would suffer from frequency, urgency, dysuria, feeling of incomplete emptying and pain (20, 21). These symptoms have a negative impact in the general health status, sexual activity, and work performance in about 78% of cases (22). After a stent insertion, the quality of life was reported to be affected in 45%–80% of the patients (23). Another major problem of current use stents is the high rate of development of encrustations. These increase the probability and severity of adverse effects including flank pain, infection, irritative urinary symptoms, stent fragmentation, stent migration, hematuria, hydronephrosis, renal failure and even death (24-26). One of the major factors for the development of encrustations is the time that stent is left inside the body. El-Faqih *et al.* (27) reported encrustation rate of 9.2% if the stent was kept for up to 6 weeks; however, encrustation rate rose to 76.3% if the stent was left in place for up to 12 weeks. So the management of patients after stent insertion is a longstanding challenge in order to perform the treatment and, at the same time, minimizing the side effects. The stent removal is a surgical procedure done in ambulatory. It is performed under local anesthesia. And it requires an endoscope and forceps. It is usually done by a urologist assisted by a nurse. A resorbable ureteral stent would be a major breakthrough in the management of these patients as it would obviate the need for multiple procedures and would minimize the risk of encrustation and other adverse side effects. Another major breakthrough in urological management would be a stent capable of delivering drugs at a controlled rate. The urothelium is source of oncological disorders as Carcinoma in Situ (CIS). Up to date the only effective treatment for CIS is immunotherapy instillation. The instillation is effective in the bladder but delivering into the ureter and renal pelvis is a technical challenge. Currently there is no effective way of performing such treatment. A ureteral stent that is in close contact to target area capable of delivering such drugs would represent another revolution in the management of these patients.

I-2. BIOMATERIALS IN URETERAL STENTS

I-2.1. Polymeric ureteral stents

An ureteral stent is a thin tube, which is inserted in the ureter to prevent or to treat the obstruction of urine flow from the kidney to the bladder (28). Ideal ureteral stent should reach a similar performance of what archived with cardiovascular stents, combining perfect efficacy in a long-term indwelling with no stent-related complications. But, what we learn from all of these years is what works in vascular environment may not be directly appropriate in ureteral stents (3, 9). Ureteral stents can be used as a temporary measure in order to prevent damage to a blocked kidney until a procedure to remove the stone is performed. Indwelling times for these cases are typically from 15 up to 60 days and in this case polymeric-based stents are more common (15, 29). Polyethylene, a synthetic polymer, was one of the first materials to be used, due the rigidity of the plastic for stent placement, but was discarded due the tendency to fragment as well as its stiffness and brittleness properties (30). Since then, silicone has been the standard gold biomaterial because is a very biocompatible material that resulted in decreased of infections and encrustations and is one of the most lubricious materials available (31). However regarding the mechanical properties for stent placement this material is difficult to handle due their softness and elasticity, particularly in the presence of tortuous ureters and extrinsic compression. Polyurethane (PU), combines the elastic properties of silicone with the rigidity of polyethylene and because of this feature it is one of the materials that are nowadays used in stents, together with polyvinyl chloride (PVC) and ethylene vinyl acetate (EVA) (2). PU still is not the ideal biomaterial to be used in ureteral stents because is a stiff biomaterial and cases of ureteral erosion and ulceration in animal studies and discomfort in patients have been reported (32, 33). Companies have been focus in development of new proprietary materials and new blend of materials that are more comfortable and soft to limit the discomfort of the patients and at the same time to be easier to handle by the surgeons during the placement in the urinary tract. Percuflex®, is one of the most common materials used in ureteral stents and is property of Boston Scientific Corporation (Marlborough, MA, USA), together with C-Flex®, property of Consolidated Polymer Technologies (Clearwater, FL, USA), Silitek® property of Surgitek (Racine, WI, USA) and Tecoflex® property of Thermedics (Wilmington, MA, USA).

I-2.2. Metal Ureteral Stents

Metal-based stents have been developed in last years with the objective to overcome the disadvantages of polymeric-based ureteral stents, including low load resistance. Pauer and Lugmayr in 1992 (34) for the first time introduced the concept and these have shown to be more adequate in the treatment of malignant ureteral obstruction (MUO) or retroperitoneal fibrosis (35-39). Metal-based stents, as polymer-based stent, have problems like biofilm formation, infections and migration. But a common problem of metal stent is that it induces local tissue hyperplasia, with ingrowth of urothelial tissue through the structure of the stent which in a long term may result in recurrent obstruction (36, 39). Metal-based stents can have different designs including the conventional double-J stents and self-expandable. Resonance™ stent (Cook Medical, USA), is a double-J stent composed by nickel-cobalt-chromium-molybdenum-alloy, with the objective to be applied in malignant ureteral cases to provide long term urinary function (40). Kadlec *et al* in 2013, reported a five-year experience with Resonance™ stent in 47 patients with chronic ureteral obstruction for both malignant and benign disease, with a total of 139 metallic stents used. The results showed 28% failure rate due to patient's pain, renal insufficiency, stent migration and encrustation with an average indwelling time of 8 months. Apart from there complications, this study showed that Resonance™ metallic stents are an adequate management strategy for benign and malignant ureteral obstruction (41). Regarding self-expandable metal stents, long term follow-up studies in humans have been made with a thermos-expandable metallic stent, Memokath® 051 (Pnn Medical, Denmark)(42) and a self-expandable metal mesh stent (36). The results of these studies continue to show common complications as stent migration, encrustation, fungal infections, hyperplastic reaction and tumour ingrowth. Novel metal stent designs have been suggested in order to overcome all the complications mentioned above. More flexible, drug-eluting metallic stents as well biodegradable stents are the concepts that are receiving more attention and showing more potential to overcome the common complications associated with metal and polymeric ureteral stents. Flexible metal stents is one of the areas of research with the focus to develop more comfortable metal stents for patients. The design of these metal stents makes them more flexibles, allowing them to adapt to the morphology of the ureters when the patients moves. Spiral-coiling and snake (golden-plated) configuration of metal stent are two different designs of the metal stent called Passage™ (Prosurge, USA). This stent has proven to increase the flexibility and the durable radial compression (43). In a recent study, Passage™ stent was compared with Resonance™ and

with double-J metal stent called Silhouette® (Applied Medical, USA) composed by polyurethane and metal. The study showed that Passage™ stent had higher resistance to radial compression and much lower tensile strength compared with others (43). The lower tensile strength of the stents showed to increase the patient comfort and avoid stent migration. Higher resistance to extrinsic radial compression is essential to avoid obstruction in case of stent compression or tumour ingrowth (39, 43). Other metal stents are also reported in some recent studies: the Allium URS (Allium Medical, Israel) is composed of an undulating nitinol wire fully covered with a thin membrane of ElastEon (polyurethane and silicone elastomer) and Uventa™ (TaeWoong Medial, South Korea) has a two layered nitinol mesh tubular body with a polytetrafluoroethylene layer between them (44, 45). Metal stents have been successfully applied in coronary vessels, however, in urology, new materials are necessary to develop in order to avoid stent-related problems.

I-3. URETERAL STENTS COATINGS

Surface coatings for ureteral stents normally address the issues of stent tolerability and the prevention of inflammation and encrustation and infection by inhibiting bacterial adhesion and growth on the stent surface, together with urinary crystal formation and adherence. Different approaches have been developed and tested, in *vitro*, in animal models and in humans. Distinctive strategies have been made based upon the application of anti-adhesive surfaces by surface charge modification, hydrophilicity and/or roughness; drug-eluting and antimicrobial (silver, antibiotics, others) compounds and a dynamic surface (biodegradable ureteral stents) (**Figure I-2**). The several stent coatings strategies developed and studied in the past 20 years are extensively reported in **Table I-1**.

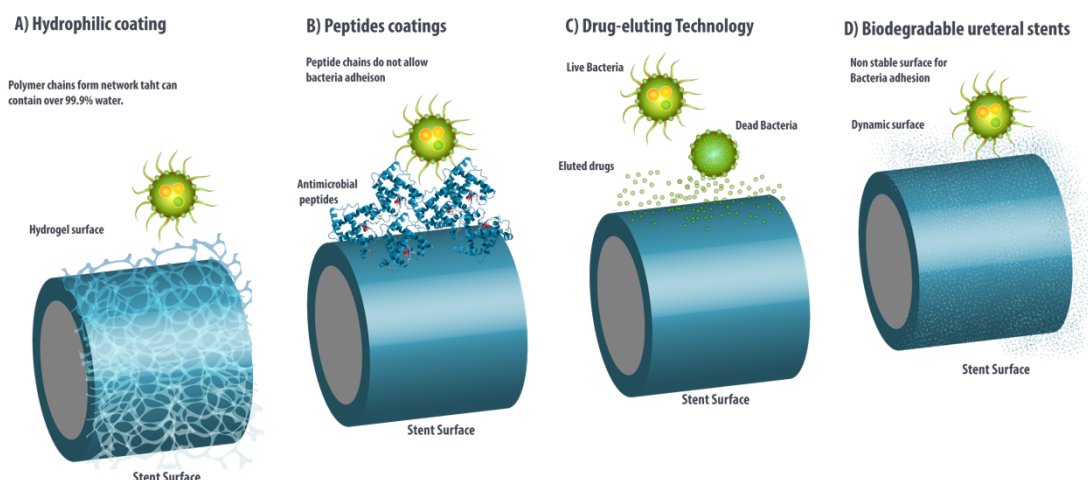


Figure I-2 Strategies to avoid the ureteral stent-associated problems, a) Hydrophilic coatings have a significant water content decrease the bacterial fixation b) Ureteral stents surface coated with antimicrobial peptides, not allowing the bacterial reach the stent surface and break up the bacterial membrane c) Drug-eluting technology, stent release specific drugs (antibiotics) in the ureter, allowing it to interact with the bacteria d) biodegradable ureteral stents, with dynamic surface due the constant degradation would provide non stable surface for bacteria to attach.

I-3.1. Hydrophilic Coating

Hydrogels constitute a group of polymeric materials with hydrophilic nature that renders them capable of holding large amounts of water in their three-dimensional networks. Due to their significant water content they have mechanical properties, very similar to natural tissues like flexibility for example (46). Hydrophilic coatings on ureteral stent surfaces have drastically decrease the friction, increasing the lubricity and elasticity, and act as a deterrent to hydrophobic bacterial surfaces and crystal deposits within the urine (47). These properties facilitate the stent placement in a dry state, but when in contact with the urine, the hydrogel starts to absorb and accumulate water in its polymer network, making it more flexible and more comfortable for the patient (15). The studies reported in literature using hydrogels as a coating, are summarized in **Table I-1**. These studies have been shown that relating to encrustation and infection in some cases reduce (30) and in other study shown an increase (48), but regarding the patient comfort the results are satisfactory. Hydrogel coating also have been used as a support for the delivery of active compounds like anti-inflammatory drugs and antibiotics (18, 47).

I-3.2. Glycosaminoglycan coatings

Glycosaminoglycan (GAG) coating have also been tested as a surface coating for ureteral stents. GAGs are a common constituent of urine and is a natural inhibitor of crystal formation. Zupkas *et al* coated a silicone surface with pentosan polysulfate (PPS) (49) and showed that were able to reduce the encrustation compared with the uncoated silicone stents. Other novel stent coatings include phosphorylcholine (PC) (50), a constituent of human erythrocytes that mimics a natural lipid membrane, and poly-N-vinyl pyrrolidone (PVP) (51) that is a hydrophilic coating, that absorbs water similaring to a hydrogel. Heparin is a highly-sulfated glycosaminoglycan used as an anticoagulant in vascular medicine and has been shown to inhibit bacterial adhesion (52). Due the high negative charge, its relative safety and their prior use in vascular stents, heparin has been applied to coating ureteral stents. Its ability to reduce the bacterial adhesion and encrustation formation (Endo-Sof™ and Radiance™, Cook Medical, USA) was been tested and Riedl *et al* (52) compared heparin-coated and uncoated PU ureteral stents in a human trial. In their work they observed that, in contrast to uncoated PU stents, heparin-coated stents did not show any biofilm or crystal deposits after being in humans for up to 6 weeks, effectively inhibiting the encrustation process. Other human trial reported by Cauda *et al* support the results observed by Riedl, in a long-term study involving patients with bilateral ureteral obstructions treated with heparin-coated ureteral stent into one ureter, and an uncoated control stent into the other ureter. After 1 month, the uncoated stents showed encrustation and bacterial biofilm formation while the heparin-coated stents remained visibly free of encrustation as long as 10 months. Heparin-coated ureteral stents have been introduced in the market and have been shown to be successful in decreasing encrustation and biofilm formation in human trials, but no significant improvement in the patient discomfort and pain control (52-54) has been reported.

I-3.3. Biostable coatings

Another class of materials that have been applied for ureteral stent coatings is plasma deposited diamond-like carbon coatings (DLCs) in an attempt to prevent encrustation. This material has been suggested based upon its monocrystalline structure, outer monomolecular layer of non-polar hydrogen atoms and the possibility to be applied as a thin film on surface. The coating is biocompatible, super lubricious, chemically inert and extremely durable. Laube *et al* (55) did a

human trial with ten patients who needed temporary a stent and were treated with 26 DLC-coated stent. The indwelling average time was 14 weeks. The results demonstrated that this coating decreased the friction, the biofilm formation and the encrustation. Different thicknesses of the coating layer were also studied and films with lower thickness, 100-200 nm (1.8 refractive index), have shown the highest resistance to bacterial adhesion and encrustation development in *in vitro* test. Additional coating exhibiting super lubricious properties is the polytetrafluoroethylene (PTFE) or commercially call Teflon®. PTFE coefficient of friction (0.05-0.1) is one of the lowest of any known substance, it is also resistance to *Van der waals* forces, normally used by bacteria for initial adhesion to the stent surface. These properties make it a promising material to prevent bacterial adhesion and biofilm formation. In last years, different *in vitro* studies demonstrated that PTFE-coated ureteral stents reduce protein and bacterial adhesion against the controls, other studies also found hydrophobic-like proteins and bacteria are not affected (14, 56). Arguinarena *et al*(57) did a 2-years human trial in 20 patients using an expanded PTFE-coated nitinol stent and shown the safety, the resistance to calcification and effectiveness in cases of ureteral stenosis. Polycarbonate (PC) elastomer coated wire stents were studied in dog model. The results of using this biostable material for coating the wire stents have shown to be success in preventing inflammation and for urothelial hyperplasia (58).

I-3.4. Biomimetic coatings

A novel coating, mPEG- DOPA₃, consisting of a mussel strong adhesive protein mimic – 3,4-dihydroxyphenylalanine (DOPA), combined to an antifouling PEG layer, also has the ability to avoid biofouling in the marine environment. Ko *et al* (59), applied this coating to silicone disks and the results shown strong resistance to bacterial adhesion and biofilm formation, *in vitro*. In 2009, another study *In vivo*, using a rabbit *E. coli* cystitis model (60), showed that DOPA-coated stents were successful in preventing bacterial adhesion, however it was incapable to avoid non-bacterial mediated encrustation. A highlight in this coating should be made because it has shown to prevent bacterial adhesion of the common found uropathogens, *in vitro*. More research will need to be done, particularly with clinical trials for an optimal understanding of the ability of this coating to avoid stent related symptoms.

Other study shown the use of hydrogel coating as a support for a controlled release of Immunoglobulin-G and shown the ability to reduce the bacterial adhesion, *in vitro* (61).

Table I-1 Ureteral stents coatings

Year	Material	Structure	Degradation	Ref
1997/1998	Poly-L-lactide-co-glycolide (PLGA)	Self-reinforced co-polymer L-lactide and glycolide containing 80% lactic acid and 20% glycolic acid with 20% barium sulfate additive	Dependent on the urine pH; Stable at pH lower than 7.0, dissolves in 48h in pH greater or equal to 7.0	(29, 62)
1999	Poly-L,D-lactide copolymer (PLA)	Double-helical spiral self-reinforced poly-L,D-lactide copolymer (SR-PLA 96; L/D ratio 96/4)	Degradation in blocks, fragments remain after 12 weeks causing obstruction.	(63-66)
2002	Poly-L-lactide-co-glycolide (PLGA)	Self-reinforced co-polymer L-lactide and glycolide containing 80% lactic acid and 20% glycolic acid.	PLGA stents degraded in 6–8 weeks and was feasible after Acucise endopyelotomy in a porcine model compared with control but with less favorable biocompatibility.	(67)
2002	Poly-L-lactide-co-glycolide (PLGA)	SR-PLGA horn stent, (PLGA; L:G ratio 80/20)	The degradation time of the material was 2 to 2,5 months	(68)
2002	Poly-L-lactic and poly-L-glycolic acid (SR-PLGA) copolymer	Self-reinforced poly-L-lactic and poly-L-glycolic acid (SR-PLGA) copolymer spiral design urethral stent	Stent degraded in 6–8 weeks and resisted encrustation at 4 weeks in artificial urine	(69, 70)
2003	Alginate-based	Alginate with a proprietary polymer that is made radiopaque using 7% by weight bismuth sub-carbonate powder	Designed to stay in place for at least 48 hours after uncomplicated ureteroscopy	(71, 72)
2010	L-lactide and glycolide with lactic acid, glycolic acid	Biodegradable copolyester components and L-lactide and glycolide with lactic acid, glycolic acid, and barium for radiopacity	Dissolves within 1 to 4 weeks in a porcine model	(16, 73)
2011	Poly-L-lactic acid (PLLA) and Poly-DL-lactic acid (PDLLA)	The stent used in this experiment was manufactured using poly-L-lactic acid (PLLA) and poly-DL-lactic acid (PDLLA) mixed together in mass proportion. A 25% barium sulphate additive	Stable for more than 120 days in a canine model	(74)
2012	Magnesium-based	Mg–4 wt % yttrium (MgY) alloy, Mg–3 wt % aluminum–1 wt % zinc (AZ31) and commercially pure Mg (98% purity with aluminum as major impurities), and these alloys with thermal oxide layer on the surfaces (MgY ₂ O ₃ and Mg ₂ O)	Stable during 3 days in AUS, microcracks on surface by corrosion.	(75, 76)
2014	PGA and PLGA multifilaments	Designed a braided thin-walled biodegradable ureteral stent made of PGA and PLGA multifilaments, using textile techniques	Stents began to degrade at 1 week, and had completely degraded by the 4th	(77, 78)

			week in a canine model
2015	Poly(ϵ caprolactone) (PCL)/poly(lactide-co-glycolide) (PLGA)	Nanostructured ureteral stent. Poly(ϵ caprolactone) (PCL)/poly(lactide-co-glycolide) (PLGA) ureteral stent composed of nanofibers with micropores fabricated by double-needle electrospinning	Stent gradually degraded from the distal end to proximal terminal, and all stents were completely degraded at 10 weeks post-insertion. (79)
2015	Polysaccharides-based	Hydrogel of Gelatin/Alginate and Gelatin/Gellan Gum blends fabricated by supercritical fluid process.	Complete dissolution of the stent occurred between 14 and 60 days in artificial urine (15, 18)

I-4. BIODEGRADABLE URETERAL STENTS MATERIAL

Despite the fact that novel coating stent designs have been improved over the last years the core ureteral stent has one basic drawback, it requires a secondary procedure to remove the stent if the suture is removed. Avoiding the ureteral stent removal procedure, it is expected a decrease in patient morbidity and also a decrease on the treatment cost. In the last years different studies with different materials have been reported in the literature, attempting to developed a biodegradable ureteral stents. This type of ureteral stent design is one of the most appealing stent designs with high potential to overcome the actual ureteral stent-associated complications (11). The biomaterial to be used in biodegradable ureteral stent should be biocompatible, maintain intact the properties after sterilization, the degree of swelling and degradation rate should take in consideration the treatment time, always allowing the flow of the urine from the kidney to the bladder (2). Biodegradable ureteral stents concept will eliminate the “forgotten stent” problem, that consists on the ureteral stents which remain more time than it is necessary for the treatment, most probably leading to bacterial infection and more serious cases of encrustation (20). The benefit of the biodegradable ureteral stent is the fact that the physical properties of the stent surface are constantly changing as the stent degrades due to erosion, decreasing the bacterial adhesion and encrustation development. Additionally, biodegradable materials might be favorable for patient comfort because tend to be softer. One of the key points involving the design of biodegradable ureteral stents is the control of degradation profile, i.e. rate and direction of the degradation. Lange *et al* suggested an early degradation of bladder coil, could prevent bladder irritation and vesicoureteric reflux during voiding (11). Some materials used in the design of biodegradable ureteral stents, can be divided in synthetic materials, natural origin materials and a more recent

research some metal biodegradable materials (**Figure I-3**). In **Table I-2** are summarized the most important studies reported in literature about different approaches of biodegradable materials used for development of biodegradable ureteral stents.

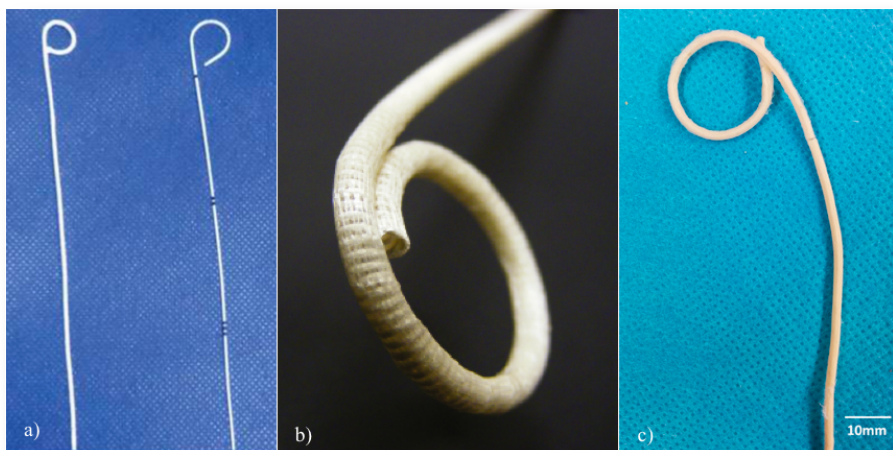


Figure I-3 Biodegradable ureteral stents a) degradable braided thin-walled ureteral stent composed of multifilaments of PGA and PLGA (4) b) Uriprene™ (Poly-Med Inc, Greenville, SC) composed of L-lactide, glycolide, and copolyester components (5) c) Natural polymer based ureteral stents composed by fully hydrogel of gelatin and alginate (15).

I-4.1. Synthetic polymers

The first concept of biodegradable ureteral stent was reported by Schlick and Planz in 1997 (29), composed by one of two property plastics (G100X-15LB and G100X-20LB) involving the concept that the degradation can be mediated by changing pharmacologically the pH of the urine (29, 62). *in vitro* studies with artificial urine solution showed that material was stable in pH<7.0 for at least 30 days, but the full degradation occurred within 48h at pH>7. The idea behind this concept is that stent could be stable in physiological urine (pH 5-6), but degradation can be triggered. This approach has some limitations when envisaging for human applications. Changing the pH of the urine it will be expected an additional crystallization in urothelial environment that can be already supersaturated. The presence of uropathogens has already been reported to increase the urine pH, which can affect the degradation of the stent *In vivo* and from the other side can

favour bacterial survival and increase calcium phosphate and struvite stones formation(80). No recent studies using this pH degradation approaches are found in literature.

Other studies showed a good performance in animal model using polylactic acid and poly (lactic-co-glycolic acid) blends as biodegradable materials (67). Lumiaho *et al* (63, 64) developed a biodegradable ureteral stents using a degradable polylactic acid in two porcine model studies and the results have shown satisfactory drainage characteristics with antireflux properties but regarding the degradation the stent degraded in blocks and the biocompatibility results were insufficient. The same material was used in a different study with a canine model and such stents had completely degraded after 12 weeks, showing good biocompatibility compared with the controls (65). Li *et al* reported a study demonstrating the effectiveness of polylactic acid ureteral stents in preventing hydronephrosis in a canine model of ballistically induced ureteral injury. Poly (lactic-co-glycolic acid) (PLGA) is other material extensively studied as a degradable material for biodegradable ureteral stent design. A study using PLGA-based ureteral stent demonstrated good radiographic and flow characteristics in a porcine model after endopyelotomy, but unsatisfactory biocompatibility (67). In a similar study no complications were observed using PLGA-based horn ureteral stents after antegrade endopyelotomy (68). Lumiaho *et al*, in 2011, continued the study of biodegradable ureteral stents using a short biodegradable helical spiral ureteral stents, with the same material, and the results shown better drainage and antireflux properties compared double-J stent control, but the biocompatibility was not reported (66). UriprenTM ureteral stent (Poly-Med Inc.,USA) was developed from a radiopaque, glycolic-lactic-acid formula (81). The materials used to construct this biodegradable ureteral stents are materials similar to those found in absorbable sutures (82). In a first study, UriprenTM stent degraded in 7-10 weeks. However, while it provided excellent drainage with minimal hydronephrosis compared with the controls (biostable stents), difficulty of insertion was experienced due too soft axial rigidity of the stent. This study has shown less bacterial adhesion in the UriprenTM biodegradable stent in comparison to the controls but the authors concluded that the time frame of degradation was too long. In a more recent study, the authors improved the UriprenTM stent formulation with a reinforcement to provide better axial rigidity which resulted in favourable insertion and better handling characteristics. This new generation demonstrated a faster degradation profile, 2-4 weeks, while supporting excellent drainage and decreasing the incidence of hydronephrosis, demonstrating less irritation compared with biostable ureteral stents (16, 83). The problem of the use this class of materials is the tendency to degraded

by hydrolysis, creating blocks that can affect the urine flow, and also can be a starting point for bacterial adhesion and biofilm formation. Zhang *et al* reported a canine model study using a manufactured braided thin-walled biodegradable ureteral stent using multifilament's of PGA and PLGA and barium sulfate. The stent shows a good biocompatibility and physical characteristics. The degradation started at 1 week and complete degradation was achieved after 4 weeks. In this study it is not clear the way that stent degraded and the authors do not refer if they had any presence of block during the degradation. These synthetic materials studied until now, were successful applied in absorbable sutures but the same results cannot be expected in the design of biodegradable ureteral stents due to the amount of bulk material that needs to be degraded in a fast and homogeneous way.

I-4.2. Natural origin polymers

Natural origin polymers have been extensively studied as biodegradable materials specially in tissue engineering and regenerative medical applications (15, 84). Lingeman *et al* (71, 72) reported the first studies using a natural origin polymer based material to fabricate biodegradable ureteral stents. This biodegradable ureteral stent was one of the most extensive clinical evaluated and was made by a proprietary alginate-polymer-based formulation. Phase I and Phase II clinical trials in 88 patients demonstrated that alginate-based stent facilitated urinary drainage with good biocompatibility. The stent was designed to be intact during 48h and after this the stent started to degrade. The clinical trials have shown an insufficient degradation rate and resulted in the need for second intervention to remove the fragments of the patients. The studies reported that the average time to fully achieve stent degradation was 15 days, but three patients kept fragments after 3 months, requiring extracorporeal shockwave lithotripsy and ureteroscopic manipulation for fragments removal. The authors of this chapter are currently involved in the development of a fully hydrogel natural origin based biodegradable ureteral stent. The principle behind the development of a fully hydrogel biodegradable ureteral stent relies on the advantages of hydrophilic coatings and the dynamic surfaces of the stent that authors believe to be an interesting approach to avoid bacterial adhesion and biofilm formation. A first study, involved a variety of different alginate, gellan gum and gelatin blends(15). To developed this biodegradable stents, the authors used a process called supercritical carbon dioxide (scCO₂), that, after solvent exchange and drying process, help to enhance the mechanical properties of the hydrogel stent. The *in vitro* study demonstrated that

polysaccharides-based stent was able to maintained their mechanical properties during the degradation. The degradation occurs, *in vitro*, between 2 weeks and 2 months and can be tailored changing the ratio of raw materials used. These materials have shown no significant differences results regarding bacterial adhesion to gram-negative and significant differences were observed for gram-negative bacteria compared with a biostable control stent. Authors evaluated the biocompatibility *in vitro* and no differences were found compared with a Biosoft Duo stent, as a control (Porges, Coloplast, Denmark) (15). These type of stent are also being investigated as a drug-eluting stents for different urological clinical scenarios explained in the drug-eluting stents section of this chapter (17, 18).

I-4.3. Magnesium-based metal

A new class of materials suggested in literature to be used as a based material for the development of biodegradable ureteral stents is magnesium and its alloys. Magnesium is a lightweight and biodegradable metallic material with advantageous properties for use in medical devices, such in cardiovascular applications. Magnesium-based stents are expected to corrode gradually *In vivo*, with an appropriate host response elicited by released corrosion products, then dissolve completely upon fulfilling the treatment (85). Lock *et al* (75, 76) investigated the antibacterial and biodegradable properties of magnesium and its alloys for biodegradable ureteral stent applications. In this study the authors used Mg–4 wt % yttrium (MgY) alloy, Mg–3 wt % aluminum–1 wt % zinc (AZ31) and commercially pure Mg (98% purity with aluminum as major impurities), and these alloys with thermal oxide layer on the surfaces. The results have shown that magnesium alloys decreased *Escherichia coli* viability and reduced the colony formation units after 3-day incubation period in an artificial urine solution (AUS) when compared with commercial polyurethane stent. Furthermore, the results of magnesium degradation have shown an increase of magnesium ion concentration in AUS and consequently an increase of pH (more alkaline). The degradation of magnesium-based materials only was measured during the 3 days. Macroscopic photographs showed all materials had micro cracks on surface in the first day, with a decrease of magnesium concentration on surface after 3 days. *In vivo* or clinical trials have not been undertaken but the *in vitro* testing look promising for the clinical translation of biodegradable metallic ureteral stents.

Table I-2 Biodegradable Ureteral Stents

Year	Material	Structure	Degradation	Ref
1997/1998	Poly-L-lactide-co-glycolide (PLGA)	Self-reinforced co-polymer L-lactide and glycolide containing 80% lactic acid and 20% glycolic acid with 20% barium sulfate additive	Dependent on the urine pH; Stable at pH lower than 7.0, dissolves in 48h in pH greater or equal to 7.0	(29, 62)
1999	Poly-L,D-lactide copolymer (PLA)	Double-helical spiral self-reinforced poly-L,D-lactide copolymer (SR-PLA 96; L/D ratio 96/4)	Degradation in blocks, fragments remain after 12 weeks causing obstruction.	(63-66)
2002	Poly-L-lactide-co-glycolide (PLGA)	Self-reinforced co-polymer L-lactide and glycolide containing 80% lactic acid and 20% glycolic acid.	PLGA stents degraded in 6–8 weeks and was feasible after Acucise endopyelotomy in a porcine model compared with control but with less favorable biocompatibility.	(67)
2002	Poly-L-lactide-co-glycolide (PLGA)	SR-PLGA horn stent, (PLGA; L:G ratio 80/20)	The degradation time of the material was 2 to 2,5 months	(68)
2002	Poly-L-lactic and poly-L-glycolic acid (SR-PLGA) copolymer	Self-reinforced poly-L-lactic and poly-L-glycolic acid (SR-PLGA) copolymer spiral design urethral stent	Stent degraded in 6–8 weeks and resisted encrustation at 4 weeks in artificial urine	(69, 70)
2003	Alginate-based	Alginate with a proprietary polymer that is made radiopaque using 7% by weight bismuth sub-carbonate powder	Designed to stay in place for at least 48 hours after uncomplicated ureteroscopy	(71, 72)
2010	L-lactide and glycolide with lactic acid, glycolic acid	Biodegradable copolyester components and L-lactide and glycolide with lactic acid, glycolic acid, and barium for radiopacity	Dissolves within 1 to 4 weeks in a porcine model	(16, 73)
2011	Poly-L-lactic acid (PLLA) and Poly-DL-lactic acid (PDLLA)	The stent used in this experiment was manufactured using poly-L-lactic acid (PLLA) and poly-DL-lactic acid (PDLLA) mixed together in mass proportion. A 25% barium sulphate additive	Stable for more than 120 days in a canine model	(74)
2012	Magnesium-based	Mg–4 wt % yttrium (MgY) alloy, Mg–3 wt % aluminum–1 wt % zinc (AZ31) and commercially pure Mg (98% purity with aluminum as major impurities), and these alloys with thermal oxide layer on the surfaces (MgY ₂ O ₃ and Mg ₂ O)	Stable during 3 days in AUS, microcracks on surface by corrosion.	(75, 76)
2014	PGA and PLGA multifilaments	Designed a braided thin-walled biodegradable ureteral stent made of PGA and PLGA multifilaments, using textile techniques	Stents began to degrade at 1 week, and had completely degraded by the 4th week in a canine model	(77, 78)
2015	Poly(ε caprolactone) (PCL)/poly(lactide-	Nanostructured ureteral stent. Poly(εcaprolactone) (PCL)/poly(lactide-co-glycolide)	Stent gradually degraded from the distal end to proximal terminal, and all stents were	(79)

	co-glycolide) (PLGA)	(PLGA) ureteral stent composed of nanofibers with micropores fabricated by double-needle electrospinning	completely degraded at 10 weeks post-insertion.	
2015	Polysaccharides-based	Hydrogel of Gelatin/Alginate and Gelatin/Gellan Gum blends fabricated by supercritical fluid process.	Complete dissolution of the stent occurred between 14 and 60 days in artificial urine	(15, 18)

I-5. DRUG-ELUTING URETERAL STENTS

Apart from the coatings strategies, developed in last years, ureteral stent design has evolved to include drug-eluting technology. Drug-eluting technology is an easy way technology to incorporated, which has been used extensively in cardiovascular applications (86). Different strategies have been studied, with different active compounds and they have shown to be most promising for the inhibition of bacterial adhesion, biofilm formation and encrustation. Strategies for avoiding the inflammation in the surround urothelial tissues were also reported. In **Table I-3** the most relevant studies are summarized and the different approaches along the last 10 years using anti-inflammatory and antibacterial drug elution technology in ureteral stents are presented.

I-5.1. Anti-bacterial eluting

Many strategies to avoid bacterial adhesion on stent surface have been applied, some with significant success in controlling bacterial development and biofilm formation. Chew *et al* (87) have developed a triclosan-eluting stent. Triclosan is a biocide with antibacterial and antifungal properties. The results of the study with triclosan-eluting stents showed that the triclosan elution is able to inhibited the growth of *E. faecalis*, *S. aureus*, *P. mirabilis* and *K. pneumoniae*, and decrease the expression of *E. coli in vitro* and in animals studies. Additionally, in the animal studies, a decrease of inflammation was observed in the bladder of animals implanted with triclosan-eluting stents comparing with controls, suggesting that triclosan-stents not only address the infection but also the discomfort cause by the ureteral stent. However, when evaluated in human trials the results showed limited success (9, 87-89). A sustained release of chlorhexidine, has been developed and demonstrated inhibition on formation of biofilm on the urinary catheter surface, *In vitro* (90). Another strategy reported in literature includes antibiotic loading in hydrogel-coated stents (47). Studies using combinations of silver nitrate (91, 92), rifampin (93) and ofloxacin (92)

have been tested in animal models while stents with cefazolin, tobramycin, gentamicin, ceftriaxone, and ciprofloxacin alone or in combination with *N*-acetylcysteine have only been tested *In vitro* and with good results (94). The main challenge in this type of approaches is to maintain an efficient release and resistance of antibiotic during all treatment time. A novel anti-quorum and cationic proteins coated stents have also been tested as a strategy to prevent the bacterial adhesion and mineral encrustation. Quorum-sensor inhibitor RNAlII-inhibiting peptide (RIP)-coated ureteral stent has shown to reduce bacterial growth and biofilm formation after 5 days in rat bladders infected with *S. aureus*. The inhibition was higher when teicoplanin was also administered (95). Minardi *et al.*, in 2007, reported a study using an antimicrobial peptide called tachyplesin III that coated the stent surface and was implanted in rat infected with *P. aeruginosa*, with or without intraperitoneal (IP) piperacillin/tazobactam. The results showed that the use of this system prevented biofilm formation and growth of *P. aeruginosa* by up to 1000 times. More recent, studies with cathelicidin (BMAP-28) impregnated in ureteral stents were also evaluated (96). Cathelicidin is a polypeptide that serve a critical role in mammalian innate defense against bacterial infection. The BMAP-28-stent showed a reduction of bacterial adhesion alone and when used in combination with vancomycin. These studies show that the antimicrobial peptide works in synergy with the antibiotic, making the approach more effective. However, while these peptide-coated systems with antibiotic are very promise in inhibiting the bacterial adhesion and biofilm formation, human trials are need to corroborate the results observed in animal model.

1-5.2. Anti-inflammatory eluting

Drug-eluting technology has also investigated in order to prevent stent-associated discomfort and pain symptoms using anti-inflammatory compounds. Liatsikos *et al.* developed a paclitaxel-eluting metal stent that has proven to decrease the inflammatory response and hyperplasia in the surrounding tissues of the implant site when tested in a pig model (97). As far we know this particular stent is still waiting human clinical trials. Human trials with non-steroidal eluting stents showed limited success in pain and discomfort reducing, possibly because of limited drug delivery to the ureteral tissues. Krambeck *et al.* in 2010 reported a study with ketorolac-eluting stent (Lexington™, Boston Scientific) that showed a substantial pain reduction in a subset of patients after ureteroscopy (98). Indomethacin, another nonsteroidal anti-inflammatory drug (NSAID), when impregnated in the stents has shown to decrease inflammatory mediators in rabbit urethra model,

but did not succeed in the decrease of fibrosis (99). Halofuginone-coated stents were study in rats with urethral damage and successfully suppressed spongiosfibrosis (100). Kallidonis *et al.*, in 2011, reported a study with zotarolimus-eluting stent (ZES) that have shown promising anti-inflammatory and antihyperplastic activity in pig and rat ureters (101). Dexamethasone-eluting stent were produced and tested *In vitro*. Dexamethasone was eluted from multilamellar liposome coatings applied to the metal stents. The results showed slow release of dexamethasone over 48 hours period in AUS, proving the concept, but further studies are needed(102).

I-5.3. Biodegradable designs

Biodegradable ureteral stent technology will have an important function in the future of ureteral stent design. With the degradation feature this class of stent can address new clinical scenarios in urology (2). As described above, different coatings and eluting technologies have been applied in ureteral stents design in general in order to avoid bacterial adhesion and mineral encrustation. Combination of this new knowledge into the design of biodegradable ureteral stents is a new area. Kotsar *et al* (103), in 2009, reported a human trial study with a biodegradable braided poly (lactic-co-glycolic acid) urethral stent that was design to elute 5 α -reductase inhibitor directly into the prostate of patients with benign prostatic hyperplasia (BPH) and urinary retention. In this study the release was not sustainable, with 50% of the patients requiring insertion of a suprapubic catheter within 1 month. The authors of this chapter have published, in 2015, a study reporting the development of a ketoprofen-eluting biodegradable ureteral stent (18). As far we know this was the first description of a drug-eluting degradable ureteral stent. Ketoprofen is a NSAID that has been shown excellent to treat renal colic. The objective of the development of this new stent is to help patients in the future reducing associated stent complications and at the same time avoiding the procedure for stent removal. The kinetic of ketoprofen release was studied *In vitro* in artificial urine solution. The study involved a variety of biodegradable natural polymers in different concentrations and the results demonstrated that gellan gum-based stents were able to be impregnated with the most ketoprofen compared with alginate-based biodegradable stents(18). The release of 50% of ketoprofen occurs in the first 10 h and then the other 50% occurs over the next 60 h. These results should to be confirmed in a human trial study. The authors of this review are also currently involved in the development of an anti-cancer biodegradable ureteral stent to target upper urinary tract urothelial tumors (17). In this case the conventional method of drug administration is via drug

instillation. This has several drawbacks, such as high concentration dosage required, increased side effects, short residence time and poor bioavailability. To avoid these problems, the authors proposed the use of biodegradable ureteral stents impregnated by supercritical fluid CO₂ with four different anti-cancer drugs (paclitaxel, doxorubicin, epirubicin and gemcitabine). The anti-cancer drugs eluted by the degradable stent showed to be able to reduce 75% of urothelial cancer cell (T24) after 72 hours, *In vitro*, with no toxicity observed in the non-cancer cells (HUVEC cells), used as a control. The use of biodegradable ureteral stents in urology clinical practice not only reduces the stent-related symptoms but also open new treatment options.

Table I-3 Drug-eluting Technologies

Year	Type	material	Methodology	Result	ref
1997	In vitro study	Antibiotic immersed stent and biodegradable prostatic stents; Silicone, silver-coated, hydrogel-coated, PGA and PLA ureteral stents	Stents incubated with E. coli and E. faecalis with and without immersion in tobramycin, ceftriaxone, or ciprofloxacin solutions.	Bacterial adhesion was not influenced by stent material surface. Ceftriaxone, or ciprofloxacin solutions drastically reduced bacterial adhesion while tobramycin did not.	(104, 105)
2000	In vitro study	Liposome-coated metal stents	Gradual release of dexamethasone during 48 hours from multilamellar liposomes in artificial urine was assessed.	The principle was proven with a suitable release.	(106)
2000	In vitro study	Silver nitrate-coated SR-PLLA ureteral stent	Study of the bacterial adhesion inhibition with five urophatogens (Pseudomonas aeruginosa, Enterococcus faecalis, Proteus mirabilis and two strains of Escherichia coli) in silver nitrate-coated PLLA ureteral stents	Silver nitrate coating reduced the amount of bacteria in urine. All urophatogens do not adhered to the stent except for E. faecalis.	(91)
2002	Animal study	Silver nitrate-/ofloxacin-coated SR-PLLA stents	Evaluate the biocompatibility, encrustation and biodegradation properties of silver nitrate and ofloxacin. Stents coated were placed in 18 male rabbit posterior urethra for 1 or 6 months.	Silver nitrate provide possibilities of preventing bacterial adhesion and encrustation to biodegradable stents.	(92)
2005	Animal study	Paclitaxel eluting polyurethane urethral stent	Evaluate a paclitaxel-eluting stent in respect to the reduction of tissue hyperplasia after stent placement in a 20 canine urethral model.	Lower hyperplastic reaction and less degree of stenosis in paclitaxel-coated stents group.	(107)
2006	In vitro study	Triclosan eluting ureteral stent	Triclosan eluted from a drug-loaded ureteral stent was suspended in artificial urine with bacterial pathogens (Escherichia coli, Proteus mirabilis, Enterococcus faecalis, Klebsiella pneumoniae, Staphylococcus	Triclosan coated influence significantly the decreasing of bacterial adhesion on stents surface.	(87)

			aureus, <i>Pseudomonas aeruginosa</i>) to assess bacterial adherence to the stent.	
2006	Animal study	Triclosan eluting Percuflex stent	48 male rabbits were instilled transurethrally with <i>P. mirabilis</i> . A stent curl from a triclosan eluting, Percuflex Plus or Optima ureteral stent was placed intravesically. Urine was cultured on days 1, 3 and 7. Stents were assessed for encrustation and viable organisms.	<i>P. mirabilis</i> growth decrease in presence of triclosan-eluting stents. No differences in encrustation while less inflammation observed in bladder. (89)
2007	Animal study	Paclitaxel eluting metal stent	Compare the standard bare metal stents (BMS) with 10 Paclitaxel-Drug Eluting Stent (DES) in the ureter of 10 pigs during 21 days. Patency was measured by radiograph of the nephrostomy tract.	Paclitaxel-DES, generated less inflammation and/or hyperplasia of the surrounding tissues, thus maintaining ureteral patency. (97)
2007	Animal study	Quorum-sensor inhibitors RNAIII-inhibiting peptide (RIP)	Ureteral stents coated with the quorum-sensing inhibitor RNAIII-inhibiting peptide (RIP) were implanted in rat bladders infected with <i>S. aureus</i> . Stents and urine were cultured on agar plates.	Coating ureteral stents with RIP increased the efficacy of teicoplanin in preventing ureteral stent-associated staphylococcal infections. (95)
2007	Animal study	Cationic peptides-tachyplepsins III	Tachyplepsin III alone or combined with piperacillin-tazobactam (TZP) coated stent segments were implanted by subcutaneous pouch model in rat infected with <i>P. aeruginosa</i> .	Coating ureteral stents with Tachyplepsin III alone or in combination with TZP is able to inhibit bacterial growth up to 1,000 times. (108)
2008	Animal study	Cathelicidin BMAP-28 immersed stent	Efficacy of stents coated with BMAP-28 alone and in combination with vancomycin in Rat model with infection due to <i>E. faecalis</i> and <i>S. aureus</i> . After 5 days implantation, the biofilm was evaluated.	The results highlight the potential usefulness of the BMAP-28 coating with IP combination in preventing ureteral stent-associated in gram-positive infections. (96)
2009	In vitro study	Ciprofloxacin/N-Acetylcysteine (NAC)	Evaluate the effect of ciprofloxacin (CIP), N-acetylcysteine (NAC) alone and in combination, on biofilm production and pre-formed mature biofilms on ureteral stent surfaces.	CIP/NAC combinations had the highest inhibitory effect on biofilm production and the highest ability to eradicate pre-formed mature biofilms. (94)
2009	Human study	Triclosan eluting stent	Eight patients with long-term stents were enrolled prospectively for 3 months with pre and postoperative antibiotics; After 3 months, the control stent was removed, and a triclosan-eluting stent was placed for 3 months with no antibiotics.	Antibiotic use with control stents resulted in bacterial antibiotic resistance, which was not the case with the triclosan-eluting stents. The triclosan-eluting stent alone is not sufficient to reduce device-associated (9)

				infections.	
2009	Animal study	Triclosan eluting and heparin-coated proprietary stent	Heparin-coated stents, triclosan-eluting stent and control stents were incubated in artificial urine with <i>E. coli</i> , <i>K. pneumoniae</i> , <i>E. faecalis</i> , <i>S. aureus</i> and <i>P. aeruginosa</i> for 7 days. Bacterial adhesion was quantified.	Heparin coating did not decrease bacterial adherence to ureteral stents. Drug eluting antimicrobials have an inhibitory effect on bacterial adherence.	(109)
2010	Animal study	Ketorolac eluting stent	A total of 92 pigs were each implanted with a control stent and administered oral ketorolac during 5 days, or stented with 7, 13 and 15% ketorolac coated stents. Ketorolac levels were measured.	Ketorolac-eluting ureteral stents proved to be safe in a porcine model. Ureteral tissues displayed the highest levels of ketorolac and dose-dependent manner.	(73)
2010	Human study	Ketorolac eluting stent	Prospective, double-blind study; 276 patients randomized received, after ureteroscopy, ketorolac-eluting stent or control stent. The primary end point was an intervention for pain defined as unscheduled physician contact, change in pain medication or early stent removal.	The safety of the ketorolac loaded stent was confirmed. A trend toward a treatment benefit was noted for patients receiving drug loaded stents, specifically young male patients appeared to require less pain medication.	(98)
2011	Animal study	Zotarolimus eluting stent (ZES)	10 pigs and 6 rabbits were inserted with a ZES and bare metal stent (BMS) in each ureter. CT or IVU were performed every week for the following 4 weeks for pigs and 8 weeks for rabbits and renal scintigraphies on week 3. Luminal and intraluminal patency evaluated by optical coherence tomography, ureter histology.	ZESs in the pig and rabbit ureter were not related to hyperplastic reaction resulting in stent occlusion. These stents were related to significantly lower hyperplastic reaction in comparison with BMSs while inflammation rates were similar for both stent types.	(101)
2012	Human study	Triclosan eluting stent	20 patients prospectively randomized were stented during 7-15 days with triclosan eluting stent alone or control stent plus 3 days levofloxacin.	Triclosan eluting stent had no marked impact on biofilm formation, encrustation or infection development in short-term stented patients, but decrease pain on activity and urination.	(10)
2012	In vitro study	Chlorhexidine (CHX) eluting stent	Evaluated growth inhibition on ureteral stent segments coated with chlorhexidine (CHX). The tests were conducted using common urinary pathogens: Enterococci, <i>Pseudomonas</i> , and <i>Escherichia coli</i> . Coated stent segments were inserted into bacterial suspensions and counting by culture and turbidity	Bacterial growth measured as turbidity and as colony-forming units showed a significant inhibition effect of initial bacteria adhesion to the CHX coated stent compared with the controls.	(90)

2012	Animal study	Rifampin and tigecycline immersed ureteral stents	Efficacy of tigecycline and rifampin alone or combined in preventing ureteral stent infection due to <i>E. faecalis</i> inoculated rat bladders.	Rifampin in combination with tigecycline demonstrated no bacterial cultivated in urine or in stent.	(93)
2012	Animal study	Indomethacin eluting absorbable urethral stent	Evaluate the effect of an indomethacin-eluting biodegradable urethral stent on the production of inflammatory cytokines <i>in vitro</i> and the degradation and biocompatibility of the new stent <i>in vivo</i> during 3 months.	Indomethacin-eluting can be safely added to biodegradable stents without major influence on the degradation time. Less severe epithelial polyposis at 3 weeks, but no difference at 3 months.	(99)
2015	In vitro study	Ketoprofen-eluting biodegradable stent	Biodegradable ureteral stent impregnated with Ketoprofen by CO ₂ high pressure vessel. Ketoprofen release evaluated <i>in vitro</i> .	50% of ketoprofen release occurred in the first 10 h and then the final 50% over the next 60 h, while stent degrade during 2 weeks.	(18)

I-6. TISSUE-ENGINEERED STENTS

From the last developments in stent-engineering developments, we expect these devices to be applied in other fields or in new clinical scenarios in particularly in the regeneration the ureters and urethra. One of the most innovative ideas for ureteral stents is their application in tissue engineering field. *Amiel et al (110)*, to the best of our knowledge, were the first to suggest the use of a natural urethral stent made of polylactic-co-glycolic acid (PLGA) in combination with autologous chondrocytes. These systems would be advantageous due to its biocompatibility. In this study the authors investigated the feasibility of engineering cartilage stents *In vitro* and *In vivo*. *Xu et al (111)* engineered an artificial ureter and performed a transplantation of *In vitro* expanded autologous urothelial cells (chondrocytes) onto an *In vivo* prefabricated capsular absorbable stent using tissue engineering methods. The absorbable stent made by PLLA were transplanted into the subcutaneous of rat model for a period until 3 weeks to induce the formation of connective tissue capsules on their surfaces, and the results of this study showed that absorbable stents could be an alternative cell carrier for tissue engineered ureters, especially with embedding time from 2 to 3 weeks. Stents coating with autologous tissue should be more biocompatibility and have a more favorable host response compared with conventional stents. Collagen and fibroblasts was found in stents surface after explanation indicating tissue restoration (112).

I-7. CONCLUSIONS AND FUTURE PERSPECTIVES

Ureteral stents continue to be an indispensable medical device in the daily urological clinical practice, even featuring various complications such bacterial adhesion, development of encrustation and patients discomfort. To date none of the technological developments has lead to the “ideal stent”, but much progress has been made in the stent design by improving the physical characteristics of the biomaterials and the application of new coatings. Developments regarding biodegradable metal-based stents could, in the future, be applied in design of stents that can maintain patency and degrade in the desired time period. The development of biodegradable materials that can be combined with drug-eluting technologies shows to be a promise in improving patient’s symptoms both by the degradation and the elution of drugs, that could help reduce the most frequent complications. The new technologies developed are envisaged to be applied not only in the next generation of ureteral stents but the application of these ureteral stents will open new treatment possibilities in a variety of different urological clinical scenarios

REFERENCES

1. Bonissent A, Gauthier E, Finney JL. Monte-Carlo Study of the Crystal-Melt Interface. *Acta Crystallogr A*. 1978;34:S209-S.
2. Al-Aown A, Kyriazis I, Kallidonis P, Kraniotis P, Rigopoulos C, Karnabatidis D, et al. Ureteral stents: new ideas, new designs. *Therapeutic advances in urology*. 2010;2(2):85-92.
3. Lange D, Elwood CN, Chew BH. *Biomaterials in Urology - Beyond Drug Eluting and Degradable - A Rational Approach to Ureteral Stent Design* 2011. 459-74 p.
4. Chew BH, Lange D. Ureteral stent symptoms and associated infections: a biomaterials perspective. *Nature Reviews Urology*. 2009;6(8):440-8.
5. Venkatesan N, Shroff S, Jeyachandran K, Doble M. Effect of uropathogens on in vitro encrustation of polyurethane double J ureteral stents. *Urological research*. 2011;39(1):29-37.
6. Dellis A, Joshi HB, Timoney AG, Keeley FX, Jr. Relief of Stent Related Symptoms: Review of Engineering and Pharmacological Solutions. *Journal of Urology*. 2010;184(4):1267-72.
7. Beiko DT, Knudsen BE, Denstedt JD. Reviews in endourology - Advances in ureteral stent design. *Journal of Endourology*. 2003;17(4):195-9.
8. Chew BH, Denstedt JD. Technology Insight: novel ureteral stent materials and designs. *Nat Clin Pract Urol*. 2004;1(1):44-8.
9. Cadieux PA, Chew BH, Nott L, Seney S, Elwood CN, Wignall GR, et al. Use of Triclosan-Eluting Ureteral Stents in Patients with Long-Term Stents. *Journal of Endourology*. 2009;23(7):1187-94.

10. Mendez-Probst CE, Goneau LW, MacDonald KW, Nott L, Seney S, Elwood CN, et al. The use of triclosan eluting stents effectively reduces ureteral stent symptoms: a prospective randomized trial. *BJU International*. 2012;110(5):749-54.
11. Lange D, Bidnur S, Hoag N, Chew BH. Ureteral stent-associated complications[mdash]where we are and where we are going. *Nat Rev Urol*. 2015;12(1):17-25.
12. Norris RD, Sur RL, Springhart WP, Marguet CG, Mathias BJ, Pletrow PK, et al. A prospective, randomized, double-blinded placebo-controlled comparison of extended release oxybutynin versus phenazopyridine for the management of postoperative ureteral stent discomfort. *Urology*. 2008;71(5):792-5.
13. Beddingfield R, Pedro RN, Hinck B, Kreidberg C, Feia K, Monga M. Alfuzosin to Relieve Ureteral Stent Discomfort: A Prospective, Randomized, Placebo Controlled Study. *Journal of Urology*. 2009;181(1):170-6.
14. Yang L, Whiteside S, Cadieux PA, Denstedt JD. Ureteral stent technology: Drug-eluting stents and stent coatings. *Asian Journal of Urology*. 2015;2(4):194-201.
15. Barros AA, Duarte ARC, Pires RA, Sampaio-Marques B, Ludovico P, Lima E, et al. Bioresorbable ureteral stents from natural origin polymers. *J Biomed Mater Res B*. 2015;103(3):608-17.
16. Chew BH, Lange D, Paterson RF, Hendlin K, Monga M, Clinkscales KW, et al. Next Generation Biodegradable Ureteral Stent in a Yucatan Pig Model. *Journal of Urology*. 2010;183(2):765-71.
17. Barros A, Browne S, Oliveira C, Reis RL, Lima EE, Duarte AR, et al. Targeting urothelial tumors of upper urinary tract with drug-eluting stents impregnated by supercritical fluids. *Frontiers in Bioengineering and Biotechnology*. 2016.
18. Barros AA, Oliveira C, Reis RL, Lima E, Duarte ARC. Ketoprofen-eluting biodegradable ureteral stents by CO2 impregnation: In vitro study. *International Journal of Pharmaceutics*. 2015;495(2):651-9.
19. Zimskind PD, Fetter TR, Wilkerson JI. Clinical Use of Long-Term Indwelling Silicone Rubber Ureteral Splints Inserted Cystoscopically. *Journal of Urology*. 1967;97(5):840-&.
20. Haleblan G, Kijvikai K, de la Rosette J, Premingert G. Ureteral stenting and urinary stone management: A systematic review. *Journal of Urology*. 2008;179(2):424-30.
21. Zhou L, Cai X, Li H, Wang KJ. Effects of alpha-Blockers, Antimuscarinics, or Combination Therapy in Relieving Ureteral Stent-Related Symptoms: A Meta-Analysis. *J Endourol*. 2015;29(6):650-6.
22. Irani J, Siquier J, Pires C, Lefebvre O, Dore B, Aubert J. Symptom characteristics and the development of tolerance with time in patients with indwelling double-pigtail ureteric stents. *Bju International*. 1999;84(3):276-9.
23. Joshi HB, Stainthorpe A, MacDonagh RP, Keeley FX, Timoney AG. Indwelling ureteral stents: Evaluation of symptoms, quality of life and utility. *Journal of Urology*. 2003;169(3):1065-9.
24. Acosta-Miranda AM, Milner J, Turk TMT. The FECal Double-J: A Simplified Approach in the Management of Encrusted and Retained Ureteral Stents. *Journal of Endourology*. 2009;23(3):409-15.
25. Monga M, Klein E, Castaneda-Zuniga WR, Thomas R. The Forgotten Indwelling Ureteral Stent: A Urological Dilemma. *The Journal of Urology*. 153(6):1817-9.
26. Nikkhou K, Kaimakliotis HZ, Singh D. Fractured Retained Ureteral Stent in a Patient Lost to Follow-up. *Journal of Endourology*. 2011;25(12):1829-30.
27. Lam JS, Gupta M. Tips and tricks for the management of retained ureteral stents. *Journal of Endourology*. 2002;16(10):733-41.

28. Chung SY, Stein RJ, Landsittel D, Davies BJ, Cuellar DC, Hrebinko RL, et al. 15-year experience with the management of extrinsic ureteral obstruction with indwelling ureteral stents. *The Journal of urology*. 2004;172(2):592-5.
29. Schlick RW, Planz K. Potentially useful materials for biodegradable ureteric stents. *Brit J Urol*. 1997;80(6):908-10.
30. Gorman SP, Tunney MM, Keane PF, Van Bladel K, Bley B. Characterization and assessment of a novel poly(ethylene oxide)/polyurethane composite hydrogel (Aquavene (R)) as a ureteral stent biomaterial. *J Biomed Mater Res*. 1998;39(4):642-9.
31. Jones DS, Garvin CP, Gorman SP. Design of a simulated urethra model for the quantitative assessment of urinary catheter lubricity. *Journal of materials science Materials in medicine*. 2001;12(1):15-21.
32. Marchesani G. Polyurethane and silicone: myths and misconceptions. *J Intraven Nurs*. 1995;18(6):330-2.
33. Marx M, Bettmann MA, Bridge S, Brodsky G, Boxt LM, Richie JP. The Effects of Various Indwelling Ureteral Catheter Materials on the Normal Canine Ureter. *J Urology*. 1988;139(1):180-5.
34. Pauer W, Lugmayr H. Metallic Wallstents - a New Therapy for Extrinsic Ureteral Obstruction. *Journal of Urology*. 1992;148(2):281-4.
35. Kulkarni R, Bellamy E. Nickel-titanium shape memory alloy Memokath 051 ureteral stent for managing long-term ureteral obstruction: 4-year experience. *Journal of Urology*. 2001;166(5):1750-4.
36. Liatsikos EN, Karnabatidis D, Katsanos K, Kallidonis P, Katsakiori P, Kagadis GC, et al. Ureteral Metal Stents: 10-Year Experience With Malignant Ureteral Obstruction Treatment. *Journal of Urology*. 2009;182(6):2613-7.
37. Masood J, Papatsoris A, Buchholz N. Dual Expansion Nickel-Titanium Alloy Metal Ureteric Stent: Novel Use of a Metallic Stent to Bridge the Ureter in the Minimally Invasive Management of Complex Ureteric and Pelviureteric Junction Strictures. *Urol Int*. 2010;84(4):477-8.
38. Papatsoris AG, Buchholz N. A Novel Thermo-Expandable Ureteral Metal Stent for the Minimally Invasive Management of Ureteral Strictures. *Journal of Endourology*. 2010;24(3):487-91.
39. Sountoulides P, Kaplan A, Kaufmann OG, Sofikitis N. Current status of metal stents for managing malignant ureteric obstruction. *Bju International*. 2010;105(8):1066-72.
40. Borin JF, Melamud O, Clayman RV. Initial experience with full-length metal stent to relieve malignant ureteral obstruction. *Journal of Endourology*. 2006;20(5):300-4.
41. Kadlec AO, Ellimoottil CS, Greco KA, Turk TM. Five-Year Experience with Metallic Stents for Chronic Ureteral Obstruction. *Journal of Urology*. 2013;190(3):937-41.
42. Agrawal S, Brown CT, Bellamy EA, Kulkarni R. The thermo-expandable metallic ureteric stent: an 11-year follow-up. *Bju International*. 2009;103(3):372-6.
43. Hendlin K, Korman E, Monga M. New Metallic Ureteral Stents: Improved Tensile Strength and Resistance to Extrinsic Compression. *Journal of Endourology*. 2012;26(3):271-4.
44. Moskovitz B, Halachmi S, Nativ O. A New Self-Expanding, Large-Caliber Ureteral Stent: Results of a Multicenter Experience. *Journal of Endourology*. 2012;26(11):1523-7.
45. Kim JH, Song K, Jo MK, Park JW. Palliative care of malignant ureteral obstruction with polytetrafluoroethylene membrane-covered self-expandable metallic stents: initial experience. *Korean J Urol*. 2012;53(9):625-31.
46. Augst AD, Kong HJ, Mooney DJ. Alginate Hydrogels as Biomaterials. *Macromolecular Bioscience*. 2006;6(8):623-33.

47. John T, Rajpurkar A, Smith G, Fairfax M, Triest J. Antibiotic pretreatment of hydrogel Ureteral Stent. *Journal of Endourology*. 2007;21(10):1211-5.
48. Desgrandchamps F, Moulinier F, Daudon M, Teillac P, LeDuc A. An in vitro comparison of urease-induced encrustation of JJ stents in human urine. *British Journal of Urology*. 1997;79(1):24-7.
49. Zupkas P, Parsons CL, Percival C, Monga M. Pentosanpolysulfate coating of silicone reduces encrustation. *Journal of Endourology*. 2000;14(6):483-8.
50. Stickler DJ, Evans A, Morris N, Hughes G. Strategies for the control of catheter encrustation. *International Journal of Antimicrobial Agents*. 2002;19(6):499-506.
51. Tunney MM, Gorman SP. Evaluation of a poly(vinyl pyrrolidone)-coated biomaterial for urological use. *Biomaterials*. 2002;23(23):4601-8.
52. Riedl CR, Witkowski M, Plas E, Pflueger H. Heparin coating reduces encrustation of ureteral stents: a preliminary report. *International Journal of Antimicrobial Agents*. 2002;19(6):507-10.
53. Cauda F, Cauda V, Fiori C, Onida B, Garrone E. Heparin coating on ureteral Double J stents prevents encrustations: An *in vivo* case study. *Journal of Endourology*. 2008;22(3):465-72.
54. Tenke P, Riedl CR, Jones GL, Williams GJ, Stickler D, Nagy E. Bacterial biofilm formation on urologic devices and heparin coating as preventive strategy. *International Journal of Antimicrobial Agents*. 2004;23:S67-S74.
55. Laube N, Kleinen L, Bradenahl J, Meissner A. Diamond-like carbon coatings on ureteral stents - A new strategy for decreasing the formation of crystalline bacterial biofilms? *Journal of Urology*. 2007;177(5):1923-7.
56. Lopez-Lopez G, Pascual A, Perea EJ. Effect of plastic catheter material on bacterial adherence and viability. *J Med Microbiol*. 1991;34(6):349-53.
57. Arguinarena FJT, del Busto EF. Self-expanding polytetrafluoroethylene covered nitinol stents for the treatment of ureteral stenosis: Preliminary report. *Journal of Urology*. 2004;172(2):620-3.
58. Leveillee RJ, Pinchuk L, Wilson GJ, Block NL. A new self-expanding lined stent-graft in the dog ureter: Radiological, gross, histopathological and scanning electron microscopic findings. *Journal of Urology*. 1998;160(5):1877-82.
59. Ko R, Cadieux PA, Dalsin JL, Lee BP, Elwood CN, Razvi H. First prize: Novel uropathogen-resistant coatings inspired by marine mussels. *J Endourol*. 2008;22(6):1153-60.
60. Pechey A, Elwood CN, Wignall GR, Dalsin JL, Lee BP, Vanjecek M, et al. Anti-adhesive coating and clearance of device associated uropathogenic *Escherichia coli* cystitis. *J Urol*. 2009;182(4):1628-36.
61. Rojas IA, Slunt JB, Grainger DW. Polyurethane coatings release bioactive antibodies to reduce bacterial adhesion. *Journal of Controlled Release*. 2000;63(1-2):175-89.
62. Schlick RW, Planz K. In vitro results with special plastics for biodegradable endoureteral stents. *Journal of Endourology*. 1998;12(5):451-5.
63. Lumiaho J, Heino A, Tunninen V, Ala-Opas M, Talja M, Valimaa T, et al. New bioabsorbable polylactide ureteral stent in the treatment of ureteral lesions: An experimental study. *Journal of Endourology*. 1999;13(2):107-12.
64. Lumiaho J, Heino A, Kauppinen T, Talja M, Alhava E, Valimaa T, et al. Drainage and antireflux characteristics of a biodegradable self-reinforced, self-expanding X-ray-positive poly-L,D-lactide spiral partial Ureteral stent: An experimental study. *Journal of Endourology*. 2007;21(12):1559-64.

65. Lumiaho J, Heino A, Pietilainen T, Ala-Opas M, Talja M, Valimaa T, et al. The morphological, in situ effects of a self-reinforced bioabsorbable polylactide (SR-PLA 96) ureteric stent; An experimental study. *Journal of Urology*. 2000;164(4):1360-3.
66. Lumiaho J, Heino A, Aaltomaa S, Valimaa T, Talja M. A short biodegradable helical spiral ureteric stent provides better antireflux and drainage properties than a double-J stent. *Scand J Urol Nephrol*. 2011;45(2):129-33.
67. Olweny EO, Landman J, Andreoni C, Collyer W, Kerbl K, Onciu M, et al. Evaluation of the use of a biodegradable ureteral stent after retrograde endopyelotomy in a porcine model. *Journal of Urology*. 2002;167(5):2198-202.
68. Talja M, Multanen M, Valimaa T, Tormala P. Bioabsorbable SR-PLGA horn stent after antegrade endopyelotomy: A case report. *Journal of Endourology*. 2002;16(5):299-302.
69. Isotalo T, Talja M, Valimaa T, Tormala P, Tammela TLJ. A Bioabsorbable self-expandable, self-reinforced poly-L-lactic acid urethral stent for recurrent urethral strictures: Long-term results. *Journal of Endourology*. 2002;16(10):759-62.
70. Laaksovirta S, Isotalo T, Talja M, Välimaa T, Törmälä P, Tammela TLJ. Interstitial Laser Coagulation and Biodegradable Self-Expandable, Self-Reinforced Poly-L-Lactic and Poly-L-Glycolic Copolymer Spiral Stent in the Treatment of Benign Prostatic Enlargement. *Journal of Endourology*. 2002;16(5):311-5.
71. Lingeman JE, Schulsinger DA, Kuo RL. Phase I trial of a temporary ureteral drainage stent. *Journal of Endourology*. 2003;17(3):169-71.
72. Lingeman JE, Preminger GM, Berger Y, Denstedt JD, Goldstone L, Segura JW, et al. Use of a temporary ureteral drainage stent after uncomplicated ureteroscopy: Results from a phase II clinical trial. *Journal of Urology*. 2003;169(5):1682-8.
73. Chew BH, Davoudi H, Li J, Denstedt JD. An In Vivo Porcine Evaluation of the Safety, Bioavailability, and Tissue Penetration of a Ketorolac Drug-Eluting Ureteral Stent Designed to Improve Comfort. *Journal of Endourology*. 2010;24(6):1023-9.
74. Li G, Wang ZX, Fu WJ, Hong BF, Wang XX, Cao L, et al. Introduction to biodegradable polylactic acid ureteral stent application for treatment of ureteral war injury. *Bju International*. 2011;108(6):901-6.
75. Lock JY, Draganov M, Whall A, Dhillon S, Upadhyayula S, Vullev VI, et al. Antimicrobial properties of biodegradable magnesium for next generation ureteral stent applications. *Conf Proc IEEE Eng Med Biol Soc*. 2012;2012:1378-81.
76. Lock JY, Wyatt E, Upadhyayula S, Whall A, Nunez V, Vullev VI, et al. Degradation and antibacterial properties of magnesium alloys in artificial urine for potential resorbable ureteral stent applications. *Journal of biomedical materials research Part A*. 2014;102(3):781-92.
77. Zhang MQ, Zou T, Huang YC, Shang YF, Yang GG, Wang WZ, et al. Braided thin-walled biodegradable ureteral stent: Preliminary evaluation in a canine model. *International Journal of Urology*. 2014;21(4):401-7.
78. Zou T, Wang L, Li WC, Wang WZ, Chen F, King MW. A resorbable bicomponent braided ureteral stent with improved mechanical performance. *J Mech Behav Biomed*. 2014;38:17-25.
79. Wang XQ, Shan HL, Wang JX, Hou YC, Ding JX, Chen QH, et al. Characterization of nanostructured ureteral stent with gradient degradation in a porcine model. *Int J Nanomed*. 2015;10:3055-64.
80. Lange D, Chew BH. Ureteral stents: design and materials. *Biomaterials and Tissue Engineering in Urology*. 2009:85-103.
81. Hadaschik BA, Paterson RF, Fazli L, Clinkscales KW, Shalaby SW, Chew BH. Investigation of a novel degradable ureteral stent in a porcine model. *Journal of Urology*. 2008;180(3):1161-6.

82. Lange D, Chew BH. Update on ureteral stent technology. *Therapeutic advances in urology*. 2009;1(3):143-8.
83. Chew BH, Paterson RF, Clinkscales KW, Levine BS, Shalaby SW, Lange D. In Vivo Evaluation of the Third Generation Biodegradable Stent: A Novel Approach to Avoiding the Forgotten Stent Syndrome. *Journal of Urology*. 2013;189(2):719-25.
84. Silva SS, Oliveira JM, Sá-Lima H, Sousa RA, Mano JF, Reis RL. 2.211 - Polymers of Biological Origin A2 - Ducheyne, Paul. *Comprehensive Biomaterials*. Oxford: Elsevier; 2011. p. 187-205.
85. Wang J, Smith CE, Sankar J, Yun Y, Huang N. Absorbable magnesium-based stent: physiological factors to consider for in vitro degradation assessments. *Regen Biomater*. 2015;2(1):59-69.
86. Tsuji T, Tamai H, Igaki K, Kyo E, Kosuga K, Hata T, et al. Biodegradable stents as a platform to drug loading. *International Journal of Cardiovascular Interventions*. 2003;5(1):13-6.
87. Chew BH, Cadieux PA, Reid G, Denstedt JD. In-vitro activity of triclosan-eluting ureteral stents against common bacterial uropathogens. *Journal of Endourology*. 2006;20(11):949-58.
88. Cadieux P, Chew BH, Nott L, Denstedt JD. The use of triclosan eluting ureteral stents in longterm stented patients. *Journal of Urology*. 2007;177(4):103-.
89. Cadieux PA, Chew BH, Knudsen BE, DeJong K, Rowe E, Reid G, et al. Triclosan loaded ureteral stents decrease proteus mirabilis 296 infection in a rabbit urinary tract infection model. *Journal of Urology*. 2006;175(6):2331-5.
90. Zelichenko G, Steinberg D, Lorber G, Friedman M, Zaks B, Lavy E, et al. Prevention of Initial Biofilm Formation on Ureteral Stents Using a Sustained Releasing Varnish Containing Chlorhexidine: In Vitro Study. *Journal of Endourology*. 2013;27(3):333-7.
91. Multanen M, Talja M, Hallanvuo S, Siitonen A, Valimaa T, Tammela TLJ, et al. Bacterial adherence to silver nitrate coated poly-L-lactic acid urological stents in vitro. *Urological Research*. 2000;28(5):327-31.
92. Multanen M, Tammela TLJ, Laurila M, Seppala J, Valimaa T, Tormala P, et al. Biocompatibility, encrustation and biodegradation of ofloxacin and silver nitrate coated poly-L-lactic acid stents in rabbit urethra. *Urological Research*. 2002;30(4):227-32.
93. Minardi D, Cirioni O, Ghiselli R, Silvestri C, Mocchegiani F, Gabrielli E, et al. Efficacy of Tigecycline and Rifampin Alone and in Combination against *Enterococcus faecalis* Biofilm Infection in a Rat Model of Ureteral Stent. *J Surg Res*. 2012;176(1):1-6.
94. El-Feky MA, El-Rehewy MS, Hassan MA, Abolella HA, El-Baky RMA, Gad GF. Effect of Ciprofloxacin and N-acetylcysteine on Bacterial Adherence and Biofilm Formation on Ureteral Stent Surfaces. *Polish Journal of Microbiology*. 2009;58(3):261-7.
95. Cirioni O, Ghiselli R, Minardi D, Orlando F, Mocchegiani F, Silvestri C, et al. RNAIII-inhibiting peptide affects biofilm formation in a rat model of staphylococcal ureteral stent infection. *Antimicrob Agents Ch*. 2007;51(12):4518-20.
96. Orlando F, Ghiselli R, Cirioni O, Minardi D, Tomasinsig L, Mocchegiani F, et al. BMAP-28 improves the efficacy of vancomycin in rat models of gram-positive cocci ureteral stent infection. *Peptides*. 2008;29(7):1118-23.
97. Liatsikos EN, Karnabatidis D, Kagadis GC, Rokkas K, Constantinides C, Christeas N, et al. Application of paclitaxel-eluting metal mesh stents within the pig ureter: An experimental study. *Eur Urol*. 2007;51(1):217-23.
98. Krambeck AE, Walsh RS, Denstedt JD, Preminger GM, Li J, Evans JC, et al. A Novel Drug Eluting Ureteral Stent: A Prospective, Randomized, Multicenter Clinical Trial to Evaluate the Safety

- and Effectiveness of a Ketorolac Loaded Ureteral Stent. *The Journal of Urology*. 2010;183(3):1037-43.
99. Kotsar A, Nieminen R, Isotalo T, Mikkonen J, Uurto I, Kellomaki M, et al. Preclinical Evaluation of New Indomethacin-Eluting Biodegradable Urethral Stent. *Journal of Endourology*. 2012;26(4):387-92.
100. Krane LS, Gorbachinsky I, Sirintrapun J, Yoo JJ, Atala A, Hodges SJ. Halofuginone-Coated Urethral Catheters Prevent Periurethral Spongiosclerosis in a Rat Model of Urethral Injury. *Journal of Endourology*. 2011;25(1):107-12.
101. Kallidonis P, Kitrou P, Karnabatidis D, Kyriazis I, Kalogeropoulou C, Tsamandas A, et al. Evaluation of Zotarolimus-Eluting Metal Stent in Animal Ureters. *Journal of Endourology*. 2011;25(10):1661-7.
102. Mikkonen J, Uurto I, Isotalo T, Kotsar A, Tammela TLJ, Talja M, et al. Drug-eluting bioabsorbable stents - An in vitro study. *Acta Biomaterialia*. 2009;5(8):2894-900.
103. Kotsar A, Isotalo T, Juuti H, Mikkonen J, Leppiniemi J, Hanninen V, et al. Biodegradable braided poly(lactic-co-glycolic acid) urethral stent combined with dutasteride in the treatment of acute urinary retention due to benign prostatic enlargement: a pilot study. *Bju International*. 2009;103(5):626-9.
104. Cormio L, LaForgia P, LaForgia D, Siitonen A, Ruutu M. Is it possible to prevent bacterial adhesion onto ureteric stents? *Urol Res*. 1997;25(3):213-6.
105. Cormio L, LaForgia P, Siitonen A, Ruutu M, Tormala P, Talja M. Immersion in antibiotic solution prevents bacterial adhesion onto biodegradable prostatic stents. *Brit J Urol*. 1997;79(3):409-13.
106. Antimisiaris SG, Siablis D, Liatsikos E, Kalogeropoulou C, Tsota I, Tsotas V, et al. Liposome-coated metal stents: An in vitro evaluation of controlled-release modality in the ureter. *Journal of Endourology*. 2000;14(9):743-7.
107. Shin JH, Song HY, Choi CG, Yuk SH, Kim JS, Kim YM, et al. Tissue hyperplasia: Influence of a paclitaxel-eluting covered stent - Preliminary study in a canine urethral model. *Radiology*. 2005;234(2):438-44.
108. Minardi D, Ghiselli R, Cirionicy O, Giacometti A, Kamysz W, Orlando F, et al. The antimicrobial peptide Tachyplesin III coated alone and in combination with intraperitoneal piperacillin-tazobactam prevents ureteral stent *Pseudomonas* infection in a rat subcutaneous pouch model. *Peptides*. 2007;28(12):2293-8.
109. Lange D, Elwood CN, Choi K, Hendlin K, Monga M, Chew BH. Uropathogen Interaction With the Surface of Urological Stents Using Different Surface Properties. *Journal of Urology*. 2009;182(3):1194-200.
110. Amiel GE, Yoo JJ, Kim BS, Atala A. Tissue engineered stents created from chondrocytes. *J Urology*. 2001;165(6):2091-5.
111. Xu Y, Fu W, Li G, Shi J, Tan H, Hu K, et al. Autologous urothelial cells transplantation onto a prefabricated capsular stent for tissue engineered ureteral reconstruction. *Journal of Materials Science: Materials in Medicine*. 2012;23(4):1119-28.
112. Nakayama Y, Zhou YM, Ishibashi-Ueda H. Development of *in vivo* tissue-engineered autologous tissue-covered stents (biocovered stents). *J Artif Organs*. 2007;10(3):171-6.

Chapter II

Materials and Methods

Chapter II

Materials and Methods

OVERVIEW

In this chapter are described the different materials, methodologies and procedures used in the development of biodegradable ureteral stents (BUS) and drug-eluting BUS. BUS developed and studied under this thesis are based on different polymer formulations composed by gelatin, alginate, gellan gum, as main components, bismuth as radiopaque agent and polycaprolactone as a coating. In terms of production technologies, the supercritical fluid technology was used both for drying and impregnation of BUS. Within the drug-eluting BUS, different types of active pharmaceuticals compounds (APIs) were impregnated, namely (i) ketoprofen, (ii) paclitaxel, (iii) doxorubicin, (iv) epirubicin and (iv) gemcitabine. Different characterization techniques were applied to the BUS developed to evaluate morphological and mechanical properties, *in vitro* stability, biocompatibility and *in vivo* performance in a pig model. Figure II-1 presents an overview of the formulations studied as well as the respective processing and characterization methodologies. Many of the materials used in this thesis were purchased. The detailed specifications of the suppliers can be found in the experimental subsections of each chapter. Likewise, equipment suppliers are also discriminated in those subsections.

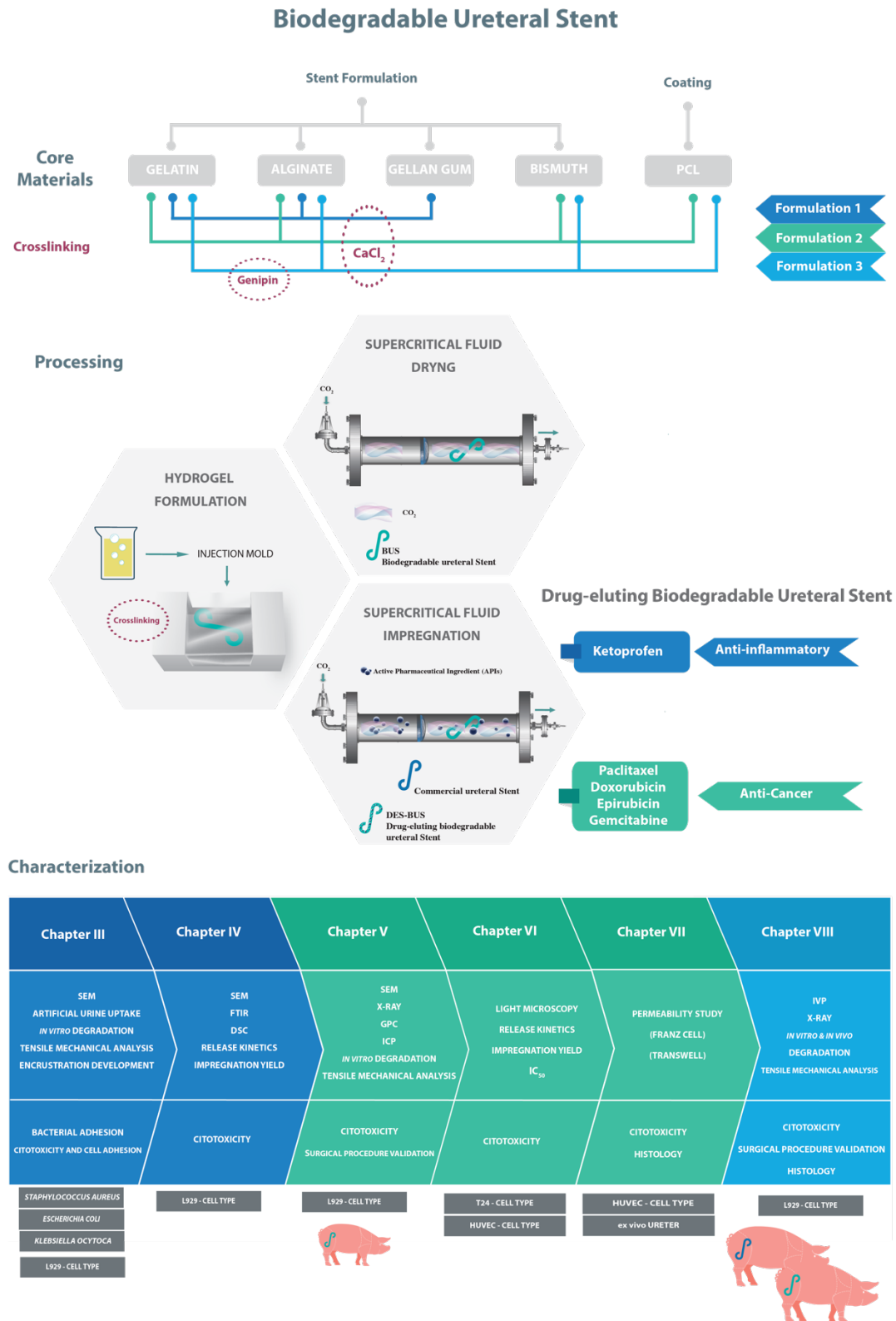


Figure II-1. Schematic overview of the materials studied, processing and characterization techniques. Essentially, five materials were used throughout the thesis for the formulation of the biodegradable ureteral stent (BUS): gelatin; alginate; gellan gum; bismuth and polycaprolactone (PCL). Two crosslinking agents were used: calcium chloride (CaCl₂) and genipin. Five active pharmaceutical ingredients (APIs) were tested in the development of drug-eluting BUS: ketoprofen (Chapter IV), paclitaxel, doxorubicin,

epirubicin and gemcitabine (chapter VI and VII). The techniques used to characterize the materials/ structures are here summarized. (SEM - Scanning electron microscopy; FTIR- Fourier transform infrared spectroscopy; DSC - Differential scanning calorimetry; GPC - Gel Permeation Chromatography; ICP – Ion coupled plasma; IC50 - half maximal inhibitory concentration; IVP – Intravenous pyelogram).

II-1. MATERIALS

II-1.1. Biodegradable ureteral stents core material

Biodegradable ureteral stents (BUS) developed under the scope of this thesis were based in natural origin polymers, such as gelatin, alginate and gellan gum. Natural origin polymers derived from renewable resources, namely from algae, animal, plant, and microorganisms, offer the advantage of specific degradation rates, chemical versatility, similar biological macromolecules, which biological environment is prepared to identify and to deal metabolically with, present a good biological performance with low cytotoxicity or adverse immunological reactions, frequently noticed with synthetic polymers(1). Therefore, the characteristics of the natural origin polymers, like the ability to uptake high amount of water and create hydrogels, are important for the design of drug-eluting devices that can also deliver active pharmaceutical compounds (APIs) locally avoiding common side effects(2). Bismuth was used in the stent formulation to provide the radiopaque properties to the developed BUS.

II-1.1.1. Gelatin

Gelatin was used as a core material in the development of BUS. Gelatin is a natural origin polymer derived from partial acid (gelatin type A) or alkaline hydrolysis (gelatin type B) of collagen obtained from different sources, such as bovine and porcine which are the most widely used(3-5). Collagen is a protein composed of linear, fiber-like structures. Different physical properties and chemical heterogeneity, such as molecular weights (MWs) and isoionic points, can be obtained depending the collagen source and the preparation technique(6, 7). Gelatin in last years has extensive been used in foods, cosmetics, pharmaceuticals and biomedical fields due to its remarkable properties, such as biodegradability, biocompatibility, low antigenicity, does not produce dangerous byproducts upon enzymatic degradation, contain motifs such as Arginine-Glycine-Aspartic acid sequences that can modulate cell adhesion, high number of accessible functional

groups for modification (e.g crosslinking) and targeting ligands (e.g drug delivery vehicles), as well commercially available at low cost and abundantly available(7, 8). Gelatin molecules are mainly composed by four groups of amino acids, being in every 1000 gelatin's amino acid residues, 330 are glycine, 132 are proline, 112 are alanine and 93 are hydroxyproline. The remainder corresponds to other different residues(4). A typical structure of gelatin is –Ala-Gly-Pro-Arg-Gly-Glu-4Hyp-Gly-Pro-(4, 9). The triple helical structure of gelatin is related with (GlycineX-Proline)_n representation, where X signifies the amino acids mostly e, arginine, methionine, lysin and valine. Gelatin surface has mixed anion and cation character (polyampholyte). Nonetheless, at lower pH gelatin is positively charged and negatively charged at higher pH(5, 10). Gelatin is polyampholyte approximately at pH 9 (for gelatin type A) and pH 5 (for gelatin type B)(11). At ideal concentrations, gelatin solutions are in the sol state at around 40°C and change into gels when they are cooled down to room temperature. This gelation normally occurs by physical crosslinking, which results in the formation of intersection regions and finally a three-dimensional branched network(12, 13). The sol-gel transformation is due to a conformational disorder-order alteration of the gelatin chains forming thermo-reversible networks by associating helices in intersection regions stabilized by hydrogen bonds(7, 12, 14). Physico-chemical characteristics of gelatin gels can be modified using a chemical crosslinking. The most commonly used chemical crosslinkers include formaldehyde, glutaraldehyde, polyepoxy compounds, dimethyl suberimidate, carbodiimides, and acyl azide, and are normally used to bond functional groups of amino acids(7-9, 15). However, these compounds present generally cytotoxicity conditioning their use in biomedical applications(15). In this thesis, biodegradable ureteral stents (BUS) were developed using gelatin type A from porcine skin. Besides the physical crosslinking used in all chapters in **chapter IX**, genipin was used as a chemical crosslinking. Genipin is naturally occurring reagent extracted from the fruits of *Gardenia jamisnoides Ellis* with low toxicity(8, 15, 16). Genipin is a chemical crosslinking reacting with amino acid or proteins and polysaccharides, and has the advantage to have lower toxicity than most of the synthetic crosslinkers mentioned above. Citotoxicity of genipin has been shown to be 10,000 times less toxic than glutaraldehyde(17). The concentration and the number of amino groups available to react with genipin molecules will influence the degree of crosslinking(18-20). Genipin was used as crosslinker of gelatin in BUS formulation 3 in order to improve the *In vivo* stability of the BUS.

II-1.1.1.1 Genipin crosslinking gelatin

To date, chemical crosslinking is the most popular approach to crosslink gelatin. Chemical crosslinking agents can covalently link amine residues or covalently link carboxylic acid and amine residues. Genipin binds to the gelatin network structure, typically by bridging the free amine groups of lysine. The crosslinking reaction between genipin and gelatin is not fully understood but it has been hypothesized that happens by two distinct reactions (**figure II 2**). First a rapid nucleophilic attack of a lysine amino group to the ring structure of genipin causes the dihydropyran ring opening and the creation of a tertiary amine (Michael addition). The second reaction is slower and results in the crosslinking process by nucleophilic replacement of lysine amino group with a second piece of gelatin(21). During the reactions, a blue pigment is presumably formed through the oxygen radical-induced polymerization and dehydrogenation of several intermediary pigments(15, 21). This gelatin crosslinking process is slower compared with other the crosslinking reactions, namely using glutaraldehyde(15, 17, 21). In the preparation of BUS the time of reaction revealed to be ideal for the injection of the polymer solution into the mold.

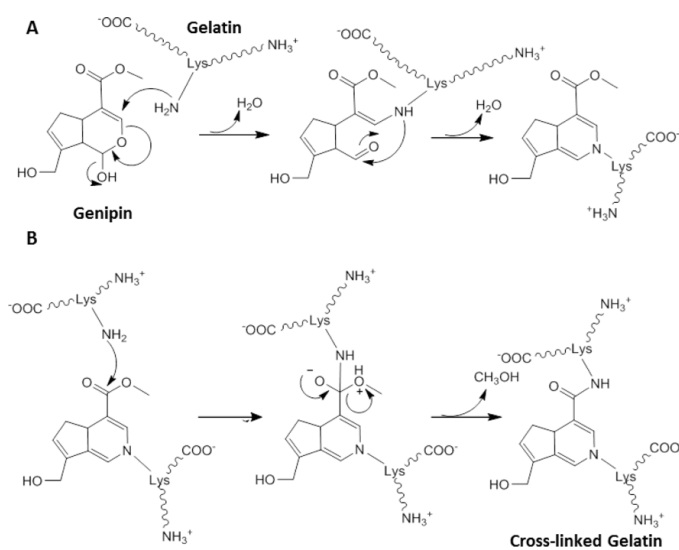


Figure II-2 Crosslinking reaction of gelatin by genipin with: a) first reaction through Michael addition to form stable intermediate; and b) second reaction with nucleophilic substitution of free lysine amine molecules into genipin activated ester. Adpated from Rose *et al.*(13)

II-1.1.2. Alginate

Alginate is one of the most studied polysaccharides as a biomaterial, being relatively abundant in nature (22). Alginate is an anionic polymer typically extracted from brown algae, such as

Laminaria hyperborea and *lessonia*, after an alkaline process. Succinctly, after filtration, alginate salt is obtained after the addition of calcium chloride or sodium. Alginic acid can be after obtained by treatment with diluted hydrochloric acid. Ultimately, upon purification and conversion, a water-soluble sodium alginate powder is obtained(23). Structurally, alginate is a linear unbranched copolymer composed by homopolymeric blocks of consecutive or alternating β (1 \rightarrow 4) linked D-mannuronic acid (M-blocks) and α (1 \rightarrow 4) linked L-gluronic acid elements (G-Blocks) (**Figure II 3**)(23, 24). The source of alginate influence the length and distribution of the M and G-blocks along the polymer chain(25). Moreover, both blocks present carboxyl groups that can be deprotonated exceeding the pH values of 3.2 and 4, respectively for G and M-blocks(23, 26). Consequently, alginate above the $pK_a \approx 3.4$ or 3.65 for glucuronic and mannuronic acid units, respectively, behaves as polyacid and exhibits polyanionic behavior, and the carboxyl groups became protonated(27, 28). Alginate has been extensively used to produce hydrogels for biomedical applications due to its low toxicity, *In vivo* biocompatibility, low cost as well as bacteriostatic, fungistatic, anti-microbial, haemostatic properties and mild gelation conditions(24). Alginate hydrogels are normally produced by an ionic crosslinking, due has an ionotropic sol transition, requiring the presence of ions for gelation(27-30). The type of ions used influences the stability of the ionic crosslinking, being stronger with divalent cations (such as Ca^{2+} , Mg^{2+} , Ba^{2+}) compared with monovalent cations (such as Na^+ and K^+). Ionic interactions are established between the G-blocks presents in the polymer chain of the alginate and the divalent cations through interactions with the carboxylic groups(23). The formation of a three-dimensional network that is frequently described by the “egg-box” model is developed due the replace of the hydrogen bonds between the carboxyl group of D- mannuronate and the 2-OH and 3-OH groups of the subsequent L- guluronate by divalent ions, by the creation of ionic inter-chain bridges(28, 31). These properties make alginate a suitable biomaterial to blend with gelatin and to be used in the BUS development.

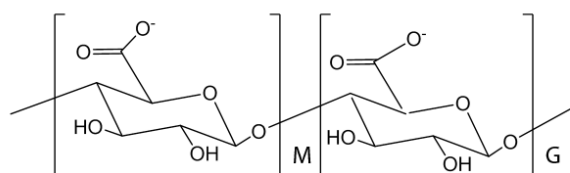


Figure II-3 Chemical structure of Alginate (M: manuronic repeating unit; G: glucuronic repeating unit).

II-1.1.3. Gellan Gum

Gellan gum is an anionic extracellular polysaccharide, produced by aerobic submerged fermentation of *Sphingomonas elodea*(32-34). Gellan gum is a linear and anionic polymer composed by approximately, 60% glucose, 20% glucuronic acid, and 20% rhamnose as a repeating unit, and two acyl groups, acetate and glycerate bound to glucose residue adjacent to glucuronic (**Figure II 4**)(33). Gellan gum can be found in two different forms, native (high acyl form) or deacetylated (low acyl) and is frequently coupled with significant amounts of impurities, such as cell protein that can be purified by filtration or centrifugation. Gellan gum in high acyl form shows two acyl groups on the glucose residue unlike in the low acyl form that is removed by alkaline treatment(32). Gellan gum is a thermally reversible gel with excellent stability and high gel strength. Nevertheless, in its high acyl form, gellan gum creates transparent, elastic and flexible gels, while in the low acyl form originate brittle gels(33, 35, 36). These characteristics and due to the capacity of forming injectable solutions and creating hydrogels with decreasing temperatures (physical crosslinking) and addition of ions (ionic crosslinking) have encouraged different applications and techniques to use it in food applications, in cosmetics, and as a drug delivery system(35, 37). The sol-gel transition of gellan gum is ionotropic, as in alginate(36, 37). Thus, the presence of cations is necessary for the formation of a stable hydrogel. The physical hydrogels should have a quite low water uptake (because the carboxylic groups are involved in the formation of the double helices) and, at the same time, a relevant elastic behaviour, which increases with the amount of the junction zones(34). On the other hand, chemical hydrogels, due to the presence of disordered chains, should have a high-water uptake (inversely proportional to the crosslinking degree) and, correspondingly, a small elastic behaviour(32). Under the scope of this thesis the gellan gum was used in the formulation of BUS in **chapter III and IV**.

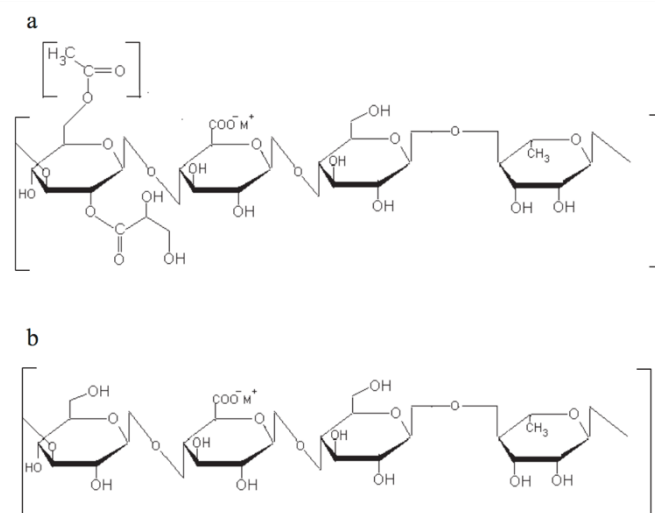


Figure II-4 Repeating units of chemical structure of a) native and b) deacetylated gellan gum.

II-1.1.4. Bismuth (III) carbonate basic

Bismuth subcarbonate was used in **chapter IV** until **chapter VIII (formulation 2 and 3)** to induce the radiopaque properties on BUS developed. Today's medical devices such as stents are used to diagnose and treat smaller and more distal areas of the vascular or urological pathway, requiring smaller device components than ever before. Many of these devices must be visible under fluoroscopy to ensure proper placement during the surgical procedure; yet, plastics used for the manufacture of these medical devices are inherently transparent to x-ray and fillers must be blended into the polymers to provide the required radiopacity (38). Bismuth Subcarbonate ($\text{Bi}_2\text{O}_3(\text{CO}_3)_2$) is one of these fillers and tends to have more radiopacity than barium compounds and can be used in smaller amounts than barium for similar results(39). The use of bismuth subcarbonate has been limited because reported of heat stability issues as it tends to degrade at 225°C(39). However, under the scope of this thesis the process used to produce the BUS used mild temperature conditions, the highest temperature being 90°C.

II-1.2. Biodegradable ureteral stents coating material

Poly (ϵ -caprolactone) (PCL) was used in chapter **chapter V** until **chapter VIII** as coating material to improve the mechanical properties of the BUS developed (**formulation 2 and 3**). PCL is a synthetic biodegradable aliphatic polyester which has attracted considerable attention in last

years, particularly in the biomedical field of absorbable surgical sutures, drug-eluting systems, and 3D scaffolds, for use in tissue engineering. The versatility of this polymer allows the development of microspheres, microcapsules, nanoparticles, pellets, implants, and films(40-43). This polymer is biodegradable in physiological conditions, because the ester bonds present in its structure are hydrolyzed into non-toxic natural metabolites and are eliminated from the body(44, 45). PCL is hydrophobic, semicrystalline, with a melting point of around 60°C and a glass transition temperature of about -60 °C. PCL is a Food and Drug Administration (FDA) approved material(42, 43, 46).

II-2. PRODUCTION OF BIODEGRADABLE URETERAL STENTS

Biodegradable ureteral stents (BUS) were produced from natural origin polysaccharides following a combination of template gelation and critical point carbon dioxide drying steps. **Figure II 5** shows the schematic representation of the processing steps used to prepare the BUS and their evolution along this thesis from the ideation phase to scale-up.

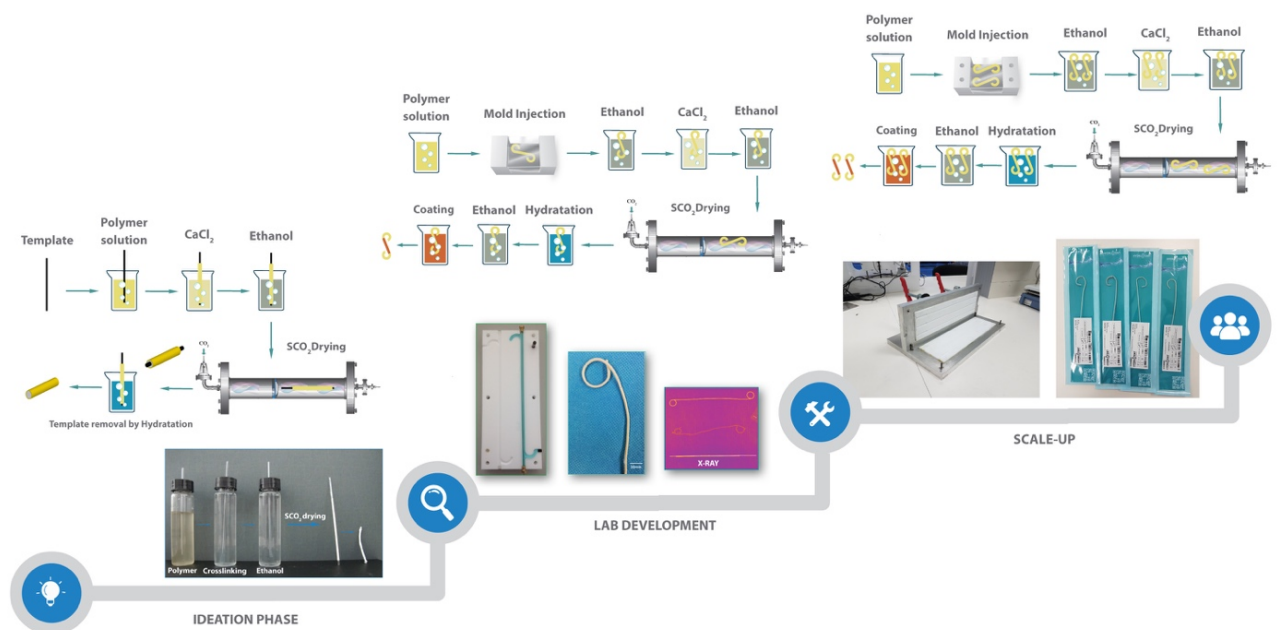


Figure II-5 Schematic representation of methodologies adopted to fabricate the biodegradable ureteral stents and their evolution.

In **chapter III** a tubular structure was prepared by first dissolving the polymers in hot distilled water (90°C) at different concentrations, and stirred for 1h. A template of appropriate geometry

was dipped in the polymeric solution and immersed at room temperature in a stirred CaCl_2 crosslinking solution. This step allows the gelification of the polymer surrounding the template. After this the gellified polymer was immersed in ethanol and dried in a high-pressure vessel by supercritical carbon dioxide (scCO_2) at 40°C and 100 bar for 2h, in a continuous mode. The conditions were chosen in order to ensure complete miscibility between the CO_2 and ethanol. After the drying process the tubular structures were immersed in distilled water in order to remove the template and to obtain the hollow tube which was then dried at room temperature.

A first injection mold was designed and used in **chapter IV** and **V**. Small changes in the methodology were introduced in order to obtain a hollow tube with the real ureteral stent size and adequate mechanical properties. Briefly, polymers were dissolved in hot distilled water (70°C) at different concentrations. The solutions were stirred for 1h and the polymeric solution was injected in the mold. After 1h the BUS was taken out of the mold and placed in an alcohol solution (100% ethanol) for 1h, for compact the polymeric layers of the stent wall. The stents were then transferred into a crosslinking solution of calcium chloride (CaCl_2) at room temperature to promote the crosslinking of the alginate. After crosslinking, the stents were relocated in an alcoholic solution (100% ethanol) to obtain an alcohol gel which was then dried in a high-pressure vessel with scCO_2 under controlled pressure (100 bar) and temperature (40°C) and a continuous flow of the scCO_2 during 90min. Finally, the dried BUS were immersed in distilled water for 30 min and in ethanol 100%, for 1h, to remove the template, and were left to dry at room temperature conditions, during 1 day. To enhance the mechanical performance of the BUS after the first surgical *In vivo* failure a coating was applied to the BUS by the end of process. BUS were coated by immersion in a 10% of polycaprolactone (PCL) resin 787 ($\text{Mw } 80,000 \text{ g mol}^{-1}$) dissolved in chloroform. The stents were dried at ambient conditions overnight.

In **chapter V**, **VI** and **VII**, the procedure steps were the same but a new mold was designed to allow the preparation of more stents simultaneously. The formulation of the BUS was modified along the thesis in order to obtain a successful *In vivo*, porcine model, biodegradable ureteral stent.

In **chapter VIII**, genipin was added to the initial stent formulation to promote the gelatin crosslinking while calcium chloride crosslink the alginate polymer network. **Table II 1** present the different formulations used to prepare the BUS and drug-eluting BUS along the thesis.

Table II-1 Polymer, cross-linking agent concentrations and active pharmaceutical compounds (APIs) used along the thesis.

Chapter	Polymer Conc. (wt%)	Gelatin %	Alginate %	Gellan Gum %	Bismuth %	PCL %	Cross-linking	APIs
III	6	-	100	-	-	-		
	4	-	-	100	-	-	0.24 M CaCl ₂	-
	6	40	60	-	-	-		
	4	40	-	60	-	-		
IV	6	40	60	-	-	-	0.24 M CaCl ₂	Ketoprofen
	4	40	-	60	-	-		
V	6	85	10	-			0.24 M CaCl ₂	
		65	30	-			0.48 M CaCl ₂	
		50	45	-	5	10	1 M CaCl ₂	
		45	50	-				
VI and VII	6	65	30	-	5	10	0.48 M CaCl ₂	Paclitaxel Doxorubicin Epirubicin Gemcitabine
VIII	6	65	30	-	5	10	0.48M CaCl ₂ 15mM Genipin	-

Two essential processes were used in the preparation of BUS; supercritical carbon dioxide drying and supercritical fluid impregnation for the development of drug-eluting BUS.

II-2.1.1. Supercritical carbon dioxide drying

Supercritical fluid drying is one alternative process to conventional drying procedures that uses supercritical fluid as the drying medium. This technique has been developed in recent years and has found its space in polymer processing(18, 47, 48). Advantages of this process compared with the conventional is the fact that no surface tension effects occur, i.e. no liquid-gas phase transitions occur during the drying process. Surface tension is what commonly causes problems in drying highly porous materials since the solid structures can collapse as the water in liquid phase is removed due to conventional drying (e.g. freeze-drying). Supercritical fluids have distinctive properties regarding density and solubility that are similar to liquids and their compressibility is similar to that of the gases(49). Carbon dioxide (CO₂) is being used progressively and encouraged at small, pilot, or large scales to dehydrate high-value natural bioactive ingredients, aerogels or scaffolds fabrication(50-52). **Figure II 6** shows the phase diagram of CO₂. The critical temperature of supercritical CO₂ (scCO₂) is as low as 31.1°C, which can be appropriate for thermosensitive materials to avoid thermal degradation. The structure shapes can be simply controlled by operating

conditions, modifying the temperature and pressure of the system(52-55). scCO_2 drying process was used to dry the BUS due their advantages compared with the conventional dry processes. Under the scope of this thesis the scCO_2 process demonstrated to be an important step to enhance the mechanical properties of the BUS and in keeping the BUS lumen open upon hydration (**chapter V**).

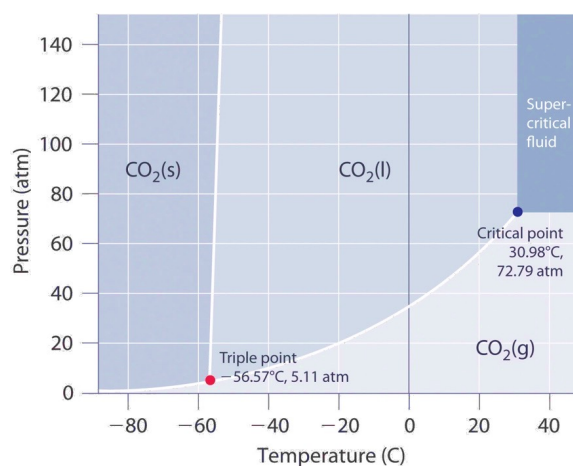


Figure II-6 The Phase Diagram of Carbon Dioxide. Adapted from Silberberg *et al*(56)

II-2.1.2. Supercritical fluid impregnation process²

Supercritical CO_2 (scCO_2) assisted impregnation has been used for loading active pharmaceuticals ingredients (APIs) in order to developed drug-eluting biodegradable ureteral stents. The preparation of drug-release products using an impregnation process demands the use of a mobile phase dissolve and transport the APIs, which at the same time should be able to swell the polymeric matrix, allowing the diffusion of the drug into the polymer bulk, increasing the impregnation rate (50). Typically, the preparation of drug-release systems requires three steps: solubilization of the APIs in an adequate solvent, APIs diffusion through the polymer matrix and removal of the residual solvent (57). In **Figure II 7** the schematic representation of the three phases of the impregnation process is presented.

² This section is based on the following publication:

Barros AA, Silva J, Craveiro R, Paiva A, Reis RL, Duarte ARC, "Green solventes for enhanced impregnation processes in biomedicine", Accepted in Current opinion in green and sustainable chemistry, 2017.

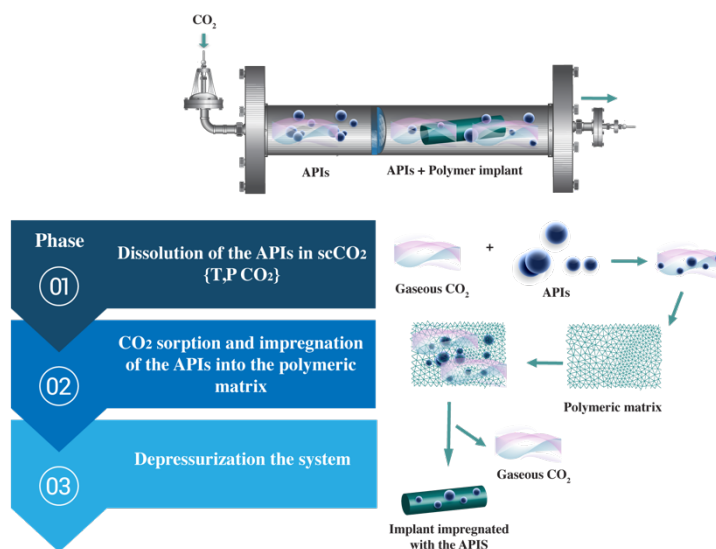


Figure II-7 Schematic representation of the three phases of the impregnation process.

In this sense, scCO_2 assisted impregnation has proven to be feasible when the pharmaceutical compound is soluble in carbon dioxide and the polymer can be swollen by the supercritical fluid. Different yields of impregnation can be obtained by scCO_2 assisted impregnation. The principal factors that affect the yield directly are the pressure and temperature of the system due to the influence on density and solvent capacity of CO_2 . According to Kazarian et al.(58, 59) there are mainly two mechanisms which describe scCO_2 assisted impregnation. One is highly dependent on the swelling ability of the polymeric matrix, when in contact of the scCO_2 the drug is solubilized in CO_2 and is placed in contact with the polymer, upon depressurization, the CO_2 rapidly leave the polymer matrix, the solubilized drug precipitates and is deposited within the polymeric matrix. Second mechanism said to be more dependent on the affinity of the CO_2 with the drug and the drug towards the polymeric matrix. One of the major advances of this manufacturing process is the fact that after impregnation the drug-eluting device can be recovered free of any solvent residue and the impregnation is carried under mild temperature and pressure conditions which enables the impregnation of thermosensitive APIs (60, 61). scCO_2 have been in the last decades claimed as a good candidate to replace conventional organic solvents in order to developed a sustainable chemical process and to meet the regulatory requirements (61, 62). scCO_2 offers advantages over other impregnation solvents mostly due to the diffusivity and the density properties of scCO_2 which can be adjusted by pressure and temperature control thus making scCO_2 a flexible media for impregnation (57). CO_2 , it is an environmentally friendly, non-flammable, non-toxic, highly abundant and low cost solvent. Furthermore, the recovered CO_2 can be easily separated from other

compounds such as APIs and/or co-solvent and recycled (60). In this thesis, scCO₂ impregnation was used in **chapter IV** for the impregnation of an anti-inflammatory compound (ketoprofen) and in **chapter VI** and **VII** for the impregnation of anti-cancer drugs (paclitaxel, doxorubicin, epirubicin and gemcitabine).

II-3. METHODS

The next section will give further details on the methods and rationale used for the characterization of the BUS developed and described in the previous section.

II-3.1. Physicochemical characterization of BUS developed

II-3.1.1. Scanning Electron Microscopy

Scanning Electron Microscopy (SEM) is an imaging techniques that gives high resolution 2D images of a sample. By scanning sample's surface with a focused beam of electrons which interact with the atoms of the sample at various depths, scattered electrons produce diverse type of signals which are detectable by the SEM equipment, and transformed into a 2D image. SEM provides qualitative information regarding sample's surface morphology, including microstructure, lumen and wall thickness, topography and composition. The morphology of produced hollow tubes, in **chapter III**, was analyzed on a Leica Cambridge S360 scanning electron microscopy (SEM). The samples were fixed with mutual conductive adhesive tape on aluminum stubs and covered with gold/palladium using a sputter coater.

SEM, in **chapter III**, was also used to monitor the deposition of crystals in the surface of the hollow tubes after immersion in AUS. This technique was also used in **chapter IV** to analyze the morphology of the ketoprofen-eluting stents before and after impregnation process (JEOL SEM, model JSM-6010LV). The samples were fixed with conductive adhesive tape on aluminum stubs and covered with gold/palladium using a sputter coater. In **chapter V** was used the same equipment to analyze the BUS before and after the coating.

II-3.1.2. Artificial Urine Uptake and swelling studies

BUS are composed by polyelectrolytes with abundant hydrophilic groups such as hydroxyl, amine, and carboxyl groups, which can promote urine uptake (63, 64). Thus, the study of the swelling kinetic of these stents when immersed in artificial urine solution (AUS) is important to predict the behaviour of BUS *In vitro* and *In vivo*. The AUS uptake capability of the samples was measured, in **chapter III**, for a period up to 60 days after immersion in AUS. Pre-weighted stents were immersed in 10 mL of AUS and placed in a water bath at 37C, 60° rpm for 1, 7, 14, 28, and 60 days. All the experiments were executed in triplicate. At the predetermined time periods, the samples were weighted in order to determine the uptake capability of the stents. AUS uptake was determined using the following equation:

$$\text{Artificial Urine Uptake (\%)} = \frac{W_w - W_f}{W_f} \times 100$$

Equation II-1 Determination of Artificial Urine Uptake

where w_w is the weight of the wet sample and w_f is the final weight (dried after immersion). The presented data is the average of at least three measurements.

To determine the swelling of the stent, images of dry and wet samples were taken using a Stereo Microscope 1 Lamp (Schott KL 200), stemi 1000 model (ZEISS), with a magnification 32 and the swelling of the matrix was evaluated by the measurement of the thickness of the wall using Image J software. The presented results are an average of at least five measurements (\pm SD) of each sample.

II-3.2. Study the biodegradation of the BUS developed in Artificial Urine Solution

II-3.2.1. *In vitro* and *In vivo* degradation studies

Biodegradable ureteral stents should have a degradation rate that takes into account the treatment time. The main challenge of these biodegradable devices is to have a uniform and homogenous degradation. Along the thesis the degradation of BUS developed was evaluated *In vitro* and *In vivo* as function of the weight loss of the BUS. In the *In vitro* degradation BUS samples (10 mg) were immersed in AUS. Samples immersed were dried and weighted to determine the

weight loss at predetermined time points. In **chapter VIII**, the *In vitro* and *In vivo* degradation of the BUS was compared. The values of *In vivo* degradation were assessed from the stents taken from the pigs sacrificed at day 5, 7 and 10 days. The weight loss of stents for both *In vitro* and *In vivo* was calculated according to the following equation:

$$\% \text{ Weight loss} = \frac{W_f - W_i}{W_i} * 100$$

Equation II-2 Determination of wight loss.

Where W_f is the final weight of the stent (dried after immersion/placement) and W_i is the initial weight of the stent.

II-3.2.2. Tensile mechanical tests

The mechanical performance of stents is an important property that needs to be full characterized *In vitro* to understand the behavior *In vivo*. Along the thesis, the mechanical properties of BUS were studied using an Instron universal testing machine (INSTRON 5540, Instron Int. Ltd, High Wycombe, UK) with a load cell of 1 kN. The universal testing machine is a testing instrument designed to test the strength of a wide variety of materials in tension, compression, or bending mode. The primary function of this assay is to create a stress-strain curve. Figure II 8 shows the setup with the BUS as well as the typical stress-train curve. From this test we can obtained values of Young modulus (E), ultimate stress (σ_{max}) and ultimate strain (ϵ_{max}). Basically, the system is made-up of a load frame, in which a specimen of the test material is mounted, a control console that provides the calibration, test setup, and test operating controls. For tensile test the tensile force is recorded as a function of the increase in gauge length. The tensile properties of the BUS were tested during the *In vitro* degradation in **chapter III, V and VIII** at predetermined time points in AUS and during the *In vivo* degradation, in **chapter VIII**, at day 0, 5, 7 and 10. The dimensions of the specimens used were 50 mm of length, 2 mm diameter, and 0.5 mm of thickness of the stent wall. The load was placed midway between the supports with a span (L) of 30 mm. The crosshead speed was 1:5 mm min⁻¹. For each condition the specimens were loaded until core break. The *In vivo* recovered stents in **chapter VIII**, were cut in equal parts along it lenght and compared. The results presented are the average of at least three specimens and are presented as the average \pm standard deviation.

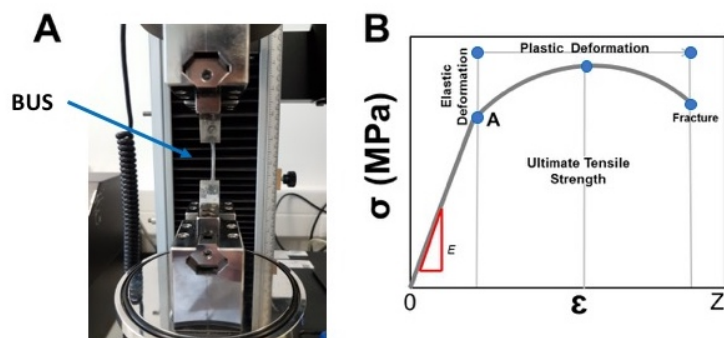


Figure II-8 A) Tensile test on BUS using a tensile universal machine and B) Typical stress-strain curve with the different regions depicted on the graph.

II-3.2.3. Gel permeation chromatography

Gel Permeation Chromatography (GPC) is a type of size exclusion chromatography used to determine the molecular weight and molecular weight distribution of a polymer. This technique involves the use of a stationary phase column with porous beads which retain smaller analytes for longer periods of time and larger analytes for lower periods of time and, consequently, analytes are eluted from the column according to their retention time, i.e. analytes with lower retention times are eluted first than analytes with longer retention times. It enables the separation of analytes from a sample according to their size and, in comparison to samples with recognized molecular weight, the molecular weight of the analytes can be determined. GPC was used in **chapter V** to analyze the degradation of the BUS. 5 mg of alginate, gelatin and bismuth were dissolved in 5 ml of an aqueous solution of sodium phosphate dibasic 0.01 M containing 0.1 M of sodium azide (pH 6.6) and used as controls, while the immersion solutions obtained by degradation test of stents at specific time point (1, 3, 6 and 9 days) were lyophilized and then dissolved in 5 ml of the same eluent. The solutions were filtered through a 0.22 μm filter and analyzed on a gel permeation chromatograph (Malvern, Viscotek TDA 305) with refractometer, right angle light scattering and viscometer detectors on a set of four columns: pre-column Suprema 5 m 8×50 S/N 3111265, Suprema 30 A° 5 m 8×300 S/N 3112751, Suprema 1000 A° 5 m 8×300 S/N 3112851 PL and Aquagel-OH MIXED 8 m 7.5×300 S/N 8M-AOHMIX-46-51, with refractive index detection (RI-Detector 8110, Bischoff). Elution was performed at 30°C using a flow rate of 1 ml min^{-1} . The elution times and the RI detector signal were calibrated with a commercial calibration

polysaccharide set from Varian that contains 10 Pullulan calibrants with narrow polydispersity and Mp (molecular mass at the peak maximum) ranging from 180 Da to 708 kDa.

II-3.2.4. Ion coupled plasma

Inductively Coupled Plasma (ICP) techniques can be very powerful tools for detecting and analyzing trace and ultra-trace elements. ICP was performed to quantify the release of Bismuth (Bi) concentration during the different degradation times (**Chapter V**). The immersion solutions from the degradation test of the stents, were filtered and analyzed. The sample absorption at specific wavelengths ($\lambda=206.17\text{nm}$ for Bi) was measured, and the bismuth concentration was determined using calibration curves previously obtained with Bismuth standard for ICP (Sigma) ($R^2 = 0.96$). Data analysis was performed as a cumulative release assay.

II-3.3. Bacterial Adhesion Studies

Bacterial infection is one of main problems associated with the conventional ureteral stents. For this reason, anti-bacterial properties of the developed BUS were evaluated. Bacterial adhesion studies were performed according to Khandwekar and Doble(65). A quantitative short-term adhesion (4h) study was performed with *Staphylococcus aureus* (NCIM 5021), a Gram-positive organism, and two Gram- negative organisms *Escherichia coli DH5 alpha* and *Klebsiella oxytoca*. These organisms were selected due to be the most common in the urinary tract infections. 100 mL of lysogeny broth (LB) medium (1% bacto tryptone, 5% bacto yeast extract, and 1% sodium chloride) was inoculated with a single colony of bacteria from a LB agar stock plate. Cells were grown at 37 °C and 200 rpm, overnight. Cells were then split between two falcon tubes, centrifuged at 3500 rpm for 20 min and resuspended in phosphate buffered saline (PBS). Cell suspension was washed twice with PBS and resuspended at a concentration of 1.3×10^8 cells/mL. Three tubes (3 mm length) of each formulation were placed in a 24-well plate and were incubated with 1 mL of the cell suspension for 4 h at 37 °C with shaking. The bacterial cells were eluted from the surfaces into 2 mL sterile PBS. The procedure involved 4 min sonication followed by 1 min mild vortexing (repeated three times) using an ultrasonic cleaner (Bandelin Sonorex Digitec) with an ultrasonic frequency of 35 kHz. A known volume of the sample was inoculated into LB agar

and incubated at 37 °C for 24 h. The colony forming units (CFUs) were counted indicating the total number of bacteria retained on the surface.

II-3.4. Drug-eluting BUS impregnation study

II-3.4.1. Impregnation Yield

The ketoprofen (**chapter IV**) and anticancer drugs (**chapter VI**) impregnation yield (I) on the biodegradable ureteral stents after scCO₂ impregnation was calculated from **Equation II 3**:

$$\text{Impregnation Yield (\%)} = \frac{m_{drug}}{m_{stent} + m_{drug}} \times 100$$

Equation II-3 Determination of impregnation Yield.

where m_{stent} is the initial mass of the stent and the m_{drug} is the mass of ketoprofen released from the stent after immersion in AUS. The total drug amount impregnated was obtained after the plateau was reached and complete degradation of the stents in AUS solution. All the experimental results are the average of three samples and are presented as average \pm standard deviation. Drugs concentration was calculated from a calibration curve prepared from standard solutions. The samples were analyzed by UV-spectroscopy using a microplate reader (SpectraMax i3, Molecular Devices, USA) at the maximum absorbance for each drug (260 nm for ketoprofen, 227 nm for paclitaxel, 254 nm for epirubicin and doxorubicin and 268 nm for gemcitabine).

II-3.4.2. *In vitro* release kinetics in AUS

The ketoprofen (**chapter IV**) and anticancer (**chapter VI**) release kinetics of developed BUS was measured in AUS. The *In vitro* ketoprofen and anticancer drugs release from the impregnated BUS was performed in triplicate. The impregnated sample were weighted and immersed in 10 ml of AUS at 37 °C with 60 rpm stirring. At pre-determined time periods (0 min, 5 min, 15 min, 30 min, 1 h, 3 h, 5 h, 7,5 h, 24 h, 48 h, 72 h, 7 days and 10 days), an aliquot (0.5 ml) of the release solution was taken and the volume replaced with fresh AUS. Drugs concentration was calculated from a calibration curve prepared from standard solutions. The samples were analyzed by UV-spectroscopy using a microplate reader (SpectraMax i3, Molecular Devices, USA) at the maximum

absorbance for each drug (260 nm for ketoprofen, 227 nm for paclitaxel, 254 nm for epirubicin and doxorubicin and 268 nm for gemcitabine).

II-3.4.3. Scanning calorimetry analysis

Differential scanning calorimeter (DSC) is an important instrument in thermal analysis being useful to understand amorphous and crystalline behaviour, eutectic transitions, curing and degree of cure, and many other material's properties used to design, manufacture, and test products. This technique allows to study the material's heat capacity (C_p) as function of the temperature. A sample of known mass is heated or cooled and the changes in its C_p are tracked as changes in the heat flow, which allows the detection of transitions such as melting, glass transitions, among others parameters. DSC was performed in **chapter IV** to confirm the amorphization of the ketoprofen upon BUS impregnation. The DSC experiments were performed using DSC Q100 V9.8 Build 296 apparatus. The samples were placed in aluminum pans and heated at a rate of 10 °C/min from 20 to 220 °C, cooled to 20 °C and heated at 5 °C/min until 200 °C. Standard calibrations were performed using indium leads.

II-3.4.4. Fourier Transformed InfraRed spectroscopy

Fourier Transform Infrared Spectroscopy (FTIR) was performed to verify the presence of the ketoprofen (**chapter IV**) after $scCO_2$ impregnation. FTIR is a cost-effective technique that identifies polymers and analyze polymer chemical modification. Fourier transformation algorithm allied to IR spectroscopy gives a spectrum of IR absorption per frequency/wavelength. Similar chemical groups absorb in the IR at similar frequencies, enabling to identify the chemical structure of a compounds, and to identify chemical modifications. IR spectrum is specific for each compound. A transmittance spectrum was obtained on an IR Prestige-21 FTIR spectrometer (Shimadzu) by performing 32 scans in each spectrum over a range of 400-4400 cm^{-1} and with a resolution of 4 cm^{-1} .

II-3.4.5. Permeability studies

In **chapter VII**, permeability studies on drug-eluting BUS impregnated with paclitaxel and doxorubicin were performed through three different membranes: polyethersulphone membrane (PES), HUVECs cell monolayer and an *ex vivo* porcine ureter. The permeability tests were conducted using two different systems, Franz-cell and Transwell® diffusion test (**Figure II 9**).

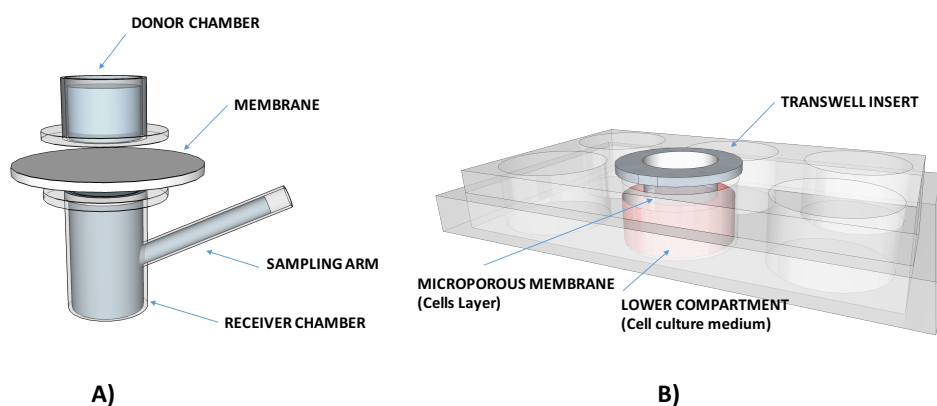


Figure II-9 Schematic representation of the a) Franz-cells and b) Transwell® diffusion test used in the permeability studies with drug-eluting BUS.

A glass Franz-type diffusion cell (PermeGear) with 8 mL receptor compartment, and an effective mass transfer area of 1 cm². Two different membranes were used using this diffusion cell, a polyethersulphone (PES) membrane (Santorius), with 150 µm thickness and 0.45 µm, pore size and an *ex vivo* porcine ureter tissue. The membranes were placed between the two compartments and held with a stainless-steel clamp. The *ex vivo* porcine ureter tissue was open and cut into 1.5 cm² sections and placed in the glass Franz-type diffusion cells with the urothelium facing the donor compartment upward. To avoid any damage of the urothelial layer this was handled with extreme caution, preventing disruption and cell detachment. The receptor compartment was immediately filled with AUS, and air bubbles were removed. Finally, the donor compartment was filled with a solution of 20 µg mL⁻¹ of drug alone (paclitaxel or doxorubicin) or with 100 mg of BUS impregnated with drugs immersed in AUS. Aliquots of 200 µL were withdrawn from the receptor compartment at fixed time points (0 min, 5 min, 15 min, 30 min, 1 h, 3 h, 5 h, 8 h) and replenished by fresh AUS (pH 5.5). The experiments were performed at 37 °C, and the receptor compartment was stirred at 400–600 rpm using a magnetic bar to eliminate the boundary layer effect.

Transwell® diffusion test was used to study the permeability of paclitaxel, doxorubicin and the stents impregnated with these drugs through a HUVEC cell monolayer. A collagen matrix (0.7%) was applied previously to the Transwells®. The HUVEC were seeded into 3 µm pore Transwell® inserts (polyester membrane, FALCON, USA) in a 6 well plate at 50,000 cells/cm². The HUVEC's were grown for 8 days on the Transwells® filters incubated at 37 °C in a 5% CO₂ with 1.5 ml of EndoGRO-VEGF medium in the insert (donor compartment) and 2.5 ml of EndoGRO-VEGF medium in the receiver compartment. The confluency of the cell monolayer cells was confirmed using an inverted microscope for cell culture (AxioVert A1 FL LED, Zeiss, USA) and images were taken at the end of the experience to ensure that the monolayer remain intact. To start the experiment, the donor solution was suctioned off and replace with a 1.5 ml of fresh EndoGRO-VEGF medium containing 20 µg mL⁻¹ of paclitaxel or doxorubicin or 100 mg of stents with drugs (medium, pH 7.8). At fixed time points (0 min, 5 min, 15 min, 30 min, 1 h, 3 h, 5 h, 8 h), 100 µl aliquots were removed from the receptor compartment and replaced with fresh medium. Between each time point the samples were maintained at 37 °C in a 5% CO₂ atmosphere. The amount of paclitaxel and doxorubicin in the receptor compartment was measured by UV, at their maximum absorbance at a wavelength of 227 nm and 254 nm respectively, using a microplate reader (Synergy HT, Bio-TEK, USA). The ureter tissue (about 5 cm) from a porcine with 70 Kg was obtained fresh from a surgical room within 5 minutes of sacrifice and immediately immersed in cold oxygenated Krebs buffer and covered specimen temporarily in a cool area.

In both cases the permeability (P) of paclitaxel and doxorubicin was calculated by **equation II 4** where C_t is the concentration in the receptor compartment at time t , C_0 is the initial concentration in the donor compartment, V is the solution volume in the two compartments, and A is the effective area of permeation. The permeability coefficient can be calculated from the slope of the curve – $(V/2A) \cdot \ln(1 - 2C_t/C_0)$ versus t . (2)

$$-\ln\left(1 - \frac{2C_t}{C_0}\right) = \frac{2A}{V} \times P \times t$$

Equation II-4 Determination of permeability

The diffusion coefficient (D) of solutes across the membranes was calculated according to Fick's law of diffusion, where D is the diffusion coefficient (cm² s⁻¹); C_i and C_f are the initial and final concentrations and C_t is the concentration at time t of solute in the receptor side, respectively (mol L⁻¹); V_1 and V_2 correspond to the volume of the liquid in the donor compartment and that in the

receptor compartment (cm^3), respectively; h is the thickness of the membrane (cm); and A is the effective diffusion area of the membrane (cm^2) (66).

$$D = \frac{V_1 V_2}{V_1 + V_2} \times \frac{h}{A} \times \frac{1}{t} \ln \left(\frac{C_f - C_i}{C_f - C_t} \right)$$

Equation II-5 Determination of the diffusion coefficient

The partition coefficient (K_d) is defined as a measure of the solubility of the solute in the membrane. The partition coefficient for the system was calculated using **Equation II 6**, where P is the permeability, h is the thickness of the membrane and D is the diffusion coefficient (2, 67).

$$K_d = \frac{P \times h}{D}$$

Equation II-6 Determination of partition coefficient

II-3.5. *In vitro* biological evaluation of the developed BUS

II-3.5.1. Cells Sources

II-3.5.1.1 Cell lines

Cells lines are immortalized cells that present the ability to proliferate indefinitely either due to a random mutation or due to a programmed modification. In the present thesis mouse lung fibroblast L929 (European Collection of Cell Cultures (ECCC), UK) were used as cell line. L929 fibroblasts are widely used as preliminary cytotoxicity screenings of biomaterials. Cell lines are useful models for doing research, because they provide reliability in experimental results due to the possibility to obtain large amounts of cells for prolonged use. L929 cell line is the usual choice in many standard tests, such as material biocompatibility testing, drug cytotoxicity testing and cell biology studies (111, 112). L929 were used in **chapter III, IV** and **VIII** of this thesis.

II-3.5.1.2 Primary Cells

Primary cell cultures are typically obtained directly from a subject and have a limited lifetime. In the present thesis two different primary cell cultures were used: human umbilical vein endothelial cells (HUVECs) and human urothelial carcinoma cell line (T24). In **chapter VI and**

VII, human urothelial carcinoma cell line, T24 (ATCC, U.S.A.) was used as a cancer cell line to model the urothelial carcinoma and human umbilical vein endothelial cells, HUVEC, (ATCC, U.S.A.) as a control, non-cancerous cell line. The T24 cell line and HUVEC cells were cultured in RPMI-1640 and EGM™-2 medium, respectively, with (10% fetal bovine serum (FBS), 1 mM L-glutamine and 1% penicillin/streptomycin), cells were maintained at 37°C in a humidified 5% CO₂ atmosphere. T24 and HUVECS cells were used in the calculation of the half maximal inhibitory concentration (IC₅₀) against the anti-cancer drugs studied and for the *In vitro* anti-cancer effect of anti-cancer drug-eluting.

II-3.5.2. Cytotoxicity assay

BUS and the leachables of BUS were tested for cytotoxicity using a MTS colorimetric assay. Cell viability was evaluated by the 3-(4,5-dimethylthiazol-2-yl)-5-(3-carboxy-methoxyphenyl)-2-(4-sulphophenyl)-2H-tetrazolium (MTS) assay after 72 h. This assay is based on the bioreduction of a tetrazolium compound MTS into a water-soluble brown formazan product. The cytotoxicity of the BUS and leachable materials during the ureteral stent degradation in AUS was assessed according to ISO/10993(68). The cytotoxicity of the samples was assessed using an immortalized mouse lung fibroblasts cell line (L929) purchased from the European Collection of Cell Cultures. First, the immersion solutions obtained by degradation test at specific time point (1, 3, 6 and 9 days) of stents were lyophilized. The leachables were dissolved in basal medium DMEM (Dulbecco's modified Eagle's medium; Sigma–Aldrich, Germany) 10% FBS (heat-inactivated fetal bovine serum, Biochrom AG, Germany), and 1% antibiotic-antimycotic (Gibco, UK). In case of direct contact studies stents were placed directly in contact with cells. Cells were seeded at a density of 10,000 cells cm² and cultured in a humidified incubator at 37°C in a 5% CO₂ atmosphere. The effect of the leachables on the cellular metabolism was evaluated using a standard MTS (Cell Titer 96® Aqueous Solution Cell Proliferation Assay, Promega, USA) viability test. A latex rubber extract was used as positive control for cell death; while cell culture medium was used as negative control representing the ideal situation for cell proliferation. This was quantified by UV-spectroscopy, reading the formazan absorbance at 490 nm in a microplate reader (Synergy HT, Bio-Tek Instruments, USA). Each sample formulation and control was tested using 12 replicates.

II-3.5.3. Half maximal inhibitory concentration (IC₅₀) determination

To understand the cytotoxic limit of the anticancer drugs against the cancer and non-cancer cells, the half maximal inhibitory concentration (IC₅₀) was calculated by a cytotoxic test, in **chapter VI**. The IC₅₀ is the concentration of an inhibitor where the response (or binding) is reduced by half (**Figure II 10**). The cytotoxicity of paclitaxel, epirubicin, doxorubicin and gemcitabine was evaluated by determining the viability of T24 and HUVEC cells after exposure to medium containing the free drug at a range of concentrations from 0.01 to 2000 ng/ml. Free drugs in medium were prepared by first dissolving the anticancer drugs in DMSO (50 mg/ml) and this solution was then diluted in culture medium to achieve the desired concentration. A standard MTT assay (CellTiter 961 Aqueous One Solution Cell Proliferation Assay) was used to test cell viability and was performed on both cell lines to determine the IC₅₀ of each drug. 5000 cells per well were seeded in a 96-well plate with 100mL medium for both T24 and HUVEC cells. After incubation for 24 h, the medium in each well was aspirated and the cells were exposed to fresh medium containing the drugs at various concentrations for 4 h and 72 h. The cells after 4 h treatment were further cultured for 72h in fresh (drug-free) medium. After that, the culture medium in each well was replaced by 100 mL of medium and 20 mL of CellTiter 961 Aqueous One Solution Reagent, followed by 4 h incubation at 37°C. A latex rubber extract was used as negative control for cell death; while cell culture medium was used as positive control. Cell viability was quantified by UV-spectroscopy, reading the formazan absorbance at 490nm in a microplate reader (SpectraMax i3, Molecular Devices, USA). Each sample formulation and control was tested using 12 replicates. The IC₅₀ was determined from the fitting of the curve of cell viability, measured by MTT and the drug concentration. The fitting was performed using GraphPad software (GraphPad Prism 6.00 software, San Diego, USA).

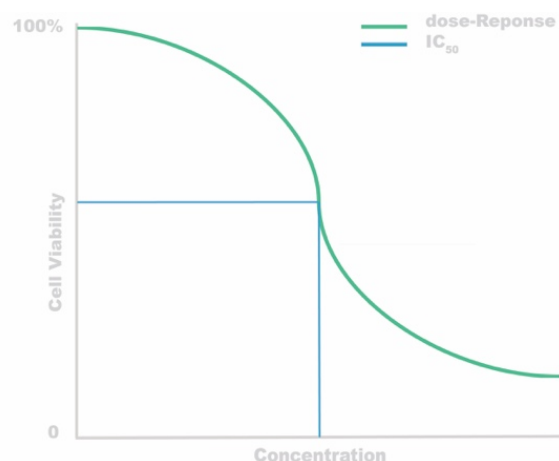


Figure II-10 Conventional method of determining IC₅₀ using the dose-response curve.

II-3.5.4. *In vitro* anti-cancer effect of anti-cancer drug-eluting BUS

The anti-cancer effect of the anti-cancer drug-eluting BUS in human urothelial carcinoma cell line was evaluated by determining the viability of T24 cells by indirect and direct contact, in **chapter VI**. HUVEC was used as non-cancerous, control cell line. The T24 cell line and HUVEC cells were cultured in RPMI- 1640 and EGMTM-2 medium, respectively with (10% fetal bovine serum (FBS), 1 mM L- glutamine and 1% penicillin/streptomycin). By indirect contact, the effect of the released drug as well as leachables from the BUS were evaluated, placing the stents in fresh medium after 4 h and 72 h. On the other hand, by direct contact 10 mg of stent was placed directly in contact with a cell layer in each well. Both tests were performed for 4h and 72h. The viability of the cells was performed using a standard MTT test. Briefly, 5000 cells per well were seeded in a 96- well plate with 100mL medium for T24 and HUVEC cells. After incubation for 24 h, the medium in each well was aspirated and the cells exposed to medium containing the extracts of the stents in the indirect contact study. In the direct contact the cells were exposed to 100 mL of fresh medium in the presence of the stent. The cells after 4 h treatment were further cultured for 72 h in fresh medium. After that, the culture medium in each well was replaced by 100 mL of medium and 20 mL of CellTiter 961 Aqueous One Solution Reagent, followed by 4 h incubation at 37°C. Cell culture medium and the non-impregnated stents (BUS and commercial stent) were used as negative controls. Each sample formulation and control was tested with 3 replicates.

II-3.6. In vivo studies of BUS development

II-3.6.1. Surgical procedure validation

The *In vivo* studies carried out in chapter **V** and **VIII** were conducted at ICVS, University of Minho, Braga, Portugal (**Figure II 11**). The BUS developed under this thesis were placed in female porcine model which is the standard model used in these types of studies. The protocols of the studies were formally approved by the institution's review board and it is in accordance with its internal ethical protocol for animal experiments. Female domestic pigs, weighing ≈ 30 kg, were used in this study. The pigs were not given food or water for 12 h before the procedure. All procedures were performed under general anesthesia and mechanical ventilation as previously described in detail(69, 70). After emptying the bladder, a semi rigid 7-Fr ureteroscope (Karl Storz, Tuttlingen, Germany) was inserted through the urethra and saline solution was instilled. The full procedure was performed according to the standard technique of ureteroscopy. A 0.035-in. flexible tip guidewire (AQUATRACK® Hydrophilic Nitinol, Cordis®, Johnson & Johnson) was inserted into the ureters under direct visualization, and then the stents were inserted over the guidewire into the kidney. The guidewire was then removed and the position of the stents was confirmed by X-ray (Examion® DR810). In **chapter V**, conventional ureteroscopy was performed in order to verify the degradation and the presence of any fragment and the morphology of the ureters after 3 and 10 days. In **chapter VIII**, a total of 7 pigs were unilaterally stented with biodegradable ureteral stent (BUS) and 3 pigs with the commercial stent. The stents were randomly placed on the right or left ureter. At day 5 one pig died and at day 7 one was euthanized, both stented with BUS and the degradation level of the stent was assessed. The other 8 were euthanized at day 10. Blood and urine samples were collected from all animals before the day of surgery. Blood tests (WBC, Hb), serum creatinine, urine culture tests were performed at day 0, 5 and 10.

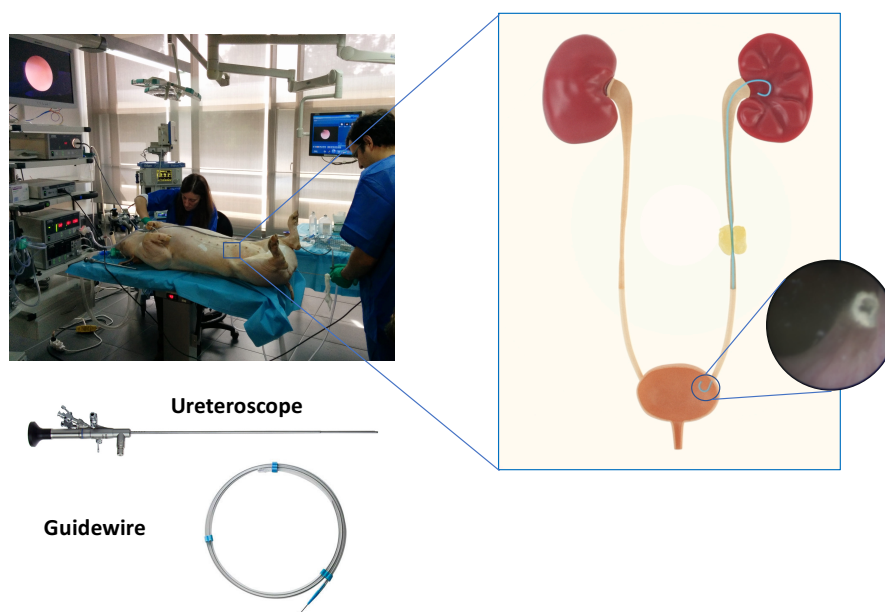


Figure II-11 Schematic representation of the BUS placement at ICVS, University of Minho, Braga, Portugal and the materials used.

II-3.6.2. Hydronephrosis level

After the placement of the BUS and the commercial stents in pig model, in **chapter VIII**, the hydronephrosis level were measured by intravenous pyelograms (IVP). IVP X-rays were carried out at 0, 1, 3, 5, 10, 20 and 30 min after intravenous injection of 1200 mg/Kg of Iohexol (Omnipaque™ 300, GE Healthcare). IVP was used to evaluate the degree of hydronephrosis at day 0, 1, 5 and 10. The renal function was measured by the rate of contrast material movement at day 0. IVP severity score is based on the time until the contrast appears in the kidneys and ureters after the intravenous injection, hydronephrosis was graded as: none – level 0 (<3min), mild – level 1 (3-10 min), moderate – level 2 (10 – 20 min) or severe – level 3 (>20 min)⁽⁷¹⁾.

II-3.6.3. Histological procedures and stainings

In **chapter VII** an *ex vivo* porcine ureter tissue and in **chapter VIII** after *In vivo* BUS degradation, porcine ureters were collected and processed in an automatic ethanol-xylene spin tissue processor for histological analysis (Microm STP 120, Thermo Scientific, USA). Afterward, samples were embedded in paraffin and cut into sections of 5 μm thickness using a microtome. Sections were subsequently deparaffinized, rehydrated, and stained.

II-3.6.3.1 Hematoxylin & eosin

Hematoxylin is a natural dye that colors in blue basophilic substances, such as the nuclei of cells, and eosin Y is a synthetic dye that colors in various shades of red acidophilic substances, the acidic proteins of the cytoplasm and connective tissue. The ureters samples collected for the permeability study (**chapter VII**) and ureters after pre-determined periods of *In vivo* BUS implanted (**chapter VIII**) were automatically processed for hematoxylin and eosin (H&E) staining. Briefly, histological sections were subsequently immersed in hematoxylin and after bluing in an ammonia solution (1% v/v) in eosin y. Samples were then mounted and analyzed by microscopy.

II-3.6.3.2 Masson's trichrome

Masson's Trichrome (MT) staining is a mixture of three different dyes that selectively colors in red the muscle fibers, in light red the cytoplasm, in blue or green the collagen and dark brown to black the cell nuclei. The ureters samples collected for the permeability study (**chapter VII**) and ureters after pre-determined periods of *In vivo* BUS implanted (**chapter VIII**) were processed for Masson's trichrome staining. Sections were stained for 5 min in a solution containing azure B (0.5 g), ammonium iron (5 g, ammonium iron sulfate (III) dodecahydrate) and distilled water (100 mL). Sections were then subsequently stained with hematoxylin and picric ethanol (1% w/v) for 5 min each. After 10 min washing in running tap water, sections were stained with the solutions from the Trichrome Stain Masson kit according to the manufacturer's specifications.

II-4. STATISTICAL ANALYSIS

All quantitative data are presented as mean \pm standard deviation (SD). Statistical analysis was performed using Graph Pad Prism 6.00 software (San Diego, USA). Statistical significances (* $p \leq 0.05$, ** $p \leq 0.01$ and *** $p \leq 0.001$) were determined using specific statistical tests described in the subsection of materials and methods in the different chapters. An average of three to twelve replicates were used.

REFERENCES

1. Silva SS, Oliveira JM, Sá-Lima H, Sousa RA, Mano JF, Reis RL. 2.211 - Polymers of Biological Origin A2 - Ducheyne, Paul. *Comprehensive Biomaterials*. Oxford: Elsevier; 2011. p. 187-205.
2. He H, Cao X, Lee LJ. Design of a novel hydrogel-based intelligent system for controlled drug release. *Journal of Controlled Release*. 2004;95(3):391-402.
3. Kosmala JD, Henthorn DB, Brannon-Peppas L. Preparation of interpenetrating networks of gelatin and dextran as degradable biomaterials. *Biomaterials*. 2000;21(20):2019-23.
4. Gorgieva S, Kokol V. Preparation, characterization, and in vitro enzymatic degradation of chitosan-gelatin hydrogel scaffolds as potential biomaterials. *Journal of Biomedical Materials Research Part A*. 2012;100a(7):1655-67.
5. Ahmad T, Ismail A, Ahmad SA, Khalil KA, Kumar Y, Adeyemi KD, et al. Recent advances on the role of process variables affecting gelatin yield and characteristics with special reference to enzymatic extraction: A review. *Food Hydrocolloid*. 2017;63:85-96.
6. Barros AA, Aroso IM, Silva TH, Mano JF, Duarte ARC, Reis RL. Water and Carbon Dioxide: Green Solvents for the Extraction of Collagen/Gelatin from Marine Sponges. *ACS Sustainable Chemistry & Engineering*. 2015;3(2):254-60.
7. Young S, Wong M, Tabata Y, Mikos AG. Gelatin as a delivery vehicle for the controlled release of bioactive molecules. *Journal of Controlled Release*. 2005;109(1-3):256-74.
8. Yao CH, Liu BS, Chang CJ, Hsu SH, Chen YS. Preparation of networks of gelatin and genipin as degradable biomaterials. *Mater Chem Phys*. 2004;83(2-3):204-8.
9. Mohanty B, Bohidar HB. Microscopic structure of gelatin coacervates. *Int J Biol Macromol*. 2005;36(1-2):39-46.
10. Pulieri E, Chiono V, Ciardelli G, Vozzi G, Ahluwalia A, Domenici C, et al. Chitosan/gelatin blends for biomedical applications. *Journal of Biomedical Materials Research Part A*. 2008;86A(2):311-22.
11. Wen C, Lu LL, Li XS. Enzymatic and Ionic Crosslinked Gelatin/K-Carrageenan IPN Hydrogels as Potential Biomaterials. *Journal of Applied Polymer Science*. 2014;131(21).
12. Balakrishnan B, Jayakrishnan A. Self-cross-linking biopolymers as injectable in situ forming biodegradable scaffolds. *Biomaterials*. 2005;26(18):3941-51.
13. Rose JB, Pacelli S, El Haj AJ, Dua HS, Hopkinson A, White LJ, et al. Gelatin-Based Materials in Ocular Tissue Engineering. *Materials*. 2014;7(4):3106-35.
14. Fan L, Du Y, Huang R, Wang Q, Wang X, Zhang L. Preparation and characterization of alginate/gelatin blend fibers. *Journal of Applied Polymer Science*. 2005;96(5):1625-9.
15. Bigi A, Cojazzi G, Panzavolta S, Roveri N, Rubini K. Stabilization of gelatin films by crosslinking with genipin. *Biomaterials*. 2002;23(24):4827-32.
16. Muzzarelli RAA. Genipin-crosslinked chitosan hydrogels as biomedical and pharmaceutical aids. *Carbohydrate Polymers*. 2009;77(1):1-9.
17. Tsai CC, Huang RN, Sung HW, Liang HC. In vitro evaluation of the genotoxicity of a naturally occurring crosslinking agent (genipin) for biologic tissue fixation. *J Biomed Mater Res*. 2000;52(1):58-65.
18. Fernandes-Silva S, Moreira-Silva J, Silva TH, Perez-Martin RI, Sotelo CG, Mano JF, et al. Porous Hydrogels From Shark Skin Collagen Crosslinked Under Dense Carbon Dioxide Atmosphere. *Macromolecular Bioscience*. 2013;13(11):1621-31.

19. Silva JM, Caridade SG, Oliveira NM, Reis RL, Mano JF. Chitosan-alginate multilayered films with gradients of physicochemical cues. *Journal of Materials Chemistry B*. 2015;3(22):4555-68.
20. Silva JM, Caridade SG, Reis RL, Mano JF. Polysaccharide-based freestanding multilayered membranes exhibiting reversible switchable properties. *Soft Matter*. 2016;12(4):1200-9.
21. Butler MF, Ng YF, Pudney PDA. Mechanism and kinetics of the crosslinking reaction between biopolymers containing primary amine groups and genipin. *J Polym Sci Pol Chem*. 2003;41(24):3941-53.
22. Quraishi S, Martins M, Barros AA, Gurikov P, Raman SP, Smirnova I, et al. Novel non-cytotoxic alginate lignin hybrid aerogels as scaffolds for tissue engineering. *J Supercrit Fluid*. 2015;105:1-8.
23. Lee KY, Mooney DJ. Alginate: Properties and biomedical applications. *Prog Polym Sci*. 2012;37(1):106-26.
24. García-González CA, Jin M, Gerth J, Alvarez-Lorenzo C, Smirnova I. Polysaccharide-based aerogel microspheres for oral drug delivery. *Carbohydrate Polymers*. 2015;117(0):797-806.
25. Johnston D, Kumar P, Choonara YE, du Toit LC, Pillay V. Modulation of the nano-tensile mechanical properties of co-blended amphiphilic alginate fibers as oradurable biomaterials for specialized biomedical application. *J Mech Behav Biomed*. 2013;23:80-102.
26. Jejurikar A, Lawrie G, Martin D, Grondahl L. A novel strategy for preparing mechanically robust ionically cross-linked alginate hydrogels. *Biomed Mater*. 2011;6(2).
27. Breger JC, Isayeva I, Langone JJ, Pollack SK, Wang NS. Novel click alginate hydrogels for use as biomaterials. *Abstr Pap Am Chem S*. 2009;238.
28. Augst AD, Kong HJ, Mooney DJ. Alginate Hydrogels as Biomaterials. *Macromolecular Bioscience*. 2006;6(8):623-33.
29. Wen C, Lu L, Li X. Mechanically Robust Gelatin–Alginate IPN Hydrogels by a Combination of Enzymatic and Ionic Crosslinking Approaches. *Macromolecular Materials and Engineering*. 2014;299(4):504-13.
30. Matricardi P, Pontoriero M, Coviello T, Casadei MA, Alhaique F. In situ cross-linkable novel alginate-dextran methacrylate IPN hydrogels for biomedical applications: Mechanical characterization and drug delivery properties. *Biomacromolecules*. 2008;9(7):2014-20.
31. Kong HJ, Kaigler D, Kim K, Mooney DJ. Controlling Rigidity and Degradation of Alginate Hydrogels via Molecular Weight Distribution. *Biomacromolecules*. 2004;5(5):1720-7.
32. Oliveira JT, Martins L, Picciochi R, Malafaya PB, Sousa RA, Neves NM, et al. Gellan gum: a new biomaterial for cartilage tissue engineering applications. *Journal of biomedical materials research Part A*. 2010;93(3):852-63.
33. Jansson PE, Lindberg B, Sandford PA. Structural Studies of Gellan Gum, an Extracellular Polysaccharide Elaborated by *Pseudomonas-Elodea*. *Carbohydr Res*. 1983;124(1):135-9.
34. Bacelar AH, Silva-Correia J, Oliveira JM, Reis RL. Recent progress in gellan gum hydrogels provided by functionalization strategies. *Journal of Materials Chemistry B*. 2016;4(37):6164-74.
35. Miyoshi E, Takaya T, Nishinari K. Rheological and thermal studies of gel-sol transition in gellan gum aqueous solutions. *Carbohydrate Polymers*. 1996;30(2-3):109-19.
36. Singh BN, Kim KH. Effects of divalent cations on drug encapsulation efficiency of deacylated gellan gum. *J Microencapsul*. 2005;22(7):761-71.
37. Oliveira JT, Santos TC, Martins L, Picciochi R, Marques AP, Castro AG, et al. Gellan Gum Injectable Hydrogels for Cartilage Tissue Engineering Applications: In Vitro Studies and Preliminary In Vivo Evaluation. *Tissue Engineering Part A*. 2010;16(1):343-53.
38. Chew BH, Duvdevani M, Denstedt JD. New developments in ureteral stent design, materials and coatings. *Expert Rev Med Devices*. 2006;3(3):395-403.
39. Glocker D, Ranade S. *Medical Coatings and Deposition Technologies*: Wiley; 2016.

40. Fanovich MA, Ivanovic J, Zizovic I, Mistic D, Jaeger P. Functionalization of polycaprolactone/hydroxyapatite scaffolds with *Usnea lethariiformis* extract by using supercritical CO₂. *Mat Sci Eng C-Mater*. 2016;58:204-12.
41. Fanovich MA, Ivanovic J, Mistic D, Alvarez MV, Jaeger P, Zizovic I, et al. Development of polycaprolactone scaffold with antibacterial activity by an integrated supercritical extraction and impregnation process. *J Supercrit Fluid*. 2013;78:42-53.
42. Tserki V, Matzinos P, Pavlidou E, Panayiotou C. Biodegradable aliphatic polyesters. Part II. Synthesis and characterization of chain extended poly(butylene succinate-co-butylene adipate). *Polym Degrad Stabil*. 2006;91(2):377-84.
43. Correlo VM, Boesel LF, Bhattacharya M, Mano JF, Neves NM, Reis RL. Properties of melt processed chitosan and aliphatic polyester blends. *Mat Sci Eng a-Struct*. 2005;403(1-2):57-68.
44. Marten E, Muller RJ, Deckwer WD. Studies on the enzymatic hydrolysis of polyesters. II. Aliphatic-aromatic copolyesters. *Polym Degrad Stabil*. 2005;88(3):371-81.
45. Hirano H, Watase S, Tanaka M. Linear polymers with sulfur in the main chain. II. Synthesis of polyesters by interfacial polycondensation of bis (4,4'-hydroxyphenyl) sulfide with several aliphatic acid dichlorides and their properties. *Journal of Applied Polymer Science*. 2004;91(3):1865-72.
46. Correlo VM, Boesel LF, Bhattacharya M, Mano JF, Neves NM, Reis RL. Hydroxyapatite reinforced chitosan and polyester blends for biomedical applications. *Macromolecular Materials and Engineering*. 2005;290(12):1157-65.
47. Martins M, Barros AA, Quraishi S, Gurikov P, Raman SP, Smirnova I, et al. Preparation of macroporous alginate-based aerogels for biomedical applications. *J Supercrit Fluid*. 2015;106:152-9.
48. Silva SS, Duarte ARC, Carvalho AP, Mano JF, Reis RL. Green processing of porous chitin structures for biomedical applications combining ionic liquids and supercritical fluid technology. *Acta Biomaterialia*. 2011;7(3):1166-72.
49. Chattopadhyay P, Gupta RB. Production of antibiotic nanoparticles using supercritical CO₂ as antisolvent with enhanced mass transfer. *Industrial & Engineering Chemistry Research*. 2001;40(16):3530-9.
50. Marizza P, Pontoni L, Rindzevicius T, Alopaeus JF, Su K, Zeitler JA, et al. Supercritical impregnation of polymer matrices spatially confined in microcontainers for oral drug delivery: Effect of temperature, pressure and time. *The Journal of Supercritical Fluids*. 2016;107:145-52.
51. Zhang J, Martin DJ, Taran E, Thurecht KJ, Minchin RF. Effect of Supercritical Carbon Dioxide on the Loading and Release of Model Drugs from Polyurethane Films: Comparison with Solvent Casting. *Macromolecular Chemistry and Physics*. 2014;215(1):54-64.
52. Tomasko DL, Li H, Liu D, Han X, Wingert MJ, Lee LJ, et al. A Review of CO₂ Applications in the Processing of Polymers. *Industrial & Engineering Chemistry Research*. 2003;42(25):6431-56.
53. Tang M, Huang YC, Chen YP. Sorption and diffusion of supercritical carbon dioxide into polysulfone. *Journal of Applied Polymer Science*. 2004;94(2):474-82.
54. Tai H, Mather ML, Howard D, Wang W, White LJ, Crowe JA, et al. Control of pore size and structure of tissue engineering scaffolds produced by supercritical fluid processing. *European Cells & Materials*. 2007;14:64-76.
55. Taberero A, Martin del Valle EM, Galan MA. Supercritical fluids for pharmaceutical particle engineering: Methods, basic fundamentals and modelling. *Chemical Engineering and Processing*. 2012;60:9-25.
56. Silberberg MS. *Principles of general chemistry*: McGraw-Hill Higher Education; 2007.

57. Champeau M, Thomassin J-M, Tassaing T, Jerome C. Drug Loading of Sutures by Supercritical CO₂ Impregnation: Effect of Polymer/Drug Interactions and Thermal Transitions. *Macromolecular Materials and Engineering*. 2015;300(6):596-610.
58. Kazarian SG, Martirosyan GG. Spectroscopy of polymer/drug formulations processed with supercritical fluids: in situ ATR-IR and Raman study of impregnation of ibuprofen into PVP. *International Journal of Pharmaceutics*. 2002;232(1-2):81-90.
59. Kazarian SG. Polymer processing with supercritical fluids. *Polymer Science - Series C*. 2000;42(1):78-101.
60. Champeau M, Thomassin JM, Tassaing T, Jerome C. Drug loading of polymer implants by supercritical CO₂ assisted impregnation: A review. *Journal of Controlled Release*. 2015;209:248-59.
61. Duarte ARC, Mano JF, Reis RL. Supercritical fluids in biomedical and tissue engineering applications: a review. *International Materials Reviews*. 2009;54(4):214-22.
62. Davies OR, Lewis AL, Whitaker MJ, Tai H, Shakesheff KM, Howdle SM. Applications of supercritical CO₂ in the fabrication of polymer systems for drug delivery and tissue engineering. *Advanced Drug Delivery Reviews*. 2008;60(3):373-87.
63. Crouzier T, Boudou T, Picart C. Polysaccharide-based polyelectrolyte multilayers. *Current Opinion in Colloid & Interface Science*. 2010;15(6):417-26.
64. Almodóvar J, Place LW, Gogolski J, Erickson K, Kipper MJ. Layer-by-Layer Assembly of Polysaccharide-Based Polyelectrolyte Multilayers: A Spectroscopic Study of Hydrophilicity, Composition, and Ion Pairing. *Biomacromolecules*. 2011;12(7):2755-65.
65. Khandwekar A, Doble M. Physicochemical characterisation and biological evaluation of polyvinylpyrrolidone-iodine engineered polyurethane. *J Mater Sci: Mater Med*. 2011;22(5):1231-46.
66. Chu L-Y, Li Y, Zhu J-H, Wang H-D, Liang Y-J. Control of pore size and permeability of a glucose-responsive gating membrane for insulin delivery. *Journal of Controlled Release*. 2004;97(1):43-53.
67. Liang SM, Zhang L, Xu H. Morphology and permeability of cellulose/chitin blend membranes. *Journal of Membrane Science*. 2007;287(1):19-28.
68. ISO/10993. Biological Evaluation of Medical Devices. Part 5. Test for Cytotoxicity, In Vitro Methods: 8.2 Test on Extracts. 1992.
69. Lima E, Rolanda C, Osorio L, Pego JM, Silva D, Henriques-Coelho T, et al. Endoscopic Closure of Transmural Bladder Wall Perforations. *Eur Urol*. 2009;56(1):151-7.
70. Oliveira CAR, Ferreira C, Quattrone C, De Sio M, Autorino R, Pinto JC, et al. Endoscopic Closure of Transmural Bladder Wall Perforations. *Journal of Endourology*. 2012;26:A501-A.
71. Chew BH, Paterson RF, Clinkscales KW, Levine BS, Shalaby SW, Lange D. In Vivo Evaluation of the Third Generation Biodegradable Stent: A Novel Approach to Avoiding the Forgotten Stent Syndrome. *J Urology*. 2013;189(2):719-25.

Chapter III

Biodegradable ureteral stents from natural origin polymers

Chapter III

Biodegradable ureteral stents from natural origin polymers[‡]

ABSTRACT

In this work, stents were produced from natural origin polysaccharides. Alginate, gellan gum and a blend of these with gelatin were used to produce hollow tube (stents) following a combination of templated gelation and critical point carbon dioxide drying. Morphological analysis of the surface of the stents was carried out by scanning electron microscopy. Indwelling time, encrustation and stability of the stents in artificial urine solution was carried out up to 60 days of immersion. *In vitro* studies carried out with simulated urine demonstrated that, the tubes present a high fluid uptake ability, ca. 1000%. Despite this, the materials are able to maintain their shape and do not present an extensive swelling behavior. The biodegradation profile was observed to be highly dependent on the composition of the stent and it can be tuned. Complete dissolution of the materials may occur between 14 and 60 days. Additionally, no encrustation was observed within the tested timeframe. The ability to resist bacterial adherence was evaluated with *Gram-positive Staphylococcus aureus* and two *Gram-negatives Escherichia coli DH5 alpha* and *Klebsiella oxytoca*. For *Klebsiella oxytoca* no differences were observed in comparison with a commercial stent (*Biosoft® duo, Porges*), although, for *S. aureus* all tested compositions had a higher inhibition of bacterial adhesion compared to the commercial stents. In case of *E. Coli* the addition of gelatin to the formulations reduced the bacterial adhesion in a highly significant manner compared to the commercial stents. The stents produced by the developed technology fulfill the requirements for ureteral stents and will contribute in the development of biocompatible and biodegradable urinary stents.

[‡] This chapter is based on the following publication:

Barros AA, Duarte ARC, Pires RA, Sampaio-Marques B, Ludovico P, Lima E, Mano JF, Reis RL. 2014. Bioresorbable ureteral stents from natural origin polymers. *J Biomed Mater Res Part B* 2014;00B:000–000.

III-1. INTRODUCTION

Stents have a wide range of applications in urology. Stent-based strategies are usually applied in the ureter to ensure its patency, which may be compromised, for example, by a kidney stone. This method is sometimes used as a temporary measure to prevent damage to a blocked kidney until a procedure to remove the stone is performed. Indwelling times for these cases are typically from 15 up to 60 days. In the case of tumors, stents are indicated to hold open ureters, which have been compressed in the area of the tumor or by the tumor itself. Stents, used to guaranteed drainage of urine flow through the ureter should have, in these cases, indwelling times of 12 months or longer (1). The main complications with ureteral stents are dislocation, infection, and blockage by encrustation (2, 3). Currently, nearly 100% of the people who have an urological stent are likely to develop a bacterial infection within 30 days, which increases morbidity threefold (4). Different types of temporary and permanent stents have been introduced into urological practice to relieve obstructions (5, 6). In terms of ureteral stents composition materials, the gold standard are polymeric compounds from different families, including silicone, polyurethane Siliteck, among others (7). However in some cases, polymeric stents demonstrate certain limits in their ability to resist external compression forces and in certain cases metallic materials have been introduced as they are more resistant stents (8).

Despite the fact that stent designs have improved over the years, they present one major key disadvantage, which is the fact that they have to be removed by second intervention. Avoiding a secondary procedure to remove the ureteral stents is highly desirable. The development of biodegradable ureteral stents has been pursued previously. However, regardless of early positive results with various models (9-12) these attempts were abandoned due to biocompatibility issues in porcine ureters (13) or because they degraded in inhomogeneous, premature or delayed fashion (14, 15). Hydrogels can be applied as a coating surface modification to ureteral stents. Hydrogel-coated stents have advantages such as improved material biocompatibility, hydrophilization and lubrication (16, 17). Hydrogels are polymeric networks which may present relevant mechanical properties, appropriate degradation rates, reduced biofilm formation (18-20) and constitute per se, an interesting alternative to conventional urological stents. An ideal stent for the lower urinary tract would provide adequate support to the duct wall, like the urethra or ureter, keeping the lumen open during and after the healing process, and then biodegrade totally from the body (2, 21). The

material needs to fulfill the biocompatibility demands according to the guidelines of tissue biocompatibility analysis and risk assessment of new medical devices. The rigidity of the material has to be suited to the place of application; the degradation products should be biocompatible; and the rate of degradation adequate to allow healing. The devices also need to be easily sterilized without change in the morphological and mechanical properties (22). It has been reported in the literature that the coating of polymeric stents with hydrogels is able to improve the properties of the stent, like anti-bacterial properties (2, 16), however, to our knowledge, simple hydrogel stents have not been reported. The concerns regarding existing stents are the motivation to design new biodegradable urological stent systems based on natural polymers, which present inherent biocompatibility, anti-bacterial properties and can be tailor-made into a custom suitable stent for a particular patient. The characteristics of an ideal temporary stent include easy placement under local anesthesia, minimal local side-effects, such as tissue hyperplasia or encrustation, and a low risk of migration. The device must also be easily removable or, preferably, biodegradable to reduce the necessity of further surgical intervention.

The compositions herein tested were based on polysaccharides of natural-origin, in particular alginate, gellan gum and their blends with gelatin. These polysaccharides have advantages over other polymers currently used to produce stents. As a main advantage, they are biodegradable and its use does not require a second surgery to remove the stent. The mechanical properties of these materials suggest that they can be used for this purpose, since they present elasticity and, at the same time, they allow urine flow through the obstructed region. With the properties of the proposed stents it is expected a reduction of the pain experienced by patients when compared to conventional stents as the stents prepared are softer. Furthermore, it is expected that the stent implantation is easier, due to the lubricity properties of the hydrogels, being hereafter more comfortable for the patient. Conventional stents coated with hydrogels have been reported to provide an improvement to the resistance to bacterial adhesion, and biofilm formation (23). Furthermore, the developed stents also exhibited adequate resistance to encrustation. The development of these stents with the above-mentioned properties anti-bacterial, biodegradable and appropriate geometry will be pursued in this work.

III-2. MATERIALS AND METHODS

III-2.1. Materials

Gelzan CM (gellan gum), alginic acid sodium salt, gelatin, urea, potassium chloride, calcium chloride and ethanol were purchased from Sigma-Aldrich (Germany). Potassium dihydrogen orthophosphate (99.5%) and magnesium chloride hexahydrate (99%) were obtained from Riedel-de Haën (Germany). Carbon dioxide (99.998 mol%) was supplied by Air Liquide (Portugal). All reagents were used as received.

III-2.2. Preparation of polymer solutions

Polymers were dissolved in hot distilled water (90°C) at different concentrations, and stirred for 1 hour. The polymeric solution was injected in a template of appropriate geometry and immersed at room temperature in a stirred CaCl₂ cross-linking solution. This step allows the gelification of the polymer. In **Table III-1** the concentrations of polymers and cross-linking agents used to prepare the aerogel-based stents are summarized.

Table III-1 Polymer and cross-linking agent concentrations used to prepare the stents

Polymers	Polymer conc. (wt%)	Cross-linking agent	Cross-linking agent conc. (M)
Alginate	6		
Alginate : gelatin (60:40)		CaCl ₂	0.24
Gellan gum	4		
Gellan gum : gelatin (60:40)			

III-2.3. Sample drying

Supercritical fluid drying with CO₂ is an alternative process to the conventional drying techniques, which preserves the properties of the wet gel in the dry form. The stents were dried in a high-pressure vessel with carbon dioxide at 40 °C and 100 bar for 2 hours, in a continuous

mode, with a CO₂ flow rate of 15 g/min. The conditions were chosen in order to ensure complete miscibility between the CO₂ and ethanol. Different processing times were tested and 2 hours was established as the necessary drying timeframe.

III-2.4. Characterization

III-2.4.1. Scanning electron microscopy (SEM)

The morphology of the stents was analyzed on a Leica Cambridge S360 SEM. The samples were fixed with mutual conductive adhesive tape on aluminum stubs and covered with gold/palladium using a sputter coater. After immersion in artificial urine solution (AUS) the inner section of the stents was also analyzed to monitor the deposition of crystals.

III-2.4.2. Artificial urine uptake

AUS was prepared as described by Khandwekar *et al* (23), with the composition presented in **table III-2**:

Table III-2 Composition of the artificial urine solution (AUS)

	Component	% wt/v
Solution A	Potassium dihydrogen ortho-phosphate	0.76
	Magnesium chloride hexahydrate	0.36
	Urea	1.60
Solution B	Calcium chloride hexahydrate	0.53
	Chicken ovalbumin	0.2
Urease		0.125

The AUS uptake capability of the samples was measured for a period up to 60 days by their immersion in AUS. Pre-weighted stents were immersed in 10 ml of AUS and placed in a water bath at 37°C, 60 rpm for 1, 7, 14, 28 and 60 days. All the experiments were executed in triplicate. At the predetermined time periods, the samples were weighted in order to determine the uptake capability of the stents. AUS uptake was determined using the following equation:

$$\%AUS \text{ uptake} = \frac{W_w - W_f}{W_f} \times 100$$

Equation II-1 Determination of Artificial Urine Uptake

where w_w is the weight of the wet sample and w_f is the final weight (dried after immersion). The presented data is the average of at least three measurements.

III-2.4.3. Swelling

Images of dry and wet samples were taken using a Stereo Microscope + Lamp (Schott KL 200), stemi 1000 model (ZEISS), with a magnification 2x and the swelling of the matrix was evaluated by the measurement of the thickness of the wall using Image J software. The presented results are an average of at least 5 measurements (\pm SD) of each sample.

III-2.4.4. Indwelling time

The indwelling time was measured as function of the weight loss of the samples. Samples immersed in AUS were dried and weighted to determine the weight loss, which was calculated according to the following equation:

$$\% \text{ weight loss} = \frac{W_f - W_i}{W_i} \times 100$$

Equation II-2 Determination of wight loss.

where w_f is the final weight of the sample (dried after immersion) and w_i is the initial weight of the sample. Each formulation was tested in triplicate.

III-2.5. Tensile mechanical analysis

Tensile mechanical analysis of the materials produced (A – Alginate; AG - Alginate:Gelatine, GG – Gellan Gum; GGG: Gellan Gum:Gelatine) was measured using an INSTRON 5540 (Instron Int. Ltd, High Wycombe, UK) universal testing machine with a load cell of 1 kN. The samples were hydrated before testing in simulated urine for 30 min. The dimensions of the specimens used were 5 mm of length, 2 mm width and 0.5 mm of thickness. The load was placed midway between the supports with a span (L) of 3 mm. The crosshead speed was 1:5 mm.min⁻¹. For each condition the

specimens were loaded until core break. The results presented are the average of at least 3 specimens and the results are presented as the average \pm standard deviation.

III-2.6. Encrustation development

The evaluation of the deposition of crystals on the surface of stents was performed following the procedure described by Tunney et al. (24). Samples of the different stents were immersed in AUS for predetermined time periods. They were removed and rinsed gently with distilled water to remove any salts (which might be only deposited on the surface). Energy dispersive X-ray spectroscopy (EDS) was performed together with SEM in a Link Ex-II spectroscope (Oxford Instruments, United Kingdom) for elemental analysis, with an energy of 15.0 keV. Samples were fixed as described for SEM analysis and carbon coated using high vacuum carbon deposition.

III-2.7. Bacterial adhesion studies

Bacterial adhesion studies were performed according to Khandwekar *et al* (23). A quantitative short-term adhesion (4h) study was performed with *Staphylococcus aureus* (NCIM 5021), a Gram-positive organism, and two Gram-negative organisms *Escherichia coli* DH5 alpha and *Klebsiella oxytoca*; 100mL of lysogeny broth (LB) medium (1% bacto tryptone, 5% bacto yeast extract and 1% sodium chloride) was inoculated with a single colony of bacteria from a LB agar stock plate. Cells were grown at 37°C and 200 rpm, overnight. Cells were then split between two falcon tubes, centrifuged at 3500 rpm for 20 min and resuspended in phosphate buffered saline (PBS). Cell suspension was washed twice with PBS and resuspended at a concentration of 1×10^8 cells/ml. Three tubes (3 mm length) of each formulation were placed in a 24 well plate and were incubated with 1 ml of the cell suspension for 4 h at 37°C with shaking. The bacterial cells were eluted from the surfaces into 2 ml sterile PBS. The procedure involved 4 min sonication followed by 1 min mild vortexing (repeated three times) using an ultrasonic cleaner (Bandelin Sonorex Digitec) with a ultrasonic frequency of 35 kHz. A known volume of the sample was inoculated into LB agar and incubated at 37°C for 24h. The colony forming units (CFUs) were counted indicating the total number of bacteria retained on the surface.

III-2.8. Cytotoxicity and cell adhesion studies

III-2.8.1. Cell culture

An immortalized mouse lung fibroblasts cell line (L929) purchased from the European Collection of Cell Cultures, was maintained in basal culture medium DMEM (Dulbecco's modified Eagle's medium; Sigma–Aldrich, Germany), 10% FBS (heat-inactivated fetal bovine serum, Biochrom AG, Germany) and 1% antibiotic-antimycotic (Gibco, UK). Cells were cultured in a humidified incubator at 37°C in a 5% CO₂ atmosphere.

III-2.8.2. Indirect cytotoxicity studies

The cytotoxicity of the stents developed was assessed using an immortalized mouse lung fibroblasts cell line (L929) purchased from the European Collection of Cell Cultures. The effect of the leachables released from the stents (during 24 h) on the cellular metabolism was performed using a standard MTS (Cell Titer 96® Aqueous Solution Cell Proliferation Assay, Promega, USA) viability test, in accordance with ISO/EN 10993 guidelines. A latex rubber extract was used as positive control for cell death; the extracts from a commercial stent (Biosoft® duo, Porges) was used as a reference material; while cell culture medium was used as negative control representing the ideal situation for cell proliferation. Cell viability was evaluated by the MTS assay after 72 h. This assay is based on the bioreduction of a tetrazolium compound 3-(4,5-dimethylthiazol-2-yl)-5-(3-carboxymethoxyphenyl)-2-(4-sulphophenyl)-2H-tetrazolium (MTS) into a water-soluble purple formazan product. This was quantified by UV-spectroscopy, reading the formazan absorbance at 490 nm in a microplate reader (Synergy HT, Bio-Tek Instruments, USA). Each sample formulation and control were tested using 12 replicates.

III-2.8.3. Direct contact studies

Confluent L929 cells were harvested and seeded in the stents as follows: stents were distributed in a 48-well cell culture plate (BD Biosciences, USA); samples were initially immersed in sterile PBS in order to swell; afterwards, PBS was removed and a drop (20µl) of a cell suspension with a concentration of 1 x 10⁵ cells/ml was added to each material. Cell seeding on the

commercial stent was also carried out as control. The cells-stents constructs were statically cultured for 1, 3 and 7 days under the culture conditions previously described. Cell adhesion to the surface of the materials was determined after the pre-determined culture times by the MTS assay described above. The cell-stents were transferred to a new culture plate in order to evaluate the presence of viable cells only on the surface of the developed materials. Optical density (wavelength of 490nm) was determined for each time point and compared to polystyrene tissue culture plate, used as a positive control. All cytotoxicity screening tests were performed using three replicates.

III-3. STATISTICAL ANALYSIS

Statistical analysis was performed to compare the results obtained using GraphPad Prism 5. Shapiro-Wilk test was used to verify the normality of the data obtained. Normally distributed data was analyzed by t-student test comparing each tested stent with the commercial stent, in case of bacterial adhesion study. Non-parametric tests were performed in the case of cytotoxicity and cell adhesion samples with deviation of the data from the normal distribution. Mann-Whitney test was performed to pairs of independent samples in order to compare the medians of the results. Statistical significant differences were considered when $p < 0.05$.

III-4. RESULTS

III-4.1. Stents from natural origin polymers

Stents were prepared following the processing steps represented in **Figure III-1**. The tube is formed from an initial aqueous solution of biopolymer from which gelation is induced. Gelation in the case of alginate tubes was promoted by ionic cross-linking with a CaCl_2 solution. In the case of gellan gum lowering the solution temperature induces gelation, which is a physical crosslinking method. In order to confer stability to the tubes, and avoid their premature dissolution in aqueous solutions, gellan gum, was also ionically cross-linked with KCl and CaCl_2 solution, respectively. The hydrogels were, then, dehydrated and subject to a solvent exchange step where an alcohol gel was formed. In this process, ethanol replaced water and the material was further dried using supercritical carbon dioxide (25).

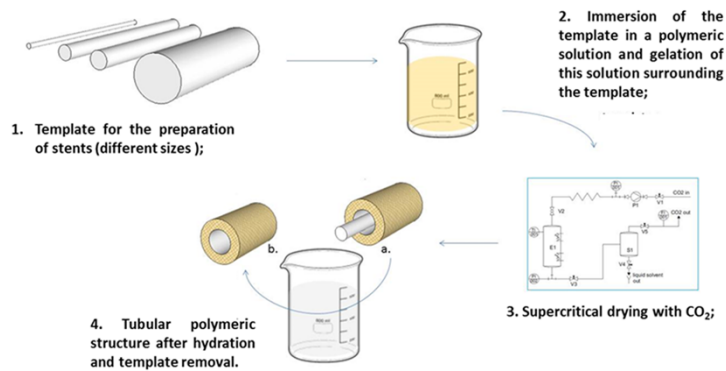


Figure III-1 Methodology used to generate the different stents.

III-4.1.1. Scanning electron microscopy

Figure III-2 presents a SEM image of the hollow tubes after drying. This procedure allowed the preparation of a stent with a diameter of 1 mm in dry state, which did not show any dependence on: the type of biopolymer used; on the polymer concentration in solution; nor on the type of crosslinking.

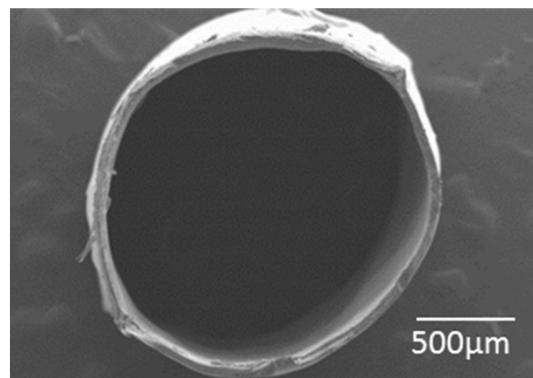


Figure III-2 SEM micrographs of the gellan gum : gelatin stent (60:40% wt/wt)

III-4.2. Characterization

III-4.2.1. Artificial urine uptake and indwelling time

The micrographs in **Figure III-3** show that, upon hydration, the inner diameter of the stents increased from 1.0 (SD \pm 0.3) to 1.8 (SD \pm 0.2) mm. These stents are able to maintain their shape

and integrity upon immersion in simulated body fluids, as observed for periods up to 60 days of immersion.

In clinical practice the indwelling time is defined as the time ranging from the implantation of the stent until its removal, which is dependent on the clinical treatment defined for each patient (26). Therefore, it would be desirable to tune the degradation of the stents to accommodate the devices for a given indwelling time. The weight loss, measured as the percentage of mass lost when immersed in AUS for a predetermined time period, was assessed for the different formulations of stents developed (**Figure III-4**).

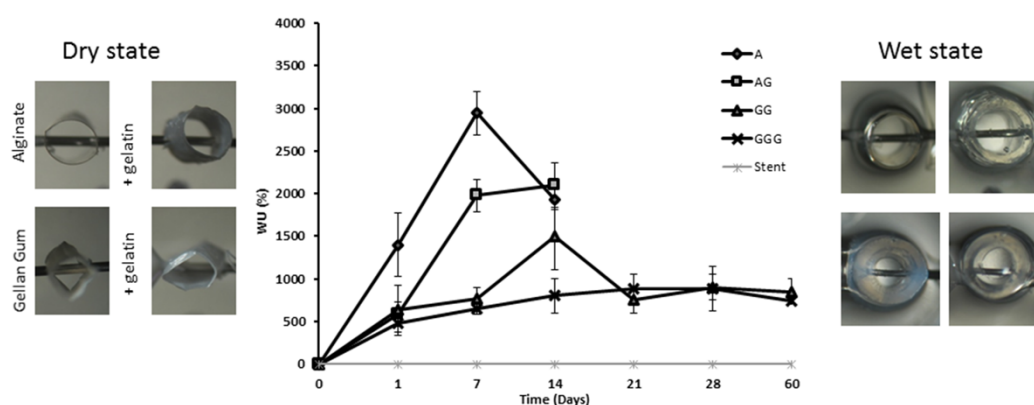


Figure III-3 AUS uptake by the developed stents (A—alginate; AG—alginate:gelatine, GG—gellan gum; GGG—gellan gum:gelatine) during a timeframe of 60 days, and swelling images using a magnifying lens (2×), showing a change in the internal diameter from 1.0 mm to 1.8 mm. Biosoft® duo, Porges Stent was used as a control.

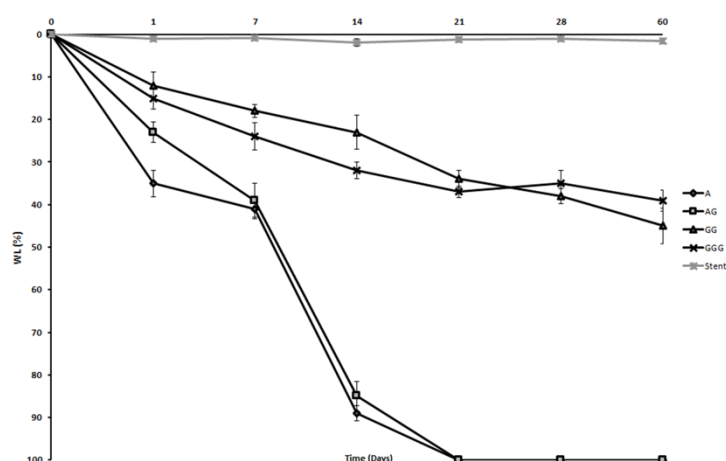


Figure III-4 Weight loss of the developed stents (A—alginate; AG—alginate:gelatine, GG—gellan gum; GGG—gellan gum:gelatine) during a time frame of 60 days (indwelling time). Biosoft® duo, Porges Stent was used as a control.

Using the processing methodology herein detailed it is possible to tune the degradation rate of the stents by selecting the materials used to produce them. Furthermore, the extent of crosslinking can confer different properties to the stents. *In vitro* performance demonstrates that the indwelling time of the proposed materials in solution can be tuned from 14 up to 60 days. The stents based on alginate were the ones that presented a faster dissolution and after 21 days of immersion the materials was completely dissolved in the solution.

III-4.2.2. Mechanical tests

The mechanical properties of the stents prepared were evaluated in tensile mode. **Table III-3** presents the results obtained for the different formulations tested. The results presented were determined in the wet state, in artificial urine solution, mimicking the real application conditions.

Table III-3 Mechanical properties of the stents prepared

	Maximum load (N)	Maximum tensile strain (%)	Young modulus (Mpa)
A	0.73 ± 0.01	11.75 ± 0.60	18.17 ± 1.04
AG	0.56 ± 0.02	15.84 ± 0.58	13.19 ± 0.82
GG	1.11 ± 0.04	20.93 ± 0.78	28.25 ± 1.47
GGG	0.96 ± 0.04	29.68 ± 0.54	26.62 ± 1.24

III-4.2.3. Encrustation development

The deposition of salts was evaluated by SEM and EDS. In **Figure III-5** is presented a micrograph of the inner surface of the stents after immersion and the corresponding EDS spectra. The results point out that no encrustation was detected in any of the materials herein proposed.

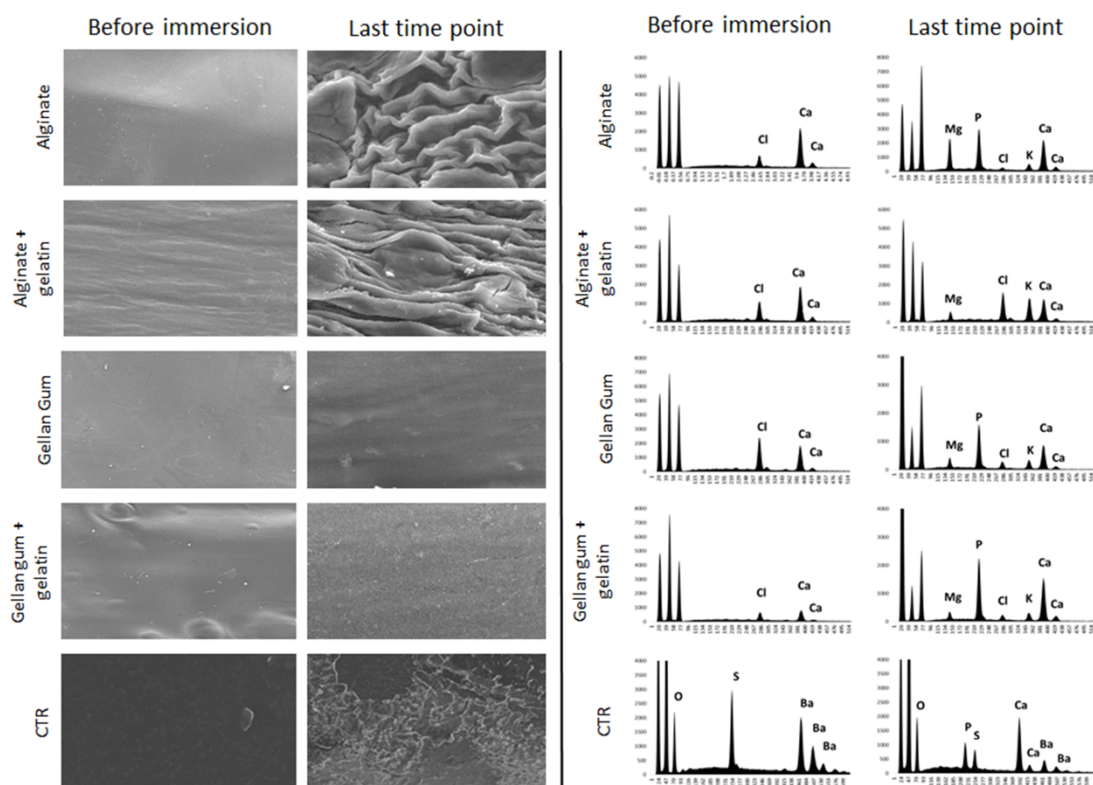


Figure III-5 SEM micrographs and EDS spectra of the surface of the stents prepared with the different polymers before and after immersion in AUS—last time point corresponds to 14 days for alginate-based stents and 60 days for gellan gum-based ones. Biosoft® duo, Porges Stent was used as a control.

III-4.2.4. Bacterial adhesion studies

Bacterial adhesion is a serious concern related with the formation of biofilm on the surface of the stents. The ability of bacteria to adhere and proliferate on the surface of the materials was studied for 3 different bacteria: *Staphylococcus aureus* (Gram-positive); and *Escherichia coli* DH5 *alpha* and *Klebsiella oxytoca* (Gram-negative) and the obtained results are presented in Figure 6. Statistical analysis indicated a significant reduction in adhesion of both *Staphylococcus aureus* and *Escherichia coli* DH5 *alpha* to alginate gelatin and gellan gum + gelatin stents in comparison with the commercial stent (~12X, ~41X and ~2X, respectively). The extent of reduction was found to be greater for *Staphylococcus aureus* when compared to *Escherichia coli* DH5 *alpha* (Figure III-6). Relatively to *Klebsiella oxytoca*, no alteration on the adhesion profile was observed for any of the tested stents. Moreover, it is relevant to notice that, the stents prepared with gelatin present

significantly lower bacterial adhesion, suggesting that these materials may be the ones that have higher potential in the development of biodegradable ureteral stents.

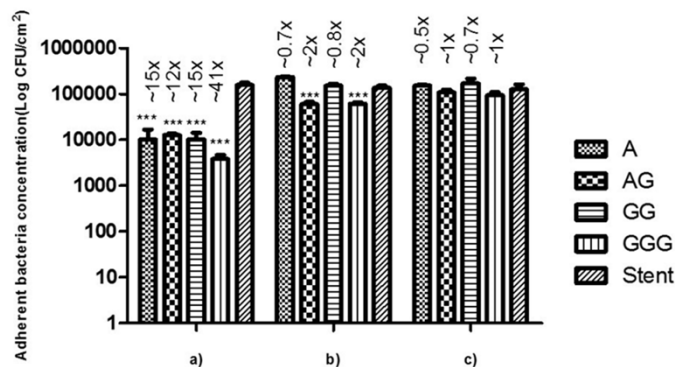


Figure III-6 Bacterial adhesion on the stents incubated with approximately 1×10^8 (a) *S. aureus* bacteria (Gram+), (b) *E. coli* DH5 alpha (Gram–), and (c) *K. oxytoca* (Gram–) for 4 h. Values indicate mean \pm standard deviation from a single experiment performed in triplicate, which was representative of three independent experiments. Fold adhesion reduction between each tested stents and the commercial stent is indicated on top of each bar. Significance of the values between each tested stents and the commercial stent was determined by the t-student test (*) $p < 0.001$. A–alginate; AG–alginate:gelatine, GG–gellan gum; GGG–gellan gum:gelatine.**

III-4.2.5. Cytotoxicity and cell adhesion studies

The cytotoxicity of the six developed stents was evaluated in accordance with the protocol described in ISO/EN 10,993 (27). As a control, the commercial stent *Biosoft® duo* (*Porges*) was used. The viability of the cells cultured in a tissue culture plate, in the presence of the stents was determined as a function of the cells cultured in DMEM culture medium. **Figure III-7a** presents the cell viability after 72 hours in contact with the material. The obtained results were compared to cell growth on tissue culture plate.

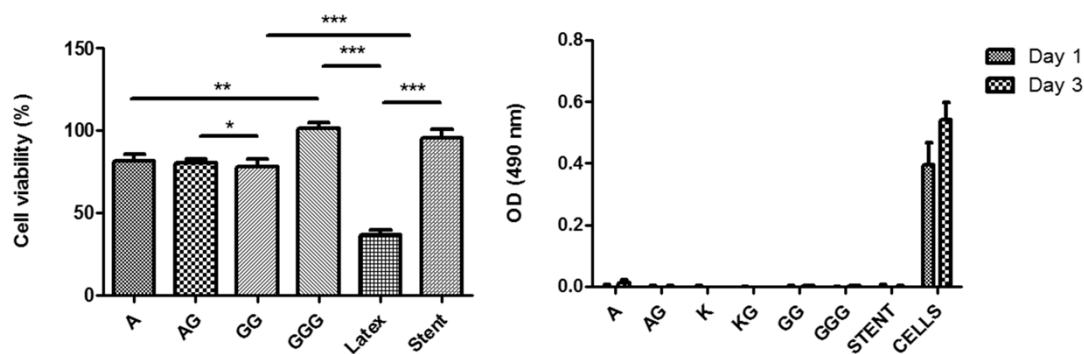


Figure III-7 Cytotoxicity and cell adhesion studies: (a) cell viability measured after 72 h and (b) cell adhesion on the surface of the different stents. Biosoft® duo, Porges Stent was used as a control. Statistical significant differences were considered as * $p < 0.001$; ** $p < 0.01$; * $p < 0.05$.**

No significant differences were observed for the cell viability in the presence of the developed stents in comparison with the one obtained for the commercial stent, which was used as a negative control.

In this context, cells were seeded directly on the surface of the stents and the adhesion was studied after 1 and 3 days of culture by MTS viability assay. Cells seeded on tissue culture plate were used as control (**Figure III-7b**).

MTS analysis revealed that no cells are present in the surface of the materials after 1 or 3 day of culture. As it can be observed from **Figure III-7b** the developed stents present a behaviour similar to the commercial stent. Clear differences between cell growth on the tissue plate and on the stent surfaces are observed. This observation would be expected due to the hydrophilic nature of the tested biopolymers. Nonetheless there are reports in the literature which indicate that cells are able to adhere and grow on the tested substrates (28-30).

III-5. DISCUSSION

An urological stent is defined as a thin tube, which is inserted in the ureter to prevent or treat the obstruction of urine flow from the kidney to bladder. Biodegradable natural-origin hydrogels present characteristics, which confer them several advantages, such as, biocompatibility, interface lubricity, as well as resistance to biofilm formation and encrustation (31). The main objective of the present research work is the preparation of hollow tubes from natural origin polymers, namely,

alginate, gellan gum and their blends with gelatin and to evaluate suitability, to be used as ureteral stents. Different blends of natural polysaccharides with gelatin have been reported in the literature (31-33). The variability of gelatin chemical composition confers this biopolymer different molecular weight and polydispersity, which *per se* have shown to substantially influence mechanical and thermal properties of physical gels (34). The combination of polysaccharides with gelatin is expected, to induce changes in the water uptake, degradation profile and the *In vitro* biological performance of the ureteral stents. These changes were particularly noticeable in the bacteria adhesion studies, which have demonstrated that the presence of gelatin in the blend lower the number of adhered bacteria.

The technology developed for the preparation of the hollow tubes, although not new, has not been applied for the purpose reported in this work (**Figure III-1**). One of the main advantages of the process is the use of supercritical carbon dioxide as drying agent. This has demonstrated several advantages over conventional drying methods, such as freeze-drying or vacuum drying (28). Both freeze-drying and vacuum drying involve a phase transition, solid-vapor and liquid-vapor, respectively. The phase transition is responsible for an interfacial tension, which results in the shrinkage and deformation of the produced matrices. On another hand, supercritical drying with carbon dioxide is a process which the matrices do not undergo any phase transition and therefore the integrity of the structures is not compromised (33). In the supercritical drying process, carbon dioxide replaces the solvent molecules within the polymeric matrix and removes the organic solvent due to their miscibility at the drying conditions. The production of hollow tubes by the proposed technology (**Figure III-2**) foresee its versatility as the change of the template allows the preparation of materials with different shapes, making it possible to control the thickness of the wall, the inner diameter and the mechanical properties. It is also possible to create a material with different layers by dipping the template, sequentially, in different polymeric solutions. Such bottom up approach to obtain multilayered hydrogels was validated before on spherical objects (25).

The biopolymers used in the preparation of the stents are highly hydrophilic. An inherent characteristic of these stents is the fact that, in the presence of water, an hydrogel is formed (35). This behavior is usually coupled with a high swelling ability, which may disrupt the structure of the matrices. The prepared stents have high water uptake ability, up to approximately 1000%, after 1 day of immersion (**Figure III-3**). However, the devices do not present an extensive swelling behavior as observed by a magnifying lens. *Augst and co-workers* refer that ionic cross-linked alginates dissolve upon losing the divalent cations responsible for the cross-linking (33). The

observed dissolution rate might also be due to the ionic change between Ca^{2+} ions by monovalent ions, which weaken the structure (36). Hydrogels of alginate occurs as a result of the formation of ionic cross-links between carboxyl groups in guluronic acid residues within the polysaccharide. Each calcium ion is then chelated by two alginate molecules, forming crosslinks, thus resulting in gelation. When immersed in distilled water alginate the mechanical properties will be conserved, however, in the presence of monovalent ions (K^+ or Na^+), in our work in artificial urine solution, ion exchange will occur with the cross-linking Ca^{2+} resulting in a rapid reduction in mechanical properties (33, 36-38).

In our experiments, the variation of the ratio of polysaccharide:gelatin did not show a significant effect on the biodegradation profile of the samples, although it has been reported that it may tune the resorption kinetics of hydrogels for a wide range of applications and conditions (32, 39). In this perspective, it is possible to design polymeric stents with the dissolution timeframe that best fits the treatment strategy (**Figure III-4**). Consequently, the need for a second surgery to remove the stent can be avoided using the proposed natural-based stents.

The mechanical properties of urinary stents are an important parameter in order to access the feasibility of the hydrogel tubes to withstand the forces applied when the stent is inserted in the patient, assuring that the material does not break obstructing the ureter and preventing the flow of urine. Results reported in the literature for a polyurethane double J stents refer an ultimate tensile strength between 18 and 35 MPa, an elongation at break between 104 and 509 % and a Young modulus between 38 and 41 MPa (40). As expected these values are significantly higher than the ones reported in our work for the hydrogels prepared. The tensile properties of the stents produced change in the presence of gelatin and the results indicate that the presence of gelatin increases the maximum tensile strain while decreasing on the other hand the maximum load and the Young modulus. Few reports in the literature provide comparable data to the one presented in this work. Nandakumar and coworkers, report the development of hydrophilic high glycolic acid–poly(DL-lactic-co-glycolic acid)/ polycaprolactam/polyvinyl alcohol blends as ureteral materials and tensile tests carried out refer tensile stresses at maximum load in the range of 0.66 up to 8.82 MPa, depending on the formulation (41). Nonetheless, the data reported was measured in thin films and not in hollow tubes. Furthermore, there is no indication that the results were determined in the wet state. Another work, by Jones and coworkers who evaluated the possibility to prepare stents from poly(ϵ -caprolactone) and poly(ϵ -caprolactone)-polyvinylpyrrolidone-iodine blends, refer also the tensile mechanical properties of the films prepared which, disregarding possible geometrical effects

is in the same order of magnitude of the polyurethane commercial stents (42). A straightforward comparison of the results should not, hereafter, be carried out. The alginate and gellan gum-based stents prepared in this work reveal good mechanical properties and provide the stability and strength necessary for manipulation during the placement process and its function in ureter.

A major concern in urology is the development of encrustation on urological stents. This phenomenon is related with the deposition of salts (present in the urine) on the surface of the stent. When encrustation occurs urine flow is blocked, causing distress and pain to the patients. Particularly relevant are magnesium salts in the form of struvite and or calcium salts in the form of hydroxyapatite. Alginate and gellan gum stents, as well as the ones prepared with their mixture with gelatin, were immersed in AUS for different time periods. In order to study this effect SEM micrographs (**Figure III-5**) show a smooth inner surface of the stents at the initial time points. The micrograph for the last data point shows some rugosity, which can be explained by the polymeric dissolution. However, these results do not indicate any evidence of deposited crystals and demonstrate that no encrustation was developed during the lifetime of the stent when in contact with AUS. Furthermore, these observations are consistent with EDS analysis presented in **Figure III-5**. The EDS spectra clearly indicated the absence of ions that could suggest struvite or hydroxyapatite formation. The Ca^{2+} and Cl^- ions detected in the spectra of all polymers are from the cross-linking agent, as they appear only the spectra of the materials before immersion and disappear after immersion in AUS. The hydrophilicity of the tested biopolymers can explain these observations, as the high hydration capacity of hydrogels prevents the deposition of soluble salts.

Concerning biofilm formation and bacterial adhesion, reports in the literature suggest that coating commercial stents with hydrogel may lead to a significant decrease in bacterial adhesion (23, 35). In the study of Khandwekar *et al.* (23) commercial stents (Tecoflex®) were compared to stents made of polyurethane (Tecoflex®) modified vinylpyrrolidone-iodine (PVP-I) complex. In their work, the PVP-I modified stent was highly hydrophilic and more lubricious than the control polyurethane. Adherence of both Gram positive *Staphylococcus aureus* (by 1×10^6 CFU/cm²) and Gram-negative *Pseudomonas aeruginosa* (by 2×10^6 CFU/cm²) was significantly reduced on the modified surfaces. Our results obtained for the commercial stent (*Biosoft® duo, Porges*), following the same experimental procedure indicated the presence of $\sim 1,8 \times 10^5$ CFU/cm² for the three tested bacteria's (*Staphylococcus aureus*, *Escherichia coli DH5 alpha* and *Klebsiella oxytoca*). The materials tested demonstrated a lower bacterial adherence, particularly for the Gram-positive bacteria *Staphylococcus aureus*, whereas a reduction of about 12X to 41X of bacterial adhesion

was observed. For the Gram-negative bacteria, the tested materials demonstrated a behavior similar to the commercial stent, although with *Escherichia coli* DH5 *alpha*, it was observed an adhesion reduction of about 2X with two of the used biomaterials (alginate gelatin and gellan gum + gelatin). These results can be explained by the bacterial cell surface structure, since cell-surface hydrophobicity is an important factor in the adherence and proliferation of microorganisms on solid surfaces (23, 24). Consistently, it was reported that *Staphylococcus aureus* has higher hydrophobicity ability in comparison with *Escherichia coli* (Cell surface hydrophobicity (CSH) of *Escherichia coli*, *Staphylococcus aureus* and *Aspergillus niger* and the biodegradation of Diethyl Phthalate (DEP) via Microcalorimetry (43, 44). Considering the implications of cell surface hydrophobicity on cell adhesion, our results suggest that including gelatin on the formulations will be a promising approach in the reduction of bacterial adhesion as demonstrated by the data described in **Figure III-6**.

Another crucial concern, in products for medical use and human consumption, is the evaluation of the cytotoxicity of the developed materials. Reports in the literature have described the non-cytotoxicity of the polysaccharides used in this study, although, it is not straightforward the extrapolation for the developed stents (45). Different processing techniques may influence the characteristics of the materials and may induce an undesirable toxic response. The experiments carried out following an ISO (27) guideline have shown that neither the materials nor its leachables are toxic as cell viability in the experiments with the developed stents is comparable to the ones in tissue cultured plates. In addition, ureteral stents should not induce cell adhesion because they could promote an abnormal cell growth which may compress the stent, and consequently constrain the normal urine flow (1). In fact, These materials have been reported for other tissue engineering applications in which it is possible to promote cell adhesion (46). It is also well documented that cells respond to particular morphological and topological cues (24). Our findings suggest that the stents prepared did not induce cell adhesion at the surface. The observed differences may be related to the processing methodology which results in a smoother surface, not favorable to cell adhesion.

III-6. CONCLUSION

The present work constitutes an important step towards the development of biodegradable urological stents. Here we described a methodology to prepare stents using natural-origin polymers templated gelation and drying, using critical point carbon dioxide, generated stents able to compete with the commercially available ones. Biopolymers, such as, alginate and gellan gum, as well as their blends with gelatin, present different advantages compared to the commercial products, such as: adequate biodegradation rates; no development of encrustation; and anti-bacterial properties. Stents prepared from alginate present the fastest biodegradation rate, corresponding to an indwelling time of 21 days. Longer indwelling periods may be achieved with the use of gellan gum. The addition of gelatin to the blends decreases the bacterial adhesion demonstrating to be a promising strategy to reduce the bacterial adhesion. Furthermore, the technology proposed is highly versatile, allowing a wide range of stent designs. The described stents, when in contact with a physiological medium, become hydrogels, exhibiting biocompatible and non-cytotoxic characteristics. The presence of a high equilibrium water content, provides soft, lubricious and flexible characteristics to the devices, similar to natural tissue. The obtained results demonstrate the feasibility to develop biodegradable stents from natural origin polysaccharides.

ACKNOWLEDGEMENTS

The research leading to these results has received funding from the European Union Seventh Framework Programme (FP7/2007-2013) under grant agreement number REGPOT-CT2012-316331-POLARIS and from the project “Novel smart and biomimetic materials for innovative regenerative medicine approaches” RL1 - ABMR - NORTE-01-0124-FEDER-000016) cofinanced by North Portugal Regional Operational Programme (ON.2 – O Novo Norte), under the National Strategic Reference Framework (NSRF), through the European Regional Development Fund (ERDF). Ricardo Pires and Belém Sampaio-Marques acknowledge their FCT post-doc grant SFRH/BPD/39333/2007 and SFRH/BPD/90533/2012, respectively.

REFERENCES

1. Waters SL, Heaton K, Siggers JH, Bayston R, Bishop M, Cummings LJ, et al. Ureteric stents: investigating flow and encrustation. *P I Mech Eng H*. 2008;222(H4):551-61.
2. Al-Aown A, Kyriazis I, Kallidonis P, Kraniotis P, Rigopoulos C, Karnabatidis D, et al. Ureteral stents: new ideas, new designs. *Therapeutic advances in urology*. 2010;2(2):85-92.
3. Lenaghan D, Clarke A, Goad J. Shockwave lithotripsy for retained encrusted ureteric stents: a review of 27 cases. *Bju Int*. 2013;111:78-9.
4. Divakaruni N, Palmer CJ, Tek P, Bjurlin MA, Gage MK, Robinson J, et al. Forgotten Ureteral Stents: Who's at Risk? *J Endourol*. 2013;27(8):1051-4.
5. Soliman BA, Shahbaz S, Brooks A, Lau H, Bariol S, Wang A, et al. Ureteric stents: how well do you know your stent? *Bju Int*. 2013;111:41-.
6. Seymour H, Patel U. Ureteric stenting - Current status. *Semin Intervent Rad*. 2000;17(4):351-65.
7. Venkatesan N, Shroff S, Jayachandran K, Doble M. Polymers as Ureteral Stents. *Journal of Endourology*. 2010;24(2):191-8.
8. Hendlin K, Korman E, Monga M. New Metallic Ureteral Stents: Improved Tensile Strength and Resistance to Extrinsic Compression. *Journal of Endourology*. 2012;26(3):271-4.
9. Assimos DG, Smith C, Schaeffer AJ, Carone FA, Grayhack JT. Efficacy of polyglycolic acid (PGA) tubing stents in ureteroureterostomies. *Urological research*. 1984;12(6):291-3.
10. Auge BK, Ferraro RF, Madenjian AR, Preminger GM. Evaluation of a dissolvable ureteral drainage stent in a Swine model. *J Urol*. 2002;168(2):808-12.
11. Lumiaho J, Heino A, Pietilainen T, Ala-Opas M, Talja M, Valimaa T, et al. The morphological, in situ effects of a self-reinforced bioabsorbable polylactide (SR-PLA 96) ureteric stent; an experimental study. *J Urol*. 2000;164(4):1360-3.
12. Kempainen E, Talja M, Riihela M, Pohjonen T, Tormala P, Alfthan O. A bioresorbable urethral stent. An experimental study. *Urological research*. 1993;21(3):235-8.
13. Olweny EO, Landman J, Andreoni C, Collyer W, Kerbl K, Onciu M, et al. Evaluation of the use of a biodegradable ureteral stent after retrograde endopyelotomy in a porcine model. *Journal of Urology*. 2002;167(5):2198-202.
14. Fu W-J, Wang Z-X, Li G, Cui F-Z, Zhang Y, Zhang X. Comparison of a biodegradable ureteral stent versus the traditional double-J stent for the treatment of ureteral injury: an experimental study. *Biomedical Materials*. 2012;7(6):065002.
15. Lingeman JE, Preminger GM, Berger Y, Denstedt JD, Goldstone L, Segura JW, et al. Use of a temporary ureteral drainage stent after uncomplicated ureteroscopy: Results from a phase II clinical trial. *Journal of Urology*. 2003;169(5):1682-8.
16. Chew BH, Duvdevani M, Denstedt JD. New developments in ureteral stent design, materials and coatings. *Expert Rev Med Devices*. 2006;3(3):395-403.
17. Chew BH, Denstedt JD. Technology insight: Novel ureteral stent materials and designs. *Nature clinical practice Urology*. 2004;1(1):44-8.
18. Li P, Poon YF, Li W, Zhu H-Y, Yeap SH, Cao Y, et al. A polycationic antimicrobial and biocompatible hydrogel with microbe membrane suctioning ability. *Nature materials*. 2011;10(2):149-56.
19. Hook AL, Chang C-Y, Yang J, Lockett J, Cockayne A, Atkinson S, et al. Combinatorial discovery of polymers resistant to bacterial attachment. *Nature biotechnology*. 2012;30(9):868-75.

20. Hasan J, Crawford RJ, Ivanova EP. Antibacterial surfaces: the quest for a new generation of biomaterials. *Trends in biotechnology*. 2013;31(5):295-304.
21. Liatsikos EN, Karnabatidis D, Kagadis GC, Katsakiori PF, Stolzenburg J-U, Nikiforidis GC, et al. Metal Stents in the Urinary Tract. *EAU-EBU Update Series*. 2007;5(2):77-88.
22. Vogt F, Stein A, Rettemeier G, Krott N, Hoffmann R, vom Dahl J, et al. Long-term assessment of a novel biodegradable paclitaxel-eluting coronary polylactide stent. *European heart journal*. 2004;25(15):1330-40.
23. Khandwekar A, Doble M. Physicochemical characterisation and biological evaluation of polyvinylpyrrolidone-iodine engineered polyurethane. *J Mater Sci: Mater Med*. 2011;22(5):1231-46.
24. Tunney MM, Keane PF, Jones DS, Gorman SP. Comparative assessment of ureteral stent biomaterial encrustation. *Biomaterials*. 1996;17(15):1541-6.
25. Duarte ARC, Santo VE, Alves A, Silva SS, Moreira-Silva J, Silva TH, et al. Unleashing the Potential of Supercritical Fluids for Polymer Processing in Tissue Engineering and Regenerative Medicine. *The Journal of Supercritical Fluids*. 2013.
26. el-Faqih SR, Shamsuddin AB, Chakrabarti A, Atassi R, Kardar AH, Osman MK, et al. Polyurethane internal ureteral stents in treatment of stone patients: morbidity related to indwelling times. *J Urol*. 1991;146(6):1487-91.
27. Biological Evaluation of Medical Devices. Part 5. Test for Cytotoxicity In Vitro Methods: 8.2 Test on Extracts., (1992).
28. Lima AC, Custódio CA, Alvarez-Lorenzo C, Mano JF. Biomimetic Methodology to Produce Polymeric Multilayered Particles for Biotechnological and Biomedical Applications. *Small*. 2013.
29. Silva T. H. MJF, and Reis R. L. Marine polysaccharide multilayers: PH responsive systems for the surface modification of tissue engineering scaffolds. *Tissue Engineering Part A*. 2008;14(5):753.
30. Duarte ARC, Mano JF, Reis RL. The role of organic solvent on the preparation of chitosan scaffolds by supercritical assisted phase inversion. *The Journal of Supercritical Fluids*. 2010.
31. Pulieri E, Chiono V, Ciardelli G, Vozzi G, Ahluwalia A, Domenici C, et al. Chitosan/gelatin blends for biomedical applications. *Journal of Biomedical Materials Research Part A*. 2008;86A(2):311-22.
32. Fan L, Du Y, Huang R, Wang Q, Wang X, Zhang L. Preparation and characterization of alginate/gelatin blend fibers. *Journal of Applied Polymer Science*. 2005;96(5):1625-9.
33. Augst AD, Kong HJ, Mooney DJ. Alginate Hydrogels as Biomaterials. *Macromolecular Bioscience*. 2006;6(8):623-33.
34. Liu Y, Geever LM, Kennedy JE, Higginbotham CL, Cahill PA, McGuinness GB. Thermal behavior and mechanical properties of physically crosslinked PVA/Gelatin hydrogels. *Journal of the mechanical behavior of biomedical materials*. 2010;3(2):203-9.
35. Cox AJ, Millington RS, Hukins DW, Sutton TM. Resistance of catheters coated with a modified hydrogel to encrustation during an in vitro test. *Urological research*. 1989;17(6):353-6.
36. Birdi G, Bridson RH, Smith AM, Mohd Bohari SP, Grover LM. Modification of alginate degradation properties using orthosilicic acid. *Journal of the mechanical behavior of biomedical materials*. 2012;6(0):181-7.
37. Dong Z, Wang Q, Du Y. Alginate/gelatin blend films and their properties for drug controlled release. *Journal of Membrane Science*. 2006;280(1-2):37-44.
38. Hunt N, Grover L. Cell encapsulation using biopolymer gels for regenerative medicine. *Biotechnol Lett*. 2010;32(6):733-42.
39. Li X, Tsutsui Y, Matsunaga T, Shibayama M, Chung U-i, Sakai T. Precise Control and Prediction of Hydrogel Degradation Behavior. *Macromolecules*. 2011;44(9):3567-71.

40. Gorman SP, Jones DS, Bonner MC, Akay M, Keane PF. Mechanical performance of polyurethane ureteral stents in vitro and ex vivo. *Biomaterials*. 1997;18(20):1379-83.
41. Nandakumar V, Suresh G, Chittaranjan S, Doble M. Synthesis and Characterization of Hydrophilic High Glycolic Acid–Poly(dl-Lactic-co-Glycolic Acid)/ Polycaprolactam/Polyvinyl Alcohol Blends and Their Biomedical Application as a Ureteral Material. *Industrial & Engineering Chemistry Research*. 2012;52(2):751-60.
42. Jones DS, Djokic J, McCoy CP, Gorman SP. Poly(epsilon-caprolactone) and poly(epsilon-caprolactone)-polyvinylpyrrolidone-iodine blends as ureteral biomaterials: characterisation of mechanical and surface properties, degradation and resistance to encrustation in vitro. *Biomaterials*. 2002;23(23):4449-58.
43. Gogra AB, Yao J, Sandy EH, Zheng S, Zaray G, Koroma BM, et al. Cell surface hydrophobicity (CSH) of *Escherichia coli*, *Staphylococcus aureus* and *Aspergillus niger* and the biodegradation of Diethyl Phthalate (DEP) via Microcalorimetry. *Journal of American Science*. 2010;6(7):78-88.
44. Schneider PF, Riley TV. Cell-surface hydrophobicity of *Staphylococcus saprophyticus*. *Epidemiology and infection*. 1991;106(1):71-5.
45. Silva TH, Duarte ARC, Moreira-Silva J, Mano JF, Reis RL. Biomaterials from Marine-Origin Biopolymers. *Biomimetic Approaches for Biomaterials Development: Wiley-VCH Verlag GmbH & Co. KGaA*; 2012. p. 1-23.
46. Oliveira JT, Martins L, Picciochi R, Malafaya PB, Sousa RA, Neves NM, et al. Gellan gum: a new biomaterial for cartilage tissue engineering applications. *Journal of biomedical materials research Part A*. 2010;93(3):852-63.

Chapter IV

Ketoprofen-eluting biodegradable ureteral stents by CO₂ impregnation: *In vitro* study

Chapter IV

Ketoprofen-eluting biodegradable ureteral stents by CO₂ impregnation: *In vitro* study[§]

ABSTRACT

Ureteral stents are indispensable tools in urologic practice. The main complications associated with ureteral stents are dislocation, infection, pain and encrustation. Biodegradable ureteral stents are one of the most attractive designs with the potential to eliminate several complications associated with the stenting procedure. In this work we hypothesize the impregnation of ketoprofen, by CO₂-impregnation in a patented biodegradable ureteral stent previously developed in our group. The biodegradable ureteral stents with each formulation: alginate-based, gellan gum-based were impregnated with ketoprofen and the impregnation conditions tested were 100 bar, 2h and three different temperatures (35°C, 40°C and 50°C). The impregnation was confirmed by FTIR and DSC demonstrated the amorphization of the drug upon impregnation. The *in vitro* elution profile in artificial urine solution (AUS) during degradation of a biodegradable ureteral stent loaded with ketoprofen was evaluated. According to the kinetics results these systems have shown to be very promising for the release ketoprofen in the first 72h, which is the necessary time for anti-inflammatory delivery after the surgical procedure. The *in vitro* release studied revealed an influence of the temperature on the impregnation yield, with a higher impregnation yield at 40°C. Higher yields were also obtained for gellan gum-based stents. The non-cytotoxicity characteristic of the developed ketoprofen-eluting biodegradable ureteral stents was evaluated in L929 cell line by MTS assay which demonstrated the feasibility of this product as a medical device.

[§] This chapter is based on the following publication:
Barros AA, Oliveira C, Reis RL, Lima E, Duarte ARC. Ketoprofen-eluting biodegradable ureteral stents by CO₂ impregnation: *In vitro* study. *International Journal of Pharmaceutics* 2015;495:651-9.

IV-1. INTRODUCTION

The double-J ureteral stent was introduced in 1978 by Finney *et al.* (1) and since then, they are usually applied in the ureter to ensure its patency, in the treatment of either benign or malignant urological diseases (2). The main complications associated with ureteral stents are dislocation, infection, pain and blockage by encrustation (3). In urological practice some clinical requirements need a temporary duration of stenting, normally few weeks, which can be covered by a biodegradable ureteral stent (2). Biodegradable ureteral stents are one of the most attractive designs with the potential to eliminate several complications associated with the stenting procedure. Particularly it avoids a second procedure to remove the stent, reduces patient morbidity and decreases of bacterial adhesion and no encrustation on the surface (4). Different biodegradable materials have been proposed to fabricate the ureteral stents with natural and synthetic polymers (5-9). On the other hand different reports suggest several coatings and eluting technologies in ureteral stents, which can improve the biocompatibility and decrease the ureteral stent discomfort (10-12). Drug-eluting stent technology allows the local delivery of a drug. The use of drug-eluting designs has been used extensively in cardiovascular applications, but in biodegradable ureteral stents it is yet an unexplored area (4, 13). Even though, different drugs have already been reported to be loaded in the conventional ureteral stents. For example, drugs like triclosan (14), with the objective to reduce stent-associated bacterial adhesion, biofilm formation and encrustation, and ketorolac (10, 15) with the purpose to improve the comfort of patient decreasing the flank pain. The first study to report the effectiveness of drug-eluting and biodegradable stents was published in 2009 showing the release of 5 α -reductase inhibitor directly into the prostate in patients with urinary retention and benign prostatic hyperplasia (BPH) (16). In the future, others drugs may be used in urologic practice like mitomycin C, paclitaxel, epirubicin and doxorubicin can be loaded in ureteral stents with different urological targets, such as chronic pelvic pain syndromes, upper tract urothelial cancer and neurogenic bladder (4).

Lange *et al.* (4) in a recent review concluded that the stent of the future will be degradable, in a control manner, and able to be coated or elute with active compounds, to address the current problems. In this work, we hypothesize the impregnation of ketoprofen, by supercritical fluid technology (SCF) in a biodegradable ureteral stent. Ketoprofen ((RS) 2-(3-benzoylphenyl)-propionic

acid) is one of the propionic acid class of nonsteroidal anti-inflammatory drugs (NSAID) with analgesic and antipyretic effects. (17-19). In current urological clinical practice ketoprofen is one of the prescribed medicines to be taken orally to decrease patient discomfort, known to be caused shortly after stent implantation (15). Supercritical fluid technology (SCF) has found its space in polymer processing, especially using supercritical carbon dioxide for processing pharmaceutical active compounds. This interest is mostly due to the mild processing conditions, the high diffusivity and low viscosity which enables delivering active compounds into polymer matrices (20-26). In literature, different studies demonstrated the solubility of ketoprofen using the supercritical carbon dioxide, which allows the impregnation of this active compound in matrices like our developed biodegradable ureteral stent (27-29). The purpose of this investigation is thus to evaluate the in vitro elution profile of ketoprofen impregnated in the biodegradable ureteral stent during its degradation.

IV-2. MATERIAL AND METHODS

IV-2.1. Materials

Gelzan CM (gellan gum), alginic acid sodium salt, gelatin, urea, urease type IX from *Canavalia ensiformis* (Jack Bean), calcium chloride, ketoprofen and ethanol were purchased from Sigma-Aldrich (Germany). Potassium dihydrogen ortho-phosphate (99.5%) and magnesium chloride hexahydrate (99%) were obtained from Riedel-de Haën (Germany). Carbon dioxide (99.998 mol%) was supplied by Air Liquide (Portugal). All reagents were used as received.

IV-2.2. Preparation of biodegradable ureteral stents

The biodegradable ureteral stents were developed according to the procedure described by Barros *et al.* (5). Briefly, the polymers were dissolved in hot distilled water (90°C) at different formulations (**Table IV-1**), and stirred for 1 hour. The polymeric solution was injected in a mold of appropriate geometry and immersed at room temperature in a stirred CaCl₂ cross-linking solution for 2 hours. This step allows the gelification of the polymer. the biodegradable ureteral stents were immersed in ethanol for 1 hour, to be subject to a solvent exchange step where an alcohol gel was formed. In this process, ethanol replaced water and the material was then dried in a high-pressure vessel with supercritical carbon dioxide at 40 °C and 100 bar for 2 hours, in semi-continuous mode.

Table IV-1 Polymer and cross-linking agent concentrations used to prepare the biodegradable stents

Formulation	Polymers	Polymer conc. (wt%)	Cross-linking Agent	Cross-linking agent conc. (M)
AG	<i>Alginate : gelatin (60:40)</i>	6	CaCl ₂	0.24
GG	<i>Gellan gum : gelatin (60:40)</i>	4		

IV-2.3. Supercritical CO₂ impregnation of ketoprofen

To remove the stents from the template a second hydration-dehydration step is necessary. The hollow tubes are dehydrated in ethanol. The two formulations of biodegradable ureteral stents alginate: gelatin (**AG**) and gellan gum : gelatin (**GG**), in the form of an alcohol gel were placed in high-pressure vessel with ketoprofen (10 mg) according the apparatus sketched in **figure IV-1**. The CO₂ supercritical impregnation conditions used for the impregnation of ketoprofen were 100 bar and 2 hours. The impregnation took place in continuous mode and three different operating temperatures were studied (35°C, 40°C and 50°C).

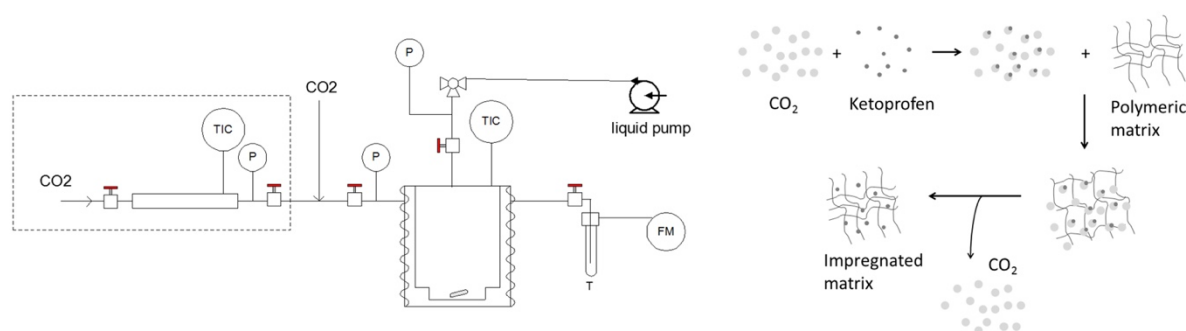


Figure IV-1 Supercritical fluid process impregnation and apparatus. TIC—temperature controller, P—pressure transducer, FM—flow meter.

IV-2.4. Characterization

IV-2.4.1. Surface Morphology

The morphology of the ketoprofen-eluting stents before and after impregnation process was analyzed on a JEOL SEM, model JSM-6010LV. The samples were fixed with mutual conductive adhesive tape on aluminum stubs and covered with gold/palladium using a sputter coater.

IV-2.4.2. Fourier transform infrared spectroscopy.

Infrared spectra of the different samples before and after impregnation was assessed by Fourier transform infrared spectroscopy (FTIR). Powdered samples were mixed with potassium bromide and the mixture was mold into a transparent pellet using a press (Pike, USA).

Transmission spectra were acquired on an IR Prestige-21 spectrometer (Shimadzu, Japan), using 32 scans, a resolution of 4 cm⁻¹ and a wavenumber range between 4400-400cm⁻¹.

IV-2.4.3. Scanning calorimetry analysis (DSC)

The DSC experiments were performed using DSC Q100 V9.8 Build 296 apparatus. The samples were placed in aluminum pans and heated at a rate of 10 °C/min from 20 to 220 °C, cooled to 20 °C and heated at 5 °C/min until 200 °C. Standard calibrations were performed using indium leads.

IV-2.4.4. In vitro release Kinetics in Artificial Urine Solution (AUS)

The release kinetics of developed ketoprofen-eluting stents was measured in artificial urine solution (AUS). AUS was prepared as described by *Khandwekar et al,(30)* with the composition presented in **table IV-2**:

Table IV-2 Composition of the artificial urine solution (AUS).

	Component	% wt/v
Solution A	Potassium dihydrogen ortho-phosphate	0.760
	Magnesium chloride hexahydrate	0.360
	Urea	1.600
Solution B	Calcium chloride hexahydrate	0.530
	Chicken ovalbumin	0.200
Urease type IX from <i>Canavalia ensiformis</i> (Jack Bean)		0.125

The *In vitro* ketoprofen release from the impregnated biodegradable ureteral stents of AG and GG was performed in triplicate. The impregnated sample were weighted and immersed in 10 ml of AUS at 37°C with 60 rpm stirring. At pre-determined time periods (0 min, 5 min, 15 min, 30 min, 1h, 3h, 5h, 7,5h, 24h, 48h, 72h, 7 days and 10 days), an aliquot (0.5 ml) of the release solution was taken and the volume replaced with fresh AUS. Ketoprofen concentration was calculated from a calibration curve prepared from standard solutions. The samples were analyzed by UV-Vis at 260 nm using a microplate reader (Synergy HT, Bio-Tek Instruments, USA) in a quartz microplate with 96 wells (Hellma).

IV-2.4.5. Diffusion coefficient calculation procedure

The release curves were modelled and the correspondent kinetic parameters were calculated using the Korsmeyer–Peppas equation, **Equation II 5** (31)

$$\frac{M_t}{M_\infty} = kt^n$$

Equation II-5 Determination of the diffusion coefficient

Where M_t and M_∞ are the absolute cumulative amounts of bioactive substance released at time t and at infinite release time, respectively; n is the release exponent, which provides information on the involved release mechanisms and k is the kinetic constant, which incorporates structural and geometric characteristics of the release material, in our case a cylinder geometry (32).

IV-2.4.6. The impregnation yield of ketoprofen-eluting biodegradable ureteral stents

The ketoprofen impregnation yield (I) on the biodegradable ureteral stents was calculated from **Equation II 3**:

$$I(\%) = \frac{m_{Ketoprofen}}{(m_{stent} + m_{Ketoprofen})} \times 100$$

Equation II-3 Determination of impregnation Yield.

Where m_{stent} is the initial mass of the stent and the $m_{ketoprofen}$ is the mass of ketoprofen released from the stent after immersion in AUS. The total drug amount impregnated was obtained after the plateau was reached and complete degradation of the stents in AUS solution. All the experimental results are the average of three samples and are presented as average \pm standard deviation.

IV-2.4.7. Indirect cytotoxicity studies

The cytotoxicity of the ketoprofen-eluting stents developed was assessed using an immortalized mouse lung fibroblasts cell line (L929) purchased from the European Collection of Cell Cultures. The effect of the leachables released from the biodegradable stents (during 24

hours) on the cellular metabolism was performed using a standard MTS (Cell Titer 96® Aqueous Solution Cell Proliferation Assay, Promega, USA) viability test, in accordance with ISO/EN 10993 guidelines. A latex rubber extract was used as positive control for cell death; while cell culture medium was used as negative control representing the ideal situation for cell proliferation. Cell viability was evaluated by the MTS assay after 72 h. This assay is based on the bioreduction of a tetrazolium compound 3-(4,5-dimethylthiazol-2-yl)-5-(3-carboxymethoxyphenyl)-2-(4-sulphophenyl)-2H-tetrazolium (MTS) into a water-soluble brown formazan product. This was quantified by UV-spectroscopy, reading the formazan absorbance at 490 nm in a microplate reader (Synergy HT, Bio-Tek Instruments, USA). Each sample formulation and control were tested using 12 replicates.

IV-3. RESULTS AND DISCUSSION

Our group previously developed an *In vitro* tested biodegradable ureteral stent from natural origin polymers (5). The results reported demonstrate that supercritical fluid processing is crucial for the development of such hollow tubes, which have a shape memory effect and when hydrated swell to the exterior and hence do not constrict the inner lumen of the stent. In this work, we developed an alginate and gellan-gum-based ketoprofen-eluting biodegradable ureteral stent and evaluated the *In vitro* elution profile in AUS. The impregnation process took place during the second drying procedure of the preparation of the stents, avoiding additional processing steps. The CO₂ supercritical impregnation conditions used for the impregnation of ketoprofen were hence, the same as used for the drying of the stents, i.e., 100 bar of pressure and 2 hours of contact time. The use of supercritical fluid impregnation in polymeric materials presents interesting advantages over conventional processes, such as the opportunity to take advantage of the high diffusivity, low surface tension of carbon dioxide and the ease to separate and recover the solvent and new polymeric material (24, 33). Upon depressurization of the process the stents are recovered in the dry form and can be used as collected.

IV-3.1. Morphological analysis

The 6 Fr double J biodegradable ureteral stent developed are illustrated in **figure IV-2**. These stents were obtained for two formulations, one alginate-based (AG) and a second one gellan gum-

based (GG). The produced ureteral stents were designed in a mold with real scale dimensions, mimicking the commercially available stents.

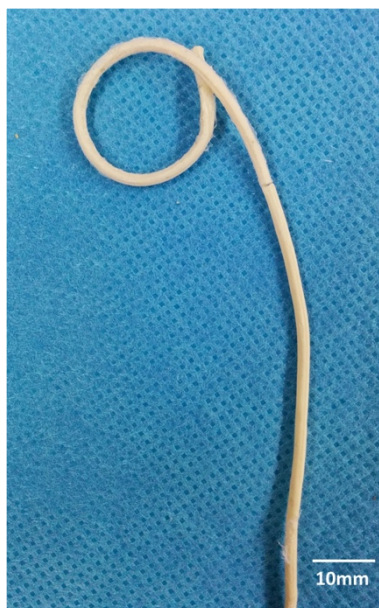


Figure IV-2 Biodegradable ureteral stent with the formulation AG (diameter 6 Fr).

In order to evaluate the influence of impregnation at the different temperatures, on the surface morphology the samples were analyzed by scanning electron microscopy (SEM). SEM images of the stents before and after ketoprofen impregnation are shown in **figure IV-3**. The images represent the surface morphology alginate-based and gellan gum-based stents impregnated at 50°C, 100 bar, AG50 and GG50. The images show the smooth surface observed before impregnation in the case of AG stents, however the GG stents present a rougher structure. Nonetheless, the surface of the stents does not seem to be affected by the CO₂ impregnation process.

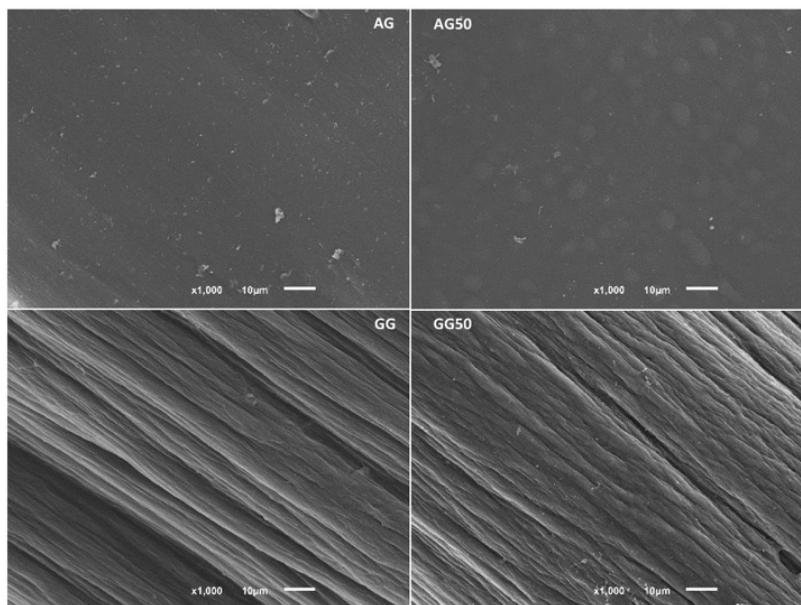


Figure IV-3 Scanning electron microscopy image of the biodegradable stents before (AG—alginate-based; GG—gellan gum-based) and after ketoprofen CO₂ impregnation (AG50, GG50–50 °C at 100 bar).

Fourier Transform Infrared Spectroscopy (FTIR) and differential scanning calorimetry (DSC) analyses were performed to verify the presence of the ketoprofen and the crystallinity of the samples after CO₂ impregnation, respectively. FTIR spectroscopy allowed the identification of most of the vibrational modes of ketoprofen present in the stents after CO₂ impregnation. FTIR spectrum of ketoprofen showed characteristic absorption peaks at 1697, and 1654 cm⁻¹ denoting stretching vibrations of aromatic C = O stretching of acid and C = O stretching of ketone, respectively. The absorption peaks at 1589 and 1446 cm⁻¹ were due to C = C stretching of aromatic ring (34). Similar absorption peaks were observed in the spectra of stents after CO₂ impregnation. In **figure IV-4**, as an example the formulations AG35 and GG35 are presented. It is noticeable the appearance of the characteristic absorption peaks of ketoprofen comparing with the standard reference spectra for AG and GG, respectively.

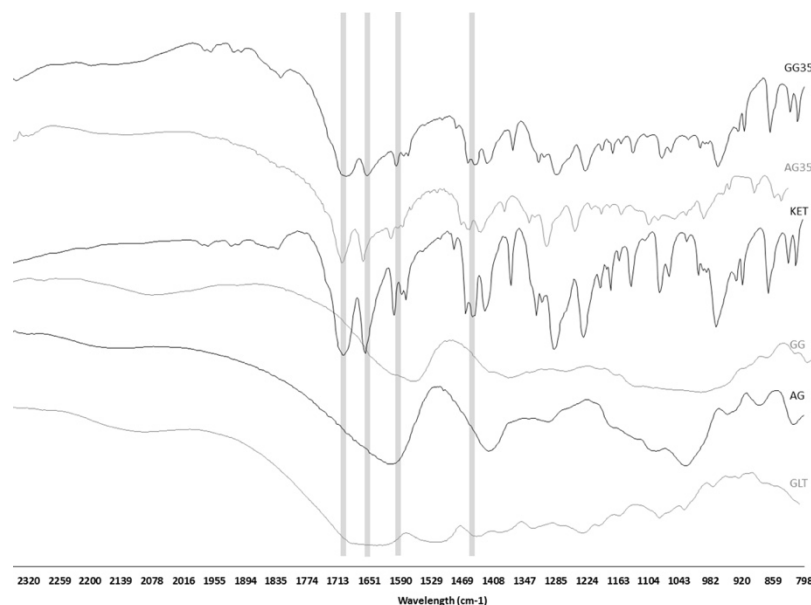


Figure IV-4 Fourier Transform Infrared Spectroscopy spectra of raw material alginate (AG), gellan gum (GG), gelatin (GLT), ketoprofen (KET) and after the ketoprofen impregnation by CO₂ (AG35, GG35–35 °C at 100 bar).

Figure IV-5 presents the thermal behavior of the pure ketoprofen and the two formulations AG and GG together with the thermal behavior of the ketoprofen-eluting stents prepared under different conditions. Ketoprofen (**Figure IV-5a**) demonstrated a characteristic peak at 96.60°C, which corresponds to its melting temperature. This highlights the fact that the raw material ketoprofen is in pure crystalline state. The thermal behavior of AG, GG and the ketoprofen-eluting stents prepared under different conditions in **Figure IV-5b** did not show any peak correspondent to crystalline ketoprofen as the initial raw material. This may be an indication that precipitating from the supercritical solution the drug presents a different crystalline state from the initial raw material. Other authors in the literature have reported this observation. (20, 21, 24, 35). The amorphization of the drugs is a preferred way in pharmaceutical sciences of enhancing the bioavailability and increasing solubility, optimizing delivery of the drug (36, 37). Hence, this is another major advantage of the supercritical impregnation process.

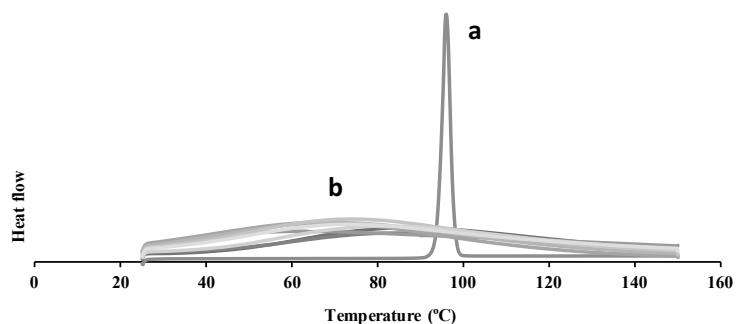


Figure IV-5 Differential scanning calorimetry spectra of ketoprofen (a) and biodegradable stents before and after the ketoprofen impregnation (b).

IV-3.2. *In vitro* release kinetics in Artificial Urine Solution (AUS)

The *In vitro* release kinetics was performed in AUS in order to mimic the real conditions *In vivo*. Released mass of ketoprofen per mass of stent impregnated at different temperatures (35°C, 40°C and 50°C) and 100 bar for a released period of 72 h in AUS is present in **figure IV-6a** for gellan gum-based and in **figure IV-6b** for alginate-based stents. The higher amount of ketoprofen released for both polymers used, was achieved at 40°C of operating condition and the lowest at 35°C. Comparing the two polymers used alginate-based stents reached the highest value of accumulative mass of 919 µg after 72h of release. In case of the gellan gum-based stent the value of accumulative mass released after 72h was 805 µg.

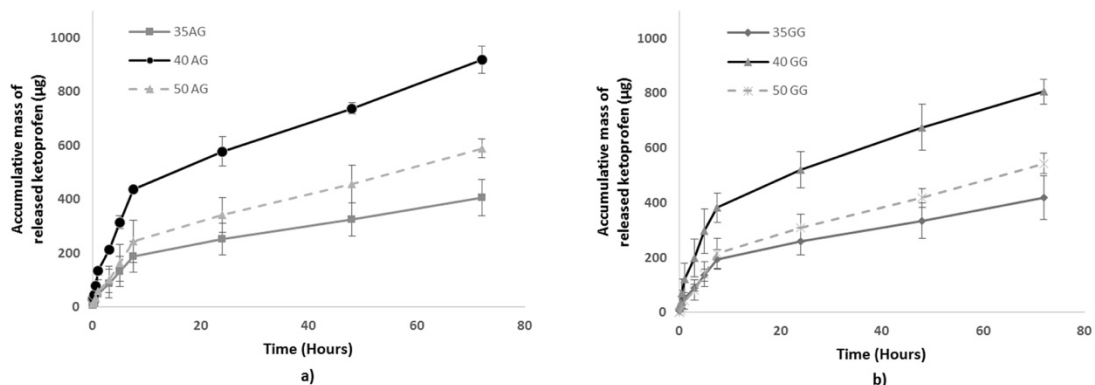


Figure IV-6 Accumulative mass of ketoprofen released of (a) alginate-based stent (b) gellan gum-based stent, impregnated at 35 °C, 40 °C, 50 °C and 100 bar during 2 h for the release period of 72 h.

Results of released kinetics modeling in terms of the percentage of total ketoprofen released for the impregnation experiment performed at 40°C are present in **figure IV-7**. As it can be observed in **figure IV-7** a fast release for both polymers was verified in the first 7h30 with nearly 40% of the total ketoprofen impregnated in biodegradable stents being released. No differences were noticeable in percentage of release comparing the gellan gum and alginate-based stent. However, a deeper analysis requires the modeling of the results obtained. The data was modeled following the Korsmeyer-Peppas equation (**Equation IV-1**). The results of the model parameters are presented in **table IV-3**. From the results, for different temperatures studied and the two formulations tested the value of released exponent (n) was calculated to be between $0.45 < n < 0.89$ implying anomalous transport of drug release mechanism. (32, 38, 39). Together with this, the study on the release kinetics constant indicates that there seems to be a much faster release from the gellan-gum based stents, as evidenced by the calculation of the constant k .

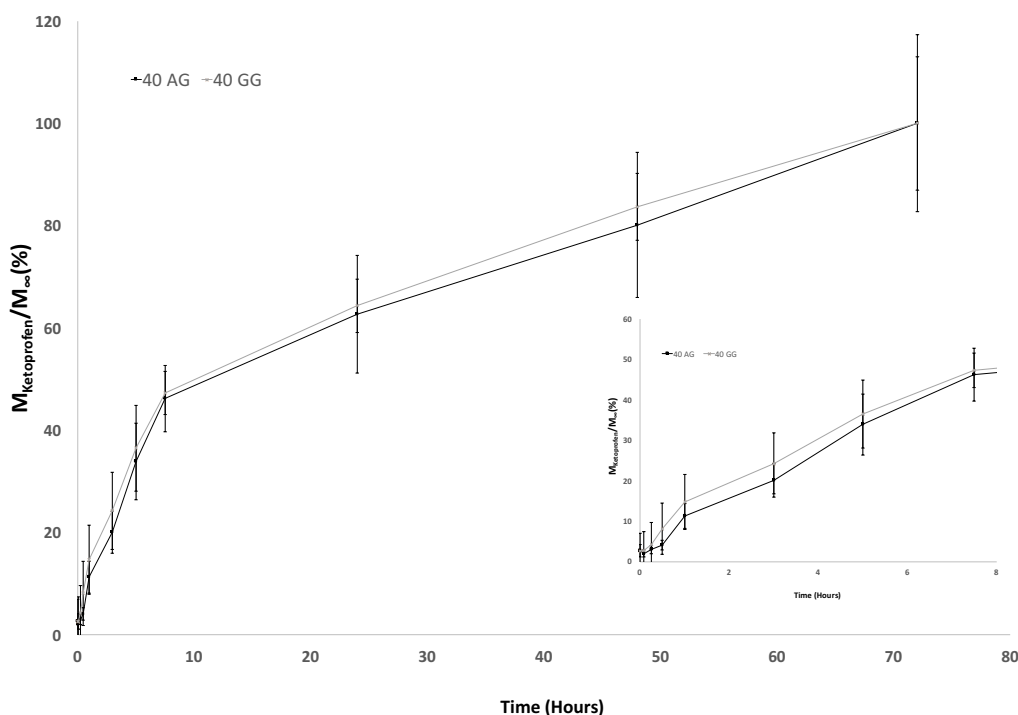


Figure IV-7 Percentage of ketoprofen released from alginate and gellan gum-based impregnated at 40 °C and 100 bar during 2 h for the release period of 72 h.

Table IV-3 Correlated parameters of the ketoprofen released kinetics.

Temperature (°C)	Formulation	<i>n</i>	<i>k</i>	R ²
35	AG	0,85	0,0203	0,96
	GG	0,75	0,0459	0,99
40	AG	0,79	0,0251	0,98
	GG	0,83	0,0486	0,95
50	AG	0,61	0,0108	0,99
	GG	0,69	0,0642	0,99

The first 3 days of indwelling are normally the time during which anti-inflammatory post-operative drugs are prescribed, due the higher risk of tissue inflammation (14). The anti-inflammatory agents are usually administered orally, which may decrease their efficacy and the ability to reach and target the site of action. Therefore, the delivery *in situ* is extremely beneficial (10, 14). The quantity and homogeneity of drug loaded into hydrogels may be limited, particularly in the case of hydrophobic drugs like ketoprofen, however this seems to be circumvented in this work. The release of drugs from hydrogels results from combination of classical diffusion in the polymer network and the limitations of mass transfer (32). The release in most hydrogels typically results in relatively rapid release of drugs from the hydrogel over the period of hours or days, particularly in the case of hydrophilic drugs due the higher water content (40). Release profile of active compounds from hydrogels can be influenced by various factors as well as the medium conditions like surface area, pH and temperature. The ketoprofen, like others non-steroidal anti-inflammatory drugs (NSAIDs), is solubility pH-dependent due their weak acid character dissolution rate in acidic conditions (41). The pH of AUS is slightly acidic (6.4) and this may have an influence in the release profile. The impregnation temperature demonstrated to have an influence in the amount of ketoprofen release, particularly due to the fact that this parameter is strongly influencing the impregnation yield.

The influence of temperature on the final loading of ketoprofen in the stents was evaluated through the determination of the yield of impregnation and the results are summarized in **table IV-4**. In our study, results demonstrate that the lowest impregnation yields were obtained for **AG35** and **GG35**, i.e, the lowest temperature operating condition, and the highest yield was obtained for **AG40** and **GG40**, at 40°C of operating condition. For the highest temperature operating condition studied (50°C) values below those obtained at 40°C in both polymers were obtained. An increase on the temperature increased the ketoprofen release in AUS. In terms of relative mass of

ketoprofen released in percentage for alginate and gellan gum-based stents the profile is similar for both polymers, however the release kinetic constant indicates that ketoprofen has a faster release when impregnated in the gellan-gum based stents in opposition to the alginate-based stents. This can be explained by the interaction of the ketoprofen with the hydroxyl group presents in hydrogel by hydrogen bonding through the carbonyl and carboxyl groups present in this drug molecule (41-43). Other possibility is due swellability of these polymers which influenced the easier released of the drug in the first 7 hours, near 40%. Because of their nature, hydrogels can be used in many different types of controlled release systems. *Peppas and co-workers* developed a theory to explain the mechanism controlling the release of the drug from the swellable materials. Hydrogel-based drug delivery systems are mainly classified as diffusion-controlled systems (Fickian diffusion) or swelling-controlled systems. However, in some cases, drug release occurs due to a combination of macromolecular relaxations and Fickian diffusion. This type of transport is known as anomalous or non-Fickian transport (31, 32, 39). In our study, the drug release mechanism seems to be by anomalous transport according the n obtained for all the conditions. For a cylinder geometry values of n between 0.45 and 0.89 were reported as an indicator for the superposition of diffusion and swelling-controlled drug released (39). The solubility of the ketoprofen in acidic conditions contributes to the diffusion of the drug and on the other hand the swelling of the alginate-based and gellan gum-based stents in AUS, quantified in the previous work (5), also contribute to the release kinetic profile of ketoprofen from the biodegradable stents developed. The combination of the diffusion of ketoprofen and the swelling of the polymer matrix suggests that the impregnation with supercritical fluids renders a more homogeneously dispersed material, in which, the drug is able to penetrate into the bulk of the material, unlike the conventional methods in which the drug is dispersed mostly on the surface.

Table IV-4 Impregnation yield of the experiments carried out during 2 h at 100 bar.

Temperature (°C)	Yield ±STD (%)		
35	AG	3,29	±0,46
	GG	4,84	±0,31
40	AG	8,74	±2,53
	GG	16,64	±3,56
50	AG	7,64	±1,87
	GG	13,29	±1,51

Additionally, the gellan gum-based stents show highest impregnation yields comparing with the alginate-based ones. The yield of SCF impregnation are influenced for different parameters like temperature, pressure, solubility of the drug in carbon dioxide and the presence of ethanol which acts as a co-solvent in the first minutes (44, 45). In this study, we evaluated the effect of three different temperatures in the impregnation yield. The other parameters were kept constant relatively to the previously described procedure (5), in order to minimize the changes in processing conditions, which may ultimately influence the properties of the stents developed. According to the work of Sabegh *et al* (27) the temperature and pressure have a direct effect on the solubility of ketoprofen in carbon dioxide. An increase on the temperature and pressure leads to an increase on the solubility of ketoprofen, but the temperature is dependent on the pressure and vice-versa, particularly due to the simultaneous effect of these two variables on density and solvation power of carbon dioxide. In the conditions studied in this work, the impregnation performed at 40°C reached higher yields for both alginate-based and gellan gum-based stents. It would be expected that at 50°C condition a higher impregnation was achieved, nonetheless, the lower value can be explained by the temperature/pressure dependency reported on the studies on ketoprofen solubility in carbon dioxide. The higher yields obtained for 40°C operating condition are justified due the higher solubility of ketoprofen in CO₂, which at 100 bar is higher than at 50°C (27-29). Comparing the two formulations gellan gum-based material present in general higher impregnation yields. This can be explained by the interaction drug-polymer. In this sense, probably the interaction ketoprofen-gellan gum is higher than ketoprofen-alginate, due to the higher density of hydroxyl groups. According to our results the impregnation of ketoprofen in alginate and gellan gum-based biodegradable stents we conclude that not only the solubility of the ketoprofen in carbon dioxide is a crucial variable in the impregnation process but also the impregnation is governed by the drug-polymer interactions (46, 47).

IV-3.3. Cytotoxicity studies

Concerning the application of the ketoprofen-eluting biodegradable stents in medical use the cytotoxicity needs to be evaluated. Although the polymeric materials used in this studied were already reported in literature as non-cytotoxic (5, 48), the concentration of the ketoprofen may induce a cytotoxic response. The cytotoxicity of the ketoprofen-eluting biodegradable stents impregnated at 35°C and 50°C was evaluated in accordance with the protocol described in ISO/EN

10-993 (49). The viability of the cells cultured in a tissue culture plate in the presence of the medium with leachables from ketoprofen-eluting biodegradable stents was determined as a function of the cells cultured in the DMEM culture medium. **Figure IV-8** presents the cell viability after 72 h in contact with the material's leachables. The obtained results were compared to cell growth on the tissue culture plate using culture media (positive control), and latex leachables, which were used as negative control. The results demonstrate that the alginate and gellan gum-based stents impregnated at different conditions do not compromise the metabolic activity of the cells.

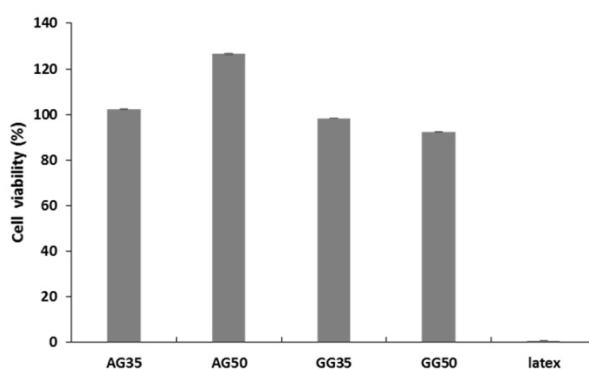


Figure IV-8 Cell viability measured after 72 h of ketoprofen-eluting biodegradable stents.

IV-4. CONCLUSION

Biodegradable stent technology coupled with the possibility to release active compounds, such as anti-inflammatory agents like ketoprofen is an important development for the future of ureteral stents. In this work, we designed a ketoprofen-eluting biodegradable ureteral stent prepared by supercritical CO₂ impregnation. The studied herein presented revealed the influence of the operating conditions, particularly temperature on the impregnation yield, which was found to be higher at 40 °C for both alginate-base stents and gellan-gum based stents. Regarding the two formulations studied, higher yields were obtained for gellan gum-based stents. According to the release kinetics profiles evaluated these systems were able to the release ketoprofen in the first 72h in artificial urine solution. These results are very promising and a good indication that the stents are able to meet the purpose for which they are designed, i.e, be able to act when fast and local delivery is desirable. The non-cytotoxicity characteristics of the developed drug-eluting biodegradable ureteral stents demonstrate the feasibility of this product as a medical device. The

elution of the drug and the same time the degradation of the stent occurs is a major progress in the state of the art in which concerns the development of new medical devices for urological practices. The next step to validate this type of systems is to evaluate the safety and effectiveness in an *In vivo* model.

ACKNOWLEDGEMENTS

The research leading to these results has received funding from ICVS/3B's – Associate Laboratory Research Grants and the European Union Seventh Framework Programme (FP7/2007-2013) under grant agreement number REGPOT-CT2012-316331-POLARIS and from the project “Novel smart and biomimetic materials for innovative regenerative medicine approaches” RL1 - ABMR - NORTE-01-0124-FEDER-000016) cofinanced by North Portugal Regional Operational Programme (ON.2 – O Novo Norte), under the National Strategic Reference Framework (NSRF), through the European Regional Development Fund (ERDF). Alexandre Barros acknowledges his FCT PhD grant SFRH/BD/97203/2013.

REFERENCES

1. Finney RP. Experience with New Double J-Ureteral Catheter Stent. *Journal of Urology*. 1978;120(6):678-81.
2. Al-Aown A, Kyriazis I, Kallidonis P, Kraniotis P, Rigopoulos C, Karnabatidis D, et al. Ureteral stents: new ideas, new designs. *Therapeutic advances in urology*. 2010;2(2):85-92.
3. Waters SL, Heaton K, Siggers JH, Bayston R, Bishop M, Cummings LJ, et al. Ureteric stents: investigating flow and encrustation. *Proceedings of the Institution of Mechanical Engineers Part H, Journal of engineering in medicine*. 2008;222(4):551-61.
4. Lange D, Bidnur S, Hoag N, Chew BH. Ureteral stent-associated complications[mdash]where we are and where we are going. *Nat Rev Urol*. 2015;12(1):17-25.
5. Barros AA, Rita A, Duarte C, Pires RA, Sampaio-Marques B, Ludovico P, et al. Bioresorbable ureteral stents from natural origin polymers. *Journal of Biomedical Materials Research Part B: Applied Biomaterials*. 2014:n/a-n/a.
6. Olweny EO, Landman J, Andreoni C, Collyer W, Kerbl K, Onciu M, et al. Evaluation of the use of a biodegradable ureteral stent after retrograde endopyelotomy in a porcine model. *Journal of Urology*. 2002;167(5):2198-202.
7. Chew BH, Lange D, Paterson RF, Hendlin K, Monga M, Clinkscales KW, et al. Next Generation Biodegradable Ureteral Stent in a Yucatan Pig Model. *The Journal of urology*. 2010;183(2):765-71.
8. Lingeman JE, Schulsinger DA, Kuo RL. Phase I trial of a temporary ureteral drainage stent. *Journal of Endourology*. 2003;17(3):169-71.

9. Schlick RW, Planz K. Potentially useful materials for biodegradable ureteric stents. *Brit J Urol.* 1997;80(6):908-10.
10. Krambeck AE, Walsh RS, Denstedt JD, Preminger GM, Li J, Evans JC, et al. A Novel Drug Eluting Ureteral Stent: A Prospective, Randomized, Multicenter Clinical Trial to Evaluate the Safety and Effectiveness of a Ketorolac Loaded Ureteral Stent. *The Journal of Urology.* 2010;183(3):1037-43.
11. Laroia ST, Laroia AT. Drug-eluting stents. A review of the current literature. *Cardiology in review.* 2004;12(1):37-43.
12. Mikkonen J, Uurto I, Isotalo T, Kotsar A, Tammela TL, Talja M, et al. Drug-eluting bioabsorbable stents - an in vitro study. *Acta Biomater.* 2009;5(8):2894-900.
13. Tsuji T, Tamai H, Igaki K, Kyo E, Kosuga K, Hata T, et al. Biodegradable stents as a platform to drug loading. *International Journal of Cardiovascular Interventions.* 2003;5(1):13-6.
14. Mendez-Probst CE, Goneau LW, MacDonald KW, Nott L, Seney S, Elwood CN, et al. The use of triclosan eluting stents effectively reduces ureteral stent symptoms: a prospective randomized trial. *BJU International.* 2012;110(5):749-54.
15. Chew BH, Davoudi H, Li J, Denstedt JD. An *in vivo* porcine evaluation of the safety, bioavailability, and tissue penetration of a ketorolac drug-eluting ureteral stent designed to improve comfort. *J Endourol.* 2010;24(6):1023-9.
16. Kotsar A, Isotalo T, Juuti H, Mikkonen J, Leppiniemi J, Hänninen V, et al. Biodegradable braided poly(lactic-co-glycolic acid) urethral stent combined with dutasteride in the treatment of acute urinary retention due to benign prostatic enlargement: a pilot study. *BJU International.* 2009;103(5):626-9.
17. Kantor TG. Ketoprofen: A Review of Its Pharmacologic and Clinical Properties. *Pharmacotherapy: The Journal of Human Pharmacology and Drug Therapy.* 1986;6(3):93-102.
18. Rutyna R, Popowicz M, Wojewoda P, Nestorowicz A, Bialek W. [Pre-emptive ketoprofen for postoperative pain relief after urologic surgery]. *Anestezjologia intensywna terapia.* 2011;43(1):18-21.
19. Vane JR, Botting RM. Anti-inflammatory drugs and their mechanism of action. *Inflamm res.* 1998;47(2):78-87.
20. Duarte ARC, Simplicio AL, Vega-Gonzalez A, Subra-Paternault P, Coimbra P, Gil MH, et al. Impregnation of an Intraocular Lens for Ophthalmic Drug Delivery. *Current Drug Delivery.* 2008;5(2):102-7.
21. Milovanovic S, Stamenic M, Markovic D, Ivanovic J, Zizovic I. Supercritical impregnation of cellulose acetate with thymol. *The Journal of Supercritical Fluids.* 2015;97(0):107-15.
22. Duarte ARC, Mano JF, Reis RL. Supercritical fluids in biomedical and tissue engineering applications: a review. *International Materials Reviews.* 2009;54(4):214-22.
23. Cooper AI. Polymer synthesis and processing using supercritical carbon dioxide. *J Mater Chem.* 2000;10(2):207-34.
24. Kikic I, Vecchione F. Supercritical impregnation of polymers. *Current Opinion in Solid State & Materials Science.* 2003;7(4-5):399-405.
25. Mishima K. Biodegradable particle formation for drug and gene delivery using supercritical fluid and dense gas. *Advanced Drug Delivery Reviews.* 2008;60(3):411-32.
26. Tomasko DL, Li HB, Liu DH, Han XM, Wingert MJ, Lee LJ, et al. A review of CO₂ applications in the processing of polymers. *Industrial & Engineering Chemistry Research.* 2003;42(25):6431-56.
27. Sabegh MA, Rajaei H, Esmailzadeh F, Lashkarbolooki M. Solubility of ketoprofen in supercritical carbon dioxide. *The Journal of Supercritical Fluids.* 2012;72(0):191-7.

28. Stassi A, Bettini R, Gazzaniga A, Giordano F, Schiraldi A. Assessment of solubility of ketoprofen and vanillic acid in supercritical CO₂ under dynamic conditions. *J Chem Eng Data*. 2000;45(2):161-5.
29. Macnaughton SJ, Kikic I, Foster NR, Alessi P, Cortesi A, Colombo I. Solubility of anti-inflammatory drugs in supercritical carbon dioxide. *J Chem Eng Data*. 1996;41(5):1083-6.
30. Khandwekar A, Doble M. Physicochemical characterisation and biological evaluation of polyvinylpyrrolidone-iodine engineered polyurethane (Tecoflex®). *J Mater Sci: Mater Med*. 2011;22(5):1231-46.
31. Korsmeyer RW, Peppas NA. Effect of the morphology of hydrophilic polymeric matrices on the diffusion and release of water soluble drugs. *Journal of Membrane Science*. 1981;9(3):211-27.
32. Ritger PL, Peppas NA. A simple equation for description of solute release I. Fickian and non-fickian release from non-swellable devices in the form of slabs, spheres, cylinders or discs. *Journal of Controlled Release*. 1987;5(1):23-36.
33. Champeau M, Thomassin J-M, Tassaing T, Jerome C. Drug Loading of Sutures by Supercritical CO₂ Impregnation: Effect of Polymer/Drug Interactions and Thermal Transitions. *Macromolecular Materials and Engineering*. 2015;300(6):596-610.
34. Vijaykumar Nagabandi*1 RT, K.N. Jayaveera3. Formulation development and evaluation of liquid systems to improve the dissolution rate of naproxen2011.
35. Mehling T, Smirnova I, Guenther U, Neubert RHH. Polysaccharide-based aerogels as drug carriers. *Journal of Non-Crystalline Solids*. 2009;355(50–51):2472-9.
36. Kaushal AM, Gupta P, Bansal AK. Amorphous Drug Delivery Systems: Molecular Aspects, Design, and Performance. 2004;21(3):62.
37. Kawabata Y, Wada K, Nakatani M, Yamada S, Onoue S. Formulation design for poorly water-soluble drugs based on biopharmaceutics classification system: Basic approaches and practical applications. *International Journal of Pharmaceutics*. 2011;420(1):1-10.
38. Carreras N, Acuña V, Martí M, Lis MJ. Drug release system of ibuprofen in PCL-microspheres. *Colloid Polym Sci*. 2013;291(1):157-65.
39. Siepmann J, Peppas NA. Modeling of drug release from delivery systems based on hydroxypropyl methylcellulose (HPMC). *Advanced Drug Delivery Reviews*. 2001;48(2–3):139-57.
40. Hoare TR, Kohane DS. Hydrogels in drug delivery: Progress and challenges. *Polymer*. 2008;49(8):1993-2007.
41. García-González CA, Jin M, Gerth J, Alvarez-Lorenzo C, Smirnova I. Polysaccharide-based aerogel microspheres for oral drug delivery. *Carbohydrate Polymers*. 2015;117(0):797-806.
42. Gorle BSK, Smirnova I, Arlt W. Adsorptive crystallization of benzoic acid in aerogels from supercritical solutions. *J Supercrit Fluid*. 2010;52(3):249-57.
43. Lozano HR, Martínez F. Thermodynamics of partitioning and solvation of ketoprofen in some organic solvent: buffer and liposome systems. *Revista Brasileira de Ciências Farmacêuticas*. 2006;42:601-13.
44. Kazarian SG, Vincent MF, West BL, Eckert CA. Partitioning of solutes and cosolvents between supercritical CO₂ and polymer phases. *The Journal of Supercritical Fluids*. 1998;13(1–3):107-12.
45. Tomasko DL, Li H, Liu D, Han X, Wingert MJ, Lee LJ, et al. A Review of CO₂ Applications in the Processing of Polymers. *Industrial & Engineering Chemistry Research*. 2003;42(25):6431-56.
46. Kazarian SG, Vincent MF, Bright FV, Liotta CL, Eckert CA. Specific Intermolecular Interaction of Carbon Dioxide with Polymers. *Journal of the American Chemical Society*. 1996;118(7):1729-36.

47. Kazarian SG, Martirosyan GG. Spectroscopy of polymer/drug formulations processed with supercritical fluids: in situ ATR-IR and Raman study of impregnation of ibuprofen into PVP. *International Journal of Pharmaceutics*. 2002;232(1-2):81-90.
48. Silva TH, Alves A, Ferreira BM, Oliveira JM, Reys LL, Ferreira RJF, et al. Materials of marine origin: a review on polymers and ceramics of biomedical interest. *International Materials Reviews*.57(5):276-306.
49. (ISO): IOFS. ISO 10993-5:1999. Biological Evaluation of Medical Devices. Part 5: Tests for in Vitro Cytotoxicity; . Geneva, Switzerland2009.

Chapter V

Gelatin-based biodegradable ureteral stents with enhanced mechanical properties

Chapter V

Gelatin-based biodegradable ureteral stents with enhanced mechanical properties **

ABSTRACT

A first generation of biodegradable ureteral stents based on natural origin polymers developed in a previous work has proven to be an interesting alternative to conventional stents, but it has however demonstrated to fail upon the first *In vivo* validation in a pig model. In this work, with the objective to overcome the low mechanical performance encountered and to make the biodegradable ureteral stents by origin polymers a success *In vivo*, four formulations with different concentrations of gelatin and alginate and different concentrations of crosslinking agent were tested in order to obtain higher mechanical properties. Bismuth was added to confer radiopaque properties to the stent. Not only a new formulation was developed but also the processing method to fabricate the stents was optimized. The biodegradable ureteral stents were coated with a biodegradable polymer. X-ray scan demonstrated the radiopacity of this second generation of biodegradable stents. The degradation of the biodegradable ureteral stents was assessed in artificial urine solution and it was observed that the degradation of the materials occurs *In vitro* between 9 and 15 days. Degradation was followed by weight loss of the samples and by chemical analysis of the solutions both by inductive couple plasma (ICP) and gel permeation chromatography (GPC). Formulation with highest amount of gelatin has shown good mechanical performance in terms of tensile properties when compared with the commercial stent (Biosoft® duo, Porges, Coloplast), and the crosslinking concentration has shown not to have a great influence on the mechanical behavior of the stents. The *In vivo* performance of this second

** This chapter is based on the following publication:

Barros A, Oliveira C, Lima E, Duarte ARC, Reis RL. Gelatin-based biodegradable ureteral stents with enhanced mechanical properties. *Applied Materials Today*. December 2016; (5): 9-18.

generation of the ureteral stents was herein validated. The biodegradable ureteral stents were placed in the ureters of a female pig, following the normal surgical procedure. The animals remained asymptomatic, with normal urine flow, the stents remain intact during the first 3 days and after 10 days the ureteral stents were totally degraded. This new formulation combined with a new production process overcome the problems verified with the first generation of natural-based biodegradable stents

V-1. INTRODUCTION

The most frequent adverse effects reported by patients experiencing ureteral stenting are pain and difficulties in urinary tract (1). These problems can significantly impact patient quality of life with loss days of working, urinary leakage and sexual difficulties (2). In last years, new ureteral stent designs have been tested with novel polymers, coatings and the incorporation of active compounds in an attempt to significantly reduce the most common problems like bacterial infection and encrustation (2-4). Lange et al (1) in a recent review concluded that the stent of the future will be degradable, in a control manner, and possible to coat or elute active compounds. No biodegradable ureteral stent is currently available on the market, although in the past years there has been a crescent interest in this field (1). Polymers like polylactic acid, polyglycolic acid, poly(lactic-co-glycolic acid) and alginate-based materials have been used to develop the biodegradable ureteral stents (5-9). Lumiaho, J. et al reported an *In vivo* studies in pig model using polylactic acid and poly(lactic-co-glycolic acid) based stents which have shown good properties like antireflux properties and favourable drainage but the biocompatibility and the degradation profile were proven to be insufficient for clinical use (5, 10, 11). The same ureteral stents showed a different behaviour in a canine model, presenting a good biocompatibility and degradation which occurred in 12 weeks (12). Other studies using poly(lactic-co-glycolic acid)-based ureteral stents reported favorable radiopaque and drainage properties, but the biocompatibility was compromised, according to what is reported in the literature (5, 13-15). The degradation of the ureteral stents must be uniform and homogenous or dissolving based on directionality, preventing the formation of fragments during the degradation process that can block the ureter (1, 6, 16). Uriprene stent (Poly-Med, USA), a radiopaque, glycolic-lactic acid based stent has been designed to degrade in the direction of the bladder coil to renal coil preventing ureteral obstruction secondary to degrading stent fragments (1). The *In vivo* pig model studies of Uriprene reported a good stability and biocompatibility, with a predictable degradation during 2–4 weeks while maintaining drainage. In our previous study, we reported an ureteral stent produced with natural-based polymers processed by critical point drying with carbon dioxide (16). This study was however not the first in literature to report alginate-polymer-based temporary ureteral stents. Lingeman et al (9, 17) showed in a phase

I and phase II clinical trials that these ureteral stents were designed to be intact at least 48 h before degradation with facilitated urinary drainage, favorable tolerability and safety profiles. The problem of these alginate-based stents is the fact that it presented a nonhomogeneous dissolution profile and fragmentation resulting in the need for secondary procedures to remove fragments in some patients.

To avoid these problems, we hypothesized the use of two biodegradable materials instead of one, with the objective to reinforce the mechanical properties of the stent (18). Additionally, the combination of template gelation with critical point carbon dioxide drying also contribute to enhance the features of the stent. In the first generation biodegradable ureteral stents were produced using alginate, gellan gum and a blend of these with gelatin. The bacterial adhesion of Gram-positive and Gram-negative was assessed and compared with a commercial stent (Biosoft® duo, Porges, Coloplast) showing a decrease of adhesion. The biodegradation profile was observed to be highly dependent on the composition of the stent, with a complete dissolution of alginate-based during 14 days and the gellan gum-based up to 60 days (16). A first generation of biodegradable ureteral stents based on natural origin polymers developed previously has proven to be an interesting alternative, but it has however demonstrated to have mechanical properties upon the first *In vivo* validation. Following these results, we developed a second generation of these ureteral stents. Gelatin was used as a base material for these stents and a hydrophobic coating was applied to improve the mechanical properties and allow the placement of the stent *In vivo* by the conventional surgical procedure. A preliminary *In vivo* validation was performed in a pig model.

V-2. MATERIALS AND EXPERIMENTAL

V-2.1. Materials

Alginic acid sodium salt, gelatin, urea, urease type IX from *Canavalia ensiformis* (Jack Bean), calcium chloride, chlorophorm, ethanol, bismuth (III) carbonate basic, sodium phosphate dibasic and sodium azide were purchased from Sigma-Aldrich (Germany). Potassium dihydrogen orthophosphate and magnesium chloride hexahydrate were obtained from Riedel-de Haën (Germany).

Bismuth standard for ICP was obtained from Sigma-Aldrich (Germany). Polycaprolactone resin PCL 787, commercially available as TONETM polymer, was obtained from Union Carbide Chemicals and Plastics Division, Bound Brook, New Jersey. Carbon dioxide (99.998 mol %) was supplied by Air Liquide (Portugal). All reagents were used as received without any further purification.

V-2.2. Preparation of second generation of biodegradable ureteral stents

Polymers were dissolved in hot distilled water (70°C) at different concentrations as described in **table V-1**. The solutions were stirred for 1 hour and the polymeric solution was injected in a mold to obtain a tubular structure. After 1 hour the piece was taken out of the mold and placed in an alcohol solution (100% ethanol) for 1 hour. The stents were then transferred into a crosslinking solution of calcium chloride (CaCl₂), with different concentrations (**table V-2**) at room temperature. After crosslinking, the stents were relocated in an alcoholic solution (100% ethanol) to obtain an alcohol gel which can be dried in a high-pressure vessel with supercritical carbon dioxide (scCO₂) under controlled pressure (100 bar) and temperature (40°C) and a continuous flow of the scCO₂ during 90 minutes. Finally, the dried stents were immersed in distilled water for 30 min and in ethanol 100%, for 1 hour, to remove the template. The stents were finally dried at room temperature conditions, during 1 day. The coating of the stents was performed by immersion in a 10% of polycaprolactone (PCL) resin 787 (Mw 80,000 g mol⁻¹) dissolved in chloroform. The stents were dried at ambient conditions overnight. Commercial Biosoft® duo, Porges, Coloplast used as a control in this study is also shown.

Table V-1 Summary of the formulations tested to prepare the different biodegradable ureteral stents.

Formulation	Material conc. (wt. %)			
	1	2	3	4
Alginate	10	30	45	50
Gelatin	85	65	50	45
Bismuth (III) carbonate basic	5	5	5	5
Coating	10% PCL resin PCL 787			

Table V-2 Crosslinking agent concentrations used to prepare the different biodegradable ureteral stents.

Crosslinking agent	Crosslinking agent conc. (M)		
	CaCl ₂	0.24 ^a	0.48 ^b

^aFormulation 2 ; ^bFormulation 1, 2, 3 and 4

V-2.3. Scanning electron microscopy

The morphology of the biodegradable stents was analysed on a JEOL SEM, model JSM-6010LV. The samples were fixed with mutual conductive adhesive tape on aluminium stubs and covered with gold/palladium using a sputter coater.

V-2.4. Postoperative X-ray

The radiopaque characteristics of the biodegradable ureteral stent developed were evaluated in a postoperative X-ray equipment located at the Department of Imaging Hospital de Braga, Portugal. The radiographs were taken in abdomen mode with magnification of 0.27x.

V-2.5. Degradation Study

The degradation of biodegradable stents was measured as function of the weight loss of the samples. Samples (10 mg) were immersed in artificial urine solution (AUS) prepared according Khandwekar *et al* (19) with the composition presented in **table V-3**. Samples immersed were dried and weighted to determine the weight loss, which was calculated according to the following equation:

$$\% \text{ Weight loss} = \frac{(W_f - W_i)}{W_i} \times 100$$

Equation II-2 Determination of wight loss.

Where W_f is the final weight of the sample (dried after immersion) and W_i is the initial weight of the sample. Each formulation was tested in triplicate.

Table V-3 Composition of the artificial urine solution (AUS).

	Component	% wt/v
Solution A	Potassium dihydrogen ortho-phosphate	0.76
	Magnesium chloride hexahydrate	0.36
	Urea	1.60
Solution B	Calcium chloride hexahydrate	0.53
	Chicken ovalbumin	0.2
Urease type IX from <i>Canavalia ensiformis</i> (Jack Bean)		0.125

V-2.5.1. Gel permeation chromatography (GPC)

5 mg of alginate, gelatin and bismuth were dissolved in 5 ml of an aqueous solution of sodium phosphate dibasic 0.01 M containing 0.1 M of sodium azide (pH 6.6) and used as a controls, while the immersion solutions obtained by degradation test of stents formulation 2 at specific time point (1, 3, 6 and 9 days) were lyophilized and then dissolved in 5ml of the same eluent. The solutions were filtered through a 0.22 μ m filter and analysed on a gel permeation chromatograph (Malvern, Viscotek TDA 305) with refractometer, right angle light scattering and viscometer detectors on a set of four columns: pre-column Suprema 5 μ m 8 \times 50 S/N 3111265, Suprema 30 Å 5 μ m 8 \times 300 S/N 3112751, Suprema 1000 Å 5 μ m 8 \times 300 S/N 3112851 PL and Aquagel-OH MIXED 8 μ m 7.5 \times 300 S/N 8M-AOHMIX-46-51, with refractive index detection (RI-Detector 8110, Bischoff). Elution was performed at 30°C using a flow rate of 1 ml min⁻¹. The elution times and the RI detector signal were calibrated with a commercial calibration polysaccharide set from Varian that contains 10 Pullulan calibrants with narrow polydispersity and Mp (molecular mass at the peak maximum) ranging from 180 Da to 708 kDa.

V-2.5.2. Inductive coupled plasma (ICP)

The immersion solutions from the degradation test of the stents, formulation 2, were filtered and analyzed by inductive coupled plasma (ICP) to follow Bismuth (Bi) concentration during the different degradation times. The sample absorption at specific wavelengths ($\lambda = 206.17$ nm for Bi) was measured, and the bismuth concentration was determined using a calibration curves previously obtained with Bismuth standard for ICP (Sigma) ($R^2 = 0.96$).

V-2.5.3. Cytotoxicity evaluation of the leachables

The cytotoxicity of the leachable materials during the ureteral stent degradation in AUS was accessed according to ISO/10993 (20). The cytotoxicity of the samples was assessed using an immortalized mouse lung fibroblasts cell line (L929) purchased from the European Collection of Cell Cultures. First, the immersion solutions obtained by degradation test at specific time point (1, 3, 6 and 9 days) of stents formulation 2 were lyophilized. The leachables were dissolved in basal medium DMEM (Dulbecco's modified Eagle's medium; Sigma-Aldrich, Germany) 10% FBS (heat-inactivated fetal bovine serum, Biochrom AG, Germany), and 1% antibiotic-antimycotic (Gibco, UK). Cells were cultured in a humidified incubator at 37 C in a 5% CO₂ atmosphere. The effect of the leachables on the cellular metabolism was performed using a standard MTS (Cell Titer 96® Aqueous Solution Cell Proliferation Assay, Promega, USA) viability test. A latex rubber extract was used as positive control for cell death; while cell culture medium was used as negative control representing the ideal situation for cell proliferation. Cell viability was evaluated by the MTS assay after 72 h. This was quantified by UV-spectroscopy, reading the formazan absorbance at 490 nm in a microplate reader (Synergy HT, Bio-Tek Instruments, USA). Each sample formulation and control was tested using 12 replicates.

V-2.6. Tensile mechanical analysis

Tensile mechanical analysis of the biodegradable stents was evaluated using an INSTRON 5540 (Instron Int. Ltd, High Wycombe, UK) universal testing machine with a load cell of 1 kN. The

wet samples were hydrated before testing in AUS for 4 hours. The dimensions of the specimens used were 5 mm of length, 2 mm width, and 0.5 mm of thickness. The load was placed midway between the supports with a span (L) of 3 mm. The crosshead speed was 1:5 mm min⁻¹. For each condition the specimens were loaded until core break. The results presented are the average of at least three specimens and the results are presented as the average \pm standard deviation.

V-2.7. Surgical procedure and *In vivo* placement validation

The *In vivo* placement validation study was conducted at Minho University, Braga, Portugal, after formal approval by the institution's review board and in accordance with its internal ethical protocol for animal experiments. Females domestic pigs, weighing \approx 30 kg, were used to validate the procedure and the stent degradation. The pigs were not given food or water for 12 h before the procedure. All procedures were performed under general anesthesia and mechanical ventilation as previously described in detail (21, 22). After emptying the bladder, a semi rigid 7 Fr ureteroscope (Karl Storz, Tuttlingen, Germany) was inserted through the urethra and saline solution was instilled. The full procedure was according the standard technique of ureteroscopy. A 0.035-inch flexible tip guidewire (AQUATRACK® Hydrophilic Nitinol, Cordis®, Johnson & Johnson) was then inserted in the ureters. The biodegradable ureteral stents (6Fr with 22 cm length) were guided by the guidewire until placed in the right and in the left ureter the commercial stent (Biosoft® duo, Porges, Coloplast) was placed as a control. Conventional ureteroscopy was performed in order to verify the degradation and the presence of any fragment and the morphology of the ureters after 3 and 10 days.

V-2.8. Statistical analysis

All data values are presented as mean \pm standard deviation (SD). Statistical analysis was performed using Graph Pad Prism 6.00 software (San Diego, USA). Statistical significances (*p < 0.05, **p < 0.01 and ***p < 0.001) were determined using one-way analysis of variance (ANOVA) for an average of three to twelve replicates, followed by post hoc Tukey's test for all pairwise mean comparisons.

V-3. RESULTS AND DISCUSSION

In our previous work, we developed a biodegradable ureteral stent based on different natural polymers. One of the drawbacks of these stents was the poor mechanical properties that result in failure upon *In vivo* implantation.

To prepare the second generation of biodegradable ureteral stents made by origin polymers new formulations were tested and the method of injection molding and drying was optimized. Gelatin and alginate are very hydrophilic polymers. In order to delay the hydration of the materials upon implantation we decided to coat the hydrogel with a polymeric layer of polycaprolactone resin PCL 787. Polycaprolactone resin PCL 787 was chosen as it is a safe material and has a fast degradation in comparison with other biodegradable polymers. The biodegradable ureteral stents are prepared from an initial aqueous solution of alginate-gelatin from which gelation is induced by decreasing the temperature followed by an ionic crosslinking with a CaCl_2 solution. Gelatin and alginate were chosen because of their versatility to form gels and the results obtained in the previous study (16) combining gelatin with other polysaccharides it is possible to induce changes in the water uptake, degradation profile and particularly were benefices regarding bacteria adhesion. In this work we have added bismuth to the formulation. The use of bismuth in the new formulation provides radiopaque properties to the ureteral stent due the inherent radiopaque characteristics of this compound. This material was already used and prove to be safe and it is already FDA approved (23). After crosslinking a combination of steps in ethanol and supercritical carbon dioxide was further employed to dry the biodegradable ureteral stents. Supercritical drying process parameters were kept as in the first version of these stents as they had already been optimized supercritical fluid drying process used is a process in which the matrices do not undergo any phase transition and therefore the integrity of the lumen of the stents is not compromised (24). Different other drying methods were tested namely air drying but the integrity of the lumen of the stents was compromised, unlike what was observed when using supercritical fluid CO_2 .

V-3.1. Morphology

Figure V-1 presents the SEM images of the cross-sections of biodegradable ureteral stent developed according to the formulation 2. In **figure V-1 a** we can see the uncoated stent and in figure 1b the stent with PCL coating. **Figures V-1c** and **V-1d** are the magnifications of stent wall. It is possible to distinguish the two layers, outer layer from PCL coating and the inner layer the alginate-gelatin plus bismuth matrix. From the SEM images we can observe a poor interfacial bonding between the polymers (alginate/gelatin and PCL 787). The inner diameter, i.e. the lumen of the stent is 2 mm. The inner and outer diameter and the length of the stents are only dependent on the injection mold used to prepare them, and do not depend on the formulation tested. Like in the first generation of the biodegradable ureteral stents the surface obtained without coating is similar (16).

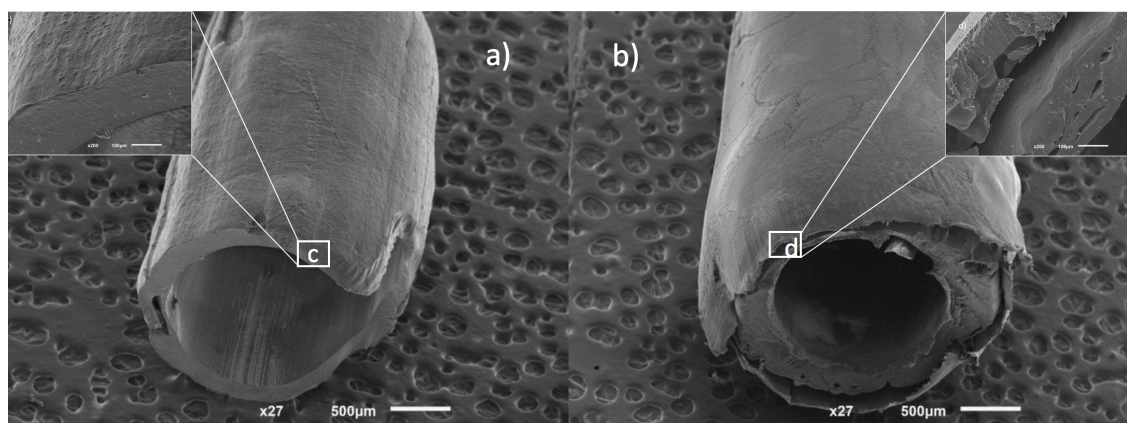


Figure V-1 SEM micrographs of the biodegradable ureteral stent (6 Fr, formulation 2, 0.48M) a) before coating, b) after coating, c) higher magnification of one-layer hydrogel d) higher magnification of two layers coating and hydrogel.

V-3.2. X-Ray validation

An important feature of the ureteral stents is its radiopacity. The possibility to assess by postoperative X-ray, localize the stent in the body and follow the degradation during time is of major importance and for this we used a standardized product, namely bismuth (III) carbonate basic, however, others can be used. In **figure V-2** it is possible to confirm the radiopacity, in wet state, of the biodegradable ureteral stent developed (**figure V-2b**) in comparison with commercial stent

(figure V-2a). In this work we used a lower concentration of this compound in the formulation as compared to the Lingeman *et al* (23), demonstrating that low amounts are suitable to provide this feature to the stent.

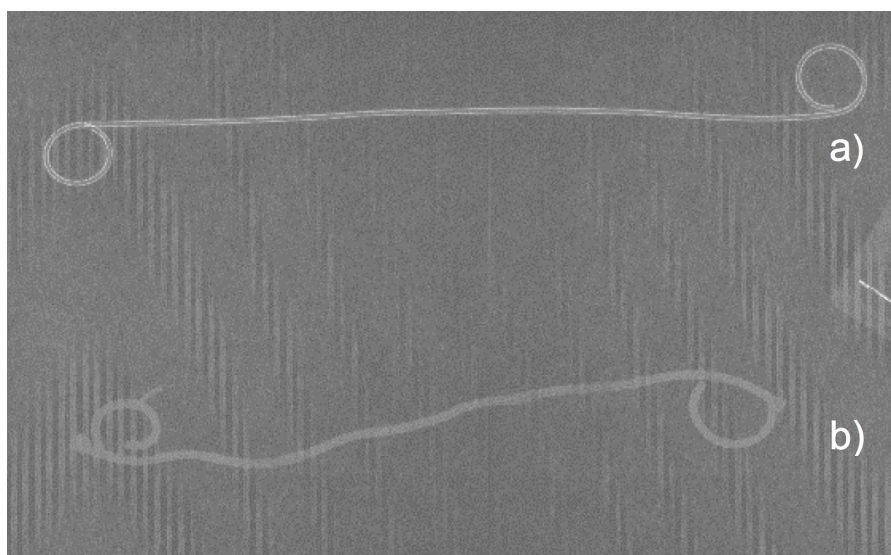


Figure V-2 Radiograph in abdomen mode of a) commercial ureteral stent (Biosoft® duo, Porges, Coloplast) and b) biodegradable ureteral stent developed (formulation 2, 0.48M).

V-3.3. *In vitro* degradation study

The *In vitro* degradation of the biodegradable ureteral stents with the different formulations and different concentrations of crosslinking agent was assessed measuring the weight loss of the samples. The weight loss, measured as the percentage of mass lost when immersed in AUS for a predetermined time period is presented in **figure V-3**. All the conditions tested demonstrated *In vitro* that no degradation occurs during the first 3 days of immersion. After 9 days, the stents have shown complete degradation. Comparing the different formulations tested, the results suggest that higher concentration of alginate formulations 4 and 5, **figure V-3a**) increase the degradation time. Comparing the different concentrations of crosslinking agent (**figure V-3b**) the results show that stronger cross-linking lower is the degradation even though not statistically significant. This can be justified due to the presence of more calcium crosslinks with guluronic acid (G) blocks, increasing their covalently cross linked network (25). The divalent cations of the ionic crosslinking agent, bind

exclusively to the G-blocks of the adjacent alginate chains, since the structure of the L-guluronate offers a greater flexibility than the D-mannuronate chains. By creating ionic inter-chain bridges, divalent ions replace the hydrogen bonds between the carboxyl group of D-mannuronate and the 2-OH and 3-OH groups of the subsequent L-guluronate, originating the gelation of aqueous alginate solutions (26, 27). The G-block length, concentration of polymer and molecular weight are thus critical factors affecting the physical properties of alginate and its resultant degradation. On the other hand, gelatin can form hydrogels by increasing and decreasing temperature, which is merely a physical crosslinking phenomena. The mechanism behind the crosslinking of gelatin molecules is a conformational change from a random coil to a triple helix. The degradation occurs then because the noncovalent associations are easily disrupted at temperatures higher than 30–35°C, therefore at body temperature (28). This helps to understand that with higher amounts of gelatin in the formulation a faster degradation will take place. In our previous study, the alginate-based ureteral stents showed a slower degradation comparing with this work, for the same reason (16). The

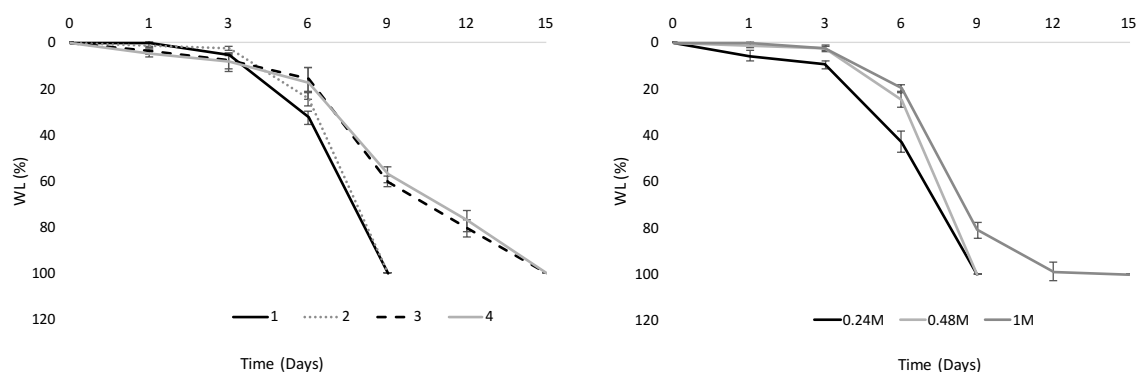


Figure V-3 Weight loss of developed biodegradable ureteral stents a) Different formulations tests and b) Formulation 2 with different crosslinking concentration.

polymer blend with the alginate is however unknown and hence a work correlation is difficult to establish compared with our formulation.

V-3.4. Gel permeation chromatography (GPC)

The polymeric leachables from the ureteral stent degradation at 1, 3, 6 and 9 days were first lyophilized and then dissolved in an appropriate eluent to be analyzed by GPC. As a control the raw materials alginate and gelatin was injected. GPC pattern of alginate and gelatin show an overlap of

the eluting peaks between 18 ml and 21 ml of retention volume and hence it is not easy to distinguish both. The leachables are composed essentially by the mixture of alginate and gelatin present in the biodegradable ureteral stent formulation. The overlap of the raw materials makes it difficult to identify separately the presence of the alginate and gelatin. However, it is possible to see an increasing intensity of the peaks on the elution curve with degradation time. Considering the retention volume of the peaks on the different elution curves, we observe a major contribution of gelatin instead of alginate. This was expected because this formulation (formulation 2) is composed of 65% gelatin and 30% alginate.

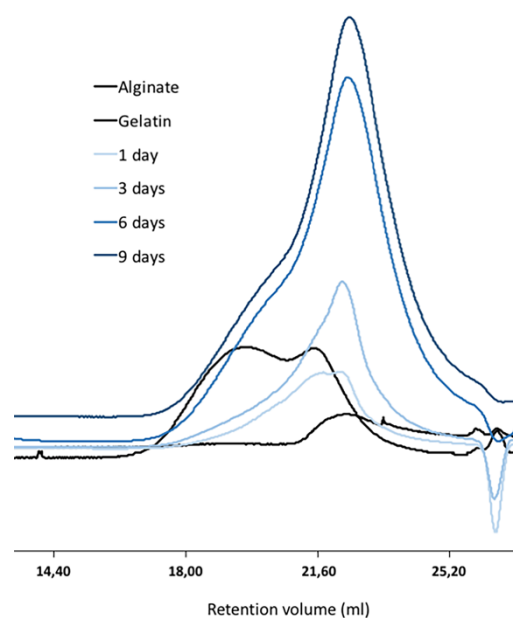


Figure V-4 GPC chromatograms of stent raw materials (alginate and gelatin) and the leachables at 1, 3, 6 and 9 days' time points.

V-3.5. Inductive Couple Plasma (ICP)

The ICP analysis of bismuth concentration in the immersion solutions from different time points from formulation 2 is present in **table V-4**. The results show a gradual release of bismuth during the degradation process from the stent to the artificial urine solution. According to the degradation profile (**figure V-3a**) of ureteral stents, formulation 2, and the bismuth measured in the immersion solutions we can see that the release of bismuth is associated with the degradation

and it does not occur due to swelling of the stent or diffusion from the stent to the AUS. To support this observation and considering a homogenous distribution of bismuth in the stent, it would be expected to have a correlation between the degradation profile and the amount of bismuth in solution. On day 3 the ureteral stent with formulation 2 presents a degradation around 5%, corresponding the value of bismuth in solution is 0.271 g/L, that is approximately 5% of the total bismuth present in the stent. The same is observed at time point day 6 in which the value 1.285 g/L is 20% of the total bismuth and again is close to the value of the degradation observed in **figure V-3a**.

Table V-4 Concentration of bismuth obtained by ICP, in immersion solution (AUS) during the degradation.

Days	Bismuth (g/L)	Std	Release (%)
1	0.0570	0.0058	~ 1%
3	0.271	0.0496	~ 5%
6	1.285	0.0600	~ 20%
9	5.953	0.1912	100%

V-3.6. Leachables cytotoxicity

The cytotoxicity of the leachables obtained from stent degradation was evaluated in accordance with the protocol described in ISO/EN 10.993 (20). The viability of the cells cultured in a tissue culture plate, in the presence of the leachables, was determined as a function of the cells cultured in Dulbecco's modified Eagle medium (DMEM) culture medium. **Figure V-5** presents the cell viability after 72 h in contact with the material dissolved in the culture medium. Significant differences were observed for the cell viability in the presence of the leachables in comparison with the latex, which was used as a positive control. The results demonstrate that there is no toxic interaction between the leachables from day 1 to day 9 and L929 cells.

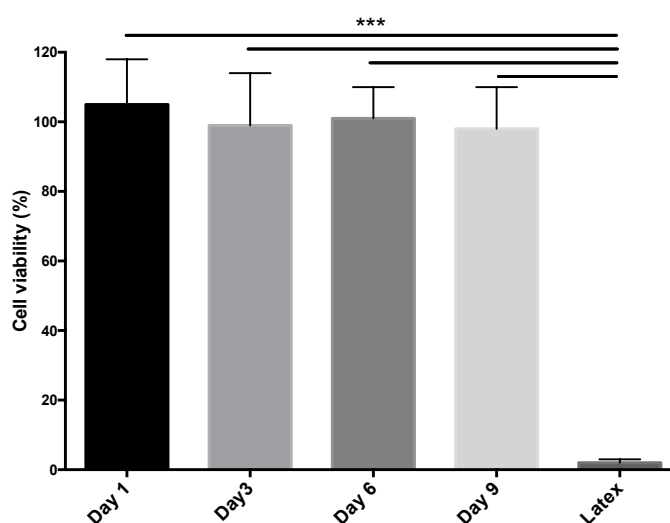


Figure V-5 Cytotoxicity study by cell viability measured after 72 h.

V-3.7. Tensile mechanical tests

The tensile mechanical properties like maximum load (N), maximum tensile strain (%) and Young modulus (MPa) of the biodegradable ureteral stents developed are presented in **figure V-6 and figure V-7**. **Figure V-6** presents the results in dry and wet state of the four different formulations of stents when using a concentration of 0.48M crosslinking agent. As a control the tensile results for the commercial stent (Biosoft® duo, Porges, Coloplast) are also presented. Comparing all studied formulations, significant differences were observed before and after hydration and with and without coating, in terms their mechanical properties. In all formulations and as expected of hydration in AUS (**figure V-6d**) the values of tensile properties decrease in terms of Young modulus but increase in terms of maximum tensile strain. Furthermore, the ureteral stents after hydration become more elastic than in dry state. The results for the hydrated samples are far more important for the clinical purpose as if complications occur it may be necessary to pull out the stent. Regarding the highest values, the maximum load was 78.7 N and in terms of Young's modulus it was 49.8 MPa after hydration for the coated stents of formulation 2. Compared with 41.2 N and 24.6 MPa, respectively, for the commercial stent. On the other hand, in terms of maximum tensile strain (%) or elongation at break the control present values around 736.5 % compared with 339.1 % obtained for formulation 2. In general, the contribution of

gelatin seems to increase the mechanical properties of the biodegradable stents. The hydration of the stents further contributes to increase the elasticity of the material. Analyzing the effect of the PCL coating it also contributes to increase the elasticity and the ductility of the stents with significant differences. With the objective to study the influence of calcium ions concentration as crosslinking agent three different concentrations were tested with the formulation 2. This formulation was selected according the results obtained, due to the balance in terms of ductility and elasticity of biodegradable ureteral stent.

Figure V-7 shows herein the results for the ureteral biodegradable stent with formulation 2, using different concentrations of crosslinking agent, namely 0.24M, 0.48M and 1M. Comparing the different concentrations, the results suggest that the crosslinking concentration does not have a great impact in the final mechanical properties of the biodegradable ureteral stent although, a slight increase is observed in the calcium ions concentration. These results have been previously reported in the literature. The presence of calcium ions enhances the crosslink of alginate matrix. Nonetheless we do not observed in this work significant changes in the mechanical properties changing the calcium concentration (29).

The maximum tensile strain (%) during the degradation process were measured (**figure V-7d**) and the results show decrease of the mechanical properties during time of degradation. Nonetheless on day 6, before the complete degradation, the ureteral stent (formulation 2) shows an average maximum tensile near 200 %. Although the mechanical properties decrease during the degradation process the properties seem to be enough to maintain the function of the ureteral stent before the total degradation. These observations are extremely important in case there is the clinical need to remove the stents without compromising the obstruction of the ureter by possible fragments left.

In the first generation of biodegradable ureteral stents made by natural polymer the values obtained were three times lower compared with the second generation (16). Clearly, increasing the gelatin concentration, the modification of the fabrication process and an incorporation of a new biodegradable coating allow the preparation of a biodegradable ureteral stent capable to be used *In vivo* following conventional ureteroscopy an ideal ureteral stent is expected to have adequate performance in terms of mechanical properties.

Comparing our maximum tensile strain results with a resorbable ureteral stents made from PGA and PLGA (15, 30) the natural origin materials here used present higher elongation comparing with the synthetic materials. In terms of global mechanical performance obtained in this study demonstrated to be similar or better than commercial stent available, Biosoft® duo, Porges, Coloplast.

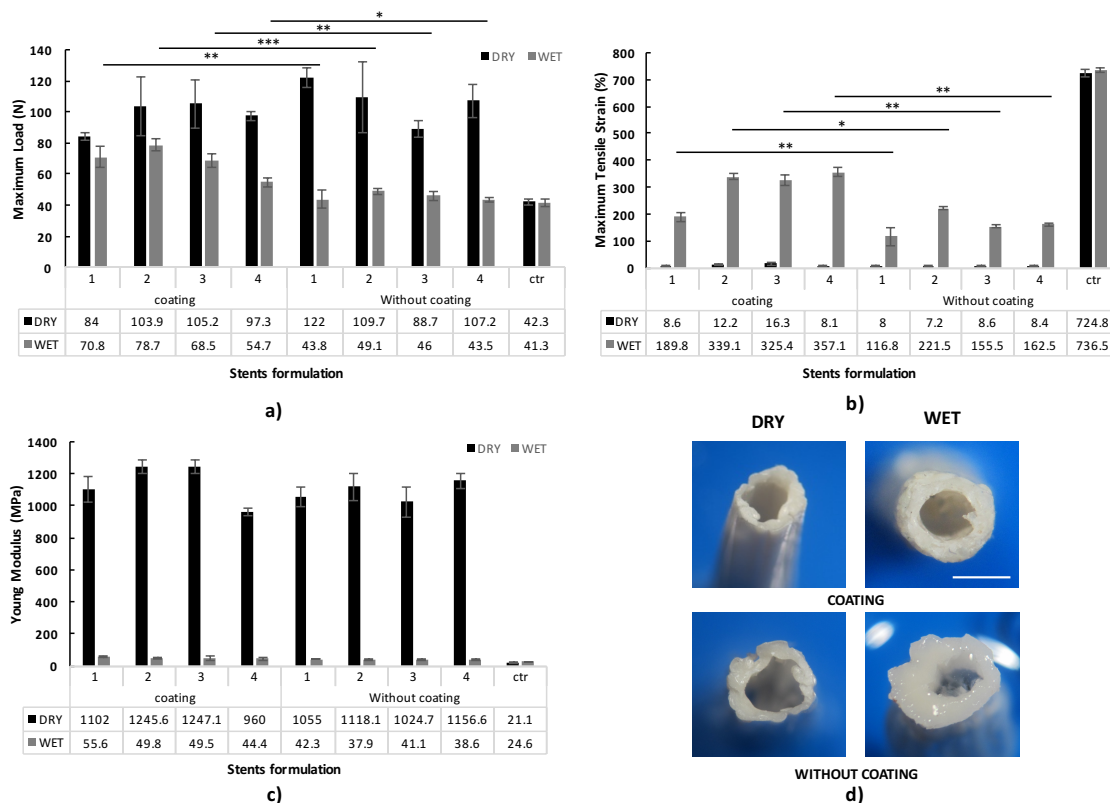


Figure V-6 Mechanical properties of the biodegradable stents (0.48M crosslinking concentration) before and after PCL coating in terms of a) maximum load (N) b) maximum tensile strain (%) and c) young modulus (MPa). d) Images of biodegradable stents before and after coating in dry state and in wet state immersion in AUS (scale bar 2mm). Ctr - (Biosoft® duo, Porges, Coloplast). Values are represented as average \pm SD, n = 3. Statistical differences (*p < 0.05, **p < 0.01) using one way-ANOVA followed by a Tukey post-test.

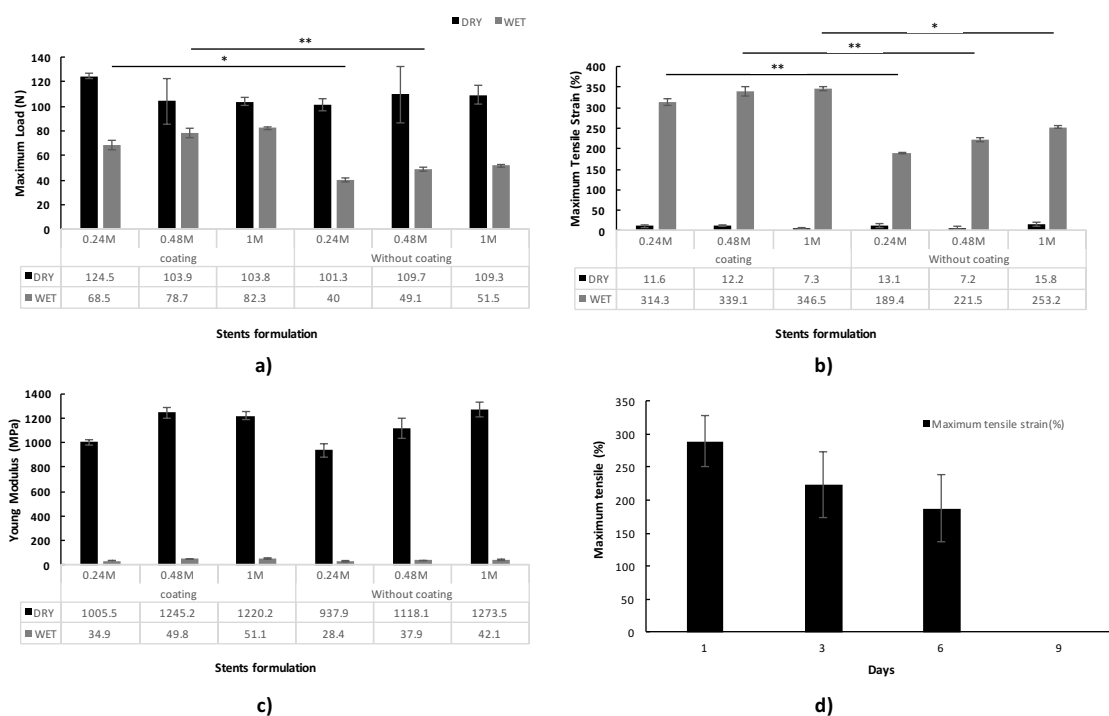


Figure V-7 Mechanical properties of the biodegradable stents prepared with the formulation 2 with different concentrations of crosslinking agent before and after PCL coating in terms of a) maximum load (N), b) maximum tensile strain (%), c) young modulus (MPa) and d) maximum tensile strain (%) of ureteral stent formulation 2 during the degradation time. Values are represented as average \pm SD, n = 3. Statistical differences (*p < 0.05, **p < 0.01) using one way-ANOVA followed by a Tukey post-test.

V-3.8. *In vivo* placement technique validation

The validation of the stent placement *In vivo* was performed in different female domestic pigs. Conventional ureteroscopy was employed to implant the developed stents. The first stent tested *In vivo* was the first generation of biodegradable ureteral stents based on natural origin polymers reported by Barros *et al* (16). The first generation demonstrated upon surgical procedure the stents slipped perfectly into the cystoscope and the hydrophilic guidewire into the bladder through the urethra. The ureteral stent developed remains intact throughout the procedure and is not fragmented and removal proved to be easy. However, it was not ductile enough in order to be able to be positioned correctly in the ureter. On the contrary, this new second generation of biodegradable ureteral stents, was successfully implanted *In vivo*. The new formulation together with the PCL 787 coating and the poor interfacial bonding between the polymers is an important

feature for the success of the *in vivo* studies. The PCL 787 layer provides a hydrophobic layer that delay the hydration of the material upon implantation and after implantation it will be delaminated from the surface of the stent. The thin layer delaminated is eliminated in the early stages of implantation and after 3 days we did not observed any fragments of PCL in the bladder or ureter. The biodegradable ureteral stents of this second generation at formulation 2 were placed in the right ureters without any complication and as a control a commercial stent (Biosoft® duo, Porges, Coloplast) was placed in the left ureter, following the conventional surgical procedure. In **figure V-8** it is possible to see the second generation of biodegradable stent placed in the ureters of the pig model. During the experiments, all the animals remained asymptomatic and with a normal urine flow. After 3 days, an ureteroscopy was performed to evaluate the morphology of the ureters and the stents. The biodegradable stent remains intact and maintain its stability (**figure V-8c**). Furthermore, no undesired side effects were observed in ureters (**figure V-8d**). On day 10, we performed again an ureteroscopy. At this time point the stents had completely degraded and no signs of fragments of the biodegradable ureteral stents were found. The morphology of the ureters remains normal with no major signs of inflammation or adverse reactions (**figure V-8e and V-8f**) at least at macroscale level. These biodegradable ureteral stents prepared from formulation 2 were demonstrated to be intact during the first 3 days and after 10 days they are completely degraded and no stent residues were observed in the urinary tract. Three independent experiments were carried out and all procedures lead to the same observation. In comparison with the first generation of stents reported in our previous work we herein demonstrate the improvement of the mechanical properties of the biodegradable stent allowing its placement in the ureter and validation of its degradability within 10 days. However, an extensive *In vivo* study needs to be performed to be able to validate clinically the material produced.

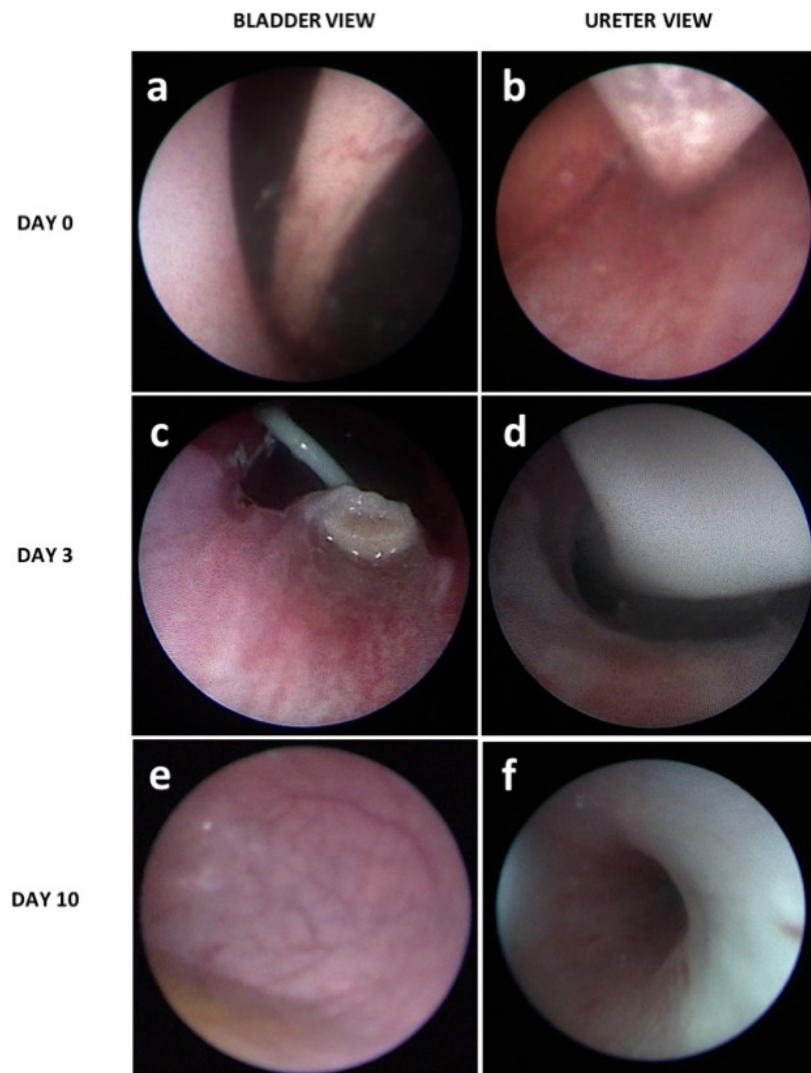


Figure V-8 Conventional ureteroscopy of the stented ureter *in vivo* in a pig model: a) biodegradable ureteral stent placement b) biodegradable ureteral stent inside the right ostium pig ureter at placement time c) biodegradable ureteral stent after 3 days at the entrance of the right ostium pig ureter d) after 3 days with the biodegradable ureteral stent (image taken in the middle of the stent) e) after 10 days of the biodegradable ureteral stent f) right ostium pig ureter after the degradation at day 10.

V-4. CONCLUSIONS

The results obtained from the experiments performed demonstrate that different mixtures of alginate and gelatin and different concentrations of crosslinking agent can be used to obtain a biodegradable ureteral stent from natural origin polymers which may be used for the treatment of urological disorders. In this work, we show that this second generation of stents, presents radiopaque properties even in the wet state. Furthermore, we demonstrate that in *vitro* a higher concentration of gelatin in the biodegradable stent resulted in higher mechanical properties, and a higher concentration of alginate slows the degradation in *vitro*. The leachables and the degradation products have shown to be non-cytotoxic and the degradation of the stent has shown to be homogenous as the degradation occurs by erosion of the material. The second generation of biodegradable ureteral stents herein developed could be implanted following the conventional surgical procedure performed daily in the clinical practice. The ureteral stent remains intact during the first 3 days starting to degrade after that. Full degradation is achieved after 10 days, without any presence of stent remaining's inside the ureter. The stents developed demonstrated to be safe and fulfilled the function of keeping the flow of urine from kidney to bladder while implanted in the ureter.

ACKNOWLEDGEMENTS

The research leading to these results has received funding from the European Union Seventh Framework Programme (FP7/2007-2013) under grant agreement number REGPOT-CT2012-316331-POLARIS and from the project “Novel smart and biomimetic materials for innovative regenerative medicine approaches” RL1 - ABMR - NORTE-01-0124-FEDER-000016) cofinanced by North Portugal Regional Operational Programme (ON.2 – O Novo Norte), under the National Strategic Reference Framework (NSRF), through the European Regional Development Fund (ERDF). Alexandre Barros acknowledges his FCT PhD grant SFRH/BD/97203/2013.

REFERENCES

1. Lange D, Bidnur S, Hoag N, Chew BH. Ureteral stent-associated complications[mdash]where we are and where we are going. *Nat Rev Urol*. 2015;12(1):17-25.
2. Mendez-Probst CE, Goneau LW, MacDonald KW, Nott L, Seney S, Elwood CN, et al. The use of triclosan eluting stents effectively reduces ureteral stent symptoms: a prospective randomized trial. *BJU International*. 2012;110(5):749-54.
3. Krambeck AE, Walsh RS, Denstedt JD, Preminger GM, Li J, Evans JC, et al. A Novel Drug Eluting Ureteral Stent: A Prospective, Randomized, Multicenter Clinical Trial to Evaluate the Safety and Effectiveness of a Ketorolac Loaded Ureteral Stent. *The Journal of Urology*. 2010;183(3):1037-43.
4. Liatsikos EN, Karnabatidis D, Kagadis GC, Rokkas K, Constantinides C, Christeas N, et al. Application of paclitaxel-eluting metal mesh stents within the pig ureter: An experimental study. *Eur Urol*. 2007;51(1):217-23.
5. Olweny EO, Landman J, Andreoni C, Collyer W, Kerbl K, Onciu M, et al. Evaluation of the use of a biodegradable ureteral stent after retrograde endopyelotomy in a porcine model. *Journal of Urology*. 2002;167(5):2198-202.
6. Al-Aown A, Kyriazis I, Kallidonis P, Kraniotis P, Rigopoulos C, Karnabatidis D, et al. Ureteral stents: new ideas, new designs. *Therapeutic advances in urology*. 2010;2(2):85-92.
7. Venkatesan N, Shroff S, Jayachandran K, Doble M. Polymers as Ureteral Stents. *Journal of Endourology*. 2010;24(2):191-8.
8. Chew BH, Lange D, Paterson RF, Hendlin K, Monga M, Clinkscales KW, et al. Next Generation Biodegradable Ureteral Stent in a Yucatan Pig Model. *Journal of Urology*. 2010;183(2):765-71.
9. Lingeman JE, Schulsinger DA, Kuo RL. Phase I trial of a temporary ureteral drainage stent. *Journal of Endourology*. 2003;17(3):169-71.
10. Lumiaho J, Heino A, Tunninen V, Ala-Opas M, Talja M, Valimaa T, et al. New bioabsorbable polylactide ureteral stent in the treatment of ureteral lesions: An experimental study. *Journal of Endourology*. 1999;13(2):107-12.
11. Lumiaho J, Heino A, Kauppinen T, Talja M, Alhava E, Valimaa T, et al. Drainage and antireflux characteristics of a biodegradable self-reinforced, self-expanding X-ray-positive poly-L,D-lactide spiral partial Ureteral stent: An experimental study. *Journal of Endourology*. 2007;21(12):1559-64.
12. Lumiaho J, Heino A, Pietilainen T, Ala-Opas M, Talja M, Valimaa T, et al. The morphological, in situ effects of a self-reinforced bioabsorbable polylactide (SR-PLA 96) ureteric stent; An experimental study. *Journal of Urology*. 2000;164(4):1360-3.
13. Talja M, Multanen M, Valimaa T, Tormala P. Bioabsorbable SR-PLGA horn stent after antegrade endopyelotomy: A case report. *Journal of Endourology*. 2002;16(5):299-302.
14. Lumiaho J, Heino A, Aaltomaa S, Valimaa T, Talja M. A short biodegradable helical spiral ureteric stent provides better antireflux and drainage properties than a double-J stent. *Scand J Urol Nephrol*. 2011;45(2):129-33.

15. Zou T, Wang L, Li WC, Wang WZ, Chen F, King MW. A resorbable bicomponent braided ureteral stent with improved mechanical performance. *J Mech Behav Biomed*. 2014;38:17-25.
16. Barros AA, Duarte ARC, Pires RA, Sampaio-Marques B, Ludovico P, Lima E, et al. Bioresorbable ureteral stents from natural origin polymers. *J Biomed Mater Res B*. 2015;103(3):608-17.
17. Schlick RW, Planz K. Potentially useful materials for biodegradable ureteric stents. *Brit J Urol*. 1997;80(6):908-10.
18. Wen C, Lu L, Li X. Mechanically Robust Gelatin–Alginate IPN Hydrogels by a Combination of Enzymatic and Ionic Crosslinking Approaches. *Macromolecular Materials and Engineering*. 2014;299(4):504-13.
19. Khandwekar A, Doble M. Physicochemical characterisation and biological evaluation of polyvinylpyrrolidone-iodine engineered polyurethane. *J Mater Sci: Mater Med*. 2011;22(5):1231-46.
20. Biological Evaluation of Medical Devices. Part 5. Test for Cytotoxicity In Vitro Methods: 8.2 Test on Extracts., (1992).
21. Lima E, Rolanda C, Osorio L, Pego JM, Silva D, Henriques-Coelho T, et al. Endoscopic Closure of Transmural Bladder Wall Perforations. *Eur Urol*. 2009;56(1):151-7.
22. Oliveira CAR, Ferreira C, Quattrone C, De Sio M, Autorino R, Pinto JC, et al. Endoscopic Closure of Transmural Bladder Wall Perforations. *Journal of Endourology*. 2012;26:A501-A.
23. Lingeman JE, Preminger GM, Berger Y, Denstedt JD, Goldstone L, Segura JW, et al. Use of a temporary ureteral drainage stent after uncomplicated ureteroscopy: Results from a phase II clinical trial. *Journal of Urology*. 2003;169(5):1682-8.
24. Duarte ARC, Santo VE, Alves A, Silva SS, Moreira-Silva J, Silva TH, et al. Unleashing the Potential of Supercritical Fluids for Polymer Processing in Tissue Engineering and Regenerative Medicine. *The Journal of Supercritical Fluids*. 2013.
25. Kong HJ, Kaigler D, Kim K, Mooney DJ. Controlling Rigidity and Degradation of Alginate Hydrogels via Molecular Weight Distribution. *Biomacromolecules*. 2004;5(5):1720-7.
26. Blandino A, Macías M, Cantero D. Formation of calcium alginate gel capsules: Influence of sodium alginate and CaCl₂ concentration on gelation kinetics. *Journal of Bioscience and Bioengineering*. 1999;88(6):686-9.
27. Jejurikar A, Lawrie G, Martin D, Grondahl L. A novel strategy for preparing mechanically robust ionically cross-linked alginate hydrogels. *Biomedical materials*. 2011;6(2).
28. Mohanty B, Bohidar HB. Microscopic structure of gelatin coacervates. *Int J Biol Macromol*. 2005;36(1-2):39-46.
29. Augst AD, Kong HJ, Mooney DJ. Alginate Hydrogels as Biomaterials. *Macromolecular Bioscience*. 2006;6(8):623-33.
30. Zhang MQ, Zou T, Huang YC, Shang YF, Yang GG, Wang WZ, et al. Braided thin-walled biodegradable ureteral stent: Preliminary evaluation in a canine model. *International Journal of Urology*. 2014;21(4):401-7.

Chapter VI

Drug-eluting biodegradable ureteral stent: new approach for urothelial tumors of upper urinary tract

Chapter VI

Drug-eluting biodegradable ureteral stent: new approach for urothelial tumors of upper urinary tract cancer^{††}

ABSTRACT

Upper urinary tract urothelial carcinoma (UTUC) accounts for 5-10% of urothelial carcinomas and is a disease that has not been widely studied as carcinoma of the bladder. To avoid the problems of conventional therapies, such as the need for frequent drug instillation due to poor drug retention, we developed a biodegradable ureteral stent (BUS) impregnated by supercritical fluid CO₂ (scCO₂) with the most commonly used anti-cancer drugs, namely paclitaxel, epirubicin, doxorubicin, and gemcitabine. The release kinetics of anti-cancer therapeutics from drug-eluting stents was measured in artificial urine solution (AUS). The *In vitro* release showed a faster release in the first 72h for the four anti-cancer drugs, after this time a plateau was achieved and finally the stent degraded after 9 days. Regarding the amount of impregnated drugs by scCO₂, gemcitabine showed the highest amount of loading (19.57 $\mu\text{g}_{\text{drug}}/\text{mg}_{\text{polymer}}$: 2% loaded), while the lowest amount was obtained for paclitaxel (0.067 $\mu\text{g}_{\text{drug}}/\text{mg}_{\text{polymer}}$: 0.01% loaded). A cancer cell line (T24) was exposed to graded concentrations (0.01 to 2000 ng/ml) of each drugs for 4 and 72 hours to determine the sensitivities of the cells to each drug (IC₅₀). The direct and indirect contact study of the anti-cancer biodegradable ureteral stents with the T24 and HUVEC cell lines confirmed the anti-tumoral effect of the BUS impregnated with the four anti-cancer drugs tested, reducing around 75% of the viability of the T24 cell line after 72h and demonstrating minimal cytotoxic effect on HUVECs.

^{††} This chapter is based on the following publication:

Barros AA, Browne S, Oliveira C, Lima E, Duarte ARC, Healy K, Reis RL. Drug-eluting biodegradable ureteral stent: new approach for urothelial tumors of upper urinary tract cancer. *International Journal of Pharmaceutics*. 2016; 513(1-2):227-237.

VI-1. INTRODUCTION

Upper tract urothelial carcinoma (UTUC) can be located in the lower (bladder and urethra) or upper (renal pelvis and ureter) urinary tract (1). UTUC are aggressive urologic cancers with propensity for multifocality, local recurrence, and metastasis (2). They are uncommon compared to bladder cancer, but 60% of UTUCs are invasive at diagnosis. Urothelial carcinomas (UCs) are the fourth most common type of tumors (3). The treatments available fall into two categories: a kidney-sparing surgery with the application of the adjuvant topical agents such as bacillus Calmette-Guêrin (BCG) vaccine, mitomycin C or other anti-cancer drugs; and, in the majority of the cases, radical nephrectomy is performed, followed by chemotherapy. The UTUC are urothelial tumors, therefore drugs such paclitaxel, doxorubicin and gemcitabine are expected to have a similar therapeutic efficacy as in bladder cancer (2, 4). Some studies examined the role of chemotherapy for UTUC, and there appears to be an overall survival and disease-free survival benefit for anti-cancer drugs based adjuvant chemotherapy (4).

Drugs like paclitaxel, mitomycin C, doxorubicin and gemcitabine have been reported in different studies as a drugs that can be incorporated in polymeric materials in order to obtain an intravesical drug delivery (IDD) system in urological tract (5-7) .For intravesical chemotherapy, hydrophobic anti-cancer drugs offer a distinctive benefit of superior permeability through the urothelium as compared to hydrophilic drugs (6, 8). One innovative idea explored by Lifshitz et al. (MitoGel™) is the use of an hydrogel with mitomycin C which solidifies at body temperature and can provide prolonged retention of the therapeutic agent and a slow, sustained release (9).

In this study we hypothesized a new concept for the delivery of these anti-cancer drugs using a drug-eluting biodegradable ureteral stent, combining hydrogel technology with conventional ureteral stents. Different drug-eluting ureteral stents have been used extensively in cardiovascular and different applications (10, 11), but in urology it is still a new area (12). Some studies reported the impregnation of drugs like triclosan (Triumph®) (13) and ketorolac (Lexington™) (14) in polyurethane based stents, with the objective to reduce bacterial adhesion, biofilm formation and encrustation to improve patient comfort by decreasing flank pain. These studies have demonstrated that in preclinical and clinical tests, drug-eluting conventional double-J ureteral stents have limited effectiveness possibly because of poor drug delivery to the ureteral tissues (12-14).

In this context, the idea is to use a biodegradable ureteral stent to increase the contact-time between the anti-cancer drugs and the ureter. In addition, after the drug has been delivered the stent degrades without the need for a second procedure to remove the stent (**figure VI-1**). In our previous work we developed a biodegradable ureteral stent from natural polymers (15, 16). This biodegradable ureteral stent allows for the facile incorporation of drugs, that can then be locally released. As a proof of concept ketoprofen was impregnated in the stent as this anti-inflammatory agent is commonly prescribed in urology after surgical procedures (15).

In this work, three hydrophobic anticancer drugs, paclitaxel, doxorubicin, epirubicin and one hydrophilic drug, gemcitabine were impregnated by supercritical fluid technology in a biodegradable ureteral stent. The impregnation of drugs in a polymeric matrix requires always the use of a mobile phase able to dissolve and carry the active pharmaceutical ingredient. When this mobile phase has additionally the ability to swell and stretch the polymer matrix, it facilitates to a great extent the diffusion of the drug into the bulk of the matrix, hence, increasing drug impregnation (17, 18). When the mobile phase uses a fluid in its supercritical state, a high purity product, free of residual solvents is obtained, since no organic solvents are involved in the process. The most commonly used supercritical fluid is carbon dioxide, due to its mild critical parameters (critical pressure 74 bar and critical temperature 31 °C), non-toxicity and non-flammability (19). Furthermore, the use of supercritical fluids can take advantage of their high diffusivity in polymers, in combination with the high solubility and plasticizing action (20-23).

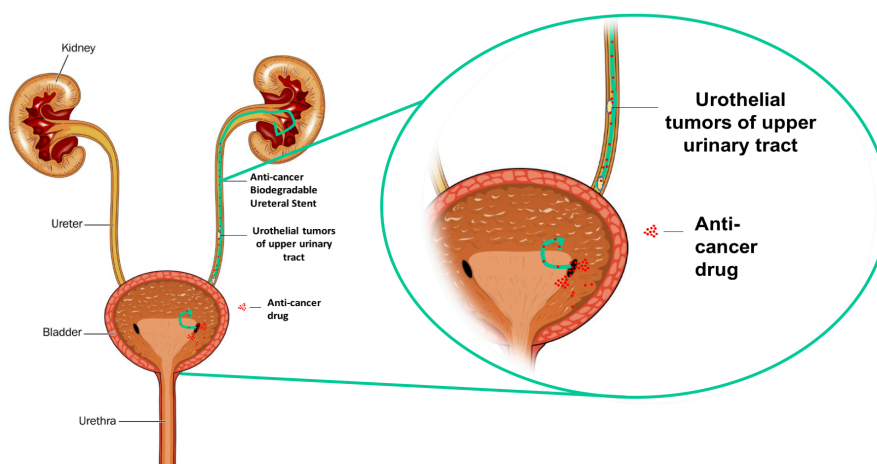


Figure VI-1 Illustration of the concept of anti-cancer drug eluting biodegradable ureteral stent as a potential drug delivery system for UTUC therapy.

VI-2. MATERIAL AND METHODS

VI-2.1. Materials

Alginic acid sodium salt, gelatin, calcium chloride, chlorophorm, ethanol and bismuth (III) carbonate basic were purchased from Sigma-Aldrich (Germany). Potassium dihydrogen ortho-phosphate (99.5%) and magnesium chloride hexahydrate (99%) were obtained from Riedel-de Haën (Germany). Polycaprolactone resin PCL 787, commercially available as TONE™ polymer, was obtained from Union Carbide Chemicals and Plastics Division, Bound Brook, New Jersey. Artificial urine solution (AUS), paclitaxel 99.5% (PA), doxorubicin 98% (DOX), epirubicin 99% (EP) and gemcitabine 99% (GEM) were obtained from Fisher Scientific (U.S.A.). Carbon dioxide (99.998 mol %) was supplied by Air Liquide (Portugal). All reagents were used as received without any further purification.

VI-2.2. Preparation of biodegradable ureteral stents

Biodegradable ureteral stents (BUS) were developed according to the procedure described by Barros et al.(15). The stents were composed of 30% alginic acid sodium salt, 65% of gelatin and 5% of bismuth (III) carbonate. The cross-linking solution was calcium chloride (CaCl_2) at 0.48M. Briefly, polymers were dissolved in hot distilled water (70°C). The solution was stirred for 1 hour and the polymeric solution was injected in a mold to obtain a tubular structure. After 1 hour the piece was taken out of the mold and placed in an alcohol solution (100% ethanol) for 1 hour. BUS were then transferred into a crosslinking solution of calcium chloride (CaCl_2), at room temperature. After crosslinking, BUS were relocated in an alcoholic solution (100% ethanol) to obtain an alcohol gel. BUS were dried using a high-pressure vessel with supercritical carbon dioxide (scCO_2) at 40 °C and 100 bar for 90 min, in continuous mode. The coating of the stents was performed by immersion in a 10% of polycaprolactone (PCL) resin 787 ($\text{Mw } 80,000 \text{ g mol}^{-1}$) dissolved in chloroform.

VI-2.3. Supercritical CO_2 impregnation of anti-cancer drugs

The prepared BUS were placed in a high-pressure vessel with anticancer drugs (10 mg) according to figure VI-2. The anti-cancer drugs were impregnated in the stents with and without the

presence of a co-solvent. The scCO₂ impregnation conditions used were 100 bar at 40°C. Carbon dioxide was liquefied and pumped to the desired pressure using a membrane pump (MCPV-71, Haskel, Germany). Impregnation took place in batch mode for 90 min followed by fast depressurization of the system. When a co-solvent was employed, 10% ethanol was used. A commercial non-degradable ureteral stent (Biosoft® duo, Porges, Coloplast) was impregnated with the same drugs at the same conditions, and used as a control. To enhance the mechanical properties of the stent a PCL coating was applied. To evaluate the effect of coating on the release of the drugs the condition BUS + Co-Solvent was prepared twice and one of this batches was coated with PCL resin. The nomenclature used for each condition is presented in table VI-1.

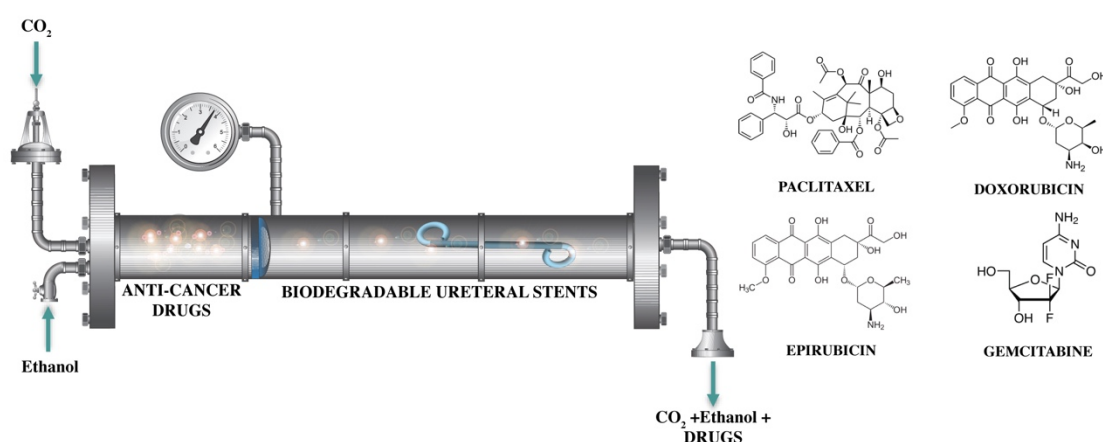


Figure VI-2 Supercritical fluid process impregnation and apparatus of the anticancer drugs used in biodegradable ureteral stent.

Table VI-1 Nomenclature of each condition study of anti-cancer drugs impregnated by supercritical fluid process.

	BUS	BUS + Co-Solvent*	(BUS+Co-Solvent) + PCL Coating	Commercial stent
Paclitaxel (PA)	PA _{bio}	PA _{EtOH}	PA _{coat}	PA _{com}
Epirubicin (EP)	EP _{bio}	EP _{EtOH}	EP _{coat}	EP _{com}
Doxorubicin (DOX)	DOX _{bio}	DOX _{EtOH}	DOX _{coat}	DOX _{com}
Gemcitabine (GEM)	GEM _{bio}	GEM _{EtOH}	GEM _{coat}	GEM _{com}

VI-2.4. Characterization

VI-2.4.1. Impregnation yield

The anticancer drugs impregnation yield (I) was calculated from **Equation II 3**:

$$I(\%) = \frac{m_{drug}}{m_{stent} + m_{drug}} \times 100$$

Equation II-3 Determination of impregnation Yield.

Where m_{stent} is the polymer mass at the beginning of the process and the m_{drug} is the mass of the respective anticancer drug released after complete degradation of the stents in AUS. Anti-cancer drugs concentration was calculated from a calibration curve prepared from standard solutions. The samples were analyzed by UV-spectroscopy using a microplate reader (SpectraMax i3, Molecular Devices, USA) at the maximum absorbance for each drug (227nm for PA, 254nm for EP and DOX and 268nm for GEM). All the experiments were performed in triplicate.

VI-2.4.2. Determination of anti-cancer drugs release from biodegradable ureteral stents.

The release kinetics of developed anti-cancer drug-eluting biodegradable ureteral stents was measured in artificial urine solution (AUS). The *In vitro* release of anti-cancer drugs (paclitaxel, epirubicin, doxorubicin and gemcitabine) from the impregnated biodegradable ureteral stents was performed in triplicate. 10 mg of impregnated sample were weighted and immersed in 10ml of AUS at 37°C with 60 rpm stirring. At pre-determined time periods (0 min, 5 min, 15 min, 30 min, 1 h, 3 h, 5 h, 7.5 h, 24 h, 48 h, 72 h, 6 days and 10 days), an aliquot of 0.5 ml of the release solution was taken and the volume replaced with fresh AUS. The concentration of drug was determined by UV-spectroscopy as described above.

VI-2.4.3. Cell culture

In this study we used a human urothelial carcinoma cell line, T24 (ATCC, U.S.A.) as a cancer cell line to model the urothelial carcinoma and human umbilical vein endothelial cells,

HUVEC, (ATCC, U.S.A.) as a control, non-cancerous cell line. The T24 cell line and HUVEC cells were cultured in RPMI-1640 and EGM™-2 medium, respectively, with (10% fetal bovine serum (FBS), 1 mM L- glutamine and 1% penicillin/streptomycin), Cells were maintained at 37 °C in a humidified 5% CO₂ atmosphere.

VI-2.4.4. In vitro efficacy of anti-cancer drugs against T24 cells and HUVECs - IC₅₀ determination

The cytotoxicity of paclitaxel, epirubicin, doxorubicin and gemcitabine was evaluated by determining the viability of T24 and HUVEC cells after exposure to medium containing the free drug at a range of concentrations from 0.01 to 2000 ng/ml. Free drugs in medium were prepared by first dissolving the anticancer drugs in DMSO (50 mg/ml) and this solution was then diluted in culture medium to achieve the desired concentration. A standard MTT assay (CellTiter 96® Aqueous One Solution Cell Proliferation Assay) was used to test cell viability and was performed on both cell lines to determine the half maximal inhibitory concentration (IC₅₀) of each drug. 5000 cells per well were seeded in a 96-well plate with 100 µL medium for both T24 and HUVEC cells. After incubation for 24 h, the medium in each well was aspirated and the cells were exposed to fresh medium containing the drugs at various concentrations for 4 h and 72 h. The cells after 4 h treatment were further cultured for 72 h in fresh (drug-free) medium. After that, the culture medium in each well was replaced by 100 µL of medium and 20 µL of CellTiter 96® Aqueous One Solution Reagent, followed by 4 h incubation at 37 °C. A latex rubber extract was used as negative control for cell death; while cell culture medium was used as positive control. Cell viability was quantified by UV-spectroscopy, reading the formazan absorbance at 490 nm in a microplate reader (SpectraMax i3, Molecular Devices, USA). Each sample formulation and control was tested using 12 replicates.

The IC₅₀ was determined from the fitting of the curve of cell viability, measured by MTT and the drug concentration. The fitting was performed using GraphPad software (GraphPad Prism 6.00 software, San Diego, USA).

VI-2.4.5. In vitro anti-cancer effect of anti-cancer drug-eluting biodegradable ureteral stents by indirect and direct contact with T24 cells and HUVECs

The anti-cancer effect of the anti-cancer drug-eluting biodegradable ureteral stents in human urothelial carcinoma cell line was evaluated by determining the viability of T24 cells by indirect and direct contact. HUVEC was used as non-cancerous, control cell line. The T24 cell line and HUVEC cells were cultured in RPMI-1640 and EGM™-2 medium, respectively with (10% fetal bovine serum (FBS), 1 mM L- glutamine and 1% penicillin/streptomycin). By indirect contact, the effect of the released drug as well as leachables from the biodegradable ureteral stents were evaluated, placing the stents in fresh medium after 4 h and 72 h. On the other hand, by direct contact 10 mg of stent was placed directly in contact with a cell layer in each well. Both tests were performed for 4 h and 72 h. The viability of the cells was performed using a standard MTT test. Briefly, 5000 cells per well were seeded in a 96-well plate with 100 µL medium for T24 and HUVEC cells. After incubation for 24 h, the medium in each well was aspirated and the cells exposed to medium containing the extracts of the stents in the indirect contact study. In the direct contact the cells were exposed to 100 µL of fresh medium in the presence of the stent. The cells after 4 h treatment were further cultured for 72 h in fresh medium. After that, the culture medium in each well was replaced by 100 µL of medium and 20 µL of CellTiter 96® Aqueous One Solution Reagent, followed by 4 h incubation at 37 °C. Cell culture medium and the non-impregnated stents (BUS and commercial stent) were used as negative controls. Each sample formulation and control was tested with 3 replicates.

VI-2.4.6. Light microscopy

Cells cultured on the bottom of the well plate, after 4 and 72 h direct contact were observed by light microscope (Axio Imager Z1m, Zeiss, Germany) in order to visually assess the effect on morphology. Images were taken with a magnification of 10x of T24 cells after 4 h and 72 h of exposure by direct contact to biodegradable ureteral stents impregnated with the anti-cancer drugs. Control experiments were carried out in T24 cells and drug-free stents for 72 h.

VI-2.4.7. Statistical analysis

All data values are presented as mean \pm standard deviation (SD). Statistical analysis was performed using Graph Pad Prism 6.00 software (San Diego, USA). Statistical significances ($p < 0.05$, $**p < 0.01$ and $***p < 0.001$) were determined using one-way analysis of variance (ANOVA) for an average of three to twelve replicates, followed by post hoc Tukey's test for all pairwise mean comparisons.

VI-3. RESULTS AND DISCUSSION

VI-3.1. Preparation of biodegradable ureteral stents impregnated with anticancer drugs

The biodegradable ureteral stents from natural origin polymers were prepared as previously described (**Figure VI-3**), and the anticancer drugs were loaded in **BUS** by $scCO_2$, as illustrated in **Figure VI-2**. $scCO_2$ offers advantages over other impregnation solvents as it is an environmentally friendly, non-flammable, and non-toxic solvent, highly abundant and low cost. Furthermore, at the end of the impregnation process, and after the depressurization step, the final product is obtained in a dry form avoiding the need for subsequent drying and purification steps. Furthermore, the solvent can be recycled and reused (24).

According to Kazarian et al. (25, 26) there are mostly two mechanisms which describe impregnation by supercritical fluids. One is the simple deposition of the drugs in the swollen matrix when the system is depressurized. In this mechanism, the drug is solubilized in CO_2 and is placed in contact with the polymeric matrix for a predetermined time. After this procedure, and upon depressurization, the CO_2 molecules rapidly leave the polymer matrix, the solubilized drug precipitates and is deposited within the polymeric network. This mechanism is highly dependent on the swelling ability of the polymeric matrix when in contact of the supercritical fluid. On the other hand, a second mechanism of impregnation described by Kazarian et al., is said to be more dependent on the affinity of the drug towards the polymeric matrix.

The conditions used for the impregnation of anti-cancer drugs were the same as used for the drying of the stents (100 bar at 40°C and 90 min) with and without the presence of a co-solvent.

The addition of polar solvents to scCO₂ such as ethanol is known to increase the solubility of many polar substances, like the drugs used in this study, which have a large molecular weight and/or molecular polarity and hence low solubility in carbon dioxide (27). The use of 10% ethanol was determined by the solubility of drugs in supercritical CO₂ reported in literature (28-30).

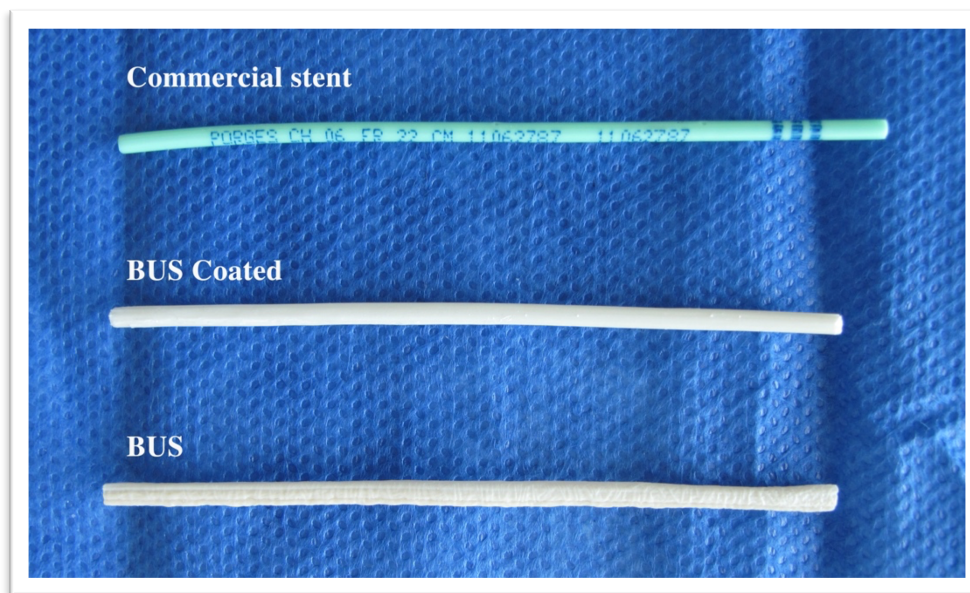


Figure VI-3 Section of commercial non-degradable ureteral stent (Biosoft® duo, Porges, Coloplast) BUS coated with PCL resin and BUS stents prepared after impregnation.

The impregnation efficiency of anti-cancer drugs in the biodegradable ureteral stents (**BUS**) was determined as a function of mass (μg) of anti-cancer drugs per mass (mg) of the polymer. The results are presented in **Table VI-2**. In the **Drug_{EtOH}** conditions, the amount of anti-cancer drug impregnated in the stents is higher, as it would be expected due to the co-solvent effect of ethanol in the enhancement of drug the solubility in CO₂. The amount of impregnated paclitaxel in pure scCO₂ (**PA_{bio}**) was 0.046 $\mu\text{g mg}^{-1}$, whereas those in **PA_{EtOH}** condition was 30% higher (0.067 $\mu\text{g mg}^{-1}$). A similar percentage was reported by Yoda et al. (27) in which the authors report the impregnation of paclitaxel in an amorphous poly(DL-lactic acid) (PDLLA) matrix. The amount of paclitaxel impregnated by Yoda et al. in PDLLA was 2-3 times higher compared with the alginate/gelatin matrix obtained in this work. This can be justified by the higher affinity of the drug-CO₂ solution in the hydrophobic PDLLA matrix (25). Furthermore, PDLLA may also have greater swelling in the presence of scCO₂ than the alginate/gelatin polymer blend (27, 31). Regarding the other drugs, the results show a 15% increase in the impregnation yield for EP, 12% for DOX and 8% for GEM when ethanol was used as a co-solvent. In the case of the Biosoft® duo, Porges, Coloplast

stents the amount of drug impregnated is 6-times lower compared with **BUS** impregnated with paclitaxel under the same conditions. The lower amount of drug impregnated can be related with lower swelling ability of the polymeric matrix of the commercial stent in scCO₂ and/or by lower affinity of the drugs with composition material of the Biosoft® duo, Porges, Coloplast stent.

Table VI-2 Quantity of drug impregnated by scCO₂ (operating conditions 90 min, 100 bar and 40 °C) (µg drug /mg polymer).

	Paclitaxel	Epirubicin	Doxorubicin	Gemcitabine
Drug_{Bio}	0.046 ±0.001	1.498 ±0.070	3.297 ±0.153	18.183 ±0.769
Drug_{ETOH}	0.067 ±0.001	1.779 ±0.032	3.748 ±0.202	19.572 ±0.053
Drug_{Com}	0.014 ±0.001	0.118 ±0.022	0.208 ±0.057	2.312 ±0.131

VI-3.2. *In vitro* release kinetics in Artificial Urine Solution

The release of anti-cancer drugs from the impregnated BUS and Commercial ureteral stents was performed in AUS at 37°C in order to mimic the conditions *In vivo*. Artificial Urine solution (pH 5.5) was chosen as the release medium and this medium was regularly replaced to provide sink conditions. Figure VI-4 shows the release profile of the drugs from the stents. Similar release for the four anticancer drugs impregnated in the BUS was observed. Comparing the condition where the BUS is coated (Drug_{coat}) with the non-coated conditions, it is possible to conclude that the PCL coating of the BUS did not affect the release of the drugs in AUS. The PCL layer is delaminated from the surface of the stent due to the poor interfacial adhesion between the hydrophilic polymers gelatin + alginate and the hydrophobic PCL. Upon immersion in the physiological AUS the PCL coating detaches from the surface, hence no significant differences between the release profile of the different drugs from the coated or uncoated stents are observed. In the case of the Commercial stent all drugs impregnated are released in the first 24 h. For the biodegradable system, it is noticeable that in the first 4 h a release of nearly 50% of the amount drug impregnated and the remaining drug was sustainably released until 72 h in AUS. The stent degraded after 9 days.

In the non-degradable stent, we observed a faster release when compared with the BUS. This faster release may be justified due the poor impregnation on the synthetic polymer. In this case due to the highly dense polymer network the drugs did not penetrate deeply into the bulk of the polymeric matrix, but rather are located on or close to the surface of the stents and hence are

more easily released to the medium (6). In the case of the biodegradable stent, it is composed of 94% water with a highly porous polymer network. Furthermore, the acidic and high ionic strength of AUS may swell the stent facilitating the release. The release profile of these four anti-cancer drugs shown in figure VI-4 is promising for intravesical chemotherapy in UTUCs (6).

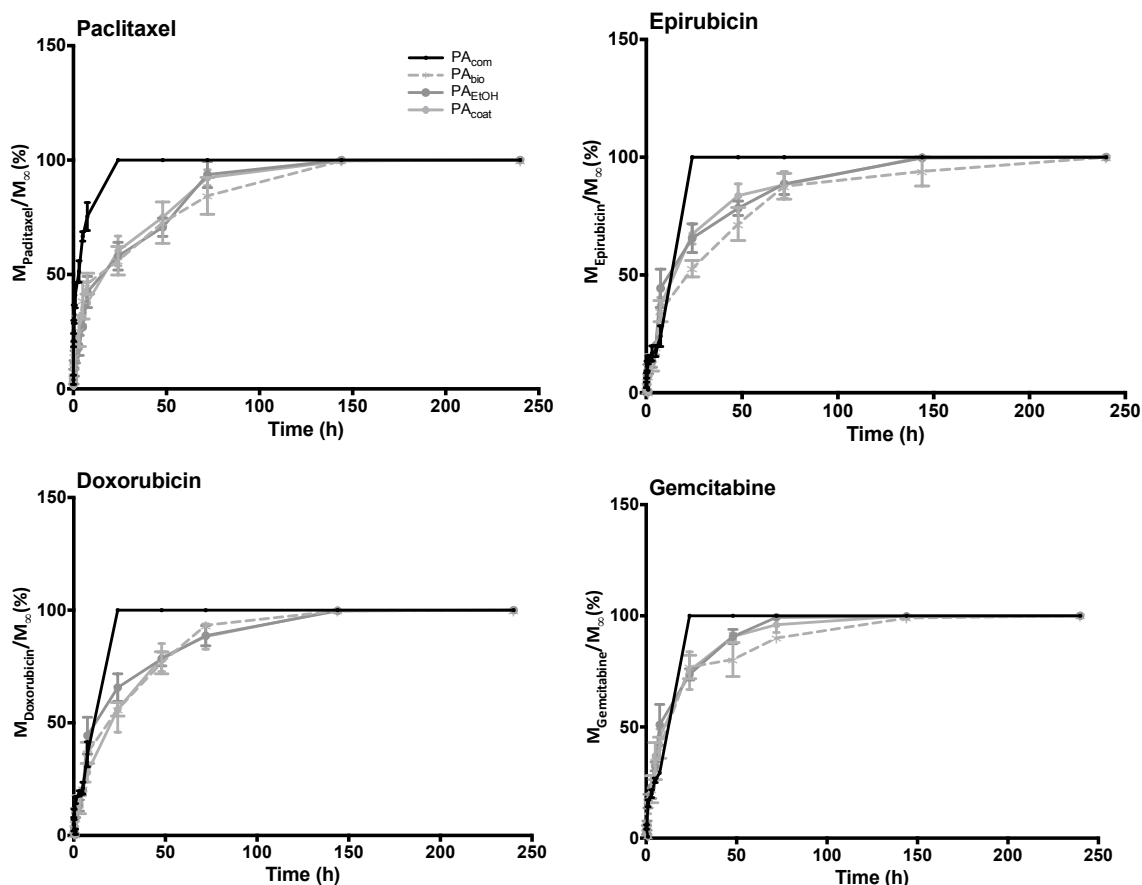


Figure VI-4 Cumulative anti-cancer drugs release from biodegradable and non-biodegradable ureteral stents in Artificial Urine Solution AUS (pH 5.5) at 37°C, for different conditions tested. The stent degraded after 9 days.

VI-3.3. Determination of IC_{50} of anti-cancer drugs against T24 and HUVEC

The effect of the anti-cancer drugs when in contact with T24 and HUVEC cells was investigated by a cell viability test, namely the MTT assay. From this, the IC_{50} was calculated for each of the four drugs in each of the two cell lines. In this case, IC_{50} is a measure of the concentration needed to inhibit cell survival, and is routinely used to specify the *In vitro* potency of a drug (32). The T24 cell line was chosen as a muscle invasive urothelial cancer and the HUVEC cells were used as non-cancerous control cells. The cytotoxicity evaluation was carried out either

after 4 h or 72 h of exposure of the cells to the free drugs at different concentrations (**figure VI-5**). The four anti-cancer drugs showed to have a concentration-dependent inhibition profile of the survival of both the cancer cell line and HUVEC cells. In **figure VI-5** it is possible to see, for both cell types the trend of concentration-dependent cytotoxicity. These are similar, in all cases and as it would be expected the 72h exposure present a higher killing efficacy. Comparing the results between the two cells it is possible to conclude that the cancer cells are much more sensitive to the anti-cancer drugs compared with the HUVEC cells.

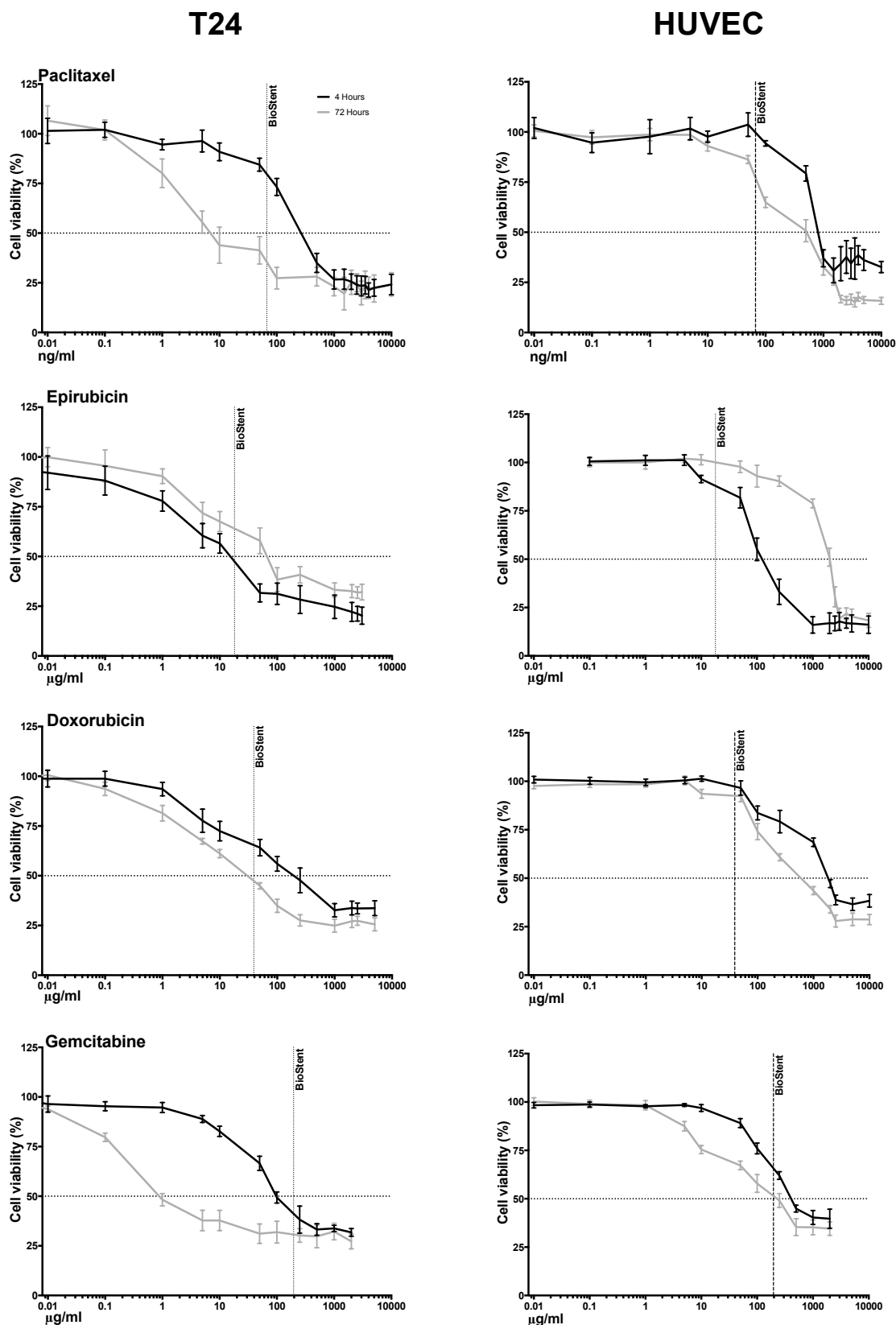


Figure VI-5 In vitro viability of T24 cells and HUVEC cells after exposure to the anti-cancer drugs at different concentrations for 4 h or 72 h. Cell viability is expressed as % of control.

Vertical line represents the amount of drug impregnated by scCO₂ in BUS. Data shown is the average of at least 3 independent experiments.

In **Figure VI-5**, a vertical line is plotted which corresponds to the amount of drug impregnated in **BUS** for each drug. The results show for all drugs that the amount of drugs impregnated in **BUS** is higher than IC₅₀ value of T24 cells and lower than IC₅₀ value of HUVEC cells. Importantly, this shows that the **BUS** impregnated in this study may have a cytotoxic effect against T24 cells but no effect against HUVEC cells. In the case of gemcitabine, the amount of drugs in **BUS** is still lower than the IC₅₀ of HUVECs but the amount of drug in theory has the ability to affect the HUVEC cells, reducing the cell viability near to 50% during the 72 h. In the case of direct contact method no effect on HUVECs was observed, Browne et al, suggested that delayed release can reduce the toxicity (33).

The four drugs have shown different cytotoxicity concentrations for the T24 and HUVEC cells. The results show to have time- and concentration-dependent cytotoxicity of T24 and HUVEC against the anti-cancer drugs tested. The IC₅₀ values are presented in **Table VI-3**. For T24, IC₅₀ at 4 h exposure time for paclitaxel is 281.98 ng/ml which is ~3 times lower than the corresponding value for HUVEC (849.81 ng/ml). When the exposure time is increased to 72 h the difference between the two [cells are even higher 7.30 ng/ml for T24 and 501.50 ng/ml to HUVEC cells. For the other drugs, the cells seem to be less sensitive. In these cases, the IC₅₀ values are in the range of µg/ml and not ng/ml as observed in paclitaxel profile. Comparing with the literature, the value obtained for paclitaxel after 72 h (7.30 ng ml⁻¹) is higher than with the IC₅₀ value obtained by Hadaschik et al. (2.85 ng ml⁻¹) (5). Lu et al. (6) and Yu et al. (34) report the IC₅₀ of doxorubicin for T24 cancer cells and the results have also shown to be concentration-dependent cytotoxicity, but presenting a different range of IC₅₀ values, 11.6 ng ml⁻¹ and 4 µg ml⁻¹, respectively. In the case of the gemcitabine, Papadopoulos et al. (7) reported an IC₅₀ of 0.79 µg ml⁻¹ which is comparable with our data.

Table VI-3 IC50 of the anti-cancer drugs at 4 h and 74 h for the T24 and HUVEC cells (± STD)

	IC ₅₀	Paclitaxel (ng/ml)	Epirubicin (µg/ml)	Doxorubicin (µg/ml)	Gemcitabine (µg/ml)
T24	4h	281.98 ± 3.06	67.02 ± 2.34	187.07 ± 5.18	98.97 ± 1.29
	72h	7.30 ± 0.88	15.74 ± 1.02	29.28 ± 10.01	0.89 ± 0.27
HUVEC	4h	849.81 ± 6.48	2051.08 ± 33.21	2149.32 ± 58.21	413.57 ± 2.68
	72h	501.50 ± 7.67	139.11 ± 13.64	646.60 ± 21.35	237.24 ± 16.73

VI-3.4. In vitro study of anti-tumoral effect of anti-cancer biodegradable ureteral stents

The anti-cancer effect of the biodegradable ureteral stents developed here was evaluated by determining the viability of both T24 cells and HUVEC by indirect and direct contact of the stents with cells. **Figure VI-6** presents the results for four drugs tested by indirect contact against T24 cancer cell after 72 h of exposure. The controls used were the T24 cells in a drug-free medium and the stents without drugs impregnated. The T24 cancer cells display similar behaviour when in contact with drug-loaded stents as to when exposed to the different drugs tested. After 4 h and 72 h in contact with drug-released-medium the viability of cancer cells decreases in most cases around 25% and 50%, respectively. The condition when ethanol was used as a co-solvent (**Drug_{EtOH}**), and thus had more drug impregnated in the stent, also presents a higher killing efficacy, around 65% for all drugs after 72 h of exposure. Considering the effect of the coating of the BUS (**Drug_{COAT}**) these present a slightly lower efficacy when compared with the non-coated stents. On the other hand, the commercial stent (**Drug_{Com}**) shows a significantly lower killing efficacy (~10%) which may be due the lower amount of drug impregnated in the stent as observed in the impregnation results.

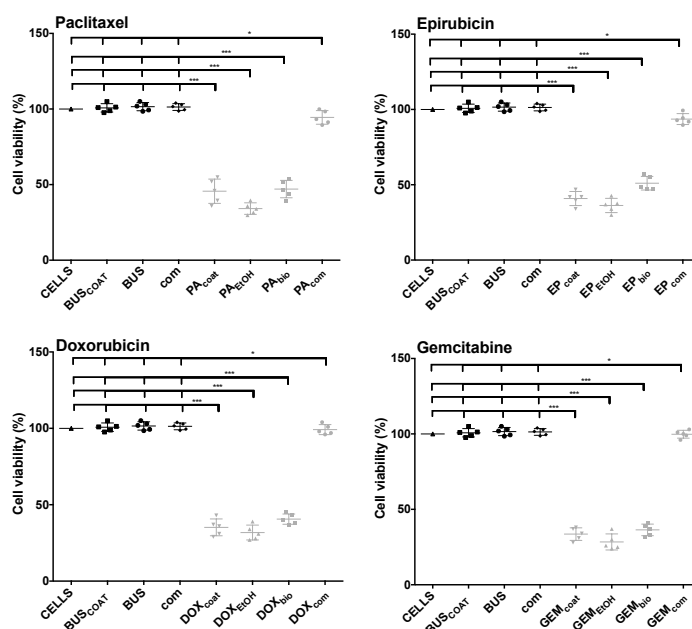


Figure VI-6 Cell viability of T24 cancer cell line after 72 h exposure by indirect contact. Statistical significant differences were considered as *p < 0.05, **p < 0.01 and ***p < 0.001.

The results obtained and the new concept of using ureteral stents with anti-cancer drugs for the treatment of carcinomas in the ureter justify the evaluation of the cancer cells viability in a closer way. The impregnated stents were placed in direct contact for 4 h and 72 h with the T24 cancer cells and as a control HUVEC were also used. **Figure VI-6** shows the cytotoxicity assay of T24 cancer cell line and HUVEC cells after 72 h exposure by direct contact. A similar result to what was observed by indirect contact for T24 cancer cells, comparing the different conditions tested with killing efficacy of the impregnated stents. Nonetheless, all the conditions present a higher killing efficacy increasing around 10% in comparison with the indirect contact results. **Drug_{EtOH}** conditions have once again shown have the highest anti-cancer effect, due to the higher amount of drug impregnated. The HUVEC cells, used as control cells, did not show compromised viability after incubation for 72 h in any of the conditions tested. Looking back to **figure VI-5** it was expected see a cytotoxic effect particularly in the conditions with gemcitabine in contact with HUVEC cells, due to the close concentration of drug impregnated in the stent with the IC_{50} value determined, but this was not observed and the cell viability remained nearly 100%. Thus, the amount of anti-cancer drug impregnated in biodegradable ureteral stents by $scCO_2$ had a killing efficacy of 75 % in T24 cancer cells, but this did not affect the non-cancer cells (HUVEC).

In the treatment of UTUC there is still no standard chemotherapy defined. The doses used for e.g in bladder cancer are in the order of 50 mg m² for paclitaxel, 30 mg m² for doxorubicin and epirubicin, and 75 mg m² for gemcitabine during the first 1- 3days. It is hence, difficult to establish a comparison between the concentrations determined here (table VI-2) and the values reported. Nonetheless, the *In vitro* results presented here indicate that the systems developed have a significant potential in the delivery of such drugs in the upper urinary track, with a demonstrated *In vitro* efficacy. To increase the killing efficacy of the BUS more than one drug could be impregnated into the polymer matrix (35), as different studies have demonstrated the higher cytotoxic and synergistic effect of combining more than one drugs administrated such as cisplatin with paclitaxel (5, 36).

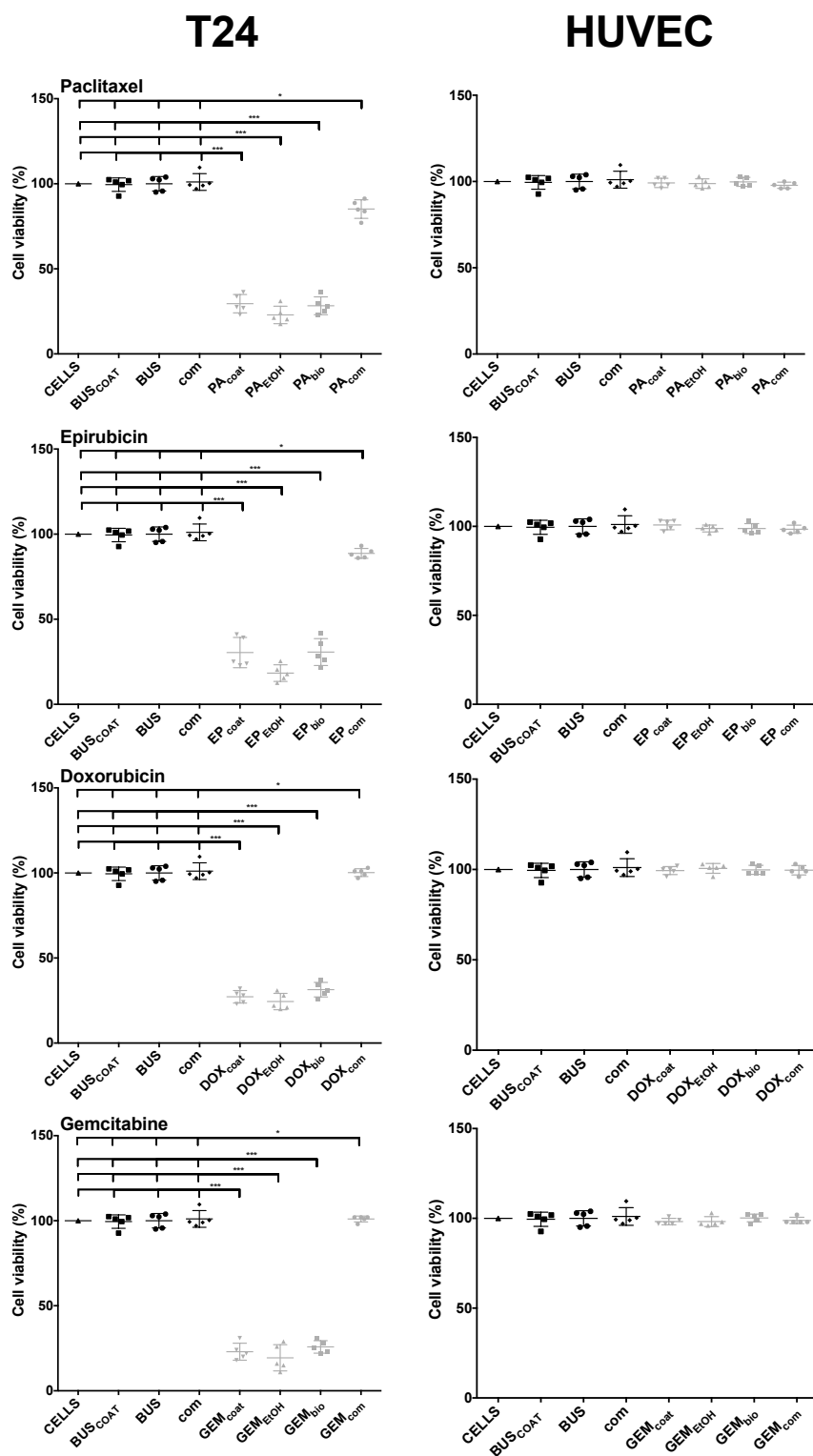


Figure VI-7 Cell viability of T24 cancer cell line and HUVEC cells after 72 h exposure by direct contact. BUScoat is the BUS with the PCL coating without anti-cancer drugs impregnated. Statistical significant differences were considered as *p < 0.05, **p < 0.01 and *p < 0.001.**

The effect of the biodegradable ureteral stents impregnated with the different anti-cancer drugs in the T24 cancer cells was investigated by light microscopy. Figure VI-8 shows the light microscopy images of T24 cancer cells in contact with the BioStent impregnated with the four different anti-cancer drugs tested. In controls, it is possible to see that the cells are normal confluent. After 4 h exposure time it is possible to see that majority of the T24 cells are confluent with some cells starting to be in a rounded shape. When the exposure time is increased to 72 h the cells shown only the rounded shape morphology, confirming the killing efficacy of the impregnated biodegradable ureteral stent against to T24 cancer cells.

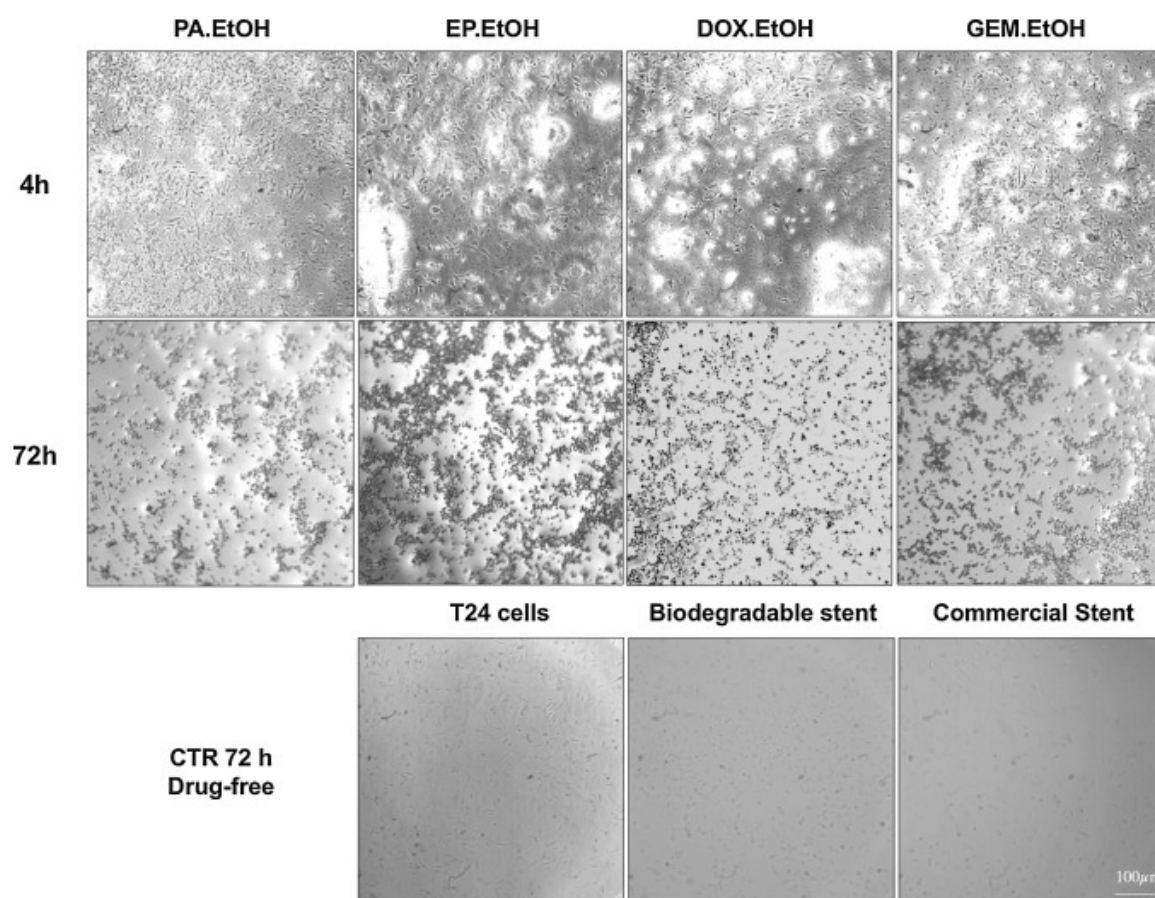


Figure VI-8 Light microscopy images (10x) of T24 cells morphology after 4 h and 72 h of exposure by direct contact to biodegradable ureteral stents impregnated with the anti-cancer drugs. Control experiments were carried out in T24 cells and drug-free stents for 72 h.

VI-4. CONCLUSION

Biodegradable ureteral stents and a commercial stent (non-degradable) were impregnated with four anti-cancer drugs (paclitaxel, epirubicin, doxorubicin and gemcitabine) by supercritical carbon dioxide (scCO₂). The anti-cancer drugs were successfully impregnated into the biodegradable ureteral stents and the release was sustainable in an artificial urine solution. In all cases, when BUS was used as support a release of 100 % of the impregnated drug was achieved after 72 h. In the case of the commercial stent the amount of drug impregnated was lower and the release was faster for all drugs, achieving 100% release within 24 h. The *In vitro* killing efficacy by direct contact with the anti-cancer biodegradable stents was similar for all the drugs tested. Our results indicate that the impregnated biodegradable ureteral stents developed may serve as carriers of anticancer drugs and potentially be an effective and sustained IDD system for upper tract urothelial carcinoma therapy.

ACKNOWLEDGEMENTS

This research was supported by the Urology Research Grant Jaba Recordati 2015 from Portuguese Urology Association, from ICVS/3B's – Associate Laboratory Research Grants and the European Union Seventh Framework Programme (FP7/2007-2013) under grant agreement number REGPOT-CT2012-316331-POLARIS. The project “Novel smart and biomimetic materials for innovative regenerative medicine approaches” RL1 - ABMR - NORTE-01-0124-FEDER-000016) co-financed by North Portugal Regional Operational Programme (ON.2 – O Novo Norte), under the National Strategic Reference Framework (NSRF), through the European Regional Development Fund (ERDF) is also acknowledged. Alexandre Barros acknowledges his FCT PhD grant SFRH/BD/97203/2013, the Healy lab for the work was performed at UC Berkeley and the FLAD Grant for internship in UC Berkeley 2015/CON5/CAN8.

REFERENCES

1. Babjuk M, Burger M, Zigeuner R, Shariat SF, van Rhijn BWG, Compérat E, et al. EAU Guidelines on Non-Muscle-invasive Urothelial Carcinoma of the Bladder: Update 2013. *Eur Urol*. 2013;64(4):639-53.
2. Audenet F, Yates DR, Cussenot O, Rouprêt M. The role of chemotherapy in the treatment of urothelial cell carcinoma of the upper urinary tract (UUT-UCC). *Urologic Oncology: Seminars and Original Investigations*. 2013;31(4):407-13.
3. Munoz JJ, Ellison LM. UPPER TRACT UROTHELIAL NEOPLASMS: INCIDENCE AND SURVIVAL DURING THE LAST 2 DECADES. *The Journal of Urology*. 2000;164(5):1523-5.
4. Hellenthal NJ, Shariat SF, Margulis V, Karakiewicz PI, Roscigno M, Bolenz C, et al. Adjuvant Chemotherapy for High Risk Upper Tract Urothelial Carcinoma: Results From the Upper Tract Urothelial Carcinoma Collaboration. *The Journal of Urology*. 2009;182(3):900-6.
5. Hadaschik BA, Ter Borg MG, Jackson J, Sowery RD, So AI, Burt HM, et al. Paclitaxel and cisplatin as intravesical agents against non-muscle-invasive bladder cancer. *BJU International*. 2008;101(11):1347-55.
6. Lu S, Neoh KG, Kang E-T, Mahendran R, Chiong E. Mucoadhesive polyacrylamide nanogel as a potential hydrophobic drug carrier for intravesical bladder cancer therapy. *European Journal of Pharmaceutical Sciences*. 2015;72(0):57-68.
7. Papadopoulos E, Yousef G, Scorilas A. Gemcitabine impacts differentially on bladder and kidney cancer cells: distinct modulations in the expression patterns of apoptosis-related microRNAs and BCL2 family genes. *Tumor Biol*. 2015;36(5):3197-207.
8. Audenet F, Traxer O, Bensalah K, Rouprêt M. Upper urinary tract instillations in the treatment of urothelial carcinomas: a review of technical constraints and outcomes. *World Journal of Urology*. 2013;31(1):45-52.
9. Lifshitz D, Meiron M, Konorty M, Schoenberg M. 25 Hydrogel based drug retention system for the treatment of upper tract urothelial carcinoma. *European Urology Supplements*. 2014;13(1):e25-ea.
10. Khan W, Farah S, Domb AJ. Drug eluting stents: Developments and current status. *Journal of Controlled Release*. 2012;161(2):703-12.
11. Shaikh M, Kichenadasse G, Choudhury NR, Butler R, Garg S. Non-vascular drug eluting stents as localized controlled drug delivery platform: Preclinical and clinical experience. *Journal of Controlled Release*. 2013;172(1):105-17.
12. Lange D, Bidnur S, Hoag N, Chew BH. Ureteral stent-associated complications[mdash]where we are and where we are going. *Nat Rev Urol*. 2015;12(1):17-25.
13. Mendez-Probst CE, Goneau LW, MacDonald KW, Nott L, Seney S, Elwood CN, et al. The use of triclosan eluting stents effectively reduces ureteral stent symptoms: a prospective randomized trial. *BJU International*. 2012;110(5):749-54.
14. Krambeck AE, Walsh RS, Denstedt JD, Preminger GM, Li J, Evans JC, et al. A Novel Drug Eluting Ureteral Stent: A Prospective, Randomized, Multicenter Clinical Trial to Evaluate the Safety and Effectiveness of a Ketorolac Loaded Ureteral Stent. *The Journal of Urology*. 2010;183(3):1037-43.
15. Barros AA, Duarte ARC, Pires RA, Sampaio-Marques B, Ludovico P, Lima E, et al. Bioresorbable ureteral stents from natural origin polymers. *J Biomed Mater Res B*. 2015;103(3):608-17.

16. Barros AA, Oliveira C, Reis RL, Lima E, Duarte ARC. Ketoprofen-eluting biodegradable ureteral stents by CO₂ impregnation: In vitro study. *International Journal of Pharmaceutics*. 2015;495(2):651-9.
17. Elvira C, Fanovich A, Fernández M, Fraile J, San Román J, Domingo C. Evaluation of drug delivery characteristics of microspheres of PMMA–PCL–cholesterol obtained by supercritical-CO₂ impregnation and by dissolution–evaporation techniques. *Journal of Controlled Release*. 2004;99(2):231-40.
18. Kikic I, Vecchione F. Supercritical impregnation of polymers. *Current Opinion in Solid State and Materials Science*. 2003;7(4–5):399-405.
19. Kikic I, Sist P. Applications of Supercritical Fluids to Pharmaceuticals: Controlled Drug Release Systems. In: Kiran E, Debenedetti PG, Peters CJ, editors. *Supercritical Fluids: Fundamentals and Applications*. Dordrecht: Springer Netherlands; 2000. p. 291-306.
20. Aroso IM, Craveiro R, Rocha Â, Dionísio M, Barreiros S, Reis RL, et al. Design of controlled release systems for THEDES–Therapeutic deep eutectic solvents, using supercritical fluid technology. *International Journal of Pharmaceutics*. 2015;492(1–2):73-9.
21. Berens AR, Huvarad GS, Korsmeyer RW, Kunig FW. Application of compressed carbon dioxide in the incorporation of additives into polymers. *Journal of Applied Polymer Science*. 1992;46(2):231-42.
22. Nunes AV, Rodriguez-Rojo S, Almeida AP, Matias AA, Rego D, Simplicio AL, et al. Supercritical fluids strategies to produce hybrid structures for drug delivery. *Journal of Controlled Release*. 2010;148(1):e11-e2.
23. York P, Kompella UB, Shekunov BY. *Supercritical Fluid Technology for Drug Product Development*: Taylor & Francis; 2004.
24. Champeau M, Thomassin J-M, Tassaing T, Jerome C. Drug Loading of Sutures by Supercritical CO₂ Impregnation: Effect of Polymer/Drug Interactions and Thermal Transitions. *Macromolecular Materials and Engineering*. 2015;300(6):596-610.
25. Kazarian SG. Polymer processing with supercritical fluids. *Polymer Science - Series C*. 2000;42(1):78-101.
26. Kazarian SG, Martirosyan GG. Spectroscopy of polymer/drug formulations processed with supercritical fluids: in situ ATR–IR and Raman study of impregnation of ibuprofen into PVP. *International Journal of Pharmaceutics*. 2002;232(1–2):81-90.
27. Yoda S, Sato K, Oyama HT. Impregnation of paclitaxel into poly(DL-lactic acid) using high pressure mixture of ethanol and carbon dioxide. *RSC Advances*. 2011;1(1):156-62.
28. Jiao Z, Chen Z, Wu Y, Ma S. Determination of Paclitaxel Solubility in Carbon Dioxide Using Quartz Crystal Microbalance. *Chinese Journal of Chemical Engineering*. 2011;19(2):227-31.
29. Suleiman D, Estévez LA, Pulido JC, García JE, Mojica C. Solubility of Anti-Inflammatory, Anti-Cancer, and Anti-HIV Drugs in Supercritical Carbon Dioxide. *Journal of Chemical & Engineering Data*. 2005;50(4):1234-41.
30. Vandana V, Teja AS. The solubility of paclitaxel in supercritical CO₂ and N₂O. *Fluid Phase Equilibria*. 1997;135(1):83-7.
31. Cooper AI. Polymer synthesis and processing using supercritical carbon dioxide. *Journal of Materials Chemistry*. 2000;10(2):207-34.
32. Sebaugh JL. Guidelines for accurate EC₅₀/IC₅₀ estimation. *Pharmaceutical Statistics*. 2011;10(2):128-34.
33. Browne S, Fontana G, Rodriguez BJ, Pandit A. A Protective Extracellular Matrix-Based Gene Delivery Reservoir Fabricated by Electrostatic Charge Manipulation. *Molecular Pharmaceutics*. 2012;9(11):3099-106.

34. Yu Q, Zhang J, Zhang G, Gan Z. Synthesis and Functions of Well-defined Polymer-drug Conjugates as Efficient Nanocarriers for Intravesical Chemotherapy of Bladder Cancer. *Macromolecular Bioscience*. 2015;15(4):509-20.
35. Browne S, Pandit A. Multi-modal delivery of therapeutics using biomaterial scaffolds. *Journal of Materials Chemistry B*. 2014;2(39):6692-707.
36. Pu Y-S, Chen JUN, Huang C-Y, Guan J-Y, Lu S-H, Hour T-C. CROSS-RESISTANCE AND COMBINED CYTOTOXIC EFFECTS OF PACLITAXEL AND CISPLATIN IN BLADDER CANCER CELLS. *The Journal of Urology*. 2001;165(6, Part 1):2082-5.

Chapter VII

***In vitro* and *ex-vivo*
permeability studies of
paclitaxel and doxorubicin
from drug-eluting
biodegradable ureteral stents**

Chapter VII

***In vitro* and *ex-vivo* permeability studies of paclitaxel and doxorubicin from drug-eluting biodegradable ureteral stents ‡‡**

ABSTRACT

A drug-eluting biodegradable ureteral stent (BUS) has been developed as a new approach for the treatment of urothelial tumors of upper urinary tract cancer. In a previous work, this system has proven to be a good carrier for anticancer drugs as a potential effective and sustainable intravesical drug delivery (IDD) system. BUS has revealed to reduce in 75% the viability of human urothelial cancer cells (T24) after 72 h of contact and demonstrated minimal cytotoxic effect on human umbilical vein endothelial cells (HUVECs) which were used as a control. In this work, we studied the permeability of the anticancer drugs, such paclitaxel and doxorubicin, alone or released from the BUS developed. We used three different membranes to study the permeability: polyethersulphone membrane (PES), HUVECs cell monolayer and an *ex vivo* porcine ureter. The ureter thickness was measured (864.51 μm) and histological analysis was performed to confirmed the integrity of urothelium. Permeability profiles, were measured during 8 hours, for paclitaxel and doxorubicin. The drugs *per se* have shown to have a different profile and as expected, increasing the complexity of the membrane to be permeated, the permeability decreased, being the PES more permeable and the *ex vivo* ureter tissue less permeable. The molecular weight has also shown to influence the permeability of each drug and a higher percentage for doxorubicin (26%) and lower for paclitaxel (18%) was observed across the *ex vivo* ureter. The permeability (P), diffusion (D) and partition (Kd) coefficients of paclitaxel and doxorubicin through the permeable membranes were calculated. Finally, we showed that paclitaxel and doxorubicin drugs released from the BUS were

‡‡ This chapter is based on the following publication:

Barros AA, Oliveira C, Reis RL, Lima E, Duarte ARC. - *In vitro* and *ex-vivo* permeability studies of paclitaxel and doxorubicin from drug-eluting biodegradable ureteral stents. Accepted in Journal of Pharmaceutical Sciences, 2017.

able to remain in the ex vivo ureter and only a small amount of the drugs can cross the different permeable membranes with a permeability of 3% for paclitaxel and 11% for doxorubicin. The estimated amount of paclitaxel remains in the ex vivo ureter tissue shown to be effective to affect the cancer cell and did not affect the non-cancer cells.

VII-1. INTRODUCTION

The incidence of upper urinary tract cancer (UTUC), although rare, has increased in the last 30 years and is now about 2 cases per 100,000 person/year (1). UTUC is commonly a consequence of previous bladder cancer that is the fourth most common tumor type. The diagnosis of UTUC is usually done at an advanced stage of the disease due to limited symptomology, originating poor prognosis with an overall 5-year survival rate of less than 50% (2). Normally the UTUC is significantly more invasive and violent compared with bladder cancer (2, 3). Patients with UTUC are generally given immunotherapy, such as Bacillus Calmette-Guerin (BCG) or chemotherapy, such as mitomycin C, paclitaxel or doxorubicin (4, 5). In last decade, these anti-cancer drugs have been suggested as drugs that could be incorporated in polymeric matrix in order to prepare an intravesical drug delivery (IDD) system (6-8). IDD has been the usual form of transurothelial drug delivery (9, 10). IDD overcomes the limitations of systemic therapy, demonstrated to be ineffective due the poor bioavailability and presenting severe adverse effects (11). However, in upper urinary tract, the effectiveness of IDD is limited by the poor bioavailability and the low contact time between drug and cancer cells due the peristaltic movements of the ureter and the urine flow. Upper and lower urinary tract are composed by a highly impermeable epithelial layer, called urothelium. This tissue is the primary barrier that prevents the urine compounds from going to the blood stream but limits the amount of drugs can permeate the ureter and bladder wall (12, 13). Moreover, the urine flows from the kidney to the bladder at a constant rate ($\sim 1 \text{ mL min}^{-1}$) which will dilute the concentration of instilled anti-cancer drugs (12). Due to these reasons it is expected that future developments will seek to improve the control and sustainability of chemotherapeutic approaches by using medical devices, such as ureteral stents impregnated with anti-cancer drugs (11). With the objective to increase the contact time between these anti-cancer drugs and the UTUC, our group developed a new concept for the delivery of these drugs namely using a drug-eluting biodegradable ureteral stent (**BUS**) (14). The idea is to have a local delivery with a more sustainable drug release using the hydrogel-based biodegradable ureteral stent and after the treatment the stent degrades without the need for a second intervention to remove it (14-17). In the previous work (14), we impregnated four different anti-cancer drugs three hydrophobic paclitaxel, doxorubicin and epirubicin and one hydrophilic, gemcitabine. The study demonstrated the successful impregnation of these anti-cancer drugs in the BUS by supercritical

carbon dioxide (**scCO₂**). The total release of the drugs was achieved after 72 hours and when in contact *In vitro* with urothelial cancer cell line (T24), the drugs delivered from BUS were able to kill 75% of the cancer cells (14). BUS was designed, so that, when placed *In vivo*, it swells in order to promote a closer contact with ureter wall, specifically with the cancer cells, and enhancing the bioavailability.

The aim of the current study is to understand the relation between the drugs delivered from BUS and the ureter permeability. Before the recent studies from Williams et al. (11, 13), the accepted dogma was that urothelial permeability was consistent throughout the urinary tract, but the results demonstrated an evidence of nonuniformity in urothelium barrier function between the upper urinary tract and bladder in a porcine model. Porcine is an established and well characterized model of the human urinary tract with a tissue structure, tissue composition and physiology similar to those of humans (18, 19). In this study, we used an *ex vivo* porcine model to assess the permeability of the anti-cancer drugs delivered from BUS across porcine ureter. To this end, we used the BUS impregnated with paclitaxel (**PAStent**) and doxorubicin (**DOXStent**). The permeability of the drugs alone was also study with the objective to understand the permeability properties of each particular system.

VII-2. MATERIAL AND METHODS

VII-2.1. Materials

Alginic acid sodium salt, gelatin, calcium chloride, chloroform, ethanol, bismuth (III) carbonate basic, formaldehyde solution (4%) and oxygenated Krebs buffer were purchased from Sigma-Aldrich (Germany). Potassium dihydrogen ortho-phosphate (99.5%) and magnesium chloride hexahydrate (99%) were obtained from Riedel-de Haën (Germany). Polycaprolactone resin PCL 787, commercially available as TONE™ polymer was obtained from Union Carbide Chemicals and Plastics Division, Bound Brook, New Jersey. Artificial urine solution (AUS), paclitaxel 99.5% (PA) and doxorubicin 98% (DOX) were obtained from Fisher Scientific (U.S.A.). EndoGRO-VEGF medium was supplied by Milipore (Germany). Carbon dioxide (99.998 mol %) was supplied by Air Liquide (Portugal). All reagents were used as received without any further purification.

VII-2.2. Preparation of biodegradable ureteral stents

Biodegradable ureteral stents (BUS) were developed according to the procedure described by Barros et al.(15). The ureteral stents were composed of 30% alginate sodium salt, 65% of gelatin and 5% of bismuth (III) carbonate. The cross-linking solution was calcium chloride (CaCl_2) at 0.48 M. Briefly, the polymers were dissolved in hot distilled water (70 °C). The solution was stirred for 1 h and the polymeric solution was injected in a mold to obtain a tubular structure. After 1 hour the piece was taken out of the mold, and placed in an alcohol solution (100% ethanol) for 1 h. BUS were then transferred into a crosslinking solution of calcium chloride (CaCl_2), at room temperature. After crosslinking, the BUS were relocated in an alcoholic solution (100% ethanol) to obtain an alcohol gel. The BUS were dried using a high-pressure vessel with supercritical carbon dioxide (scCO_2) at 40 °C and 100 bar for 90 min, in continuous mode.

VII-2.3. Supercritical CO_2 impregnation of Paclitaxel and Doxorubicin

The prepared **BUS** were placed in a high-pressure vessel with anticancer drugs according to **Figure VII-1**. Paclitaxel and doxorubicin were impregnated in the stents in the presence of 10% of ethanol, which was used as co-solvent. The operational scCO_2 impregnation conditions were 100 bar and 40 °C. Carbon dioxide was liquefied and pumped to the desired pressure using a membrane pump (MCPV-71, Haskel, Germany). Impregnation took place in batch mode for 90 min followed by fast depressurization of the system.

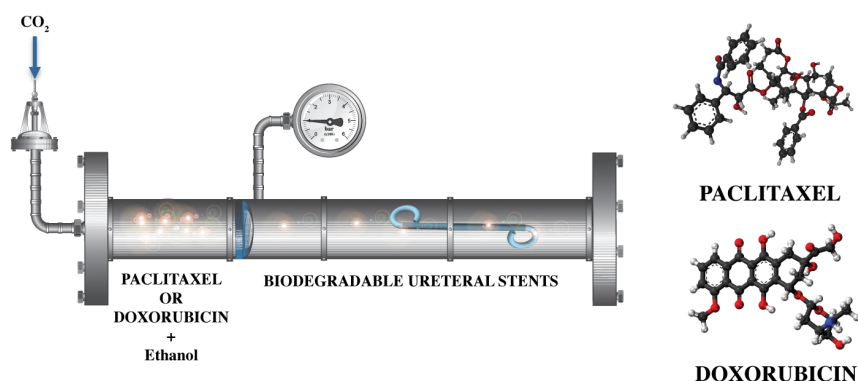


Figure VII-1 Paclitaxel and doxorubicin impregnation apparatus by supercritical fluid process in biodegradable ureteral stent, 100 bar, 90 min at 40°C.

The impregnated stents were coated by immersion in a 10 wt% solution of polycaprolactone (PCL) resin 787 (Mw 80,000 g mol⁻¹) dissolved in chloroform.

VII-2.4. Franz-cell diffusion test

VII-2.4.1. Experimental permeability setups.

The permeability tests were conducted using a glass Franz-type diffusion cell (PermeGear) with 8 mL receptor compartment, and an effective mass transfer area of 1 cm² (**table VII-1**). Two different membranes were used using this diffusion cell, a polyethersulphone (PES) membrane (Santorius), with 150 μm thickness and 0.45 μm, pore size (**figure VII-3A**) and an *ex vivo* porcine ureter tissue (**figure VII-3C**). The membranes were placed between the two compartments and held with a stainless steel clamp. The *ex vivo* porcine ureter tissue was open and cut into 1.5 cm² sections and placed in the glass Franz-type diffusion cells with the urothelium facing the donor compartment upward. Care was taken to prevent contact the urothelial layer with hands to avoid any damage. The receptor compartment was immediately filled with artificial urine solution (AUS), and air bubbles were removed. Finally, the donor compartment was filled with a solution of 20 μg·mL⁻¹ of drug alone (paclitaxel or doxorubicin) or with 100 mg of stent impregnated with drugs. Aliquots of 200 μL were withdrawn from the receptor compartment at fixed time points (0 min, 5 min, 15 min, 30 min, 1 h, 3 h, 5 h, 8 h) and replenished by fresh AUS (pH 5.5). The experiments were performed at 37 °C, and the receptor compartment was stirred at 400–600 rpm using a magnetic bar to eliminate the boundary layer effect. The amount of paclitaxel and doxorubicin in the receptor compartment was measured by UV, at their maximum absorbance at a wavelength of 227 nm and 254 nm respectively, using a microplate reader (Synergy HT, Bio-TEK, USA). The ureter tissue (about 5 cm) from a porcine with 70 Kg was obtained fresh from a surgical room within 5 minutes of sacrifice and immediately immersed in cold oxygenated Krebs buffer and covered specimen temporarily in a cool area.

VII-2.4.2. Histology and morphology of the ureter tissue layer

Tissue samples were fixed using dilute formaldehyde solution 4%, buffered at pH 6.9, sectioned and stained with Masson Trichrome and Hematoxylin and Eosin (H&E) before examination by stereo microscopy. Tissue layer depth was measured directly from the photomicrographs obtained from the inverted microscope (Axiovert 40, ZEISS), using AxioVision 4 (version 4.8.2) software (**figure VII-2C**). Measurements were calculated as the distance between the top and the base of the layer and were performed across the whole micrograph and the mean thickness of the tissue layers was calculated (**table VII-1**).

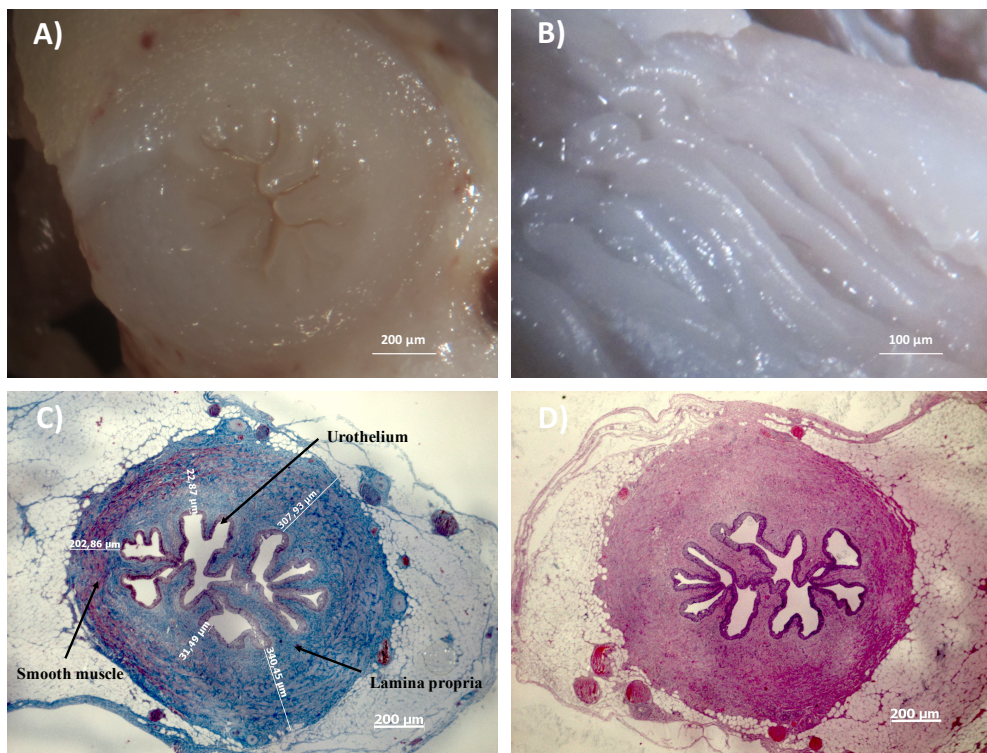


Figure VII-2 Representative Representative photomicrographs show ureter sections from single *ex vivo* porcine urinary tract obtained by stereo microscope (A and B). Masson trichrome staining (C) of ureter section with measures and Hematoxylin and Eosin (H&E) staining (D) of ureter section. Scale bar indicates 200 µm (A, C and D) and 100 µm (B).

Table VII-1 Tissue layer measurements of ex vivo porcine ureter.

	Mean Tissue Layer Thickness*
Urothelium	30.32 μm (\pm 1.24)
Lamina propria	269.87 μm (\pm 2.76)
Smooth muscle	353.28 μm (\pm 2.41)
Whole Wall	864.51 μm (\pm 2.69)

* Total of 20 measurements per layer from ureter porcine

VII-2.5. Transwell® diffusion test

VII-2.5.1. Cell culture

In this study, human umbilical vein endothelial cells, HUVEC, (Invitrogen, Canada), mimicking the ureter tissue were used. HUVEC cells were cultured in EndoGRO-VEGF complete culture media (Millipore S.A.S. France) supplemented with 10% fetal bovine serum (FBS), 1 mM L-glutamine and 1% penicillin. The culture was maintained at 37 °C in a humidified 5% CO₂ atmosphere.

VII-2.5.2. Experimental setups

Transwell® diffusion test was used to study the permeability of paclitaxel, doxorubicin and the stents impregnated with these drugs through a HUVEC cell monolayer. A collagen matrix (0.7%) was applied previously to the Transwells®. The HUVEC were seeded into 3 μm pore Transwell® inserts (polyester membrane, FALCON, USA) in a 6 well plate at 50,000 cells/cm². The HUVEC's were grown for 8 days on the Transwells® filters incubated at 37 °C in a 5% CO₂ with 1.5 ml of EndoGRO-VEGF medium in the insert (donor compartment) and 2.5 ml of EndoGRO-VEGF medium in the receiver compartment (**figure VII-3B**). The confluency of the cell monolayer cells was confirmed using an inverted microscope for cell culture (AxioVert A1 FL LED, Zeiss, USA) and images were taken at the end of the experience to ensure that the monolayer remain intact. To start the experiment, the donor solution was suctioned off and replace with a 1.5 ml of fresh

EndoGRO-VEGF medium containing 20 $\mu\text{g}\cdot\text{mL}^{-1}$ of paclitaxel or doxorubicin or 100 mg of PASTent or DOXStent (medium, pH 7.8). At fixed time points (0 min, 5 min, 15 min, 30 min, 1 h, 3 h, 5 h, 8 h), 100 μl aliquots were removed from the receptor compartment and replaced with fresh medium. Between each time point the samples were maintained at 37 °C in a 5% CO₂ atmosphere. The amount of paclitaxel and doxorubicin in the receptor compartment was measured by UV, at the maximum absorbance, i.e. a wavelength of 227 nm and 254 nm, respectively using a microplate reader (Synergy HT, Bio-TEK, USA).

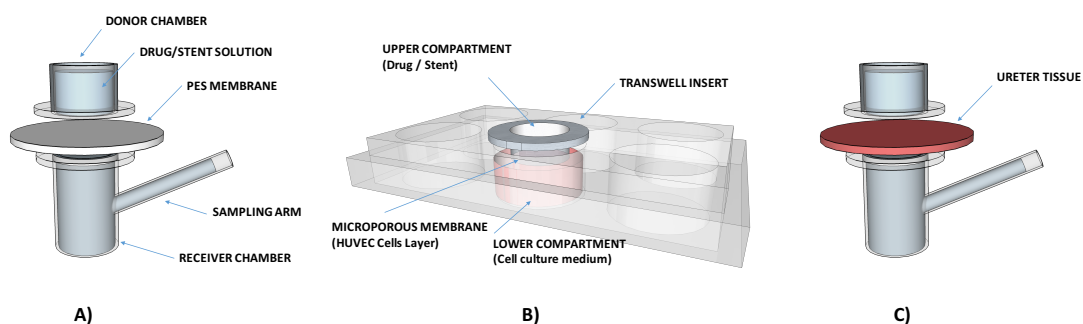


Figure VII-3 Schematic of A) Franz-type diffusion cell load with PES, B) Transwell® diffusion test with a HUVEC cells monolayer C) Franz-type diffusion cell load with porcine ureter tissue.

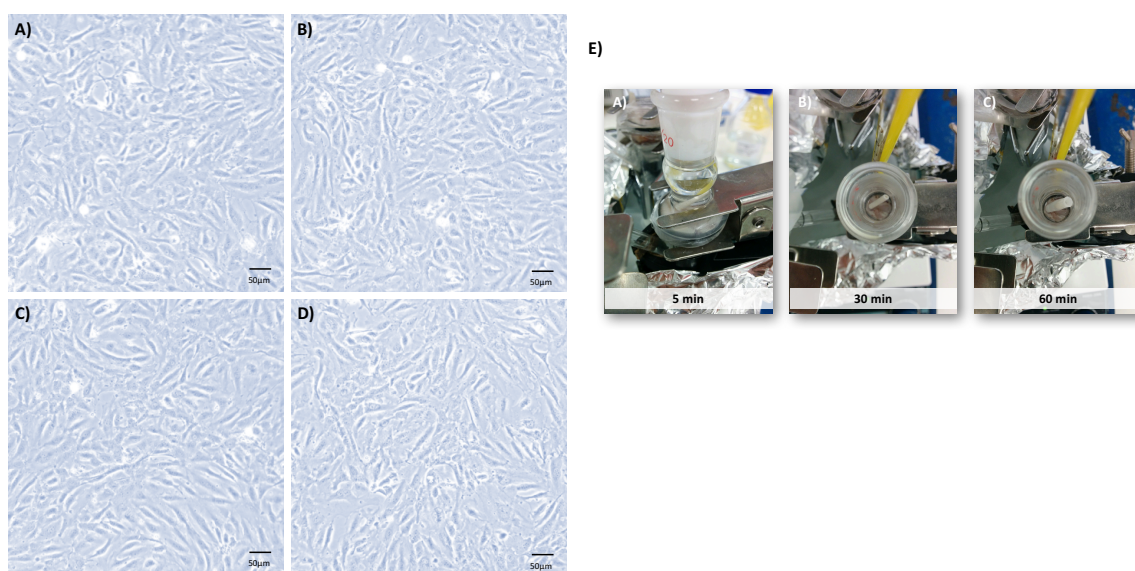


Figure VII-4 Inverted microscope images of confluent monolayer HUVEC cells on Transwell® before (A, B) and after diffusion test with paclitaxel (C) and doxorubicin (D). E) donor compartment

of Franz-cell setup with the delivery of paclitaxel from BUS and permeation through the ureter tissue after 5 min, 30 min and 60 min.

VII-2.5.3. Calculations and mathematical model

The permeability (P) of paclitaxel and doxorubicin through the membranes studied (on Franz-cells and Transwell®) was calculated by the following equation (**Equation II 4**) (20):

$$-\ln\left(1 - \frac{2C_t}{C_0}\right) = \frac{2A}{V} \times P \times t$$

Equation II-4 Determination of permeability

Where C_t is the concentration in the receptor compartment at time t , C_0 is the initial concentration in the donor compartment, V is the solution volume in the two compartments, and A is the effective area of permeation. The permeability coefficient can be calculated from the slope of the curve $-(V/2A) \cdot \ln(1 - 2C_t/C_0)$ versus t .

The diffusion coefficient (D) of paclitaxel and doxorubicin across the PES, HUVEC cell layer and ureter (*ex-vivo*) was calculated according to Fick's law of diffusion, as follows (**Equation II 5**)(21):

$$D = \frac{V_1 V_2}{V_1 + V_2} \times \frac{h}{A} \times \frac{1}{t} \times \ln\left(\frac{C_f - C_i}{C_f - C_t}\right)$$

Equation II-5 Determination of the diffusion coefficient

where D is the diffusion coefficient ($\text{cm}^2 \cdot \text{s}^{-1}$); C_i and C_f are the initial and final concentrations, and C_t is the concentration at time t of solute in the receptor side, respectively (g L^{-1}). V_1 and V_2 correspond to the volume of the liquid in the donor compartment and that in the receptor compartment (cm^3), respectively; h is the thickness of the membrane (cm) and A is the effective diffusion area of the membrane (cm^2).

The partition coefficient (K) is defined as a measure of the affinity of the solute in the membrane. The partition coefficient for the system was calculated as follows (**Equation II 6**) (22):

$$K_d = \frac{P \times h}{D}$$

Equation II-6 Determination of partition coefficient

where P is the permeability, h is the thickness of the membrane, and D is the diffusion coefficient.

Table VII-2 Characteristics of experimental setups used in the present study to assess the permeability of paclitaxel through the PES, HUVEC cell layer and porcine ureter (ex-vivo).

	Donor volume (cm³)	Receptor volume (cm³)	Membrane surface (cm²)
Franz's Cells	2.00	8.00	1.00
Transwell®	1.50	2.60	4.67

VII-2.5.4. Statistical analysis

All data values are presented as mean ± standard deviation (SD). Statistical analysis was performed using Graph Pad Prism® 6.00 software (San Diego, USA). For all comparisons 1-way ANOVA with the Tukey post hoc test for multiple comparisons was used.

VII-3. RESULTS AND DISCUSSION

In our previous work, we developed a drug-eluting biodegradable ureteral stent (**BUS**) impregnated with different anticancer drugs as a new concept for the delivery of anti-cancer drugs to urothelial tumors of the upper urinary tract (14). The idea was to use a biodegradable ureteral stent to increase the contact-time between the anti-cancer drugs and the cancer cells in the ureter and hence the bioavailability of the drugs. The direct contact study of the anti-cancer biodegradable ureteral stents with the T24 cancer cell line and HUVEC (cell line used as a control) showed a reduction around 75% of the viability of the T24 cell line after 72 h and demonstrated minimal cytotoxic effect on HUVECs (14). The aim of this study was to investigate the transurothelial delivery of paclitaxel and doxorubicin from the drug-eluting biodegradable ureteral stent using a

comparative study *In vitro* and *ex vivo* with porcine model in order to understand the efficacy of this drug-eluting stents against urothelial tumors of upper urinary tract cancer (**figure VII-3**).

VII-3.1. Permeability study of paclitaxel and doxorubicin

The permeability of paclitaxel and doxorubicin delivered from BUS was quantified, using a comparative study, with three different barriers, *In vitro* through a PES membrane, or a HUVEC cell monolayer, and using a porcine ureter *ex vivo*.

Figure VII-5 shows the representative permeability profile of paclitaxel and doxorubicin through the PES, HUVEC monolayer and *ex vivo* ureter. All the membranes demonstrated to be permeable to paclitaxel and doxorubicin. Permeability profiles have shown to be different regarding the membrane used and as expected, increasing the complexity of the membrane the permeability decreased, with PES, less complex, and *ex vivo* ureter tissue more complex. Permeability profile of the drugs through HUVEC and ureter setup show for both drugs tested, an initial lag phase in the receptor cell due to the time required for the drugs cross the HUVEC cells and the ureter tissue (23). After 8 hours, the two drugs tested show a permeation, across the PES of 65% (± 5.5) for paclitaxel and of 70 % (± 13.7) for doxorubicin, for equal period. In the ureter setup, the permeation of these drugs was near 3 times less, being 18% (± 3.2) for paclitaxel and 26% (± 9.6) for doxorubicin. The difference between the drugs permeability can be justified with the molecular weight of both, where paclitaxel weight, 853,91 g/mol, doxorubicin is smaller weighting, 543,52 g/mol. The diffusion of paclitaxel and doxorubicin in the *ex vivo* porcine ureter has shown to be lower due the complexity and higher thickness of the tissue compared with the other two membranes. Sections of ureter tissue were histologically stained with Masson trichrome and Hematoxylin and Eosin (H&E) (**figure VII-2**). The mean thickness of the tissue layers was calculated (**table VII-2**) and a value of 864.51 μm (± 2.69) was obtained. The results show a good transurothelial permeation across the porcine ureter composed by different tissues like urothelium, lamina propria and the smooth muscle, visible in **figure VII-2**, for both drugs paclitaxel and doxorubicin. Williams *et al.*(13) reported the permeability of another anti-cancer drug, namely mitomycin C (MW 334.33 g/mol) in an *ex vivo* porcine ureter obtained a 9.07 $\mu\text{g cm}^{-2}$ after 60 min instillation of 1mg ml⁻¹. Our results have shown, after the same time, lower permeability for paclitaxel (0.018 $\mu\text{g cm}^{-2}$) and higher permeability in the case of doxorubicin

($21.45 \mu\text{g cm}^{-2}$). Different studies demonstrated by concentration-depth studies a permeability dependent on the specific urothelial tissue, with a linear decrease in drug concentration over the urothelium, followed by an exponential decrease in concentration over the lamina propria and muscle (11, 13, 24, 25).

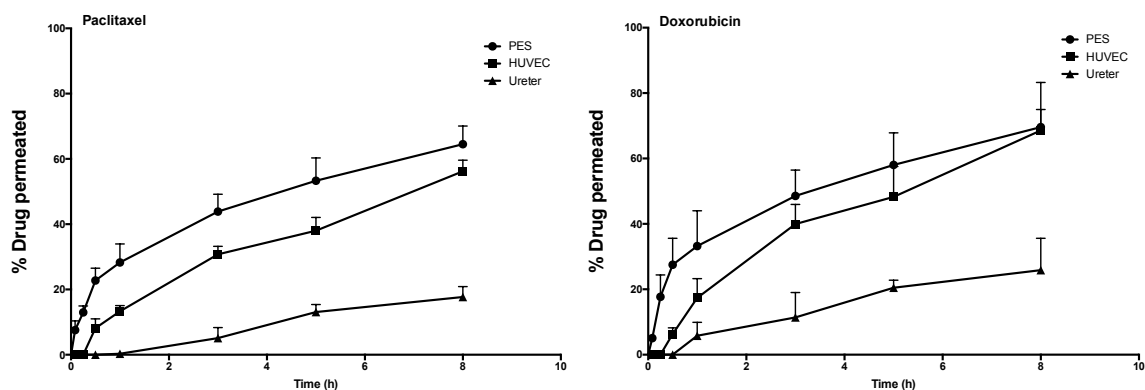


Figure VII-5 Permeation of paclitaxel and doxorubicin through PES and ex vivo porcine ureter using a Franz-cell setup and through a confluent monolayer HUVEC cells on Transwell®.

The permeability coefficient was determined (**Eq.VII-1**) in the linear permeation region (26). The permeability coefficient (P) of paclitaxel and doxorubicin decreased when the complexity of the setup increase (**table VII-3**) as expected and higher permeability coefficient was obtained for doxorubicin compared with paclitaxel. The diffusion coefficients (D) were inferred from **Eq. VII-2** and the partition coefficients (K_p) from **Eq. VII-3 (table VII-3)**. The diffusion coefficient is a fundamental factor to estimate the mass of solute diffusing in time through our different membranes (27). In our study, the diffusion coefficient demonstrated to be barrier-size and molecular weight dependent, with a higher value obtained for doxorubicin ($9.37 \times 10^{-8} \text{ cm}^2/\text{s}$) in PES membrane. The affinity of the membranes to the solutes was assessed from the calculation of partition coefficients (28, 29). *Ex vivo* ureter shows a lower K_p value meaning that, the tissue may have the ability to trap the drugs and consequently there is a decrease in the amount of drug in the receptor compartment.

Table VII-3 Permeability (P), Diffusion (D) and Partition (Kd) coefficients of paclitaxel and doxorubicin on PES, HUVEC cell layer and porcine ureter (ex vivo).

	Paclitaxel			Doxorubicin		
	D (10 ⁻⁸ cm ² /s)	K _d	P (10 ⁻⁶ cm/s)	D (10 ⁻⁸ cm ² /s)	K _d	P (10 ⁻⁶ cm/s)
PES	6.59	1.50	4.87	9.37	1.40	5.26
HUVEC Cells	3.53	1.41	1.42	6.03	1.12	2.13
Ex vivo Ureter	3.26	1.21	0.88	4.92	1.10	1.43

According to the biopharmaceutics classification system (BCS) the drugs can be categorized in four main groups based on their solubility and permeability (30). Paclitaxel and doxorubicin are BCS classified class IV drugs (31). These drugs are classified as a low solubility, low permeability resulting in poor bioavailability. They are usually not rapidly absorbed by the tissues and a high variability is expected. According to the values described in the literature a highly permeable drug is one that has a permeability higher than 6×10^{-6} cm/s (32). The permeability results obtained for paclitaxel and doxorubicin corroborate the class IV type of these drugs reported in the literature, with the values lower than 6×10^{-6} cm/s. These demonstrated the need for the development of highly efficient drug delivery systems.

VII-3.2. Permeability study of drugs delivery from biodegradable ureteral stent

The biodegradable ureteral stents (BUS) impregnated by scCO₂ with paclitaxel (PASTent) and doxorubicin (DOXStent) were prepared as previously described and illustrated in **figure VII-1** (14, 15, 17). The PASTent and DOXStent were placed in the donor compartment of the setups and the permeability of the drugs delivered from the BUS was assessed. **Figure VII-6** shows the permeability profiles for both drugs comparing the drug alone and the drugs delivered from BUS for each membrane tested. A lower permeability was observed in the three membranes for the drugs delivered from BUS compared with the permeability profile of drugs alone. These results can be justified with the release profile of the drugs from the BUS to the medium in donor compartment. Only after being released, the drug molecules start to cross the permeable membranes to the receptor compartment. Hence, it is possible to observe a higher lag phase in the permeability profile of the drugs delivered from BUS.

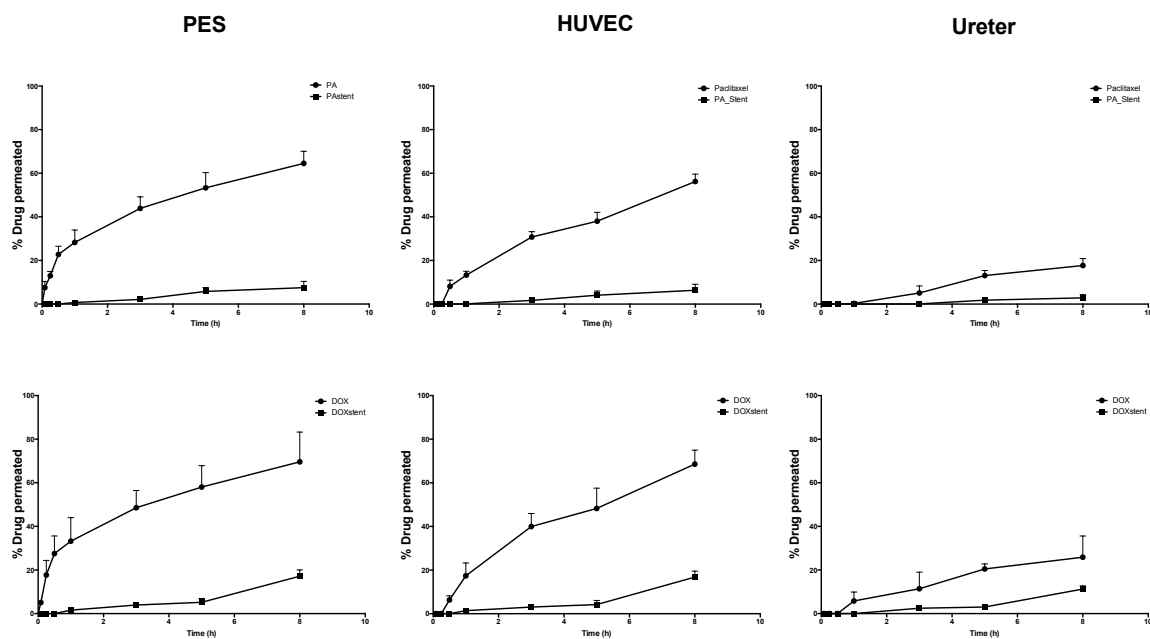


Figure VII-6 Permeability profile of Paclitaxel (PA) and Doxorubicin (DOX), and Stent impregnated with paclitaxel (PAStent) and doxorubicin (DOXStent) through PES, HUVEC cell layer and porcine ureter (*ex-vivo*).

Figure VII-6 presents the results for permeability profile of the paclitaxel (**PAStent**) and doxorubicin (**DOXStent**) delivered from the BUS in the three membranes studied in comparison with the release profile of each drug from the BUS calculated from the previous work (14). The *In vitro* release showed a faster release in the first 72 h for the anti-cancer drugs and after this time a plateau was achieved and finally the stent degraded after 9 days (14). Observing for the percentage delivered from the BUS and the drug that crossed the *ex vivo* ureter, after 8 hours, only 3% of paclitaxel and 11% of doxorubicin are detected on the for the receptor compartment.

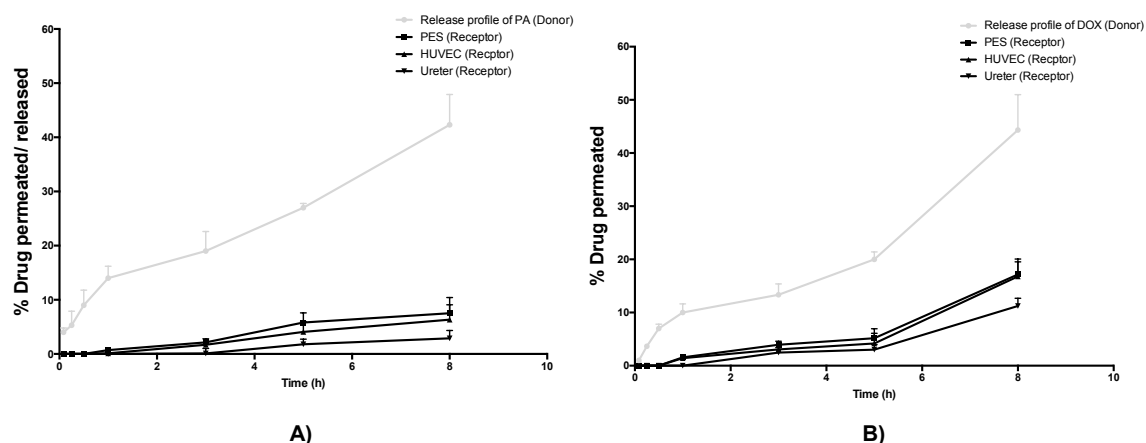


Figure VII-7 Release profile in the donor compartment and permeability profile obtained with the A) paclitaxel and B) doxorubicin delivered from BUS.

Table VII-4 presents the cumulative mass (μg) after 8 hours in the receptor compartment, in the case of PES, HUVEC monolayer cells and *ex vivo* ureter membranes, for each drug alone and the drugs delivered from BUS. From the initial 40 μg of paclitaxel (**PA**) and doxorubicin (**DOX**) dissolved directly in the donor compartment only 7.1 μg (± 1.3) and 10.3 μg (± 3.9) passed through the *ex vivo* ureter, for paclitaxel and doxorubicin respectively. In the case of drugs delivered from the BUS, the initial amount of drug is much lower. In the donor compartment 0.2 μg (± 0.1) of paclitaxel (**PAStent**) and 41.6 μg (± 6.3) of doxorubicin (**DOXStent**) have permeated through the *ex vivo* ureter. The difference between the amount of paclitaxel and doxorubicin delivered from the stent, and detected in the receptor compartment, can be justified by the different amount of paclitaxel and doxorubicin impregnated by scCO_2 in the first place. The amount of drug impregnated in each stent was calculated to be 0.067 $\mu\text{g}_{\text{drug}} \cdot \text{mg}_{\text{polymer}}^{-1}$ in case of stents impregnated with paclitaxel (**PAStent**) and 3.7 $\mu\text{g}_{\text{drug}} \cdot \text{mg}_{\text{polymer}}^{-1}$ in case of stents impregnated with doxorubicin (**DOXStent**).

Table VII-4 Drug permeated and Cumulative paclitaxel and doxorubicin mass after 8h permeation test in the receptor compartment through different membranes studied for drug alone (PA and DOX) and paclitaxel or doxorubicin release from the BUS (PAStent and DOXStent).

		Drug permeated (%)	Cumulative mass (μg)
PES membrane	PA	64.5	25.8 (± 2.2)
	PAStent	7.5	0.5 (± 0.1)
	DOX	69.6	27.8 (± 6.2)
	DOXstent	17.2	63.5 (± 4.2)
HUVEC Cells	PA	56.2	22.5 (± 1.7)
	PAStent	6.3	0.4 (± 0.1)
	DOX	68.6	27.4 (± 2.5)

	DOXstent	16.8	62.1 (±2.5)
	PA	17.7	7.1 (±1.3)
Ureter (<i>ex-vivo</i>)	PAstent	2.9	0.2 (±0.1)
	DOX	25.9	10.3 (±3.9)
	DOXstent	11.3	41.6 (±6.3)

Williams *et al* (11, 13) reported the capacity of the ureter retain the drug inside the tissue. It is essential that the drugs can remain in the ureter to increase the bioavailability and act against the tumors cells and not disperse to the blood system. **Figure VII-8** shows the estimated percentage of paclitaxel and doxorubicin after 8 hours in the *ex vivo* ureter porcine tissue. This estimation takes into account the total drug impregnated in the BUS and the amount recovered in the donor and receptor compartment. The estimated percentage of drugs in the *ex vivo* ureter was between 2.9 % (**PAstent**) and 11.3% (**DOXStent**). As previous mentioned the total released of the drugs from the stents occurs within 72h, therefore after 8h there is still a significant amount that was not released to the medium. The amount of paclitaxel (40%) and doxorubicin (38%) which was not yet released from the BUS after 8 h are in accordance with the release profile observed in **figure VII-7**. The results demonstrated that a small percentage of paclitaxel and doxorubicin are able to across the entire *ex vivo* ureter, but a higher percentage is found within the thickness of the *ex vivo* tissue. Taking into account the IC₅₀ values obtained in the previous work (14), the amount of paclitaxel estimated to be in the *ex vivo* ureter tissue after 8 hours, 0.6 µg (10%), is higher than the IC₅₀ value obtained for the human urothelial carcinoma cell T24 (0.28 µg) and lower than the IC₅₀ values obtained for HUVEC cells (0.8 µg). This suggests that the amount of drug remain in the *ex vivo* ureter can affect the cancer cells and not affect the non-cancer cells. On the other hand, the amount of doxorubicin estimated to be present in the *ex vivo* ureter (44 µg) did not reach the drug concentration required to affect the cancer cells (187 µg), according to the IC₅₀ values determined. According to our previous work, the amount of paclitaxel impregnated in the stents was less when compared with the stent impregnated with doxorubicin under the same conditions but the cancer cells T24 have shown to be more sensitive to paclitaxel than doxorubicin (14). Therefore, the results suggested the **PAstent** may be more effective an *In vivo* scenario compared with the **DOXStent**. The amount of paclitaxel and doxorubicin that was estimated to be able to cross the *ex vivo* ureter is lower than the drug trapped in the tissue. This value according the IC₅₀ values determined is such that it does not affect the non-cancer cells, providing an indication that the system could be suitable to treat such pathologies.

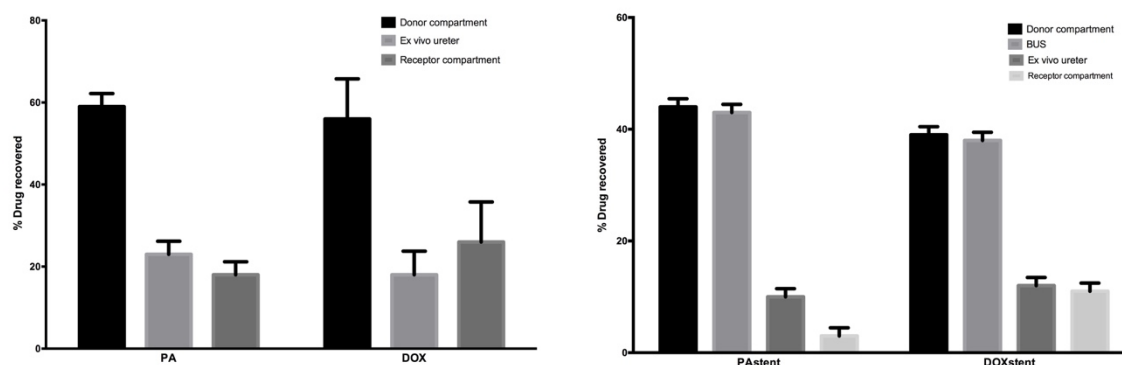


Figure VII-8 Percentage of Paclitaxel (PA) and Doxorubicin (DOX), and Stent impregnated with paclitaxel (PAStent) and doxorubicin (DOXStent) recovered after 8 h of permeability test in donor and receptor compartment, in BUS and in *ex vivo* porcine ureter.

The amount of drug to be impregnated in this type of biodegradable stent should then take into account the permeability values of the tissue, which is essential for the efficacy in *In vivo* scenario. It is still expected some loss of the drugs with the urine flow, but it is obvious that the use of biodegradable ureteral stent as an IDD can increase the contact time of the anti-cancer drugs against cancer cells. The versatility of the impregnation process together with the ability to tailor degradation of the stent allow the design of a stent with an adequate amount of the drugs to be release and have efficacy *In vivo*. An *In vivo* model would be essential to validate these results but little has been described in the literature concerning this and it is hard to find a right animal model to validate such experiments.

VII-4. CONCLUSION

In conclusion, using an *ex vivo* porcine approach we have studied the transurothelial permeation of paclitaxel and doxorubicin and verifying the permeation of this drugs delivery from a drug-eluting biodegradable ureteral stent. Three different membranes were used as a permeable membrane, PES and HUVEC monolayer cell and an *ex vivo* porcine ureter in order to determine the permeability, diffusion and partition coefficients. Using this type of approach, we can understand if the delivery of the drugs impregnated in the drug-eluting biodegradable stents will be pharmacologically viable *In vivo*. In this study, the permeability results were found to be dependent of molecular weight of drugs and naturally by the release time of the drug from the stent. Our results suggest that the amount of paclitaxel and doxorubicin impregnated in biodegradable

ureteral stents can remain in the ureter tissue and only a small fraction can cross the tissue. The amount of paclitaxel which remains in the *ex vivo* ureter seems to be effective to affect the viability of the cancer cells and not affect the HUVEC cells. Doxorubicin, on the contrary has shown higher diffusion and permeability through the membranes and the amount of drug which remains in the tissue seems to be lower than what is necessary to affect T24 cancer cells. This study supports the hypothesis that drug-eluting biodegradable ureteral stents impregnated with chemotherapy drugs may serve as sustainable IDD systems with the ability to increase the bioavailability of drugs to target upper urinary tract urothelial carcinoma, particularly those impregnated with paclitaxel.

ACKNOWLEDGEMENTS

The research leading to these results has received funding from Urology Research Grant Jaba Recordati 2015 from Portuguese Urology Association, from ICVS/3B's – Associate Laboratory Research Grants and the European Union Seventh Framework Programme (FP7/2007-2013) under grant agreement number REGPOT-CT2012-316331-POLARIS. The project “Novel smart and biomimetic materials for innovative regenerative medicine approaches” RL1 - ABMR - NORTE-01-0124-FEDER-000016) co-financed by North Portugal Regional Operational Programme (ON.2 – O Novo Norte), under the National Strategic Reference Framework (NSRF), through the European Regional Development Fund (ERDF) is also acknowledged. Alexandre Barros acknowledges his FCT PhD grant SFRH/BD/97203/2013. The authors would like to acknowledge Teresa Oliveira for the technical assistance on the histological analysis.

REFERENCES

1. Raman JD, Messer J, Sielatycki JA, Hollenbeak CS. Incidence and survival of patients with carcinoma of the ureter and renal pelvis in the USA, 1973–2005. *BJU International*. 2011;107(7):1059-64.
2. Stewart GD, Bariol SV, Grigor KM, Tolley DA, McNeill SA. A comparison of the pathology of transitional cell carcinoma of the bladder and upper urinary tract. *BJU International*. 2005;95(6):791-3.
3. Eylert MF, Hounscome L, Verne J, Bahl A, Jefferies ER, Persad RA. Prognosis is deteriorating for upper tract urothelial cancer: data for England 1985–2010. *BJU International*. 2013;112(2):E107-E13.
4. Badalament RA, Farah RN. Treatment of superficial bladder cancer with intravesical chemotherapy. *Seminars in Surgical Oncology*. 1997;13(5):335-41.
5. Malmström P-U. Intravesical therapy of superficial bladder cancer. *Critical Reviews in Oncology/Hematology*. 2003;47(2):109-26.
6. Hadaschik BA, Ter Borg MG, Jackson J, Sowery RD, So AI, Burt HM, et al. Paclitaxel and cisplatin as intravesical agents against non-muscle-invasive bladder cancer. *BJU International*. 2008;101(11):1347-55.
7. Lu S, Neoh KG, Kang E-T, Mahendran R, Chiong E. Mucoadhesive polyacrylamide nanogel as a potential hydrophobic drug carrier for intravesical bladder cancer therapy. *European Journal of Pharmaceutical Sciences*. 2015;72(0):57-68.
8. Papadopoulos E, Yousef G, Scorilas A. Gemcitabine impacts differentially on bladder and kidney cancer cells: distinct modulations in the expression patterns of apoptosis-related microRNAs and BCL2 family genes. *Tumor Biol*. 2015;36(5):3197-207.
9. Tyagi P, Tyagi S, Kaufman J, Huang L, de Miguel F. Local Drug Delivery to Bladder Using Technology Innovations. *Urologic Clinics of North America*. 2006;33(4):519-30.
10. GuhaSarkar S, Banerjee R. Intravesical drug delivery: Challenges, current status, opportunities and novel strategies. *Journal of Controlled Release*. 2010;148(2):147-59.
11. Williams NA, Bowen JL, Al-Jayyousi G, Gumbleton M, Allender CJ, Li J, et al. An ex Vivo Investigation into the Transurothelial Permeability and Bladder Wall Distribution of the Nonsteroidal Anti-Inflammatory Ketorolac. *Molecular Pharmaceutics*. 2014;11(3):673-82.
12. Williams T, Smith B. *Operating Department Practice A-Z*. 2 ed. Cambridge: Cambridge University Press; 2008 2008/003/20.
13. Williams NA, Barnard L, Allender CJ, Bowen JL, Gumbleton M, Harrah T, et al. Evidence of Nonuniformity in Urothelium Barrier Function between the Upper Urinary Tract and Bladder. *J Urol*. 2016;195(3):763-70.
14. Barros AA, Browne S, Oliveira C, Lima E, Duarte ARC, Healy KE, et al. Drug-eluting biodegradable ureteral stent: New approach for urothelial tumors of upper urinary tract cancer. *International Journal of Pharmaceutics*. 2016.
15. Barros AA, Duarte ARC, Pires RA, Sampaio-Marques B, Ludovico P, Lima E, et al. Bioresorbable ureteral stents from natural origin polymers. *J Biomed Mater Res B*. 2015;103(3):608-17.
16. Barros AA, Oliveira C, Lima E, Duarte ARC, Reis RL. Gelatin-based biodegradable ureteral stents with enhanced mechanical properties. *Applied Materials Today*. 2016;5:9-18.

17. Barros AA, Oliveira C, Reis RL, Lima E, Duarte ARC. Ketoprofen-eluting biodegradable ureteral stents by CO₂ impregnation: In vitro study. *International Journal of Pharmaceutics*. 2015;495(2):651-9.
18. Tscholl R, Tettamanti F, Zingg E. Ileal substitute of ureter with reflux-plasty by terminal intussusception of bowel Animal experiments and clinical experience. *Urology*. 1977;9(4):385-9.
19. Dixon JS, Gosling JA. Histology and fine structure of the muscularis mucosae of the human urinary bladder. *Journal of Anatomy*. 1983;136(2):265-71.
20. de Villiers MM, Otto DP, Strydom SJ, Lvov YM. Introduction to nanocoatings produced by layer-by-layer (LbL) self-assembly. *Advanced Drug Delivery Reviews*. 2011;63(9):701-15.
21. Detzel CJ, Larkin AL, Rajagopalan P. Polyelectrolyte multilayers in tissue engineering. *Tissue Eng Part B Rev*. 2011;17(2):101-13.
22. Tang Z, Wang Y, Podsiadlo P, Kotov NA. Biomedical Applications of Layer-by-Layer Assembly: From Biomimetics to Tissue Engineering. *Advanced Materials*. 2006;18(24):3203-24.
23. Sokolnicki AM, Fisher RJ, Harrah TP, Kaplan DL. Permeability of bacterial cellulose membranes. *Journal of Membrane Science*. 2006;272(1-2):15-27.
24. Kerec M, Bogataj M, Veranič P, Mrhar A. Permeability of pig urinary bladder wall: the effect of chitosan and the role of calcium. *European Journal of Pharmaceutical Sciences*. 2005;25(1):113-21.
25. Tsallas A, Jackson J, Burt H. The uptake of paclitaxel and docetaxel into *ex vivo* porcine bladder tissue from polymeric micelle formulations. *Cancer Chemotherapy and Pharmacology*. 2011;68(2):431-44.
26. Caridade SG, Monge C, Gilde F, Boudou T, Mano JF, Picart C. Free-Standing Polyelectrolyte Membranes Made of Chitosan and Alginate. *Biomacromolecules*. 2013;14(5):1653-60.
27. Liang S, Zhang L, Xu J. Morphology and permeability of cellulose/chitin blend membranes. *Journal of Membrane Science*. 2007;287(1):19-28.
28. He H, Cao X, Lee LJ. Design of a novel hydrogel-based intelligent system for controlled drug release. *Journal of Controlled Release*. 2004;95(3):391-402.
29. Matsuyama H, Tamura T, Kitamura Y. Permeability of ionic solutes in a polyamphoteric membrane. *Separation and Purification Technology*. 1999;16(2):181-7.
30. Amidon GL, Lennernas H, Shah VP, Crison JR. A Theoretical Basis for a Biopharmaceutic Drug Classification - the Correlation of *in-Vitro* Drug Product Dissolution and *in-Vivo* Bioavailability. *Pharmaceut Res*. 1995;12(3):413-20.
31. Stevens DM, Gilmore KA, Harth E. An assessment of nanosponges for intravenous and oral drug delivery of BCS class IV drugs: Drug delivery kinetics and solubilization. *Polymer Chemistry*. 2014;5(11):3551-4.
32. Reddy BBK, Karunakar A. Biopharmaceutics Classification System: A Regulatory Approach. *Dissolut Technol*. 2011;18(1):31-7.

Chapter VIII

Natural origin polymer- based biodegradable ureteral stent: *In vivo* evaluation in a porcine model

Chapter VIII

Natural origin polymers-based biodegradable ureteral stent: *In vivo* evaluation in a porcine^{§§}

ABSTRACT

We have developed a biodegradable ureteral stent (BUS) based on natural origin polymers and we evaluated its performance *In vivo*. A total of 10 female Yorkshire pigs were used in this study. Seven BUS 6-Fr stents and three commercial (Biosoft® duo, Porges, Coloplast) 6-Fr stents were unilaterally inserted by cystoscopy. Intravenous pyelography (IVP), blood and urine tests were carried out. During the *in vivo* degradation, the mechanical characteristics of stents were tested in tensile mode and compared with the *in vitro* degradation performed in artificial urine solution (AUS). After degradation pigs were euthanized. Histopathological analysis was performed. All BUS stents had completely degraded by day 10, without the presence of any fragments in the ureter and bladder. From day 1 to day 10, hydronephrosis was significantly less with the BUS in comparison with the commercial stent. Preoperative and postoperative blood and urine results were similar in all samples from the animals implanted with BUS, unlike the commercial stent group with significant differences in values of serum hemoglobin. The BUS stents collected at day 5 and day 7, after sacrificing the animals, demonstrated to have mechanical properties similar to the commercial stents and confirmed that BUS stents degraded by surface erosion. Histopathological analysis of the ureters showed that the stent-related tissue reaction of the two type of stents was different and lower histopathology changes were observed in BUS group. BUS developed is biocompatible, presents a homogenous degradation with no fragments with less

^{§§} This chapter is based on the following publication:

Barros AA, Oliveira C, Ribeiro AJ, Reis RL, Lima E, Duarte ARC. Natural origin polymers-based biodegradable ureteral stent: *in vivo* evaluation in a porcine model. Submitted 2017.

hydronephrosis and capacity to provide a temporary urine drainage as good as the non-degradable commercial stents.

VIII-1. INTRODUCTION

Ureteral stents are a versatile and indispensable medical device in the management of urological practices like to enable urine drainage during surgery of ureteral stones, after ureteroscopy and endopyelotomy, ureteropelvic junction obstruction, extracorporeal shockwave lithotripsy, and extrinsic malignant ureteral obstruction 1-2. After all these years of use and intense research, the ureteral stents commercially available still produce significant stent symptoms, like infection, encrustation, patient discomfort and all required a second procedure to take out for the stent removal by cystoscopy. Nowadays, the forgotten stent syndrome is associated with a significant morbidity which may result in kidney loss or even death³. One of the main demands in the field of ureteral stents is to confer biodegradable features to the stents. Specialists consider this to be the best approach to avoid most of the stent-associated complications^{2, 4}. Biodegradable ureteral stents would avoid the second procedure for stent removal and theoretically be more comfortable for the patients as they are made from softer materials^{2, 5}. The dynamic surface of these ureteral stents due the constant degradation will hypothetically eliminate the bacterial adhesion and encrustation problems not promoting anchor points^{2, 6}. Several biodegradable ureteral stent systems have been reported in last years, but all of them faced poor biocompatibility or unsuitable degradation⁵⁻¹¹. The use of new biomaterials has increased the biocompatibility of these internal devices, reported in recent publications¹²⁻¹⁴. The main challenge of these biodegradable devices is to have a uniform and homogenous degradation or dissolving based on directionality, preventing the formation of fragments during the degradation process that can cause obstruction^{2, 14-15}. Chew et al.¹² reported the design of a glycolic-lactic acid based stent has been designed to degrade in the direction of the bladder coil to renal coil preventing ureteral obstruction. Zhang et al.¹³ reported a different design using glycolic-lactic acid based multifilament. Using a textile technique, they design a braided thin-walled stent with the same outer diameter but with a thinner wall claiming fewer degradation products decreasing the possibility of obstruction. Both studies were done *in vivo* using a porcine and canine model, with good results regarding biocompatibility and urine drainage during the degradation. However, none of these are commercially available and problems still remains, as in both studies fragments of the stents were found in the body. In our previous studies, we reported the design of a biodegradable ureteral stent produced with natural based polymers and processed by critical point drying with carbon

dioxide^{14, 16}. Gelatin was used as a base material for these stents and a hydrophobic coating was applied to improve the mechanical properties and allow the placement of the stent *in vivo* by the conventional surgical procedure. The radiopaque hydrogel-based ureteral stent has shown to have an homogenous degradation as the degradation occurs by erosion of the material¹⁴. The leachables and the degradation products have shown to be non-cytotoxic. A preliminary *in vivo* validation was performed in a porcine model and the ureteral stent remained intact during the first 3 days and started to degrade after that. Full degradation was achieved after 4-5 days, without the presence of any stent fragments inside the ureter or bladder¹⁴. In this study, the formulation was adjusted and a new crosslinker, genipin, was added in order to increase the *in vivo* stability of the stent. Genipin is a natural crosslinking agent that have been used to crosslink natural-based polymers in many different applications¹⁷⁻¹⁸. It has already proven its feasibility, presents low toxicity and have a characteristic dark blue color when reacting with amino groups in amino acids or proteins¹⁹. We evaluated *in vitro* and *in vivo*, in a porcine model, the biodegradable ureteral stent (BUS) developed. The degradation, mechanical properties, drainage, physiological and histological results were compared with a commercially available ureteral stent (Biosoft® duo, Porges, Coloplast).

VIII-2. MATERIALS AND METHODS

VIII-2.1. Materials

Gelatin, alginic acid sodium salt, urea, urease type IX from *Canavalia ensiformis* (Jack Bean), calcium chloride, chlorophorm, ethanol, bismuth (III) carbonate basic, sodium phosphate dibasic and sodium azide were purchased from Sigma-Aldrich (Germany). Potassium dihydrogen orthophosphate and magnesium chloride hexahydrate were obtained from Riedel-de Haën (Germany). Genipin was obtained from Wako Chemicals GmbH (Germany). Polycaprolactone resin PCL 787 (Mw 80,000 g mol⁻¹), commercially available as TONE™ polymer, was obtained from Union Carbide Chemicals and Plastics Division, Bound Brook, New Jersey. Carbon dioxide (99.998 mol%) was supplied by Air Liquide (Portugal). All reagents were used as received without any further purification.

VIII-2.2. Preparation of biodegradable ureteral stents (BUS)

Biodegradable ureteral stents (BUS) were manufactured according our last publication(1), with some modifications. Briefly, gelatin, alginate sodium salt and bismuth (III) carbonate basic (65:30:5 wt.%) were dissolved in distilled water at 70°C. After the obtention of a homogenous solution, 15mM of the crosslinking agent, genipin, was added to the solution and the solution was injected in a mold to obtain a 6-Fr ureteral stent with the total length of 20 cm, wall thickness of 500 µm and internal diameter of 1000 µm. After 1 hour, the stents were taken out of the mold and placed in an alcohol solution (100% ethanol) for an additional hour. The stents were then transferred into a second crosslinking solution of 0.48M calcium chloride (CaCl₂), at room temperature, for one hour. After crosslinking, the stents were relocated in an alcoholic solution (100% ethanol) to obtain an alcohol gel which can be dried in a high-pressure vessel with supercritical carbon dioxide (scCO₂), under controlled pressure (100 bar) and temperature (40°C) and a continuous flow of scCO₂ during 90 minutes. The dried stents were immersed in distilled water for 30 min and in ethanol 100%, for 1 hour, to remove the inner template used. The stents were subsequently dried at room temperature conditions, during 1 day. The coating of the stents was performed by immersion in a 10 wt.% solution of polycaprolactone (PCL) resin 787 with 2 wt.% of bismuth (III) carbonate basic in chloroform. The stents were dried at ambient conditions overnight. The stents were sterilized with ethylene oxide at 42°C for 3h. The control group used in this study was the 6-Fr commercial double-j Biosoft® duo stents (Porges Coloplast, Denmark).

VIII-2.2.1. *In vitro* cytotoxicity

The cytotoxicity of the new stents developed was evaluated using an immortalized mouse lung fibroblasts cell line (L929) purchased from the European Collection of Cell Cultures. The effect of the leachables released from the biodegradable stents (during 24 h) on the cellular metabolism was performed using a standard MTS (Cell Titer 96® Aqueous Solution Cell Proliferation Assay, Promega, USA) viability test, in accordance with ISO/EN 10993 guide-lines(2). A latex rubber extract was used as positive control for cell death; the extracts from a commercial stent (Biosoft® duo, Porges) were used as a reference material; while cell culture medium was used as negative control representing the ideal situation for cell proliferation. Cell viability was evaluated by the 3-(4,5-dimethylthiazol-2-yl)-5-(3-carboxy-methoxyphenyl)-2-(4-sulphophenyl)-2H-tetrazolium (MTS)

assay after 72h. This assay is based on the bioreduction of a tetra-zolium compound MTS into a water-soluble brown formazan product. This was quantified by UV-spectroscopy, reading the formazan absorbance at 490nm in a microplate reader (Synergy HT, Bio-Tek Instruments, USA). Each sample was tested using 12 replicates.

VIII-2.3. *In vivo* evaluation in a porcine model

VIII-2.3.1. Stent insertion technique

The *In vivo* study was conducted at ICVS, University of Minho, Braga, Portugal. The protocol of the study was formally approved by the institution's review board and it is in accordance with its internal ethical protocol for animal experiments. A total of 10 female domestic pigs, weighing \approx 30 kg, were used in this study. The pigs were not given food or water for 12 h before the procedure. All procedures were performed under general anesthesia and mechanical ventilation as previously described in detail(3). After emptying the bladder, a semi rigid 7-Fr ureteroscope (Karl Storz, Tuttlingen, Germany) was inserted through the urethra and saline solution was instilled. The full procedure was performed according to the standard technique of ureteroscopy. A 0.035-in. flexible tip guidewire (AQUATRACK® Hydrophilic Nitinol, Cordis®, Johnson & Johnson) was inserted into the ureters under direct visualization, and then the stents were inserted over the guidewire into the kidney. The guidewire was then removed and the position of the stents was confirmed by X-ray (Examion® DR810). A total of 7 pigs were unilaterally stented with biodegradable ureteral stent (BUS) and 3 pigs with the commercial stent. The stents were randomly placed on the right or left ureter. At day 5 one pig died and at day 7 one was euthanized, both stented with BUS and the degradation level of the stent was assessed. The other 8 were euthanized at day 10.

Blood and urine samples were collected from all animals before the day of surgery. Blood tests (WBC, Hb), serum creatinine, urine culture tests were performed at day 0, 5 and 10.

VIII-2.3.2. Excretory Urogram

Intravenous pyelograms (IVP) X-rays were carried out at 0, 1, 3, 5, 10, 20 and 30 min after intravenous injection of 1200 mg/Kg of Iohexol (Omnipaque™ 300, GE Healthcare). IVP was used

to evaluated the degree of hydronephrosis at day 0, 1, 5 and 10. The renal function was measured by the rate of contrast material movement at day 0. IVP severity score is based on the time until the contrast appears in the kidneys and ureters after the intravenous injection, hydronephrosis was graded as: none – level 0 (<3min), mild – level 1 (3-10 min), moderate – level 2 (10 – 20 min) or severe – level 3 (>20 min)(4).

VIII-2.3.3. *In vitro* and *In vivo* degradation study

The *In vitro* and *In vivo* degradation of the stents was compared. The *In vitro* degradation of biodegradable ureteral stents was measured as function of the weight loss of the samples. Samples (10 mg) were immersed in artificial urine solution (AUS) prepared according to the procedure described in a previous article(1). Samples immersed were dried and weighted to determine the weight loss at 0, 1, 5, 7, 10 and 12 days. The values of *In vivo* degradation were assessed from the stents taken from the pigs sacrificed at day 5, 7 and 10 days. The weight loss of stents for both *In vitro* and *In vivo* was calculated according to the following equation:

$$\% \text{ Weight loss} = \frac{W_f - W_i}{W_i} * 100$$

Equation II-2 Determination of wight loss.

Where W_f is the final weight of the stent (dried after immersion/placement) and W_i is the initial weight of the stent.

VIII-2.3.4. Tensile mechanical analysis

The tensile properties of the biodegradable ureteral stents were tested during the *In vitro* degradation at day 0, 1, 5, 7 and 10, and for *In vivo* degradation at day 0, 5, 7 and 10. Tensile mechanical analysis of the biodegradable ureteral stents was evaluated using an INSTRON 5540 (Instron Int. Ltd, High Wycombe, UK) universal testing machine with a load cell of 1 kN. The dimensions of the specimens used were 50 mm of length, 2 mm diameter, and 0.5 mm of thickness of the stent wall. The load was placed midway between the supports with a span (L) of 30 mm. The crosshead speed was 1:5 mm min⁻¹. For each condition the specimens were loaded

until core break. The *In vivo* recovered stents were cut in equal parts along its length and compared. The results presented are the average of at least three specimens and are presented as the average \pm standard deviation.

VIII-2.3.5. Euthanasia and Necropsy

At 5, 7 and 10 days, animals were sacrificed and necropsy was performed. A midline incision was carried out to excise the kidneys, ureters and bladder en bloc. The kidneys and ureters were measured and a representative section of each organ was fixed in 10% formalin and was stained with Hematoxylin-Eosin and Masson's Trichrome. Tissues were compared between the stented groups (biodegradable vs commercial stents) as well as between the non-stented contralateral (control) ureters and stented ureters in each group. Biocompatibility parameters were assessed histopathologically and grading according to described by Chew et al(5). Histopathological grading was assigned as Normal (Grade 0) – no inflammation and normal architecture; Early stage (Grade 1) – mild edema, congestion and inflammation with some destruction of epithelium in ureters and renal pelvis mucosa in kidneys; Progressive (Grade 2) – remarkable edema, congestion and inflammation with tissue destruction; and Advanced (Grade 3) – severe edema, congestion, inflammation presence of renal parenchyma with large cystic calices in kidneys and hyperplastic mucosa and/or papillary outgrowth.

VIII-2.4. Statistical analysis

All quantitative data are presented as mean \pm standard deviation (SD). Statistical analysis was performed using Graph Pad Prism 6.00 software (San Diego, USA). Statistical significances (* $p \leq 0.05$, ** $p \leq 0.01$ and *** $p \leq 0.001$) were determined using one-way analysis of variance (ANOVA) for an average of three to twelve replicates, followed by post hoc Tukey's test for all pairwise mean comparisons. Hydronephrosis scores with time were compared using two-way repeated measures ANOVA followed by the Bonferroni post test.

VIII-3. RESULTS AND DISCUSSION

Our group developed a biodegradable ureteral stent made of natural origin polymers(1, 6). However, the stents designed still presented some drawbacks, which were overcome with this new formulation herein presented and tested. In our previous work, BUS were prepared from an initial aqueous solution of alginate and gelatin and physical and ionic gelation was induced. The gelation was first induced by decreasing the temperature followed an ionic crosslinking with a calcium chloride (CaCl_2) solution. The divalent cations (Ca^{2+}) crosslink the carboxyl groups of alginate, but gelatin is not crosslinked by the calcium chloride (CaCl_2) solution(7). In this study, we changed the formulation in order to increase *In vivo* the stability of the stent, using a new crosslinking agent, genipin. Gelatin suffered a physical crosslinking phenomena, by increasing and decreasing temperature with gelatin molecules changing the conformation from a random coil to triple helix(8). In this sense, genipin was used as a chemical crosslinker agent for gelatin, that has been proven its feasibility for biomaterials containing primary amino groups (9, 10)(**figure VIII 1a**). Genipin was chosen among the available crosslinking agents due to its natural origin and reported low toxicity(10). Supercritical drying process was used to dry the stents. **Figure VIII 1b** presents 6-Fr stents used in this study, on the left, the biodegradable ureteral stent (BUS) developed and on the right, used as a control, a commercial stent from Porges, Coloplast. **Figure VII 1c** presents the *In vitro* cytotoxicity of the new formulation of BUS. The results demonstrate that there is no cytotoxic effect of the new stent formulation with genipin on L929 cells.

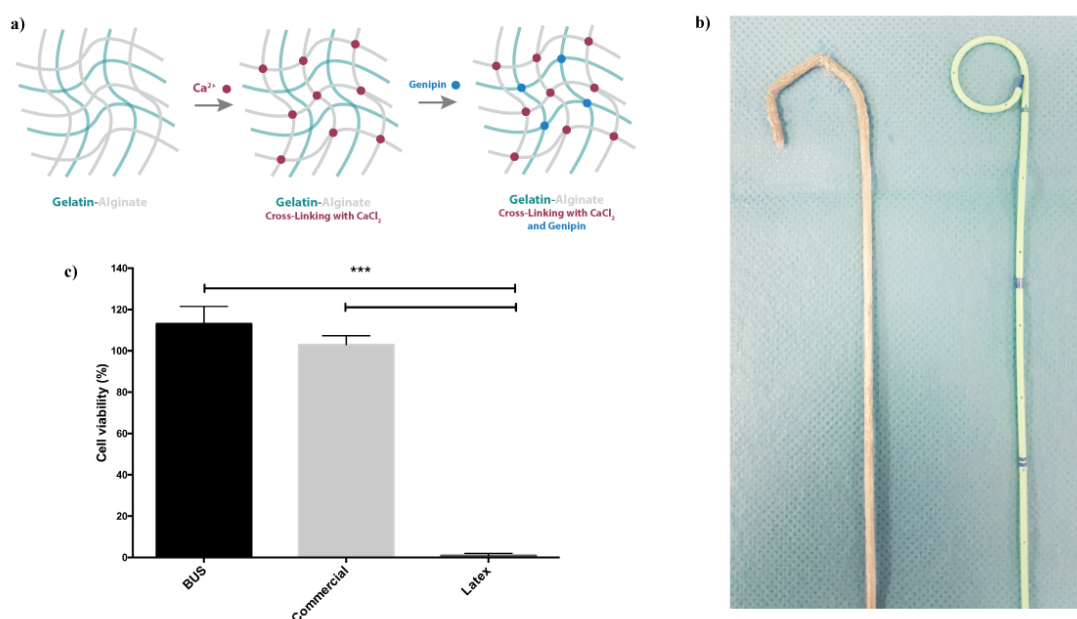


Figure VIII-1 a) Schematic illustration of the BUS cross-linking. b) 6-Fr Biodegradable ureteral stent – BUS (left) and 6-Fr Biosoft® duo, Porges, Coloplast - commercial (right). c) Cytotoxicity study by cell viability measured after 72h.

VIII-3.1. In vivo evaluation in a porcine model

Biodegradable ureteral stents (BUS) were compared *In vivo* with a commercial ureteral stents, using a porcine model. All 10 pigs were successful stented with biodegradable and commercial ureteral stents, randomly placed in right or left ureters. The duration of the *In vivo* study was 10 days. One pig implanted with BUS died at day 5, due to preexisting pneumonia, but the stent was recovered and analysed. From the 6 pigs stented with BUS only one pig demonstrated migration of the BUS stent, which occurred at day 4. The BUS stent has thus shown to have the appropriate design to remain in the ureter. All biodegradable ureteral stents were further designed to be radiopaque under X-ray, due to the bismuth present in the formulation. However, upon X-ray exposure, they were only visible in the first 24 hours, after this time BUS could not be followed by X-ray (**figure VIII 2ab**). The contrast of the stent under X-ray is higher for the commercial stent (**figure VIII 2c**) than BUS (**figure VIII 2a**).

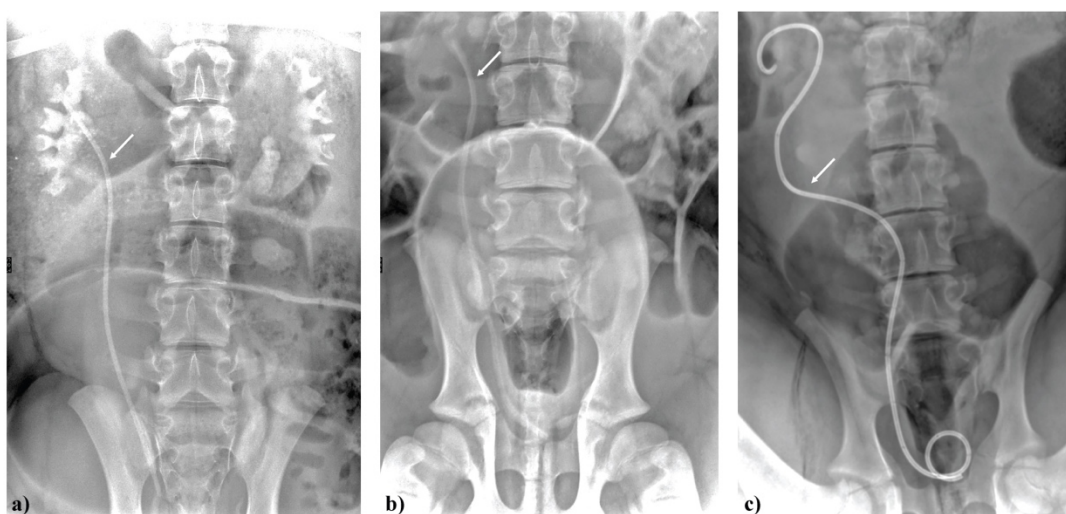


Figure VIII-2 X-ray image of biodegradable ureteral stent at a) day 0 and b) day 1. c) Commercial ureteral stent at day 1.

Hematological values of the animals were not affected by the placement of biodegradable stent. In **table VIII 1** the analytical values obtained from the blood and urine collected preoperatively (day 0) and postoperatively (day 10) are presented. A significant change in values of serum hemoglobin was noted in the commercial stent group. The results of serum WBC and urine culture showed no urinary tract infections in both groups. Creatinine levels during the study demonstrated to be relatively stable and not be affected by biodegradable or commercial stent placement.

Table VIII-1 Preoperative (day 0) and postoperatively (day 10) follow-up serum and urine parameters of commercial and BUS ureteral stent.

Group	Category	Preoperatively	Postoperatively	P-value
Commercial	Serum hemoglobin (g/dL)	10.82 ± 1.47	19.73 ± 0.89	0.03*
	Serum WBC (10 ³ /μL)	13.52 ± 2.31	15.63 ± 2.24	0.75
	Serum creatinine (μmol/L)	0.96 ± 0.16	1.00 ± 0.10	0.73
	Urine pH	7.17 ± 0.62	7.67 ± 0.47	0.99
BUS	Serum hemoglobin (g/dL)	9.40 ± 1.02	7.84 ± 3.19	0.81
	Serum WBC (10 ³ /μL)	17.31 ± 5.09	18.83 ± 5.98	0.75
	Serum creatinine (μmol/L)	0.69 ± 0.16	0.80 ± 0.20	0.99
	Urine pH	6.83 ± 0.24	8.00 ± 1.00	0.70

Data presented as average \pm SD. *significant changes.

VIII-3.2. *In vitro* and *In vivo* stent degradation

The *In vitro* degradation of the biodegradable ureteral stents was assessed measuring the weight variation of the samples. The weight loss, measured as the percentage of mass lost when immersed in AUS for a predetermined time period is presented in **figure VII 3**. BUS demonstrated *In vitro* that no degradation occurs during the first 3 days of immersion and after 12 days, the stents have shown complete degradation. Comparing the results obtained from our previous work(1), *In vitro*, with this new formulation we were able to extend the stability of the stent from 9 to 12 days. The increase of the stability of the BUS stent can be justified by the genipin crosslinking in this new stent formulation. *In vivo* degradation of the BUS was followed at predetermined time points, by direct visualization and by sacrificing the animals at day 5 and day 7. All of the five BUS were completely degraded (100% weight loss) in urine after 10 days, which was confirmed at sacrifice. No fragments of the stents were seen in the renal pelvis, ureter or bladder after sacrificed. **Figure VIII 3c** shows the BUS recovered after 5 days with the total length and a weight loss off 24% from the initial weight. At day 7, the BUS recovered shown to be also intact with a mass reduced about 38% (**figure VIII 3d**). It was visible the homogeneous degradation by erosion along the entire stent surface, while the lumen remains open. All biodegradable stents are composed with PCL coating and hydrogel core. The degradation of the stent started by the peeling of the coating, however it was observed that after 5 days not all the coating disappears. On the other hand, in the stent recovered after 7 days, only the hydrogel part of the stent was presented. The *In vivo* results show the stability of the biodegradable stent during 7 days. This stability can be justified by the counterbalancing effect of the ionic and covalent crosslinking upon variation on the urinary tract environment. Between 7 and 10 days the stents have a fast degradation (\approx 62%). This fast degradation can be justified by the urine environment (pH and ionic content) which influence a multimode of the intermolecular interactions present in BUS such as electrostatic interactions, hydrogen bonding and hydrophobic interactions, occurred after the peeling of the coating(7, 11). In addition it is important to point out that the divalent calcium cation can be chelated by the physiological conditions influencing the stability of the polymeric chains(11, 12). The *In vitro* degradation in AUS shown a similar degradation profile but the complete

degradation only occurs after 12 days, which can be justified due the dynamic conditions *In vivo*, like urine flow and peristaltic movements of the ureters. Fragments of the stent degradation is one of the problems that need to be overcome and this is still the main reason why biodegradable stents are not available in the market. The first studies in the field reported an obstruction caused by the stent degradation products. Fragments can act as a nucleation point for bacterial adhesion and/or encrustation development leading to further complications(13-17). Chew *et al.*(4, 18) developed a biodegradable stent, Uriprene, that was investigated *In vivo*, in a porcine model. Zhang *et al.*(19) developed a similar glycolic-lactic acid fiber based biodegradable ureteral stent and reported results *In vivo*, in a canine model. Both studies presented good results regarding the degradation and biocompatibility, however upon degradation they reported fragments of the stent in the renal pelvis and bladder. The time of degradation of these glycolic-lactic acids based biodegradable ureteral stents is around 4 weeks. In the clinical practice an ureteral stent is generally removed between 48 hours to 4 weeks, after an uncomplicated ureteroscopy. In our study, the time of degradation was lower, 10 days. This may limit the therapeutic prescription of these stents. However, and most important any BUS stent fragments were observed during the degradation process which occurs by surface erosion. The modification of the stent formulation, incorporating new polymers or different cross-linkings may result in higher indwelling times.

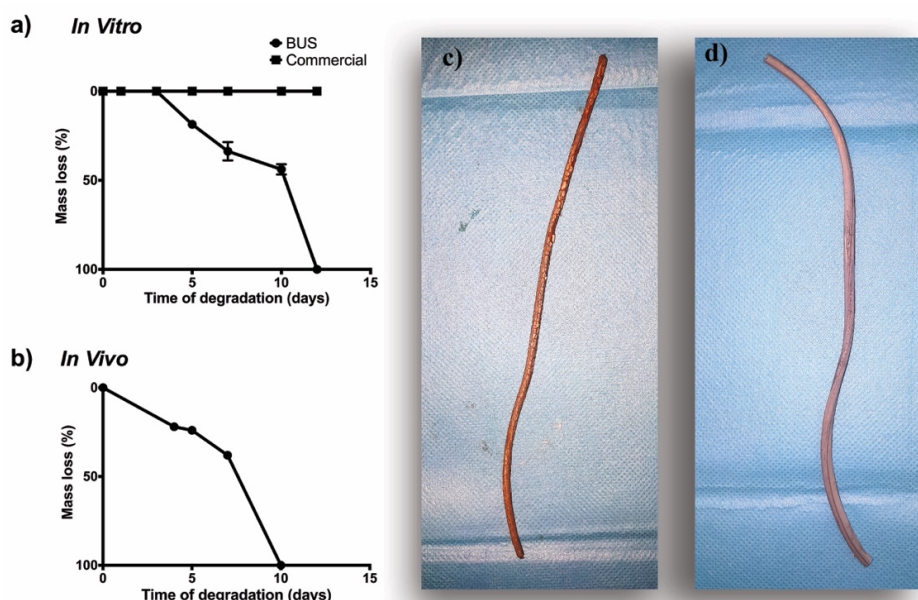
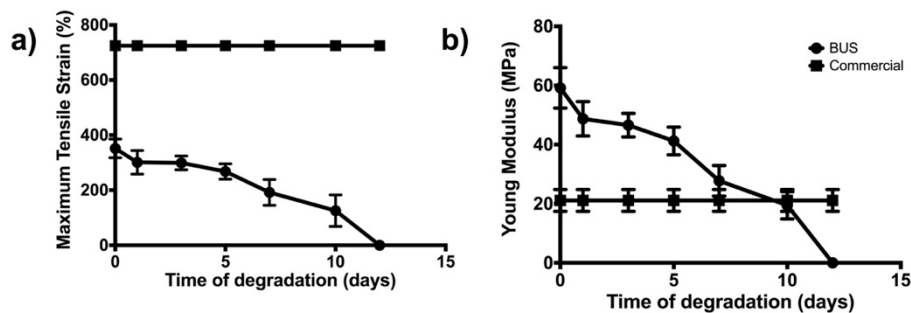


Figure VIII-3 a) In vitro BUS degradation in AUS and b) *in vivo* degradation in a porcine model. BUS intact recovered after d) 5 days and e) 7 days in a porcine model.

VIII-3.3. Tensile mechanical tests

The *In vitro* and *In vivo* tensile mechanical properties, namely maximum tensile strain (%) and Young's modulus (MPa) of the biodegradable ureteral stents during the degradation process are presented in **figure VIII 4**. As a control the tensile results for the commercial ureteral stent are also presented. As expected, during the degradation process the mechanical properties of the BUS decreased, while the commercial ureteral stents remained constant. The maximum tensile strain and Young's modulus were measured at day 0, in wet state. BUS demonstrated to have lower maximum tensile strain and higher Young's modulus compared with the commercial ureteral stent. Comparing the mechanical values obtained in our previous work, *In vitro*, it should be noted that genipin had a slight influence on the increase of the mechanical properties (49.8 MPa to 61.7 MPa of Young's modulus). The *In vitro* and *In vivo* profile obtained are similar, with *In vivo* values lower compared with *In vitro* for each time point. The *In vivo* BUS stents, were cut in equal parts before the mechanical test. The lower standard deviation obtained in each time point supports the hypothesis of homogeneous erosion degradation along the stent surface. BUS shown less 40%, at day 5 and 65%, at day 7 of maximum tensile strain after *In vivo* degradation. In terms of Young's modulus, BUS were significantly more resistant than the control until day 10 (*In vitro*) and day 7 (*In vivo*), the time that both stents presented similar values. Mechanical characteristics of ureteral stents determine their drainage ability or disability to relieve obstruction. As expected, our biodegradable ureteral stent had different physical and mechanical characteristics compared with commercial ureteral stents progressively decreasing during the degradation process. Nonetheless, the mechanical properties obtained of our biodegradable ureteral stent allowed the placement easily in a porcine model by the conventional procedure. The physical characteristics of the BUS stent also allowed the recovery of the stent in one piece, without cracking, after 7 days from the *In vivo* model.

In Vitro



In Vivo

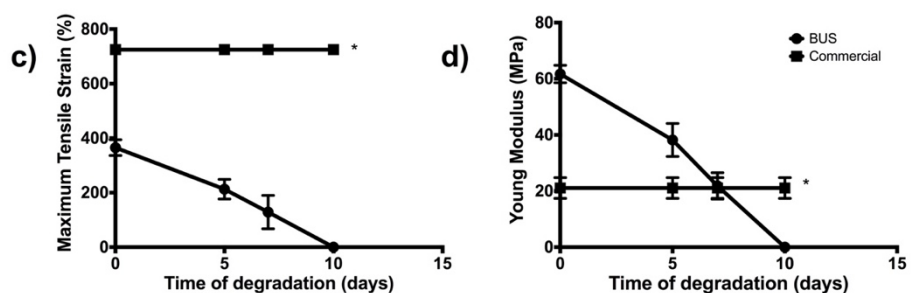


Figure VIII-4 *In vitro* and *in vivo* values of maximum tensile strain (%), young modulus (MPa) and Mass loss (%) of BUS and commercial ureteral stents. Aterisks mark – data from *in vitro* results.

VIII-3.4. Hydronephrosis

Intravenous pyelograms (IVP) X-rays were performed in all animals before the operation (day 0), and all pigs were defined as not having hydronephrosis and a healthy kidney function. **Figure VIII 5a** shows a representative image of 10-min pyelogram at day 10 after BUS degradation. **Figure VIII 5b** presents the hydronephrosis score obtained for all animals stented with BUS and commercial stents. At all time-points after stent insertion, the hydronephrosis level of all pigs was not higher than grade 2. Statistical differences were observed in hydronephrosis score on day 5 between BUS and Commercial stented pigs. The level of hydronephrosis increased significantly in the Commercial ureteral stent group by day 5 ($p \leq 0.01$) with a slightly decrease by day 10 ($p \leq 0.05$). It remained constant in the BUS group. Overall, animals stented with BUS had an average of slightly less hydronephrosis compared with the control, commercial stent. The hydronephrosis was further confirmed by the histopathological analysis. It is well documented that the placement of conventional ureteral stents may result in a certain level of hydronephrosis (20,

21). While ureteral stents can alleviate obstruction, and improve urine drainage, the urine flow is not the same as freely as that in a non-stented ureter(22). The degradation process of BUS has shown no effect on the urine flow and did not increase the hydronephrosis score. Satisfactory urine flow is one of the most important features of a ureteral stent to decrease kidney pressure caused by obstruction(21). Excitingly, hydronephrosis results suggested that BUS developed provides better flow compared with control stent. This can be supported by the water uptake capacity of hydrogel-based materials which has higher absorbing properties than the conventional material used in the non-biodegradable ureteral stents(23-25). Previous *In vivo* studies comparing biodegradable ureteral stents with commercial stents showed similar hydronephrosis score to our BUS(4, 19). One of the major complications nowadays is the discomfort and pain that patients feel due to inflammation caused by the stent movement, which can originate irritation of the kidney, ureter and bladder epithelium(5, 26). BUS stent demonstrated to cause less level of hydronephrosis compared with the conventional stent tested suggesting less pain and discomfort for the patients in the future.

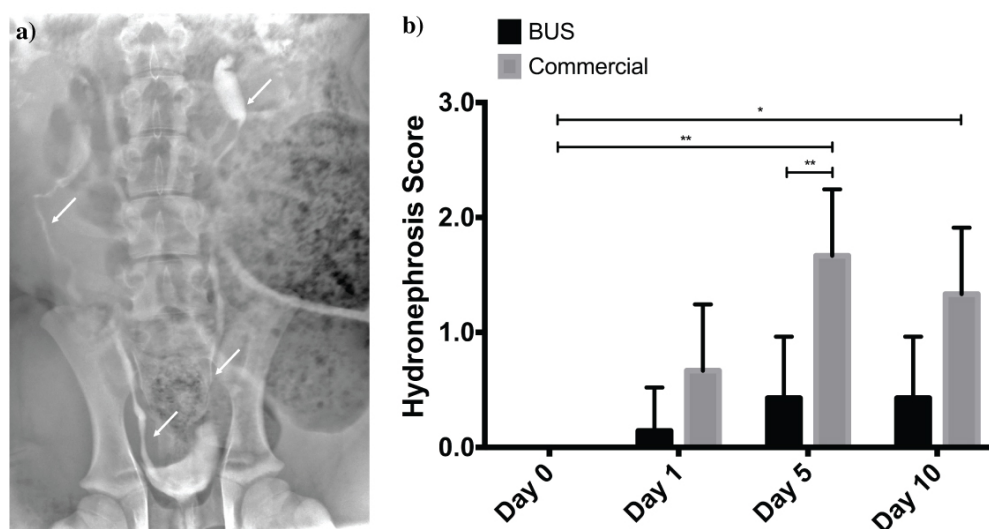


Figure VIII-5 a) A 10-min pyelogram at day 10 after BUS degradation. b) Hydronephrosis score measured by mean of IVP of all animals at day 0,1, 5 and 10 days of BUS and commercial ureteral stent, based on time until contrast (Omnipaque™ 1200mg/Kg) was seen in kidneys and ureters. 0.0, less than 3 minutes. 1.0, 3 to 10 minutes. 2.0, 10 to 20 minutes. 3.0, greater than 20 minutes. Values are represented as average. Statistical differences (*p≤0.05, **p≤0.01, *p≤0.001).**

VIII-3.5. Histopathological analysis

Ureteral stents are in close contact with uroepithelium and because of that biocompatibility of the materials used is an important requisite(19). The *In vivo* biocompatibility of BUS and commercial stents was assessed essentially based on the inflammatory reaction produced in the urothelium of the kidney and ureter. In **figure VIII 6** are presented macroscopic images representative of urinary tract collected at different time points. **Figure VIII 6a, 6b** and **6c** shows the urinary tracts from the BUS stented pigs. One case of clear hydronephrosis was observed in a pig stented with commercial stent (**figure VIII 6e**). The grade obtained by the IVP at day 10, for the same animal, was grade 2 which corresponds to moderate hydronephrosis. Based on histopathological grades for nephropathy and ureteral pathology, kidneys and ureters stented with BUS shown better pathological conditions, and hence better biocompatibility when compared with the pathological grades obtained with commercial ureteral stents (**table VIII 2**). There were no statistically significant difference between kidneys stented with BUS and commercial stent. On the other hand, statistically significant differences ($p \leq 0.05$) were obtained in ureters pathology, higher grade was obtained for ureters stented with commercial stent.

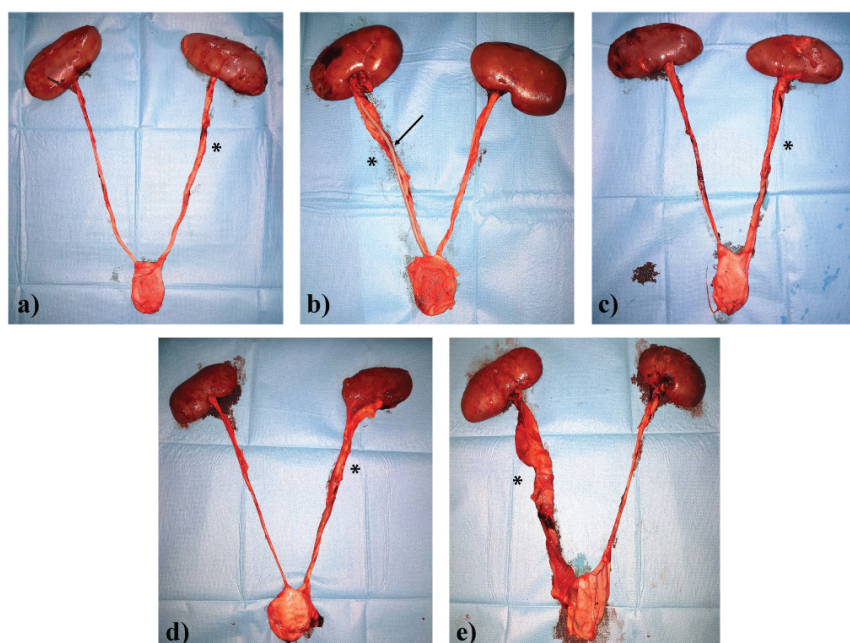


Figure VIII-6 Macroscopic images representative of urinary tract after a) 5 days, b) 7 days and c) 10 days with BUS. d) Representative image of urinary tract after stented with commercial

stent. e) Hydronephrosis case verified after stented with commercial stent. Asterisks mark the ureters that were stented. Arrow points the BUS stent after 7 days indweeling.

Table VIII-2 Biocompatibility parameters of BUS and commercial stents group in the kidney and the ureters

Group	BUS	Commercial	P-value
Nephropathy	0.17 ± 0.37	0.67 ± 0.47	0.24
Ureteral pathology	0.33 ± 0.47	1.67 ± 0.33	0.04*

Data presented as mean ±SD. *significant changes.

Stented and non-stented kidney and ureters width was measured (**figure VIII 7**). Ureters width was measured in 3 sections, upper, mid and distal. Confirming what we observed by the biocompatibility parameters, no significant differences were observed between the stented kidney and non-stented and between the two type of stents. Overall the ureteral width of BUS stented ureters was not statistically significantly larger when compared to the non-stented ureter. In contrast, commercial stented ureters were statistically significantly greater when compared to the ureters non-stented, in mid ($p \leq 0.01$), upper and distal ($p \leq 0.001$) ureter sections. Between the two groups of stents significant differences were obtained along the ureter width, ureters stented with BUS shown lower size compared with ureters stented with control, commercial stent. Similar results were observed by Chew et al.(4) demonstrating the ability of biodegradable ureteral stents to be less abrading when compared with conventional ureteral stents.

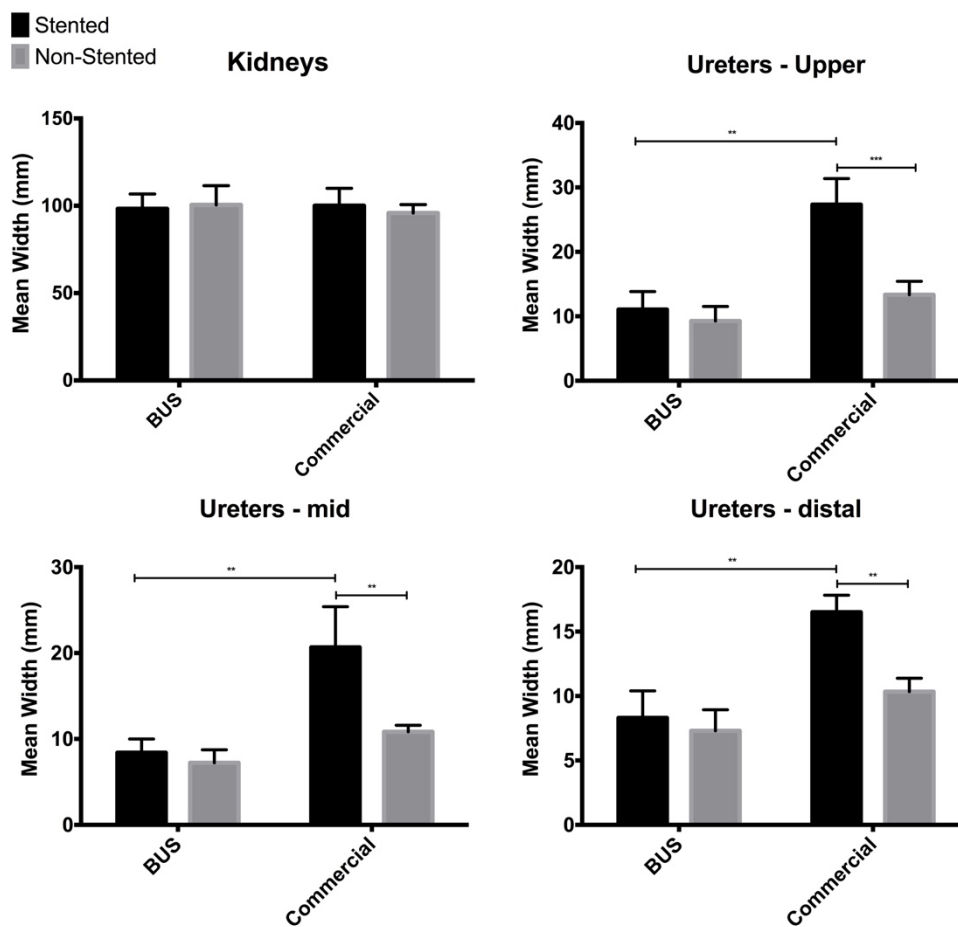


Figure VIII-7 Width of BUS and commercial stented kidneys and ureters vs respective non-stented controls, including upper, mid and distal ureter. Values are represented as average. Statistical differences (*p<0.05, **p<0.01, ***p<0.001).

Histological analysis was performed in the kidneys and ureters stented with BUS and Commercial stent, on day 10. Non-stented ureters were used as a control. **Figure VII 8** shows representative Hematoxylin and Eosin (H.E) and Masson's Trichrome (M.T.) images of the ureters. Generally, histological analysis revealed that greater ureter changes were more frequent in stented ureters than in non-stented ureters in each group. Kidneys histology, with exception of the pig with higher hydronephrosis (**figure 6e**), showed similar histological conditions compared to the control. Ureters are composed by three essential layers, a fibrous tissue (outer layer), a middle layer essential muscle and an inner layer composed by the stratified epithelium(27). It is well documented that the placement of commercial ureteral stents can cause irritation of the ureteral epithelium(5, 26). Results suggest higher ureter changes in the stented ureters compared with the

non-stented ureters. The histological analysis in the urothelium of ureter has shown a different behaviour for the two stents used in the present study. Ureter epithelium after BUS placement and degradation remains intact without any major change compared to the control. The thickness of ureter mucosa remains similar and no inflammation or hydronephrosis was observed in all animal stented with BUS. In contrast, commercial group has shown to be more aggressive to ureter epithelium. Irregular surface, edema and epithelium destruction were found in the histological samples of commercial stent group. In **figure VIII 8** it is possible to see the differences in the mucosa thickness between the control and the commercial ureteral stent group. A small edema and mucinous cytoplasmic vacuolation (mcv) of the epithelium was developed in the presence of conventional stents, the same was not observed in the presence of biodegradable ureters stent (BUS). Overall, no significant inflammatory or necrotic cells were found in each group. The histology outcomes support the results obtained and described before. Biodegradable stented animals have shown less ureters changes compared with animals stented with conventional stents, and more frequent cases of severe epithelium disintegration. Previous studies using commercial ureteral stents reported the same observations namely, presence of edemas and urothelium layer destruction (4, 26). Another work on biodegradable ureteral stents, developed with different materials, presented severe inflammatory reaction, with stent material entrenched in the ureteral wall(28). This reaction was not observed in any pig of this study. The characteristics of the base material of the stents are essential for a good preservation of ureteral histopathology. BUS is a hydrogel-based stent, shown to be ureteral urothelium friendly material, and the degradation products not induced any ureteral inflammatory response. Hydrogel-based materials have been used in the conventional stents to reduce the stent-related problems as a coating, however full hydrogel stents have not yet been introduced in the market (29). The results in this study suggest that the biodegradable ureteral stent (BUS) developed will be more comfortable for the patient with lower stent associated symptoms.

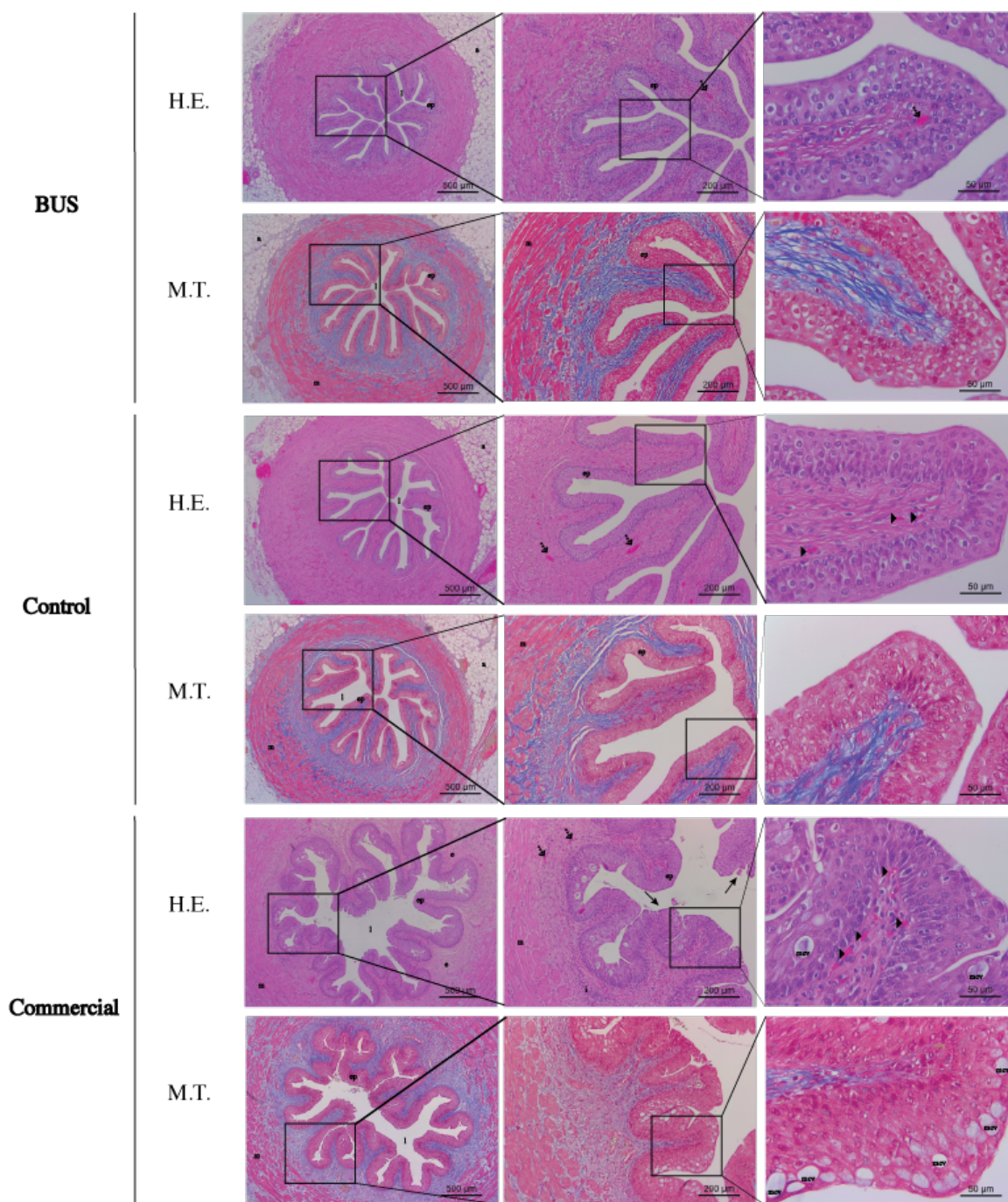


Figure VIII-8 Representative Hematoxylin and Eosin (H.E) and Masson’s Trichrome (M.T.) images of ureters stented with biodegradable ureteral stent (BUS), Commercial stent (commercial) and non-stented ureters (control), on day 10. Examples of: mcv - mucinous cytoplasmic vacuolation, i – infiltrated, m – muscle, ep- epithelium, l- lumen ureter, e – edema, a – adipose tissue, arrow - epithelium destruction; arrow dashed- blood vessels, and arrow head – erythrocytes; All images were taken with a 4x, 10x and 40x magnification microscope objectives.

VIII-4. CONCLUSIONS

In the current study, we developed a natural origin polymer-based biodegradable ureteral stent (BUS). The results supported the hypothesis of homogeneous degradation by surface erosion, within 10 days, remain intact during 7 days, in a porcine model. BUS demonstrated to lose the radiopaque lost properties after 24 hours, making it difficult to follow under X-ray. Regarding biodegradation, no ureteral obstruction was observed and no BUS fragments were found in the renal pelvis, ureter or bladder. BUS demonstrated to have encouraging physiological and histopathological responses *In vivo*. Urine drainage, based on intravenous pyelograms (IVP), was significantly better in BUS compared with the commercial ureteral stent. BUS has also shown to be more biocompatible compared with the commercial ureteral stent concerning nephropathy and uropathy. Foreign body reactions, urothelium damage and edema were barely detected on histologically sections post BUS stent implantation unlike in control stent. In the present *In vivo* study, biodegradable ureteral stents based on natural origin polymers shows advances regarding prior biodegradable stents reported in literature. Next steps will be to increase the stability of the biodegradable ureteral stent *In vivo*, not compromising the degradation by erosion, without fragments and improve the radiopaque features of the stent. Clinical studies are required to determine the feasibility in humans.

ACKNOWLEDGEMENTS

The research leading to these results has received funding from the ICVS/3B's Associated Laboratory with the project reference POCI-01-0145-FEDER-007038, from the project "Novel smart and biomimetic materials for innovative regenerative medicine approaches" RL1 - ABMR - NORTE-01-0124-FEDER-000016) cofinanced by North Portugal Regional Operational Programme (ON.2 – O Novo Norte), under the National Strategic Reference Framework (NSRF), through the European Regional Development Fund (ERDF). Alexandre Barros acknowledges his FCT PhD grant SFRH/BD/97203/2013 and Teresa Oliveira and Tírcia C. Santos for the histopathology technical assistance.

REFERENCES

1. Barros AA, Oliveira C, Lima E, Duarte ARC, Reis RL. Gelatin-based biodegradable ureteral stents with enhanced mechanical properties. *Applied Materials Today*. 2016;5:9-18.
2. ISO/10993. Biological Evaluation of Medical Devices. Part 5. Test for Cytotoxicity, In Vitro Methods: 8.2 Test on Extracts. 1992.
3. Oliveira CAR, Ferreira C, Quattrone C, De Sio M, Autorino R, Pinto JC, et al. Endoscopic Closure of Transmural Bladder Wall Perforations. *Journal of Endourology*. 2012;26:A501-A.
4. Chew BH, Paterson RF, Clinkscales KW, Levine BS, Shalaby SW, Lange D. In Vivo Evaluation of the Third Generation Biodegradable Stent: A Novel Approach to Avoiding the Forgotten Stent Syndrome. *J Urology*. 2013;189(2):719-25.
5. Chew BH, Knudsen BE, Nott L, Pautler SE, Razvi H, Amann J, et al. Pilot study of ureteral movement in stented patients: First step in understanding dynamic ureteral anatomy to improve stent comfort. *Journal of Endourology*. 2007;21(9):1069-75.
6. Barros AA, Duarte ARC, Pires RA, Sampaio-Marques B, Ludovico P, Lima E, et al. Bioresorbable ureteral stents from natural origin polymers. *J Biomed Mater Res B*. 2015;103(3):608-17.
7. Wen C, Lu L, Li X. Mechanically Robust Gelatin–Alginate IPN Hydrogels by a Combination of Enzymatic and Ionic Crosslinking Approaches. *Macromolecular Materials and Engineering*. 2014;299(4):504-13.
8. Mohanty B, Bohidar HB. Microscopic structure of gelatin coacervates. *Int J Biol Macromol*. 2005;36(1-2):39-46.
9. Yan L-P, Wang Y-J, Ren L, Wu G, Caridade SG, Fan J-B, et al. Genipin-cross-linked collagen/chitosan biomimetic scaffolds for articular cartilage tissue engineering applications. *Journal of Biomedical Materials Research Part A*. 2010;95A(2):465-75.
10. Fernandes-Silva S, Moreira-Silva J, Silva TH, Perez-Martin RI, Sotelo CG, Mano JF, et al. Porous Hydrogels From Shark Skin Collagen Crosslinked Under Dense Carbon Dioxide Atmosphere. *Macromolecular Bioscience*. 2013;13(11):1621-31.
11. Silva JM, Caridade SG, Reis RL, Mano JF. Polysaccharide-based freestanding multilayered membranes exhibiting reversible switchable properties. *Soft Matter*. 2016;12(4):1200-9.
12. Silva JM, Caridade SG, Oliveira NM, Reis RL, Mano JF. Chitosan-alginate multilayered films with gradients of physicochemical cues. *Journal of Materials Chemistry B*. 2015;3(22):4555-68.
13. Schlick RW, Planz K. Potentially useful materials for biodegradable ureteric stents. *Brit J Urol*. 1997;80(6):908-10.
14. Schlick RW, Planz K. In vitro results with special plastics for biodegradable endoureteral stents. *Journal of Endourology*. 1998;12(5):451-5.
15. Lumiaho J, Heino A, Tunninen V, Ala-Opas M, Talja M, Valimaa T, et al. New bioabsorbable polylactide ureteral stent in the treatment of ureteral lesions: An experimental study. *Journal of Endourology*. 1999;13(2):107-12.
16. Lumiaho J, Heino A, Pietilainen T, Ala-Opas M, Talja M, Valimaa T, et al. The morphological, in situ effects of a self-reinforced bioabsorbable polylactide (SR-PLA 96) ureteric stent; An experimental study. *J Urology*. 2000;164(4):1360-3.
17. Lumiaho J, Heino A, Kauppinen T, Talja M, Alhava E, Valimaa T, et al. Drainage and antireflux characteristics of a biodegradable self-reinforced, self-expanding X-ray-positive ploy-L,D-

lactide spiral partial Ureteral stent: An experimental study. *Journal of Endourology*. 2007;21(12):1559-64.

18. Chew BH, Lange D, Paterson RF, Hendlin K, Monga M, Clinkscales KW, et al. Next Generation Biodegradable Ureteral Stent in a Yucatan Pig Model. *J Urology*. 2010;183(2):765-71.

19. Zhang MQ, Zou T, Huang YC, Shang YF, Yang GG, Wang WZ, et al. Braided thin-walled biodegradable ureteral stent: Preliminary evaluation in a canine model. *International Journal of Urology*. 2014;21(4):401-7.

20. Richter S, Ringel A, Shalev M, Nissenkorn I. The indwelling ureteric stent: a 'friendly' procedure with unfriendly high morbidity. *Bju International*. 2000;85(4):408-11.

21. Tschada R, Mickisch G, Rassweiler J, Knebel L, Alken P. Success and Failure with Double J-Ureteral Stent - an Analysis of 107 Cases. *J Urologie*. 1991;97(2):93-7.

22. Ramsay JWA, Payne SR, Gosling PT, Whitfield HN, Wickham JEA, Levison DA. The Effects of Double-J Stenting on Unobstructed Ureters - an Experimental and Clinical-Study. *Brit J Urol*. 1985;57(6):630-4.

23. Hoare TR, Kohane DS. Hydrogels in drug delivery: Progress and challenges. *Polymer*. 2008;49(8):1993-2007.

24. Augst AD, Kong HJ, Mooney DJ. Alginate Hydrogels as Biomaterials. *Macromolecular Bioscience*. 2006;6(8):623-33.

25. Young S, Wong M, Tabata Y, Mikos AG. Gelatin as a delivery vehicle for the controlled release of bioactive molecules. *Journal of Controlled Release*. 2005;109(1-3):256-74.

26. Elwood CN, Lange D, Nadeau R, Seney S, Summers K, Chew BH, et al. Novel in vitro model for studying ureteric stent-induced cell injury. *Bju International*. 2010;105(9):1318-23.

27. Dixon JS, Gosling JA. Histology and fine structure of the muscularis mucosae of the human urinary bladder. *Journal of Anatomy*. 1983;136(2):265-71.

28. Olweny EO, Landman J, Andreoni C, Collyer W, Kerbl K, Onciu M, et al. Evaluation of the use of a biodegradable ureteral stent after retrograde endopyelotomy in a porcine model. *J Urology*. 2002;167(5):2198-202.

29. Yang L, Whiteside S, Cadieux PA, Denstedt JD. Ureteral stent technology: Drug-eluting stents and stent coatings. *Asian Journal of Urology*. 2015;2(4):194-201.

Chapter IX

HYDRU**TENT**
NON-DEGRADABLE IS SO 20TH CENTURY®

Business Plan

Chapter IX

Business Plan - HydrUStent

IX-1. EXECUTIVE SUMMARY

IX-1.1. Elevator Pitch:

FOR patients who need temporary urological stents, WHO need to have a second surgery for stent removal, OUR PRODUCT is a degradable stent that will revolutionize the market, PROVIDING lower treatment cost, avoiding second surgery for stent removal, while reducing the risk of infection and eliminates the cases of “forgotten” stents.

IX-1.2. Market Validation:

HydrUStent was validated through a series of contacts with Urologists, experts in the field. All the doctors answered positively when asked if they would you be willing to use biodegradable stents as long as their safety and ease of placement would be demonstrated. Dr. De La Fuente de Carvalho from Hospital de Santo António, Porto stated: “Advantages for patients and less associated costs to health system are two strong reasons for the development of this type of stents”.

IX-1.3. Problem:

Patients who have a ureteral stent require a second surgery for stent removal. Long implantation times, increase the problem of infection and encrustation, which becomes more severe when the stent is “forgotten” in the body. This is often due to lack of availability of the urologist or the patient's own move in the hospital. The crystal deposition on the surface of the stent and infections associated with these stents due to the excessive time may result in loss of the kidney or potentially even death.

IX-1.4. Solution:

HydrUStent is a biodegradable, anti-bacterial urological stent, which eliminates the need for a second surgery, required nowadays for catheter removal. HydrUStent also avoids further complications from infections, due to its antibacterial properties. HydrUStent hydrogel degrades by dissolution of the material in urine avoiding crystal deposition. The dissolution profile is controlled and depending on the material used for stent production, the degradation rate can be tuned from 15 to 60 days of implantation, according to the specific treatment requirements.

IX-1.5. Technology:

The patented technology underlying the production of HydrUStent provides the product its unique advantages. The methodology developed for the preparation of stents with a high water content makes them soft, lubricious and flexible, as well as having adequate biodegradation rates, no encrustation development and anti-bacterial properties. The ability to create a ureteral stent safe for the patient antibacterial and biodegradable it is the main technical advantage of HydrUStent.

IX-1.6. Market Opportunity:

Overall market consumes every year around 137,500 urethral stents, both in Europe (98,000) and USA (39,500), meaning an estimated global revenue of 12 million Euros with an estimated annual growth rate of 8.9%. Furthermore, nearly 78,000 stents are placed worldwide per year in the case of kidney transplants.

IX-1.7. Why Invest:

HydrUStent provides an innovative solution in ureteral stents and it is a major breakthrough in urological market. HydrUStent sales intends to reach 25% of the market by 2020, year in which the breakeven will be achieved. This corresponds to a net profit of 4,948 K€. To seize this opportunity, we need to start now.

IX-2. BUSINESS OPPORTUNITY

Urological disorders greatly affect patients' quality of life. Ureteral stents are used in urological practice in different procedures, in order to minimize pain caused by obstruction of urine flow. Different types of temporary and permanent stents have been introduced into urological practice depending on the treatment and the patients' needs. The indwelling time, i.e., the time of stent implantation, depends on the type of procedure and the complexity of the situation. Available data for Europe refers to the need to implant 97,881 ureteral stents in 2014 (estimation based on sales in 2010) in patients with kidney stones, with an annual growth rate of 8.3%, based on an estimated of a market report from 2010⁹. **Figure XI 1** presents different procedures to manage kidney stones and the number of stents implanted in different countries. The implantation time varies according to the type of procedure and is also presented in **figure IX-1**.

Market segments for urological stents	%	Indwelling time, days
Ureteroscopic lithotripsy	74%	7-14
Percutaneous nephrolithotomy	12%	7-14
Uncomplicated Kidney Stones management	8%	2-3
Benign ureteral stenosis	2%	-
Others	4%	-

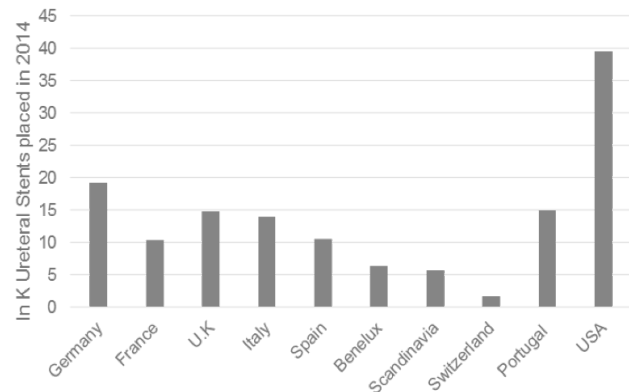


Figure IX-1 Incidence of ureteral stents in urological disorders

The need for a stent is not limited to the treatment of renal calculus. Statistics worldwide show an upward trend in demand for urological stents to address several diseases related to increase life expectancy.

Ureteral stents available on the market are far from the ideal solution. Stents are commonly associated with infections and encrustations. Currently, 80% of the people who have a urological stent are likely to develop a bacterial infection within 30 days of implantation, increasing morbidity

⁹ Stone Treatment Device Market, Report from iData Research Inc., 2010,

threefold¹⁰. So there is still an unmet medical need to reduce the risk of infection associated to urological stents. The existing commercial stents try to overcome this and the last generation of ureteral stents are coated with a hydrogel layer, i.e., HydroPlus™ (Boston Scientific), Universia™ (Cook Medical), Superglide DD™ (Teleflex), Silhouette™ (Applied Medical) and pAguamedicina™ (Q Urological) that is a fully hydrogel stent, but only in use in the pediatric market. To the best of our knowledge, CR Bard and Coloplast do not have, to the best of our knowledge stents with hydrogel coatings in their portfolio. The presence of a hydrogel layer and the high hydration capacity of hydrogels may lead to a significant decrease in bacterial adhesion, as reported in different scientific studies and prevents the deposition of soluble salts and therefore encrustation¹¹.

Some studies reported that for almost 5.9% of patients the stent is left in the body too long¹². This is often due to lack of availability of the urologist or the patient's own move to the hospital for stent removal. The encrustations and infections associated with these stents due to the excessive time may result in loss of the kidney or potentially even death. The problem of infection and encrustation becomes more severe when the stent is “forgotten”.

Another very interesting market for degradable stents is the kidney transplant market. Per year, nearly 78 000 kidney transplants are performed worldwide and each patient requires a temporary stent¹³. In this case, however, the indwelling time corresponds to 6-8 weeks post-op.

This field of research is also quite intensive in academia. The development of biodegradable ureteral stents has been pursued previously, however, despite the positive results obtained with various models, these attempts were abandoned due to biocompatibility issues in porcine ureters or because they degrade in a non-homogeneous, premature or delayed fashions. Poly-Med Inc. has acquired the Uriprene stent, a stent designed to degrade in 10 weeks. A scientific report in 2010 and 2013 claims the validation of the stent after *In vivo* studies performed in a pig model. These studies show that the degradation of the stent may result in some cases in its fragmentation which

¹⁰ Dirk Lange, Chelsea N. Elwood and Ben H. Chew (2011). Biomaterials in Urology - Beyond Drug Eluting and Degradable (Ed.), ISBN: 978-953-307-418-4, InTech

¹¹ Khandwekar A, Doble M. Physicochemical characterization and biological evaluation of polyvinylpyrrolidone-iodine engineered polyurethane. J Mater Sci Mater Med 2011;22:1231–1246

¹² Tang, V. C., et al. (2008). "Ureteric stent card register - a 5-year retrospective analysis." Ann R Coll Surg Engl 90(2): 156-159.

¹³ http://ec.europa.eu/health/blood_tissues_organ/docs/ev_20141126_factsfigures_en.pdf

may lead to the obstruction of the ureter^{14,15}. Poly-Med filed an application to start the first phase of clinical trials of Uriprene in the United States in January 2014. Although Uriprene is not a marketed product this is a direct competitor of our product, HydrUStent. In case the clinical trials are successful Uriprene can reach the market first.

HydrUStent is a biodegradable hydrogel stent designed for temporary treatments. The major opportunity is to offer the market a degradable stent capable of preventing the development of infections and encrustations and overcoming the associated problems. Despite the fact that stent designs have improved over the years, they present one major key disadvantage, which is the fact that they have to be removed surgically. Avoiding a secondary procedure to remove the ureteral stent is highly desirable, as it would decrease patient morbidity and make this technology attractive. **Figure IX 2** highlights the uniqueness of HydrUStent in comparison with commercially available stents.

The introduction of this new generation of bioresorbable urological stents in clinical practice will, in which concerns the kidney stone management:

- Reduce by 137,500 the number of surgical procedures in Europe and the United States,
- Reduce the hospital costs associated with these second surgeries by 137.5 million euros;
- Increase patients' comfort and
- Improve the quality of care.

¹⁴ Chew, B. H., et al. (2010). "Next generation biodegradable ureteral stent in a yucatan pig model." J Urol 183(2): 765-771.

¹⁵ Chew, B. H., et al. (2013). "In vivo evaluation of the third generation biodegradable stent: a novel approach to avoiding the forgotten stent syndrome." J Urol 189(2): 719-725.

Company	Ureteral Stent	Anti-Bacterial / encrustation	Hydrogel	Degradable
 Boston Scientific Advancing science for life™	HydroPlus™	✓	✓	✗
 Urological	pAguamedicina™	✓	✓	✗
 COOK MEDICAL	Universa™	✓	✓	✗
 Teleflex	Superglide DD™	✓	✓	✗
 Applied Medical	Silhouette™	✓	✓	✗
 BAIRD	Inlay™	✓	✗	✗
 Coloplast	Biosoft duo™	✓	✗	✗
 PMI POLY-MED, INC.	Uriprene™	✓	✗	✓
 Aqua Urological	HydrUStent	✓	✓	✓

Figure IX-2 Uniqueness of HydrUStent in comparison with commercially available stents

Some of the doctors we have contacted corroborate our assumptions:

“The problem of lower urinary tract symptoms (LUTS) and encrustation are the main ones. The short life of this stent means that encrustation will not be a problem, although the LUTS remain.”

Dr. Fin Macneil, Member at Royal Australian College of Surgeons (RACS) Board of Urology

“I think stent symptoms can be quite disabling. A more flexible stent would help.”

Dr. Deepak Batura, Consultant Urological Surgeon at Ealing Hospital NHS Trust

“No symptoms (LUTS) and no need to remove while still doing its job of draining the kidney”

Dr. Hilten Patel, (Professor of Surgery & Urology, and Director of Robotic Urological Surgery, University Hospital North Norway and Director of Surgical Urology Simulation Training, Bart's & The London, Queen Mary University of London)

“My reflex response is that a biodegradable stent for kidney transplantation is a gift to the surgeon and the patient.”

Dr. Peter Madras, (Kidney transplant surgeon, Lahey Health)

HydrUStent hydrogel degrades by dissolution of the material in urine circumventing the degradation in blocks and hydrolysis of the material in toxic residues, which may compromise the product biocompatibility. The dissolution profile is controlled and depending on the material used for stent production, the degradation rate in urine can be tuned from 15 to 60 days of implantation and no large crystal deposits which can obstruct the ureter are observed¹⁶.

The patented technology underlying the production of HydrUStent provides the product its unique advantages. The process developed for the preparation of stents with a high water content makes them soft, lubricious and flexible, as well as having adequate biodegradation rates, no encrustation development and anti-bacterial properties. The main technical advantage of HydrUStent is the ability to degrade within the therapeutic window, overcoming the possibility of bacterial colonization, biofilm formation and infection and being able to be eliminated from the body without the need for surgery to remove it.

In 2012, after a provocative presentation of Dr. Estevão Lima, on the panel “Ideas Out of the Box” at the 1st ICVS/3B’s Associated Laboratory meeting, the team started this project. Lima’s vision was to develop a degradable ureteral stent that could avoid stent removal as well as possible infections due to long term implantation. The team has been working together since then to design and mitigate the technological risks associated with HydrUStent. The Feature-Advantage-Benefit (FAB) analysis of HydrUStent is represented in **table IX-1**.

Table IX-1 Feature-Advantage-Benefit (FAB) model of HydrUStent

Feature	Advantage	Benefit
Degradable	Avoids second surgery	Reduce costs
Anti-bacterial	Avoids biofilm formation and encrustation	Reduce risk of infection
Hydrogel (constituted by 94% water)	Soft and flexible material	Increase patient comfort

Even though our product is targeted to urological patients our payers will be health insurances or the National Health System, depending on the country’s healthcare systems. The benefits associated will not only be advantageous for the patients but also for the payer. In Portugal the

¹⁶ Barros, A. A., et al. (2014). "Bioresorbable ureteral stents from natural origin polymers." J Biomed Mater Res B Appl Biomater.

costs associated with the procedure for stent removal were estimated to be nearly 1000 euros/patient, according to Dr. La Fuente from Santo António Hospital, Porto, Portugal. Citing Dr. La Fuente:

“Another great advantage is that it does not need a second surgery, to remove the stent, and so the patient has no job loss or admission to hospital, facilitates recovery and professional and social integration. There is a reduction in costs for the health system.”

In the United States, according to the US Medicare reimbursement plan for ureteral stent placement and removal, in 2014, the costs associated with the removal of the ureteral stent vary between 634€ and 1871 € depending on the complexity of the procedure¹⁷.

The **major benefit** for the payer is a **reduction of 60% of the costs of the kidney stone treatment, due to the fact that a second surgery is avoided**. Currently, per year, nearly 39,500 patients in the United States and 98,000 patients in Europe require a ureteral stent for kidney stone management. These account for **137,500 surgical procedures** in Europe and in the US. That can be **avoided with HydrUStent, saving up to 137.5 million Euros**. The costs estimated do not account for the infection problems that may be associated and the increase in treatment costs that may arise hereafter. The cost of commercially available stents from Coloplast, Porges is within the range of 25 to 90 euros, according to Ângelo Maria, sales representative from Iberia. These stents however do not provide the same value as HydrUStent. The HydrUStent price can be estimated at 180 €.

IX-3. BACKGROUND

The technology has been developed under a quality management system (QMS), established at the 3B´s research group. The QMS follows the ISO 9001:2008 that complies with ISO 13485 and is a quality management system standard specifically for the medical devices industry.¹⁸ In particular, this technology relates to a process based on several successive steps which comprise:

- i) formation of a flexible polymer tube from an aqueous solution of a natural polymer;
- ii) injection of

¹⁷ Lam, J. S. and M. Gupta (2002). "Tips and tricks for the management of retained ureteral stents." J Endourol 16(10): 733-741.

¹⁸ http://www.3bs.uminho.pt/sites/default/files/iso9001_2008.pdf

the polymer solution in a mold, iii) gelification of the tube by physical crosslinking iv) dehydration and drying of the product.¹⁶

According to the technology readiness level (TRL) the team classifies the proposed technology at TRL 6¹⁹, i.e., the main components have been validated and a prototype has been developed. The team has been granted 10 thousand euros funding by the Associated Laboratory ICVS/3B's to start working on the development of materials to proceed to the first *In vivo* testing. The scale up of the technology has been done and the demonstration of the product has been assessed in a pig model bringing the technology to TRL 6. The formulation is now frozen, biocompatibility, extractables and leachables testing were carried out and the results indicate that the material is indicated and do not present signs of toxicity for human use. **Figure IX 3** demonstrates the stage of development of HydrUStent and the envisaged next steps.

The project has been awarded the grand prize Innovation Award from Novo Banco (Lisboa, Portugal, 2015), has won the Venture Forum Competition (Worcester, Massachusetts, USA 2015) and was awarded an honorable mention by Bluepharma/University of Coimbra Innovation Award (Coimbra, Portugal, 2015).

The technology has been protected by a patent application submitted in Portugal. PT Patent PI106593, registered on 19/10/2013, was published in Revista de Propriedade Industrial, 77/2014, on March 21, 2014. The team has recently submitted the PCT application with reference PCT/IB2016/052875 on the 17.05.2016, related with the national patent application to the National Patent Office (INPI) with priority date of 14.05.2015 number 108476, entitled "A composition for ureteral stent and method thereof", Rui L. Reis, Ana Rita C. Duarte, Alexandre A. A. Barros, Estêvão de Lima, Carlos Oliveira e Jorge Correia-Pinto and to the European Patent Office (EPO) on the 26.05.2015 number 15169249.8. The team has submitted a patent application which entitled: "Biodegradable ureteral stents: new approach for urothelial tumors of upper urinary tract cancer", Rui L. Reis, Ana Rita C. Duarte, Alexandre A. A. Barros, Estêvão de Lima, Carlos Oliveira, to the Biodegradable ureteral stents: new approach for urothelial tumors of upper urinary tract cancer", application 109229, registered on 11/03/2016. The applicant of the patent is A4TEC, Association for the Advancement of Tissue Engineering Cell based Technologies & Therapies who has signed a technology transfer agreement to HydrUStent.

¹⁹ Technology readiness levels (TRLs) are measures used to assess the maturity of evolving technologies.

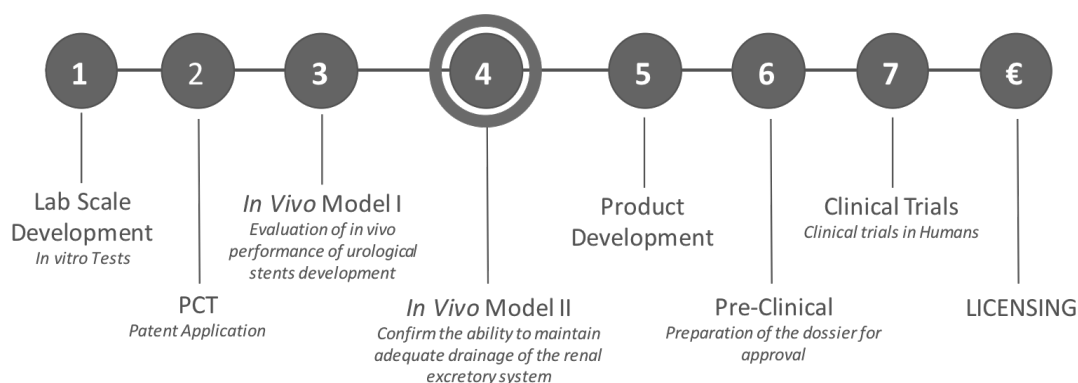


Figure IX-3 HydrUStent stage of development and next steps.

To validate our product, we prepared a survey and we have sent it to 54 urologists. The objective of the survey was to understand the problems associated with the current solutions and to evaluate the willingness to change to a new product. 47% of the doctors answered our survey.

Table IX 2 summarizes the results obtained. The doctors were also asked about the desired features a ureteral stent should have in order to meet patients’ needs and improve their comfort.

Figure IX 4 summarized the features preferred.

Table IX-2 Results obtained from the doctors survey about the problems associated with the current solutions for ureteral stents.

Question	Yes	No	Comments
Do you have experience of complaints of Lower Urinary Track Symptoms (LUTS) in your patients with double J ureteral stents?	100%	0%	Dr. Herrmann from Hannover Medical School states that: “from our database more than 60% (presents LUTS symptoms), 15 % (take) medication, 1.7% can ’t stand double Js at all”
Do you think your patients would be happy if it would be possible to avoid a second term intervention for stent removal?	92%	8%	8% stated they usually use a stent with a thread for stent removal
Do you think biodegradable double J ureteral stents would be beneficial?	100%	0%	Dr. Günter Janetschek, from the Dept. of Urology, Salzburg Medical School further refers that “This would solve the problem of the cystoscopy for removal as well as that of the “forgotten stent”.
Would you be willing to use biodegradable stents as long as their safety and ease of placement would be demonstrated?	100%	0%	_____
Do you consider that the introduction in the market of a	80%	20%	Two of the doctors referred that price would dictate the adoption of these type of stents.

**biodegradable stent would definitely
change the current clinical practice in
urology?**

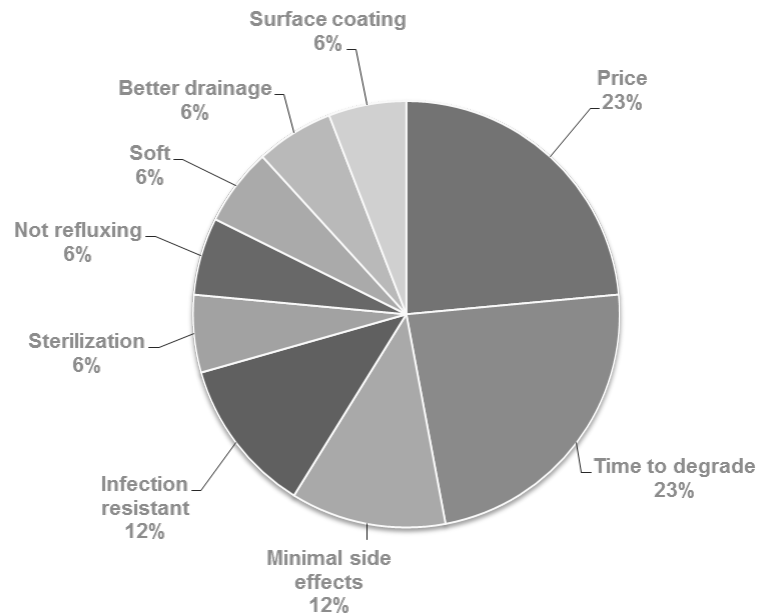


Figure IX-4 Desired features of ureteral stents as referred in the survey

Doing good with science is our vision. Our mission is to develop new medical devices that meet patient needs, improving their quality of life. The road between research and commercialization is still long and one of the goals of the team when participating in a program like BGI – Building Global Innovators – is to be able to leverage our research into marketed products, which can in fact touch people’s lives and make a difference.

We estimate that in 3 years after investment we will reach the market after having the required regulatory approvals. To successfully achieve this, we need 1.5 M Euros for the first pre-clinical and clinical trials, respectively. **Table IX 3** presents the project roadmap where the milestones and the funding required to achieve them are presented.

Table IX-3 HydrUStent project roadmap (Months after Investment)

Milestone	Completion date	Funding Need	Investment required
<i>In vivo</i> II	6 months	25 k€	25 k€
Clinical Evaluation Report	6 months	30 k€	30 k€
Production process under GMP conditions	6 months	100 k€	100 k€

IP - National applications	6 months	6 k€	6 k€
Product development	1 year	10 k€	10 k€
Personnel and administrative Costs	-	175 K€	175 K€
Subtotal		256 k€	256 k€
Completion of pre-clinical trials (GLP conditions)	1 year	100 k€	100 k€
Clinical trials	3 years	653 k€	653 k€
FDA 510k premarket application	3 years	100 k€	100 k€
Personnel and administrative Costs	-	296 k€	296 k€
Subtotal		1,149 k€	1,149k€
TOTAL		1,405 k€	1,405k€

The regulatory process is long and we believe we have the opportunity to start now. HydrUStent intends to pursue clinical trials and prepare and submit the FDA 510(k) premarket notification. A regulatory affairs consultant will be hired to ensure the success of the process. After approval the team intends to initiate sales to specialized distributors in Europe and US that have a strong foothold in the ureteral stent market.

The team intends to continue inventing new medical devices and develop a portfolio of products for urological complications, driving innovation in the urology field. The “Silver Tsunami” of an aging population and the continued rise of chronic diseases like obesity and diabetes which are connected with urological disorders offer a growth opportunity in the future. To seize this opportunity, we need to start now.

IX-4. . GO TO MARKET STRATEGY

The HydrUStent team of the University of Minho will establish a strategic partnership with the Clinical Academic Center – Braga (2CA-Braga) for the translation of research into clinical practice as a showcase pilot to demonstrate the success of the proposed new medical device. This center provides services in which clinicians and researchers monitor and manage the health status of the population while at the same time have a comprehensive clinical platform for data gathering and retrieval.

IX-4.1. Value Proposition

For the 215,500 patients who need temporary urological stents that require a second surgery for stent removal, our product is a biodegradable stent that reduces bacterial adhesion by 98%¹⁶

and decreases the treatment costs by 60%. Unlike our competitors' marketed products, our product is degradable and avoids the need for a second surgery. Our product is a kit which includes not only the biodegradable HydrUStent, but also a guidewire and a pusher for insertion. Competitors' kits also have the accessories for stent insertion.

IX-4.2. Industry Analysis/Competitive Environment

The urological medical device industry is a consolidated industry dominated by few major players, namely Boston Scientific, Cook, Coloplast and C.R. Bard. Boston Scientific and Cook Medical have a high share of their resources invested in research and development. Boston Scientific reports in their 2013 annual report an investment of 12% of sales in R&D. Boston Scientific reports in the annual report of 2012 a decrease in sales of the division of urology and women's health from 2011, but still standing at € 386 M and corresponding to 7% of the total sales of the company²⁰. This decrease is due to a contraction of the market justified by new regulations enforced by the FDA in 2011. However, in their annual report Boston Scientific shares their vision to increase the market share and growth in the urological market. A similar trend was reported in the annual report of the C.R.Bard. C.R. Bard reports in 2013, total sales of € 2.31B, of which 25% is sales in urology.²¹ C. R. Bard also reports in their 10K 2013 report a growth of consolidated sales of 1% of urological basic drainage devices, in which the stents are included. Table IX-4 summarizes the competitive landscape of the urological device market.

Table IX-4 Competitive landscape of urological device market

	HydrUstent	Boston Scientific	C.R. Bard	Coloplast	Cook Medical
Products and services	Ureteral stents	Medical devices	Medical devices	Medical devices	Medical devices
Net Sales	-	€ 5,791 M ²²	€ 2,436 M ¹⁵	€ 4.2 M ²³	€ 1,590 M
Net Income	-	€ 475 M	€ 551 M	€ 1.1 M	

²⁰ <http://www.bostonscientific.com/templatedata/imports/HTML/2012ar/downloads/BostonScientific-2012-Form-10-K.pdf>

²¹ <http://www.sec.gov/Archives/edgar/data/9892/000119312514058921/d624566d10k.htm>

²² US Dollars to Euros - exchange rate used was 0.7882 USD/EUR.

²³ DK Danish Krone to Euros - exchange rate used was 0.134 DK/EUR

Target market (urological sales)	-	€386 M	€588 M	€151 M	
Annual growth (%)	-	5%	3%	6%	7%
R&D investment		12%	9.7%	11%	
Competitive advantage	Degradable stent	Hydrogel stent with reduced risk of infection	—	—	Hydrogel stent with reduced risk of infection
State of development	<i>In vivo</i> validation	Market	Market	Market	Market

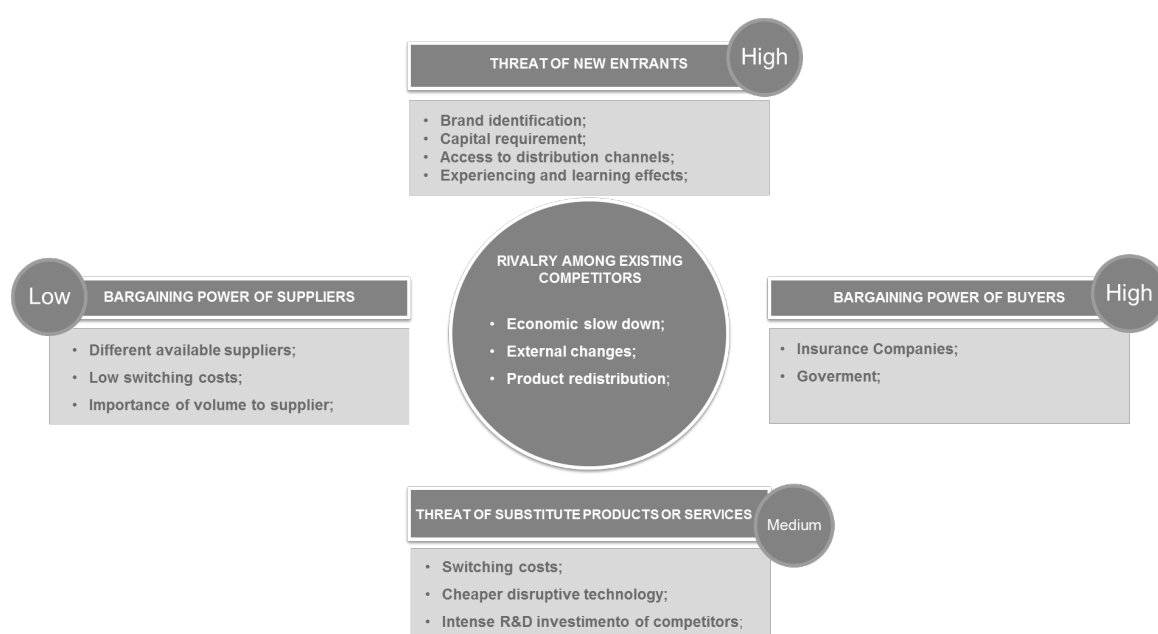


Figure IX-5 HydrUStent Porter’s five force analysis

The two features that make HydrUStent difficult to replicate by other players are the designed degradation profile and the degradation of the material itself. HydrUStent presents a slow dissolution profile in urine, which confers it the degradation properties required, in the time frame necessary for kidney stone management. Other products have been designed to degrade within two weeks of implantation, yet in some cases residues of the material block the ureter and obstruct the urine flow. The production method of HydrUStent has been patented and the unique characteristics of our product can only be achieved following the described methodology. Patent infringement by other companies can be, hereafter, policeable. The team is further working on a patent landscape report.

The major barriers to market entry are related with the threat of a new product entering the market is also possible due to the long time to market associated with the estimated time for completion of the clinical trials and the regulatory approval. HydrUStent intends to enter a fearless competitor market dominated by a few major players, however these major players do not present any degradable stent in their portfolio. BARD claimed when asked if they would see this as competition that **“it is much more an opportunity for BARD to have a differentiating product”**, Ben Jackson, Biomedical division BARD.

HydrUStent's business model (figure IX-6) takes into account the threats but also the opportunities in this market. To overcome some of the identified threats we need to engage key opinion leaders (KOL) in the urology field starting with the demonstration of our product at the European Association of Urology section on Uro-Technology²⁴. We already have validated our concept, with some members of this group, whom we have contacted to answer our survey. The endorsement of our product by this prestigious group in the area of urology, who are strong KOL's will be a starting point to gain credibility in other countries outside Europe.

HydrUStent																										
Key Partners <ul style="list-style-type: none"> • Key Opinion leaders (Physicians, Urological Associations); • Hospital Administrators; • Insurance companies • Contract Manufacturing Organization (EOM); • Distributors; 	Key Activities <ul style="list-style-type: none"> • R&D; • Supply Chain/ Operations management; • Regulatory; • Health Economics; 	Value Proposition <ul style="list-style-type: none"> • Newness; • Reduce risk of infection; • Avoid the second surgery; • Increase patient flow • for NHS and insurance companies- Reduction of treatment cost by 60% 	Customer Relationships <ul style="list-style-type: none"> • Face to Face (personal assistance, exhibitions); 	Customer Segments <ul style="list-style-type: none"> • Decision makers at Public Hospitals; • Decision makers at Private hospitals; 																						
Key Resources <ul style="list-style-type: none"> • Intellectual property; 	Channels <ul style="list-style-type: none"> • Medical device distributors; 	<table style="width: 100%; border-collapse: collapse;"> <tr> <td style="width: 50%;">Revenue Streams</td> <td style="width: 50%;"></td> </tr> <tr> <td style="vertical-align: top;"> <ul style="list-style-type: none"> • Product Sales, annual contracts with customers </td> <td style="text-align: right; vertical-align: top;"> <table style="width: 100%; border-collapse: collapse;"> <tr> <td style="width: 80%;"></td> <td style="text-align: right;">Sales</td> <td style="text-align: right;">100%</td> </tr> <tr> <td></td> <td style="text-align: right;">Cost of Good Sold</td> <td style="text-align: right;">6%</td> </tr> <tr> <td></td> <td style="text-align: right;">Gross Margin</td> <td style="text-align: right;">94%</td> </tr> <tr> <td></td> <td style="text-align: right;">Administrative & Marketing</td> <td style="text-align: right;">30%</td> </tr> <tr> <td></td> <td style="text-align: right;">R&D</td> <td style="text-align: right;">10%</td> </tr> <tr> <td></td> <td style="text-align: right;">Operating Profit</td> <td style="text-align: right;">54%</td> </tr> </table> </td> </tr> </table>			Revenue Streams		<ul style="list-style-type: none"> • Product Sales, annual contracts with customers 	<table style="width: 100%; border-collapse: collapse;"> <tr> <td style="width: 80%;"></td> <td style="text-align: right;">Sales</td> <td style="text-align: right;">100%</td> </tr> <tr> <td></td> <td style="text-align: right;">Cost of Good Sold</td> <td style="text-align: right;">6%</td> </tr> <tr> <td></td> <td style="text-align: right;">Gross Margin</td> <td style="text-align: right;">94%</td> </tr> <tr> <td></td> <td style="text-align: right;">Administrative & Marketing</td> <td style="text-align: right;">30%</td> </tr> <tr> <td></td> <td style="text-align: right;">R&D</td> <td style="text-align: right;">10%</td> </tr> <tr> <td></td> <td style="text-align: right;">Operating Profit</td> <td style="text-align: right;">54%</td> </tr> </table>		Sales	100%		Cost of Good Sold	6%		Gross Margin	94%		Administrative & Marketing	30%		R&D	10%		Operating Profit	54%
Revenue Streams																										
<ul style="list-style-type: none"> • Product Sales, annual contracts with customers 	<table style="width: 100%; border-collapse: collapse;"> <tr> <td style="width: 80%;"></td> <td style="text-align: right;">Sales</td> <td style="text-align: right;">100%</td> </tr> <tr> <td></td> <td style="text-align: right;">Cost of Good Sold</td> <td style="text-align: right;">6%</td> </tr> <tr> <td></td> <td style="text-align: right;">Gross Margin</td> <td style="text-align: right;">94%</td> </tr> <tr> <td></td> <td style="text-align: right;">Administrative & Marketing</td> <td style="text-align: right;">30%</td> </tr> <tr> <td></td> <td style="text-align: right;">R&D</td> <td style="text-align: right;">10%</td> </tr> <tr> <td></td> <td style="text-align: right;">Operating Profit</td> <td style="text-align: right;">54%</td> </tr> </table>		Sales	100%		Cost of Good Sold	6%		Gross Margin	94%		Administrative & Marketing	30%		R&D	10%		Operating Profit	54%							
	Sales	100%																								
	Cost of Good Sold	6%																								
	Gross Margin	94%																								
	Administrative & Marketing	30%																								
	R&D	10%																								
	Operating Profit	54%																								
Cost Structure <ul style="list-style-type: none"> • Human Resources (R&D / Sales); • R&D; • Outsourced manufacturing; • Consultants for regulatory affairs • Marketing; 																										

Figure IX-6 HydrUStent business model canvas

²⁴ http://www.uroweb.org/sections/uro-technology-esut/?no_cache=1

Manufacturing of HydrUStent will be outsourced. The team has contacted Stanipharm²⁵ as our contract manufacturing organization (EOM), a specialized company in the development of pharmaceutical/medical products using supercritical fluid technology in GMP conditions, located in France. The team has already identified different suppliers to guarantee the manufacturing of our product. In this sense the possibility to switch suppliers with low costs does not offer a major threat to the business.

Key activities and key resources are related with the major strengths of HydrUStent, i.e., the knowledge generated, the IP protected technology and the possibility to create a product portfolio. In this sense the team has been working on the development of drug-eluting stents, particularly for addressing upper urinary tract urethelial cancer. The team has submitted a provisional patent application.

Hospitals already buy ureteral stents and in this sense we envisage that HydrUStent will be sold to hospitals as consumable products for daily procedures. Typically medical devices are sold to healthcare providers who are not always the ultimate payers of the product. HydrUStent may also be sold directly to physicians who perform the procedure in their own private practices. The payers will be, depending on the country, the National Health System and/or insurance companies. HydrUStent will hire a sales manager in each country, where sales are planned. The presence of a sales representative will contribute to the acceleration of market penetration through a direct contact with the providers. Medical devices are mostly promoted directly to healthcare professionals. Two approaches will be followed to promote and advertise our product.

Promotion of HydrUStent to doctors, who are the influencers and to the providers, will be done by technical team at major urological conferences and meetings or trade fairs. When the product has been accepted by the medical community, HydrUStent will need a strong sales force in order to promote and disseminate the novel product and increase sales.

Distribution of HydrUStent products will be outsourced. Companies that already have an established distribution network for medical devices will be subcontracted to maximize the distribution and increase market penetration. The company sales manager will work together with the distributors in the region to promote HydrUStent sales.

²⁵ <http://www.stanipharm.fr/>

IX-4.3. Pricing and Costing

The different categories in the HydrUStent production cost of are shown and estimated in Table IX-5 for a single unit.

Table IX-5 Unit Cost breakdown for HydrUStent production

Description	Units	Product Type	Component Cost (€/unit)	Input Quantity	Yield (%)	Product Cost (€)
raw material 1 ²⁶	kg	Purchased	415.00	0.00092	90.00	0.34
raw material 2	kg	Purchased	133.00	0.00048	90.00	0.06
raw material 3	Kg	Purchased	107.40	0.00534	100.00	0.57
raw material 4	L	Purchased	4.00	0.10	100.00	0.40
raw material 5	L	Purchased	0.75	0.22	100.00	0.17
raw material 6	Kg	Purchased				
raw material 7	Kg	Purchased	1.81	0.05	100.00	0.09
Processing -stage 1	hours	Manufactured	0.2081	0.75	100.00	0.00
Labour I	hours	Purchased	6.50	1.00	100.00	0.07
Processing stage 2		Manufactured	0.2081	0.75	100.00	0.01
Labour I	hours	Purchased	6.50	5.00	100.00	0.33
Processing stage 3		Manufactured	0.2081	0.75	100.00	0.00
Labour I	hours	Purchased	6.50	3.00	100.00	0.20
Distributors						8.53 ²⁷
TOTAL						10.77

²⁶ Raw materials costs were based on the prices from Sigma-Aldrich, an academic R&D supplier. The suppliers of our raw materials will be other who sells in larger scale for production purposes.

²⁷ Quotation obtain from Palex medical (member a network of European Medical Device Distributors –EMDDA) for a 2000 stents/year for sale in Europe-www.palexmedical.com

The value generated to the payer comes from the savings that the payer will have from the elimination of a second surgery. **The cost of the treatment decreases by 60%** when HydrUStent is chosen instead of currently available stents. Our pricing will take this into consideration.

HydrUStent will be sold at **180€** each corresponding to an approximate **gross margin of 94%** per device. The price is in average twice as much as the commercially available stents. This number is justified by the 60% savings provided to hospitals with the elimination of a second intervention and the reduction of infections currently associated with ureteral stents. To justify the higher price and address Doctor's concern about pricing we will need to generate robust health economics reports that clearly show how both payers and patients economic benefits from adopting HydrUstent.

IX-5. MILESTONES AND ACTION PLAN

HydrUStent has been developed at laboratory scale and the team has already scaled up the technology for up to a prototype development. HydrUStent product development needs to be in accordance with the guidelines of FDA regulation for Ureteral Stents, 21 CFR 876.4620 (a)²⁸. Furthermore, it is also required to be in accordance with the guidelines of the European commission MEDDEV. 2.7.1 Rev.3²⁹ and the guidelines reported on the European Guidance documents NBOG BPG 2009-1 (Guidance on design dossier examination and report content)³⁰ the preparation of the dossier for approval requests the presentation of information related with: i) Manufacturer details; ii) Details relating to the application and Notified Bodies review (including staff and experts involved in the review and the aspects assessed by each, signatures of responsible reviewers etc.); iii) Device description and product specification; iv) Classification; v) Requirements regarding manufacturing; vi) Requirements regarding design and construction; vii) Pre-clinical evaluation; viii) Clinical evaluation/performance evaluation; ix) Other applicable Directives; x) Risk analysis and risk management; xi) Review of declaration of conformity; xii) Post-market surveillance and xiii) Summary of review.

²⁸ <http://www.fda.gov/MedicalDevices/DeviceRegulationandGuidance/GuidanceDocuments/ucm081346.htm>

²⁹ http://ec.europa.eu/health/medical-devices/files/meddev/2_7_1rev_3_en.pdf

³⁰ http://www.nbog.eu/resources/NBOG_BPG_2009_1.pdf

The team's objective within the next 18 months is to start the preparation of the application dossier for approval. The team will need to contract a regulatory affairs consultant with a strong insight on both US and European regulations. Particularly the team will be strongly committed to fulfill the requirements for product manufacturing, design and production as well as in the pre-clinical evaluation. The milestones, actions and timescale are hereafter envisaged to achieve this goal. Particularly pre-clinical evaluation involves the following³¹:

- 1- a list of all materials in direct or indirect contact with the patient or user, including the concentration of the materials
- 2- detailed information on biocompatibility testing and biological evaluation and must clearly show the suitability, safety and biocompatibility of all materials used (biocompatibility – EN ISO 10993)
- 3- detailed information on any studies in animal models, i.e., study objectives, methodology, results, analysis and conclusions including rationale and limitations for the selected model(s)

1 and 2 have been addressed by the team and have been reported in a scientific article published by the HydrUStent team³². The first studies on animal models have started in early March 2015 and since then the team has worked to optimize the formulation and ensure a good *In vivo* performance of the biodegradable stents. The validation in a pig model has been successfully achieved. The *In vivo* validation was performed at the ICVS – Life and Health Sciences Research Institute, where state of the art equipment is available to do so.

The Product Roadmap involves the *In vivo* validation of the product in GLP conditions and after the design and implementation of the clinical trials. HydrUStent is classified as a class II medical device. The extension of the clinical trials necessary will be done after the design of a product development plan for which the team has already met with different CRO, namely BlueClinical in Portugal, Med Pass in France and NAMSA and Health R&D, LLC in the US to provide us consultancy on this matter.

HydrUStent team has contracted legal advisors, namely Dr. Anabela Carvalho from Patents.PT to follow the PCT patent application and the family of patents hereafter. Additionally, HydrUStent

³¹ Park, J. C., et al. (1999). "Preclinical evaluation of prototype products." *Yonsei Med J* 40(6): 530-535.

³² Barros, A. A., et al. (2014). "Bioresorbable ureteral stents from natural origin polymers." *J Biomed Mater Res B Appl Biomater*.

has also worked with the attorney company Garrides and has a complete full patent landscape report on the subject.

Table IX-6 Milestone Actions and deadline set for HydrUStent development.

	Milestones	Actions	Funding €
1	In vivo validation – part II	Conduct a study of stent biocompatibility and performance with clinical evaluation in a pig model Document the evolution of drainage capacity as a function of time and the degree of degradation of the material Conduct necropsy study with histological evaluation of renal and ureteral tissue	25,000
2	Prototype product	Develop HydrUStent, following the guidelines required for the first in-human studies	80,000
	Product development	Design of brand and package	10,000
3	IP Protection	National applications	6,000

The next steps of the product development plan include the development of the HydrUStent package. The team has started working on the design of the packaging and product leaflet (Instructions for Use, or IFU). Furthermore, key validations associated with product development are selection of the guidewire and pusher from commercially available products. The second key validation is the design and development of packaging. It is necessary to select the appropriate packaging materials able to be sterilized and ensure that the sterility of the product is maintained when stored. Part of this key validation is development the product brochure and labeling of the package, in accordance with the guidelines. In this brochure, the instructions for use of HydrUStent and accessories will be described. According to the milestones defined and the resources needed the team has estimated the necessary budget, as shown in **table IX 7**.

Reducing the risk of failure of HydrUStent is the objective of the team when setting these Milestones-Actions-Deadlines. The team is actively committed towards the development of the product and has been pursuing other sources of funding to ensure that the milestones defined are achieved. Each milestone reached will increase the HydrUStent value. HydrUStent value can be further increased if KOL's validate our product. Expert urologists will be contacted to participate in the first clinical trials. In this sense they will be engaged in the project from the beginning, contributing to the promotion and validation of the product.

In case something goes wrong and we run out of funds the team will continue to raise money with different joint-venture and affiliate partners to finish product development. The team may invest their own money in the company to reach the milestones. The team is also pursuing funding

through the application of project proposals in different scientific grant proposals both via National and European scientific agencies. In case the bootstrapping strategy of the team fails the team can sell part or all of the company

IX-6. INVESTMENT AND KEY FINANCIAL INDICATORS

The team has estimated the pro forma financial statements to project the financial performance of HydrUStent through the next eight years of operation. These statements take into account the costs estimated and presented in **table IX 7** and estimated figures however they are supported on sound assumptions and market data (attached are disclosed the assumptions made). **Table IX 8** and **table IX 9** present the forecast P&L and cash flow figures, estimating that HydrUStent will be able to start commercialization by 3 years after investment.

The industry reference numbers used in these assumptions balance the uncertainty due to the very early stage of the project. The following assumptions were considered:

- The entry market segment will be uncomplicated kidney stone management (8% ureteral stent market); in the second year, we intend to consolidate this market and prepare the uteroscopic lithotripsy market to start selling in the 3rd year.
- At the same time HydrUStent intends to start selling, in 4th year for kidney transplant market
- Regarding the region segments HydrUStent will start selling in Europe in 3rd year, entry into the US in 4th year and rest of the world in 6th .
- The finance account takes into consideration the cost of stent produced including the distribution cost with a final cost of 10,70€. HydrUStent will be sold at 180€/stent.
- The industry spends on average, 10% of the revenues on R&D and 30% of the revenues on administrative and marketing expenses.

Table IX-7 Forecasted P&L statement (all figures in '000 EUR)

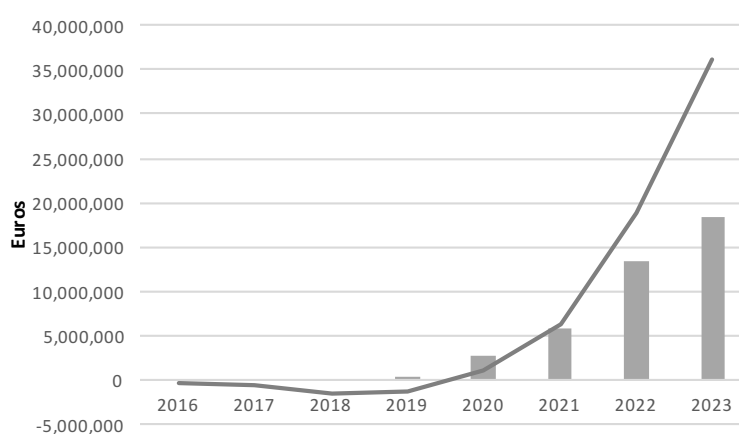
Years after investment	1	2	3	4	5	6	7	8
Total Sales	0	0	0	300	2,671	5,723	13,339	18,322
Cost of goods	0	0	0	18	163	349	815	1,120
Gross Profit	0	0	0	281	2,508	5,373	12,524	17,201
R&D	175	150	850	30	267	572	1,334	1,832
SG&G	100	90	160	175	202	202	202	310
EBITDA	(275)	(240)	(1010)	76	2,038	4,599	10,987	15,060

Net Profit	(275)	(240)	(1010)	95	2,202	4,948	11,803	16,179
-------------------	-------	-------	--------	----	-------	-------	--------	--------

Table IX-8 Forecasted Cash Flow statement (all figures in '000 EUR)

Years after investment	1	2	3	4	5	6	7	8
Net Profit	(275)	(240)	(1010)	(576)	2,202	4,948	11,803	16,179
Capex (-)	27	5	0	4	0	0	0	0
Depr./Amortization (+)	0	0	0	18	163	350	815	1,119
Free Cash Flow	(275)	(245)	(1010)	117	2,365	5,298	12,618	17,299
Cumulative Cash Flow	(275)	(492)	(1502)	(1,385)	980	6,278	18,895	36,194
Break Even Year	2020							

The financial projections in revenues and cash flow (million €) are presented in figure **IX-7**.

**Figure IX-7 Eight years' financial projections for HydrUStent**

According to the investment required; costs of product development and time to market the team projects that breakeven will be **achieved in 5th year** after investment, **the 2nd year of sales**.

Our exit strategy envisages the possibility to be acquired by one of the major players in the market. For companies like Boston Scientific or Bard it is easy to implement our product in their product portfolio, because they already have all the structure required, distribution channels secured and contacts to launch the product. The team has met BARD and Boston Scientific in their facilities in Boston, MA in the past month of September and the feedback the team had was very enthusiastic. Boston Scientific has visited our facilities late September following our meeting and was very impressed with the product, demonstrating interest in partnering with us after the first *in vivo* validation has been successfully completed.

IX-7. MAJOR RISKS AND MITIGATIONS STRATEGIES

The team has identified different types of risks associated with the proposed project. We have ranked them according to the likelihood of occurring as 1 being low risk and 5 high risk (table IX-9).

Table IX-9 Risk assessment of HydrUStent

Type of risk	Specification	Comments	Rank
Technological risks	In vivo I Animal model	This study will be a first validation of the product. The results from this study will evaluate potential changes caused by biodegradable stents, assess the complete degradation / residual catheter and evaluate evaluation in the case of fragments of their dimensions and assessment of bacterial leakage.	2
	In vivo II Animal model	The second study is a study of survival with clinical evaluation and analytical specimens with documentation of the evolution of renal function and signs of infection. It is expected to get the documentation of the evolution of drainage capacity as a function of time and the degree of degradation of the material as well as a necropsy study with histological evaluation of renal and ureteral tissue.	3
	Pre-clinical evaluation	Prepare the clinical dossier for submission.	3
	Clinical trials	The product translation from pig model to humans may fail. When approved, minimize FDA/ EMEA warning letters relating to our product.	4
Product risk	Duration risk	The extended duration of the project increases the product risk. The risk of a similar product to enter the market within this timeframe should not be disregarded.	2
	Entry of a competitor product	This does not invalidate the commercialization of HydrUStent but to be the first to market would be advantageous.	3
Regulatory risks	Quality	Defects, failures or quality issues can result in serious consequences for patients.	3
	FDA approval CE certification	The failure to be accepted as a new medical device that can be used in current clinical practice may invalidate the project.	2
Entrepreneurial risk	Business	The entrepreneurial risk will be mitigated by the team set up by the proponents of the project with the help of the network of contacts the team has.	1

IX-7.1. Mitigation strategy

From the above listed risks the team considers that the technology risks are the most likely to occur. The milestones determined by the team, namely *In vivo* studies, pre-clinical evaluation and the clinical trials have an inherent risk of failure. The probability of failure decreases as the project evolves and the milestones set are completed. The high risk associated with the first tasks can, however, be mitigated by the know-how and expertise of the team. The design of an iterative process to optimize HydrUStent will be done following the results of the *in vivo* tests. The protected technology allows the customization of the material in case unexpected side-effects are observed. The probability of failure is however present until the moment the regulatory entities certify the product and sales start.

In these projects the duration estimated may be exceeded. Longer times for product validation and product development than estimated may occur. The duration risk will be mitigated defining specific deliverables within the timeframe of the project. This will allow milestones to be reached within the expected date and no delays on the course of the project.

Chapter X

General Conclusions, Final Remarks and Future Perspectives

Chapter X

General conclusions, Final Remarks and Future Perspectives

X-1. GENERAL CONCLUSIONS AND FINAL REMARKS

Ureteral stents are a useful and crucial daily medical device in the management of numerous urological disorders. Ureteral stents are normally implanted in the treatment of urolithiasis, malignant or benign obstruction, to promote ureteral healing, manage urinary leak, or they can be placed preoperatively to aid in intraoperative ureteral identification, during particular surgical procedures. However, despite their extensive use, conventional ureteral stent technology is far from the ideal. Conventional ureteral stents are associated with clinical complications including bacterial adhesion, infection, encrustation development, pain and discomfort for the patients. A complete understanding of usual and unusual complications and past fails is required to find how ureteral stent design and clinical stent use can be improved. In past years, different methodologies have been explored, including novel stent coatings, drug-eluting stents and biodegradable ureteral stents. The major goal of the work developed under the scope of the present thesis was to develop a biodegradable ureteral stent based on natural origin polymers. The technology herein proposed and studied procured to match the main drawbacks identified in the literature in the development of biodegradable ureteral stents and overcome them. In **chapter III**, biodegradable ureteral stents were successfully developed from natural origin polysaccharides. A method combined of templated gelation and critical point drying lead to the creation of hollow tubes, using alginate and gellan gum, as well as their blends with gelatin. The have results shown adequate biodegradation rates in artificial urine solution; no development of encrustation; and anti-bacterial properties. Stents prepared from alginate presented the fastest biodegradation rate. The ureteral stents developed, when in contact with a physiological medium, become hydrogels, exhibiting biocompatible and non-cytotoxic characteristics. Biodegradable stent technology joined with the possibility to release active compounds, such as anti-inflammatory agents like ketoprofen is an important development for the future of ureteral stents. In **chapter IV**, a ketoprofen-eluting biodegradable ureteral stent was

prepared by supercritical CO₂ impregnation. The study revealed the influence of the operating conditions, particularly temperature, on the impregnation yield, which was found to be higher at 40 °C for both alginate-base stents and gellan-gum based stents. According to the release kinetics profiles, ketoprofen is released in the first 72 h in artificial urine solution. The results showed a good indication that the drug-eluting ureteral stents developed are able to meet the purpose for which they were designed, i.e, be able to act when fast and local delivery is desirable. The elution of the drug at the same time the degradation of the stent occurs is a major progress in the state of the art. In **chapter V**, the objective was to overcome the low mechanical performance demonstrated in the formulation of the stent designed in **chapter III** which fail, upon the first *In vivo* validation in a pig model. Stent formulation was revised and different concentrations of gelatin and alginate and different concentrations of crosslinking agent were tested in order to enhance the mechanical properties. Furthermore, bismuth was added to confer radiopaque properties to the biodegradable ureteral stent. This second-generation of stents, presents radiopaque properties even in the wet state. Additionally, *In vitro* results showed that a higher concentration of gelatin in the biodegradable stent resulted in higher mechanical properties, and a higher concentration of alginate slowed the degradation *In vitro*. The leachables and the degradation products have shown to be non-cytotoxic and the degradation of the stent has shown to be homogenous as the degradation occurs by erosion of the material. The *In vivo* placement under conventional procedure was successfully validated and the female pigs remained asymptomatic, with normal urine flow. The stents remain intact during the first 3 days and after 10 days the ureteral stents were totally degraded. In **Chapter VI**, using the formulation developed in the previous chapter and the supercritical carbon dioxide (scCO₂) impregnation process used in the **chapter III**, a drug-eluting biodegradable ureteral stent as new approach for urothelial tumors of upper urinary tract cancer was developed. Paclitaxel, epirubicin, doxorubicin and gemcitabine were impregnated in the biodegradable ureteral stents developed and in commercial ureteral stent, as a control. The release was sustainable in artificial urine solution and 100% of the impregnated drug was released after 72h, while stent degraded in 9 days. In the case of the commercial stent the amount of drug impregnated was lower and the release was faster for all drugs. In this case 100% of the drug was released within 24 h. The anti-cancer drug-eluting biodegradable ureteral stents developed confirmed the anti-tumoral effect against T24 urothelial cancer line reducing around 75% of cell viability after 72 h and demonstrating minimal cytotoxic effect on HUVECs which were used as control. In **chapter VII**, the permeability of paclitaxel and doxorubicin from the drug-eluting

ureteral stents developed in the previous chapter was studied, using three different membranes: polyethersulphone membrane (PES), HUVECs cell monolayer and an *ex vivo* porcine ureter. The permeability results were found to be dependent on the molecular weight of drugs and naturally by the release time of the drug from the stent. The results supported the hypothesis of biodegradable ureteral stents impregnated with chemotherapy drugs may serve as sustainable IDD systems increasing the bioavailability of drugs and the ability to target upper urinary tract urothelial carcinoma, particularly those impregnated with paclitaxel. In **chapter VIII**, the biodegradable ureteral stents developed were tested in a large *In vivo* porcine model. The study, demonstrated that biodegradable ureteral stents made from natural origin polymers developed are biocompatible, with suitable mechanical properties and present a homogenous degradation. The results obtained have proven that this biodegradable ureteral stent has the capacity to provide a temporary urine drainage as good as the non-degradable commercial stents with significantly less edema and hydronephrosis. In **chapter IX**, presents a business plan strategy towards the commercialization of the technology developed under the scope of this thesis. The business plan demonstrated the feasibility and the demand as well as the market potential of the patented technologies.

X-2. FUTURE RESEARCH DIRECTIONS

Ureteral stent design is an interesting and exciting field which has gained more attention particularly in last years. To date none of the technological developments has led to the “ideal stent”, but much progress has been made in the ureteral stent design by improving the physical characteristics of the biomaterials and the application of new coatings. The future direction in this field will incorporate all the research developed and might be in the form of a biodegradable ureteral stent engineered to be coated or impregnated with and active compounds to address not only stent-associated complications but also new clinical urologic scenarios as tumors of upper urinary tract. Developments regarding biodegradable metal-based stents could, in the future, be applied in design of stents that can maintain patency and degrade in the desired time period. The development of new biomaterials that can be triggered from an external stimulus and because of that the degradation of the stent can be controlled instantly and be another promising approach. Hydrogel-based materials with suitable mechanical properties, proved in this thesis to be a good approach to minimize inflammation and lower urothelium irritation. In the next years, new natural hydrogels or new biodegradable synthetic polymer-based can be developed and applied to the

design of ureteral stents. Supercritical fluid process has revealed in this thesis to be a unique process for drying biodegradable ureteral stents and to impregnate active compounds within the polymeric matrix. With the knowledge generated by this work, it is expected that the proposed biodegradable ureteral stents from natural origin polymers will have a strong impact in urologic field and can find the way to go to market. The most characteristic and promising feature of the proposed biodegradable ureteral stent is the unique homogenous stent-fragment free degradation process confirmed *in vivo* in a porcine model. Incontestably, the clinical trials in humans it are necessary to corroborated the promising results obtained so far.

